Thesis title:

The Method of Fundamental Solutions for certain problems in rotationally symmetric domains

Author: Theodoros Tsangaris

Department of Mathematics and Statistics

University of Cyprus

Nicosia, Cyprus

June 2005

Contents

List of Figures

Abstract

Our main objective in this thesis is the investigation of the application of the Method of Fundamental Solutions (MFS) to certain problems in rotationally symmetric domains.

In the Introduction we give a brief review of boundary methods for the solution of certain elliptic boundary value problems. One such method is the MFS and we subsequently describe its formulation for several important two and three–dimensional boundary value problems. We also present some recent developments in the use of the MFS.

In the second chapter, we investigate the application of the MFS to the Dirichlet problem for Laplace's equation in annular domains. We examine in detail the properties of the resulting coefficient matrix and its eigenvalues, and using these we prove the convergence of the method for analytic boundary data. An efficient matrix decomposition algorithm using Fast Fourier Tranforms (FFTs) is developed for the computation of the MFS approximation. The algorithm is tested on several problems confirming the theoretical predictions.

In the third chapter, we develop an efficient matrix decomposition MFS algorithm for the solution of certain biharmonic problems in annular domains. The circulant structure of the matrices resulting from the MFS discretization is again exploited by using FFTs. The algorithm is tested on several examples.

In the fourth chapter, we apply the MFS to three–dimensional problems. In particular, we consider certain axisymmetric harmonic and biharmonic problems. The coefficient matrices resulting from the MFS discretization now have block circulant structures. By exploiting these structures, we develop efficient matrix decomposition algorithms for the solution of this class of problems. The algorithms are tested on several examples.

In the fifth chapter, we present the conclusions of the thesis and give suggestions for future work.

Acknowledgements

On the occasion, I wish to express my sincere gratitude to my advisors Professor Andreas Karageorghis and Associate Professor Yiorgos–Sokratis Smyrlis. I could not have imagined having better advisors and mentors for my Ph.D. Throughout my thesis–writing period, they provided encouragement, sound advice, good teaching, good company, and lots of good ideas. I would have been lost without them. Without their help it was impossible to finish the thesis.

I would also like to thank the Univesity of Cyprus and especially the Department of Mathematics and Statistics for providing me financial support and excellent environment for learning and research.

Finally, I want to express my feelings of gratitude to my parents for their continuous support through my life.

Chapter 1

Introduction

The method of fundamental solutions (MFS) is a meshless technique for the numerical solution of certain elliptic boundary value problems which falls in the class of methods generally called boundary methods. Like the boundary element method (BEM), it is applicable when a fundamental solution of the differential equation in question is known. It shares the same advantages of the BEM over domain discretization methods, and also has certain advantages over the BEM. The MFS has the following key features:

(i) It requires neither domain nor surface discretization.

(ii) It requires no numerical integration and thus the difficulty of singular integration can be avoided.

(iii) It is easy for practical implementation.

We are primarily interested in the application of the MFS to elliptic boundary value problems governed by equations of the form

$$Lu(P) = 0, \quad P \in \Omega$$

where L is a linear elliptic partial differential operator and Ω is a bounded domain in $\mathbb{R}^2$ or $\mathbb{R}^3$. By a fundamental solution of the differential operator L, we mean a function $k(P, Q)$ such that

$$\mathcal{L}\, k(\cdot, Q) \;=\; \delta_Q, \tag{1.1}$$

where δ_Q denotes the Dirac measure on $\mathbb{R}^2$ giving unit mass to the point Q. The equation (1.1) is satisfied in the sense of distributions. The function k is defined everywhere except when $P = Q$, where it is singular. Thus Q is called the singularity of the fundamental solution.

Early uses of the MFS were for the solution of various linear potential problems in two and three space variables. The method has since been applied to a variety of situations such as plane potential problems involving nonlinear radiation-type boundary conditions, free boundary problems, biharmonic problems, problems in elastostatics and in the analysis of wave scattering fluids and solids. A survey of the MFS and related methods for the numerical solution of elliptic boundary value problems is presented in Ref. [18, 19].

1.1 Boundary Methods for the Dirichlet Problem

The basic idea in the MFS is to approximate the solution of a boundary value problem by a linear combination of fundamental solutions of the governing equation. To be more specific, let us consider the following boundary-value problem

$$\Delta u(P) = 0, \quad P \in \Omega, \tag{1.2}$$

$$u(P) = f(P), \quad P \in \partial\Omega, \tag{1.3}$$

where Ω is a bounded domain in the plane with smooth boundary $\partial\Omega$, Δ denotes the Laplacian and f is a prescribed function.

1.1.1 Indirect BIEMs

In the traditional boundary integral approach u is represented in the form of a simple-layer potential [32]

$$u(P) = \int_{\partial\Omega} \sigma(Q) \log r(P,Q)\, dS_Q, \quad P \in \overline{\Omega}, \tag{1.4}$$

where $r(P,Q)$ denotes the distance between the points P and Q, σ is the unknown source density function which is determined so that (1.3) is satisfied. Thus

$$\int_{\partial\Omega} \sigma(Q) \log r(P,Q) dS_Q = f(P), \quad P \in \partial\Omega,$$

which is a Fredholm integral equation of the first kind.

An alternative representation of u is given by the double-layer potential [32]

$$u(P) = \int_{\partial\Omega} \mu(Q) \frac{\partial}{\partial n_Q} \log r(P,Q)\, dS_Q, \quad P \in \overline{\Omega},$$

where $\frac{\partial}{\partial n_Q}$ denotes the outward normal derivative at $Q \in \partial\Omega$. In this case, μ is the unknown density function defined by the Fredholm second-kind integral equation

$$-\pi\mu(P) + \int_{\partial\Omega} \mu(Q) \frac{\partial}{\partial n_Q} \log r(P,Q)\, dS_Q = f(P), \quad P \in \partial\Omega.$$

These methods are usually referred to as indirect BIEMs.

1.1.2 Direct BIEMs

In many current applications, direct BIEMs are used. Applying Green's Third Identity in (1.2) gives [5, 32]

$$c(P)u(P) = \int_{\partial\Omega} \{u(Q) \frac{\partial}{\partial n_Q} \log r(P,Q) - \frac{\partial u}{\partial n_Q}(Q) \log r(P,Q)\}\, ds_Q + \int_{\Omega} \Delta u(Q) \log r(P,Q)\, dA_Q, \tag{1.5}$$

where $P \in \overline{\Omega}$, and

$$c(P) = \begin{cases} 2\pi, & \text{if} \quad P \in \Omega, \\ \pi, & \text{if} \quad P \in \partial\Omega, \\ 0, & \text{if} \quad P \neq \overline{\Omega}. \end{cases}$$

Since (1.2) holds in Ω, equation (1.5) gives

$$c(P)u(P) = \int_{\partial\Omega} \{u(Q) \frac{\partial}{\partial n_Q} \log r(P,Q) - \frac{\partial u}{\partial n_Q}(Q) \log r(P,Q)\}\, ds_Q. \tag{1.6}$$

Equation (1.6) can be viewed as the combination of a simple-layer potential of density $\frac{\partial u}{\partial n}$, and a double layer potential of density u.

We determine $\frac{\partial u}{\partial n}$ such that

$$\int_{\Omega} \frac{\partial u}{\partial n_Q}(Q) \log r(P,Q)\, ds_Q = -\pi f(P) + \int_{\partial\Omega} f(Q) \frac{\partial}{\partial n_Q} \log r(P,Q)\, ds_Q, \quad P \in \partial\Omega. \tag{1.7}$$

This formulation is the basis for direct BIEMs.

1.1.3 Collocation

For the numerical solution of (1.7), a set of points $Q_j,\ j=1,\dots,N$, is placed on the boundary $\partial\Omega$ with $\partial\Omega_j = \overline{Q_{j-1}Q_j}$. Also a set of observation points $P_i,\ j=1,\dots,N$ with $P_i \in \partial\Omega_i$ is chosen. We assume that $u, \dfrac{\partial u}{\partial n}$ are piecewise constant functions such that

$$u(P) = u_j, \quad \frac{\partial u}{\partial n}(P) = u_{n_j}, \quad P \in \partial\Omega_j, \quad j = 1,\dots,N.$$

We then collocate at the midpoints P_i of $\partial\Omega_i, \quad i=1,\dots,N$. This produces the system of equations

$$\pi u_i = \sum_{j=1}^{N} \left\{ u_j \int_{\partial\Omega_j} \frac{\partial}{\partial n_Q} \log r(P_i,Q)\, ds_Q - u_{n_j} \int_{\partial\Omega_j} \log r(P_i,Q)\, ds_Q \right\}, \quad j=1,\dots,N. \tag{1.8}$$

We thus obtain an $N \times N$ linear system for the unknowns $u_{n_i}, \quad i=1,\dots,N$.

The possible complications associated with this method are the following:

(i) There may be difficulties in chosing the $\{Q_j\}$, the quadrature rules and the method for approximating $\partial\Omega$.

(ii) When $j=i$, the integrals are singular.

1.2 Auxiliary boundary methods

1.2.1 Kupradze's method

Since the integrands in (1.8) are singular when $j=i$, special care must be taken when we apply a quadrature rule to approximate the corresponding integrals. In Kupradze's method [17] this difficulty is avoided by choosing the observation points P_i to lie on an auxiliary boundary $\partial\Omega_a$ enclosing the original region Ω. Since each P_i lies outside $\overline{\Omega}$ then $c(P)=0$ in (1.6) and we have the functional equation

$$\int_{\partial\Omega} \left\{ u(Q) \frac{\partial}{\partial n_Q} \log r(P,Q) - \frac{\partial u}{\partial n_Q}(Q) \log r(P,Q) \right\} ds_Q = 0.$$

In this method the choice of $\partial\Omega_a$ is crucial and not easy to make.

1.2.2 Oliveira's method

In this approach [17, 62], the solution of the problem is expressed in terms of a simple layer potential with respect to the auxiliary boundary $\partial\Omega_a$. For example, for the solution of the problem (1.2)-(1.3) we have

$$u(P) = \int_{\partial\Omega_a} \sigma_a(Q) \log r(P,Q)\, dS_Q, \quad P \in \overline{\Omega}_a. \tag{1.9}$$

If we approximate the integral in (1.9) by a quadrature rule with nodes $\{Q_j\}_{j=1}^N$, then $u(P)$ is approximated by

$$\tilde{u}_N(P) = \sum_{j=1}^{N} [\omega_j \sigma_a(Q_j)] \log r(P, Q_j), \tag{1.10}$$

where the $\{\sigma_a(Q_j)\}_{j=1}^N$ are determined by satisfying the boundary conditions on the boundary $\partial\Omega$ of Ω. Since the fundamental solution of Laplace's equation is a constant multiple of $\log r(P,Q)$, the MFS can be viewed as a discrete simple layer potential representation method. This approach is particularly useful in the development of the MFS formulations for biharmonic problems.

1.2.3 The Method of Fundamental Solutions

In the MFS [18, 19], we discretize equation (1.9) by a quadrature rule. In particular, the solution u is approximated by a function of the form

$$u_N(\boldsymbol{c}, \boldsymbol{Q}; P) = \sum_{j=1}^{N} c_j k(P, Q_j), \quad P \in \overline{\Omega},$$

where $\boldsymbol{c} = (c_1, c_2, \ldots, c_N)^T$ and $\boldsymbol{Q}$ is a $2N$-vector containing the coordinates of the singularities $Q_j,\ j = 1, \ldots, N$, which lie outside the domain of the problem $\overline{\Omega} \equiv \Omega \cup \partial\Omega$. The goal is to determine the coefficients $\boldsymbol{c}$.

A set of observations points $\{P_i\}_{i=1}^M$ is selected on $\partial\Omega$. One then applies the boundary condition at each of this points. The locations of the singularities $\{Q_j\}_{j=1}^N$ are either preassigned or determined along with the coefficients of the fundamental solutions $\{c_j\}_{j=1}^N$ so that the approximate solution satisfies the boundary conditions as well as possible.

When the locations of the singularities are fixed and preassigned, this process yields the equations

$$\mathcal{B} u_N(\boldsymbol{c}, \boldsymbol{Q}; P_i) = 0, \quad i = 1, 2, \ldots, M, \tag{1.11}$$

where the boundary condition is of the form $\mathcal{B}u = 0$. When $M = N$, equation (1.11) yields a linear system of N equations in N unknowns, whereas, when $M > N$, we have an over-determined system which leads to a linear least-squares problem.

When the locations of the singularities are to be determined along with the coefficients $\boldsymbol{c}$ there are $3N$ unknowns, comprising $\boldsymbol{c}$ and the cartesian coordinates of the N singularities $\boldsymbol{Q}$; they are determined by minimizing the functional

$$F(\boldsymbol{c}, \boldsymbol{Q}) = \sum_{j=1}^{N} \left| \mathcal{B}u_N(\boldsymbol{c}, \boldsymbol{Q}; P_i) \right|^2,$$

which is nonlinear in the coordinates of the Q_j. The minimization of this functional is usually done using readily available software such as the MINPACK routines LMDIF and LMDER [23], the Harwell subroutine `VA07AD` [30], and the NAG routine `E04UPF` [61]. The constrained optimization features of `E04UPF` are particularly useful for ensuring that, for instance, the singularities remain outside the domain of the problem. The initial placement of the singularities can influence the convergence of a least-squares routine significantly. Usually the singularities are distributed uniformly around the domain of the problem, at a fixed distance from its boundary. In this way, they may be viewed as lying on the boundary $\partial\Omega_a$, in (1.9), containing Ω.

When the MFS with an equal number of fixed singularities and boundary points, both of which are uniformly distributed, is applied to certain problems in circular domains, it leads to linear systems with coefficient matrices which are circulant or block matrices with circulant blocks ([15]). Ways of exploiting the properties of such systems for the efficient implementation of the MFS applied to harmonic and biharmonic problems are investigated in Refs. [67, 68] and in chapters 2 and 3.

1.3 MFS formulations

1.3.1 Harmonic Problems in two dimensions

The MFS with moving singularities was first proposed by Mathon and Johnston [59] for the solution of potential problems of the form

$$\begin{cases} \Delta u(P) = 0, & P \in \Omega, \\ \mathcal{B}u(P) = 0, & P \in \partial\Omega\,, \end{cases}$$

where Δ denotes the Laplace operator, u is the dependent variable, and Ω is a bounded domain in the plane with boundary $\partial\Omega$. The operator $\mathcal{B}$ specifies the boundary conditions (BCs) and is usually of the form:

$$\mathcal{B}u(P) = \begin{cases} \alpha(P) + u(P), & P \in \partial\Omega_1 \quad \text{(Diriclet BCs)} \\ \alpha(P) + \dfrac{\partial u}{\partial n}(P) & P \in \partial\Omega_2 \quad \text{(Neumann BCs)}\,, \\ \alpha(P) + \beta(P)u(P) + \gamma(P)\dfrac{\partial u}{\partial n}(P) & P \in \partial\Omega_3 \quad \text{(Robin BCs)} \end{cases} \tag{1.12}$$

where α, β and γ are prescribed functions, and $\partial\Omega = \partial\Omega_1 \cup \partial\Omega_2 \cup \partial\Omega_3$. The solution u is approximated by a function of the form

$$u_N(\boldsymbol{c}, \boldsymbol{Q}; P) = \sum_{j=1}^{N} c_j\, k_1(P, Q_j), \quad P \in \overline{\Omega},$$

where $\boldsymbol{c} = (c_1, c_2, \ldots, c_N)^T$ and $\boldsymbol{Q}$ is a $2N-$ vector containing the coordinates of the singularities Q_j, $j = 1, \ldots, N$, which lie outside the domain of the problem $\overline{\Omega}$. The function $k_1(P, Q)$ is a fundamental solution of Laplace's equation given by

$$k_1(P, Q) = -\frac{1}{2\pi} \log r(P, Q), \tag{1.13}$$

with $r(P, Q)$ denoting the distance between the points P and Q. A set of observation points $\{P_i\}_{i=1}^{M}$ is selected on $\partial\Omega$ and the coefficients $\boldsymbol{c}$ and the coordinates of the singularities $\boldsymbol{Q}$ are determined by minimizing the functional

$$F(\boldsymbol{c}, \boldsymbol{Q}) = \sum_{i=1}^{M} \left|\mathcal{B}u_N(\boldsymbol{c}, \boldsymbol{Q}; P_i)\right|^2,$$

which is nonlinear in the coordinates of the Q_j. The minimization of this functional is done using a nonlinear least square algorithm.

In the case when the singularities Q_j are fixed on the boundary $\partial\tilde{\Omega}$ of the domain $\tilde{\Omega}$ containing Ω, the coefficients $\boldsymbol{c}$ are determined so that the boundary condition is satisfied at the boundary points $\{P_i\}_{i=1}^{N}$:

$$\mathcal{B}u_N(\boldsymbol{c}, \boldsymbol{Q}; P_i) = 0, \quad i = 1, \ldots, N. \tag{1.14}$$

This yields a linear system of the form

$$G\boldsymbol{c} \;=\; \boldsymbol{f}\,, \tag{1.15}$$

for the coefficients $\boldsymbol{c}$. In the case of Dirichlet boundary conditions, the elements of the matrix G are given by

$$G_{i,j} = -\frac{1}{2\pi} \log |P_i - Q_j|, \quad i, j = 1, \dots, N. \tag{1.16}$$

1.3.2 Biharmonic Problems in two dimensions

We consider the biharmonic equation

$$\Delta^2 u(P) = 0, \quad P \in \Omega,$$

subject to the boundary conditions

$$\mathcal{B}_1 u(P) \equiv \alpha(P) + u(P) = 0, \quad \mathcal{B}_2 u(P) \equiv \beta(P) + \frac{\partial u}{\partial n}(P) = 0, \quad P \in \partial\Omega, \tag{1.17}$$

or

$$\mathcal{B}_1 u(P) \equiv \alpha(P) + u(P) = 0, \quad \mathcal{B}_2 u(P) \equiv \beta(P) + \Delta u(P) = 0, \quad P \in \partial\Omega, \tag{1.18}$$

where α and β are prescribed functions.

A first biharmonic MFS formulation [38] is based on the simple layer potential representation of biharmonic functions suggested in [18, 56]. In this formulation, the solution is approximated by a function of the form

$$u_N(\boldsymbol{c}, \boldsymbol{Q}; P) = \sum_{j=1}^{N} \Big[c_j k_1(P, Q_j) + d_j k_2(P, Q_j) \Big], \quad P \in \overline{\Omega},$$

where k_1 is the fundamental solution of Laplace's equation given by (1.13) and k_2 is the fundamental solution of the biharmonic equation given by

$$k_2(P, Q) = -\frac{1}{8\pi} r^2(P, Q) \log r(P, Q). \tag{1.19}$$

Following the MFS approach in the case of Laplace's equation, the coefficients $\boldsymbol{c_j}$, $\boldsymbol{d_j}$ and the coordinates of the singularities $\boldsymbol{Q_j}$ are determined by minimizing the functional

$$F(\boldsymbol{c}, \boldsymbol{d}, \boldsymbol{Q}) = \sum_{i=1}^{M} \Big[|\mathcal{B}_1 u_N(\boldsymbol{c}, \boldsymbol{d}, \boldsymbol{Q}; P_i)|^2 + |\mathcal{B}_2 u_N(\boldsymbol{c}, \boldsymbol{d}, \boldsymbol{Q}; P_i)|^2 \Big].$$

When the singularities are fixed, the vectors of coefficients $\boldsymbol{c}$ and $\boldsymbol{d}$ are determined so that the boundary conditions are satisfied at the collocation points $\{P_i\}_{i=1}^{N}$:

$$\mathcal{B}_1 \, u_N(\boldsymbol{c}, \boldsymbol{d}, \boldsymbol{Q}; P_i) = 0, i = 1, \dots, N, \tag{1.20}$$

and

$$\mathcal{B}_2\, u_N(\boldsymbol{c}, \boldsymbol{d}, \boldsymbol{Q}; P_i) = 0, \quad i = 1, \ldots, N. \tag{1.21}$$

This yields a linear system of the form

$$G\boldsymbol{c} \;=\; \boldsymbol{f}\,, \tag{1.22}$$

for the coefficients $\boldsymbol{c}$ and $\boldsymbol{d}$, where, in the case of boundary conditions (1.17), the elements of the matrix

$$G = \left(\begin{array}{c|c} A_{11} & A_{12} \\ \hline A_{21} & A_{22} \end{array}\right) \tag{1.23}$$

are given by

$$\begin{aligned}
(A_{11})_{i,j} &= -\frac{1}{2\pi}\log|P_i - Q_j|, \\
(A_{12})_{i,j} &= -\frac{1}{8\pi}|P_i - Q_j|^2 \log|P_i - Q_j|, \\
(A_{21})_{i,j} &= -\frac{1}{2\pi}\left(\frac{x_{P_i} - x_{Q_j}}{|P_i - Q_j|^2}n_x + \frac{y_{P_i} - y_{Q_j}}{|P_i - Q_j|^2}n_y\right), \\
(A_{22})_{i,j} &= -\frac{1}{8\pi}\left[1 + 2\log|P_i - Q_j|\right]\left((x_{P_i} - x_{Q_j})n_x + (y_{P_i} - y_{Q_j})n_y\right),
\end{aligned}$$

where n_x and n_y denote the components of the outward normal vector $\boldsymbol{n}$ to $\partial\Omega$ in the x and y directions, respectively.

A second biharmonic MFS formulation [2], is based on the Almansi representation of biharmonic functions [1, 18, 32]. Almansi showed that the general solution of the biharmonic equation can be written as

$$u(P) = r^2(P)\,\phi^{(1)}(P) + \phi^{(2)}(P), \quad P \in \overline{\Omega},$$

where the functions $\phi^{(1)}$ and $\phi^{(2)}$ are harmonic in Ω, and $r(P)$ denotes the distance of the point P from the origin, which lies in Ω. If we replace both $\phi^{(1)}$ and $\phi^{(2)}$ by simple layer potentials,

$$\phi^{(i)}(P) = \int_{\partial\Omega} \sigma^{(i)}(Q)\log r(P,Q)\, ds_Q, \quad P \in \overline{\Omega},\; i = 1, 2,$$

then

$$u(P) = r^2(P)\int_{\partial\Omega} \sigma^{(1)}(Q)\log r(P,Q)\, ds_Q + \int_{\partial\Omega} \sigma^{(2)}(Q)\log r(P,Q)\, ds_Q \quad P \in \overline{\Omega}. \tag{1.24}$$

This expression provides the motivation for the second biharmonic MFS formulation. In (1.24), the simple layer potential representation with respect to an auxiliary boundary $\partial\Omega_a$ is used and, following (1.9)–(1.10), u(P) is approximated by a function of the form

$$u_N(\boldsymbol{c}, \boldsymbol{Q}; P) = \sum_{j=1}^{N} \left[c_j\, r^2(P) + d_j\right] k_1(P, Q_j), \quad P \in \overline{\Omega},$$

where k_1 is given by (1.13).

Now consider the biharmonic equation subject to the boundary conditions [18]

$$B_1 u(P) \equiv \alpha(P) + \frac{\partial u}{\partial x_P}(P) = 0, \quad B_2 u(P) \equiv \beta(P) + \frac{\partial u}{\partial y_P}(P) = 0, \quad P \in \partial\Omega. \tag{1.25}$$

Problems of this type arise, for example, in fluid flow problems, where u denotes the stream function. They do not have unique solutions, but since the quantities of interest are usually derivatives of the solution, which give the velocity components, the nonuniqueness is inconsequential.

For the biharmonic problem with boundary conditions (1.25), Fichera [22] proposed the simple layer potential representation

$$u(P) = \int_{\partial\Omega} \left[\sigma(Q) \frac{\partial k_2}{\partial x_Q}(P, Q) + \mu(Q) \frac{\partial k_2}{\partial y_Q}(P, Q)\right] ds_Q, \quad P \in \overline{\Omega}, \tag{1.26}$$

where $k_2(P, Q)$ is given by (1.19). It follows that

$$u(P) = \int_{\partial\Omega} [\sigma(Q)(x_P - x_Q) + \mu(Q)(y_P - y_Q)] \left[k_1(P, Q) + \frac{1}{4\pi}\right] ds_Q, \quad P \in \overline{\Omega},$$

where $P = (x_P, y_P)$ and $Q = (x_Q, y_Q)$. This provides the motivation for the third biharmonic MFS formulation [39], in which the approximate solution has the form

$$u_N(\mathbf{c}, \mathbf{Q}; P) = \sum_{j=1}^{N} [c_j(x_P - x_{Q_j}) + d_j(y_P - y_{Q_j})] \left[k_1(P, Q_j) + \frac{1}{4\pi}\right], \quad P \in \overline{\Omega},$$

where $Q_j = (x_{Q_j}, y_{Q_j})$.

1.3.3 The Helmholtz equation in two dimensions

We consider the exterior Neumann boundary value problem in $\mathbb{R}^2$

$$\begin{cases} \Delta u + k^2 u = 0 & \text{in} \quad \Omega, \\ \mathcal{B}u = 0 & \text{on} \quad \partial\Omega\,, \end{cases} \tag{1.27}$$

where the boundary conditions are given by (1.12). The domain Ω is an unbounded domain in $\mathbb{R}^2$. The boundary of Ω is $\partial\Omega$. Further, we must specify the behaviour of u at infinity, namely, it must satisfy the *Sommerfeld radiation condition* (two dimensional version),

$$\lim_{r\to\infty} \sqrt{r}\left(\frac{\partial u}{\partial r} - \mathrm{i}ku\right) = 0, \tag{1.28}$$

where r is the distance of a point $P \in \Omega$ from the origin. This problem is related to the problem of radiation of time-harmonic sound waves in a compressible fluid, caused by the vibrations of an immersed obstacle.

In the MFS [41], the solution u is approximated by

$$u_N(\boldsymbol{c}, \boldsymbol{Q}; P) = \sum_{\nu=1}^{N} c_\nu\, k_3(P, Q_\nu), \quad P \in \overline{\Omega}, \tag{1.29}$$

where $\boldsymbol{c} = (c_1, c_2, \ldots, c_N)^T \in \mathbb{C}^N$ and $\boldsymbol{Q}$ is a $N-$vector containing the coordinates of the singularities Q_ν, $\nu = 1, \ldots, N$, which lie outside $\overline{\Omega}$. The function $k_3(P, Q)$ is a fundamental solution of the Helmholtz equation given by

$$k_3(P, Q) = \frac{\mathrm{i}}{4} H_0^{(1)}\big(k|P - Q|\big), \tag{1.30}$$

where $\mathrm{i} = \sqrt{-1}$ and $H_0^{(1)}$ is the Hankel function of the first kind of order zero, and with $|P-Q|$ denoting the distance between the points P and Q. The case when the singularities are not fixed is described as in section (1.2.3). In the case when the singularities Q_ν are fixed on the boundary $\partial\tilde{\Omega}$ of the domain $\tilde{\Omega}$ which contains Ω. Note that the fundamental solution k_3 satisfies the Sommerfeld radiation condition as $|P - Q| \to \infty$, for a fixed Q. In the case of moving singularities a set of observation points $\{P_i\}_{i=1}^{M}$ is selected on $\partial\Omega$ and the coefficients $\boldsymbol{c}$ and the positions of the singularities $\boldsymbol{Q}$ are determined by minimizing the functional

$$F(\boldsymbol{c}, \boldsymbol{Q}) = \sum_{i=1}^{M} \left|\mathcal{B}\, u_N(\boldsymbol{c}, \boldsymbol{Q}; P_i)\right|^2,$$

which is nonlinear in the coordinates of the Q_j. The minimization of this functional is done using a nonlinear least square algorithm. In the case when the singularities Q_j are fixed on the boundary $\partial\tilde{\Omega}$ of the domain $\tilde{\Omega}$ containing Ω, the coefficients $\boldsymbol{c}$ are determined so that the boundary condition is satisfied at the boundary points $\{P_\mu\}_{\mu=1}^{N}$, namely,

$$\mathcal{B}\ u_N(\boldsymbol{c}, \boldsymbol{Q}; P_\mu) = 0, \quad \mu = 1, \ldots, N. \tag{1.31}$$

This yields a linear system of the form

$$Gc = f, \tag{1.32}$$

for the coefficients c.

In the case where we have Dirichlet boundary conditions the elements of matrix G are given by

$$G_{\mu,\nu} = \frac{\mathrm{i}}{4}\frac{\partial H_0^{(1)}}{\partial n}(k|P_\mu - Q_\nu|), \quad \mu, \nu = 1, \ldots, N$$

Since the Hankel function $H_0^{(1)} = J_0 + \mathrm{i}Y_0$, where J_0 and Y_0 are the Bessel functions of the first and second kind, respectively ([2, 75]), the elements of the matrix G can be expressed in terms of the Bessel functions J_1 and Y_1. These can be calculated via the NAG routines `S17AFF` and `S17ADF`, respectively.

1.3.4 The Cauchy–Navier equations in two dimensions

We consider the boundary value problem in $\mathbb{R}^2$ governed by the Cauchy–Navier equations of elasticity [33]

$$\begin{cases} (\lambda+\mu)u_{k,ki} + \mu u_{i,kk} = 0 & \text{in} \quad \Omega, \\ \mathcal{B}u_i = 0 & \text{on} \quad \partial\Omega, \qquad i = 1, 2 \end{cases} \tag{1.33}$$

Here we are using the indicial tensor notation in terms of the displacements u_1 and u_2. In (1.33), λ and μ are the Lamé elastic constants. These constants can be expressed as $\lambda = \dfrac{\nu E}{(1+\nu)(1-2\nu)}$ and $\mu = \dfrac{E}{2(1+\nu)}$ where E is the modulus of elasticity, and ν is Poisson's ratio. Summation over repeated subscripts is implied and partial derivatives are denoted by $u_{i,j} = \dfrac{\partial u_i}{\partial x_j}$. The boundary of Ω is $\partial\Omega$.

Note that the Cauchy-Navier equations can also be written as

$$\begin{cases} \left(\dfrac{2-2\nu}{1-2\nu}\right)\dfrac{\partial^2 u_1}{\partial x_1^2} + \left(\dfrac{1}{1-2\nu}\right)\dfrac{\partial^2 u_2}{\partial x_1 \partial x_2} + \dfrac{\partial^2 u_1}{\partial x_2^2} = 0, \\ \\ \dfrac{\partial^2 u_2}{\partial x_1^2} + \left(\dfrac{1}{1-2\nu}\right)\dfrac{\partial^2 u_1}{\partial x_1 \partial x_2} + \left(\dfrac{2-2\nu}{1-2\nu}\right)\dfrac{\partial^2 u_2}{\partial x_2^2} = 0. \end{cases} \tag{1.34}$$

In the Method of Fundamental Solutions (MFS) the displacements u_1 and u_2 are approximated by [6]

$$u_{1_N}(\mathbf{a}, \mathbf{b}, \mathbf{Q}; P) = \sum_{j=1}^{N} a_j\, g_{11}(P, Q_j) + \sum_{j=1}^{N} b_j\, g_{12}(P, Q_j), \tag{1.35}$$

and

$$u_{2_N}(\mathbf{a},\mathbf{b},\mathbf{Q};P) = \sum_{j=1}^{N} a_j\, g_{21}(P,Q_j) + \sum_{j=1}^{N} b_j\, g_{22}(P,Q_j) \qquad P\in\overline{\Omega}\,, \tag{1.36}$$

respectively. Here $\boldsymbol{a} = (a_1, a_2, \ldots, a_N)^T \in \mathbb{R}^N$ and $\boldsymbol{b} = (b_1, b_2, \ldots, b_N)^T \in \mathbb{R}^N$ are vectors of unknown coefficients, $\boldsymbol{Q}$ is a $N-$vector containing the coordinates of the singularities Q_j, $j = 1, \ldots, N$, which lie outside $\overline{\Omega}$. The functions $G_{ij},\ i, j = 1, 2$ are the fundamental solutions of the system (1.34) and are given by

$$g_{11}(P,Q) = -\frac{1}{8\pi\mu(1-\nu)}\left[(3-4\nu)\log r_{PQ} - \frac{(x_{1_P}-x_{1_Q})^2}{r_{PQ}^2}\right], \tag{1.37}$$

$$g_{12}(P,Q) = g_{21}(P,Q) = \frac{1}{8\pi\mu(1-\nu)}\left[\frac{(x_{1_P}-x_{1_Q})(x_{2_P}-x_{2_Q})}{r_{PQ}^2}\right], \tag{1.38}$$

$$g_{22}(P,Q) = -\frac{1}{8\pi\mu(1-\nu)}\left[(3-4\nu)\log r_{PQ} - \frac{(x_{2_P}-x_{2_Q})^2}{r_{PQ}^2}\right], \tag{1.39}$$

where $r_{PQ} = \sqrt{(x_{1_P}-x_{1_Q})^2 + (x_{2_P}-x_{2_Q})^2}$, and (x_{1_Q}, x_{2_Q}), (x_{1_P}, x_{2_P}) are the coordinates of the points Q and P, respectively.

In the case of moving singularities a set of points $\{P_i\}_{i=1}^{M}$ is selected on $\partial\Omega$ and the coefficients $\boldsymbol{a}$ and $\boldsymbol{b}$ and the locations of the singularities $\boldsymbol{Q}$ are determined by minimizing the functional

$$F(\boldsymbol{a},\boldsymbol{b},\boldsymbol{Q}) = \sum_{i=1}^{M}\Big[|\mathcal{B}\,u_{1_N}(\boldsymbol{a},\boldsymbol{b},\boldsymbol{Q};P_i)|^2 + |\mathcal{B}\,u_{2_N}(\boldsymbol{a},\boldsymbol{b},\boldsymbol{Q};P_i)|^2\Big],$$

In the case the singularities $\{Q_j\}_{j=1}^{N}$ are fixed on the boundary $\partial\tilde{\Omega}$ of the domain $\tilde{\Omega}$ which contains Ω, the $2N$ coefficients $\boldsymbol{a}, \boldsymbol{b}$ are determined so that the boundary conditions are satisfied at the boundary points $\{P_i\}_{i=1}^{N}$, namely,

$$\mathcal{B}\,u_{1_N}(\boldsymbol{a},\boldsymbol{b},\boldsymbol{Q};P_i) = 0, \tag{1.40}$$

$$\mathcal{B}\,u_{2_N}(\boldsymbol{a},\boldsymbol{b},\boldsymbol{Q};P_i) = 0, \quad i = 1, \ldots, N. \tag{1.41}$$

This yields a $2N \times 2N$ linear system of the form

$$G\begin{pmatrix}\boldsymbol{a}\\ \hline \boldsymbol{b}\end{pmatrix} = \begin{pmatrix}\boldsymbol{f_1}\\ \hline \boldsymbol{f_2}\end{pmatrix}, \tag{1.42}$$

where, in the case of Dirichlet boundary conditions

$$G = \left(\begin{array}{c|c} A & B \\ \hline B & C \end{array}\right)$$

with the $N \times N$ matrices $A = (A_{i,j})$, $B = (B_{i,j})$, and $C = (C_{i,j})$, where

$$A_{i,j} = g_{11}(P_i, Q_j),$$

$$B_{i,j} = g_{12}(P_i, Q_j) = g_{21}(P_i, Q_j)$$

$$\text{and} \quad C_{i,j} = g_{22}(P_i, Q_j), \quad i, j = 1, \ldots, N\,.$$

1.3.5 The Laplace equation in three dimensions

The corresponding three–dimensional boundary value problem in three dimensions is:

$$\begin{cases} \Delta u = 0 & \text{in} \quad \Omega, \\ \mathcal{B}u = 0 & \text{on} \quad \partial\Omega, \end{cases} \tag{1.43}$$

where the boundary conditions are given by (1.12). The boundary of Ω is denoted by $\partial\Omega$.

In the MFS [18, 31] the solution u is approximated by

$$u_N(\boldsymbol{c}, \boldsymbol{Q}; P) = \sum_{j=1}^{N} c_j\, K_1(P, Q_j), \qquad P \in \overline{\Omega}, \tag{1.44}$$

where $\boldsymbol{c} = (c_1, c_2, \ldots, c_N)^T$ and $\boldsymbol{Q}$ is a $3N-$vector containing the coordinates of the singularities $Q_j,\ j = 1, \ldots, N$, which lie outside $\overline{\Omega}$. The function $K_1(P, Q)$ is a fundamental solution of Laplace's equation in $\mathbb{R}^3$ given by

$$K_1(P, Q) = \frac{1}{4\,\pi\,|P - Q|}, \tag{1.45}$$

with $|P - Q|$ denoting the distance between the points P and Q. In the case of moving singularities a set of observation points $\{P_i\}_{i=1}^M$ is selected on $\partial\Omega$ and the coefficients $\boldsymbol{c}$ and the coordinates of the singularities $\boldsymbol{Q}$ are determined by minimizing the functional

$$F(\boldsymbol{c}, \boldsymbol{Q}) = \sum_{i=1}^{M} \left|\mathcal{B}\, u_N(\boldsymbol{c}, \boldsymbol{Q}; P_i)\right|^2,$$

which is nonlinear in the coordinates of the Q_j. The minimization of this functional is done using a nonlinear least square algorithm. If the singularities Q_j are fixed, the coefficients $\boldsymbol{c}$ are determined so that the boundary condition is satisfied at the boundary points $\{P_j\}_{j=1}^N$:

$$\mathcal{B}\, u_N(\boldsymbol{c}, \boldsymbol{Q}; P_i) = 0, \quad i = 1, \ldots, N. \tag{1.46}$$

This yields an $N \times N$ linear system of the form

$$G\boldsymbol{c} \;=\; \boldsymbol{f}\,, \tag{1.47}$$

for the coefficients $\boldsymbol{c}$, where, in the case of Dirichlet boundary conditions, the elements of the matrix G are given by

$$G_{i,j} = \frac{1}{4\pi\,|P_i - Q_j|}, \quad i,\, j = 1, \ldots, N. \tag{1.48}$$

1.3.6 The biharmonic equations in three dimensions

We now consider the three–dimensional boundary value problem

$$\begin{cases} \Delta^2 u = 0 & \text{in} \quad \Omega, \\ \mathcal{B}_1\, u = 0 & \text{on} \quad \partial\Omega\,, \\ \mathcal{B}_2\, u = 0 & \text{on} \quad \partial\Omega\,, \end{cases}$$

where the boundary conditions $\mathcal{B}_1$ and $\mathcal{B}_2$ are given by (1.17) or (1.18). The boundary of Ω is $\partial\Omega$.

In the MFS [18, 20], the solution u is approximated by

$$u_N(\boldsymbol{c}, \boldsymbol{d}, \boldsymbol{Q}; P) = \sum_{j=1}^{N} c_j\, K_1(P, Q_j) + \sum_{j=1}^{N} d_j\, K_2(P, Q_j) \qquad P \in \overline{\Omega},$$

where $\boldsymbol{c} = (c_1, c_2, \ldots, c_N)^T$, $\boldsymbol{d} = (d_1, d_2, \ldots, d_N)^T$, and $\boldsymbol{Q}$, is a $3N-$vectors containing the coordinates of the singularities Q_j, $j = 1, \ldots, N$, which lie outside $\overline{\Omega}$. The function $K_1(P, Q)$ is the fundamental solution of Laplace's equation in $\mathbb{R}^3$ given by (1.45), and $K_2(P, Q)$ is the fundamental solution of biharmonic equation in $\mathbb{R}^3$ given by

$$K_2(P, Q) \;=\; \frac{1}{8\,\pi}\,|P - Q|. \tag{1.49}$$

In the case of moving singularities the functional that is minimized to yield $\boldsymbol{c}$, $\boldsymbol{d}$ and $\boldsymbol{Q}$ is

$$F(\boldsymbol{c}, \boldsymbol{d}, \boldsymbol{Q}) = \sum_{i=1}^{M} \Big[|\mathcal{B}_1\, u_N(\boldsymbol{c}, \boldsymbol{d}, \boldsymbol{Q}; P_i)|^2 + |\mathcal{B}_2\, u_N(\boldsymbol{c}, \boldsymbol{d}, \boldsymbol{Q}; P_i)|^2 \Big].$$

When the singularities are fixed, vectors of coefficients $\boldsymbol{c}$ and $\boldsymbol{d}$ are determined so that the boundary conditions are satisfied at the collocation points $\{P_i\}_{i=1}^N$:

$$\mathcal{B}_1\, u_N(\boldsymbol{c}, \boldsymbol{d}, \boldsymbol{Q}; P_i) = 0,$$

$$\mathcal{B}_2\, u_N(\boldsymbol{c}, \boldsymbol{d}, \boldsymbol{Q}; P_i) = 0, \quad i = 1, \ldots, N.$$

This yields a $2N \times 2N$ linear system of the form

$$G \begin{pmatrix} \boldsymbol{c} \\ \hline \boldsymbol{d} \end{pmatrix} \; = \; \begin{pmatrix} \boldsymbol{f_1} \\ \hline \boldsymbol{f_2} \end{pmatrix},$$

for the coefficients $\boldsymbol{c}$ and $\boldsymbol{d}$ where, in the case of boundary conditions (1.17), the elements of the matrix

$$G = \left(\begin{array}{c|c} A_{11} & A_{12} \\ \hline A_{21} & A_{22} \end{array} \right)$$

are given by

$$(A_{11})_{i,j} = \frac{1}{4\pi} \frac{1}{|P_i - Q_j|},$$

$$(A_{12})_{i,j} = \frac{1}{8\pi} |P_i - Q_j|,$$

$$(A_{21})_{i,j} = \frac{1}{4\pi} \frac{\partial}{\partial n} \left[\frac{1}{|P_i - Q_j|} \right] = -\frac{1}{4\pi} \left[\frac{(x_{P_i} - x_{Q_j})}{|P_i - Q_j|^3} n_x + \frac{(y_{P_i} - y_{Q_j})}{|P_i - Q_j|^3} n_y + \frac{(z_{P_i} - z_{Q_j})}{|P_i - Q_j|^3} n_z \right],$$

$$(A_{22})_{i,j} = \frac{1}{8\pi} \left[\frac{\partial}{\partial n} |P_i - Q_j| \right] = \frac{1}{8\pi} \left[\frac{(x_{P_i} - x_{Q_j})}{|P_i - Q_j|} n_x + \frac{(y_{P_i} - y_{Q_j})}{|P_i - Q_j|} n_y + \frac{(z_{P_i} - z_{Q_j})}{|P_i - Q_j|} n_z \right],$$

where n_x, n_y and n_z denote the components of the outward normal vector $\boldsymbol{n}$ to $\partial\Omega$ in the x, y and z directions, respectively.

1.3.7 The Helmholtz equation in three dimensions

We now consider the three-dimensional boundary value problem

$$\begin{cases} \Delta u + k^2 u = 0 & \text{in} \quad \Omega, \\ \mathcal{B}\, u = 0 & \text{on} \quad \partial\Omega, \end{cases} \tag{1.50}$$

where, as before, $\mathcal{B}$ are the boundary conditions given by (1.12). Further, u must satisfy the Sommerfeld radiation condition in three dimensions,

$$\lim_{r\to\infty} r \left(\frac{\partial u}{\partial r} - \mathrm{i} k u \right) \; = \; 0, \tag{1.51}$$

where r is the distance of a point $P \in \Omega$ from the origin. As was the case in two dimensions, this problem is related to the problem of radiation of time–harmonic sound waves in a compressible fluid, caused by the vibrations of an immersed obstacle.

In the MFS [41], the solution u is approximated by

$$u_N(\boldsymbol{c}, \boldsymbol{Q}; P) = \sum_{j=1}^{N} c_j \, K_3(P, Q_j), \qquad P \in \overline{\Omega}, \tag{1.52}$$

where $\boldsymbol{c} = (c_1, c_2, \ldots, c_N)^T \in \mathbb{C}^N$ and $\boldsymbol{Q}$ is a $3N-$ vector containing the coordinates of the singularities (sources) Q_j, $j = 1, \ldots, N$, which lie outside $\overline{\Omega}$. The function $K_3(P, Q)$ is a fundamental solution of the Helmholtz equation in $\mathbb{R}^3$ given by

$$K_3(P, Q) = \frac{1}{4\pi |P - Q|} \, \mathrm{e}^{\mathrm{i}k|P-Q|}, \tag{1.53}$$

with $|P - Q|$ denoting the distance between the points P and Q. Note that the fundamental solution K_3 satisfies the the Sommerfeld radiation condition as $|P - Q| \to \infty$, for a fixed Q. In the case when the singularities Q_ν are fixed on the boundary $\partial\tilde{\Omega}$ of the domain $\tilde{\Omega}$ which contains Ω. Note that the fundamental solution K_3 satisfies the Sommerfeld radiation condition as $|P - Q| \to \infty$, for a fixed Q. In the case of moving singularities the functional which is minimized is the

$$F(\boldsymbol{c}, \boldsymbol{Q}) = \sum_{i=1}^{M} \left| \mathcal{B} \, u_N(\boldsymbol{c}, \boldsymbol{Q}; P_i) \right|^2,$$

which is nonlinear in the coordinates of the Q_j. When the singularities $Q_{m,n}$ are fixed on the boundary $\partial\tilde{\Omega}$ of a solid $\tilde{\Omega}$ surrounding Ω the coefficients $\boldsymbol{c}$ are determined so that the boundary condition is satisfied at the boundary points $\{P_i\}_{i=1}^{N}$:

$$\mathcal{B} \, u_N(\boldsymbol{c}, \boldsymbol{Q}; P_l) = 0, \;\; l = 1, \ldots, N. \tag{1.54}$$

This yields an $N \times N$ linear system of the form

$$G\boldsymbol{c} \; = \; \boldsymbol{f} \, , \tag{1.55}$$

for the coefficients $\boldsymbol{c}$, where, in the case of Dirichlet boundary conditions, the elements of the matrix G are given by

$$G_{l,j} = \frac{1}{4\pi} \frac{e^{\mathrm{i}k|P_l - Q_j|}}{|P_l - Q_j|}, \quad l, j = 1, \ldots, N \, . \tag{1.56}$$

1.3.8 The Cauchy-Navier equations in three dimensions

We consider the boundary value problem in $\mathbb{R}^3$ governed by the Cauchy-Navier equations of elasticity

$$\begin{cases} (\lambda+\mu)u_{k,ki} + \mu u_{i,kk} = 0 & \text{in} \quad \Omega, \\ \mathcal{B}u_i = 0 & \text{on} \quad \partial\Omega\,, \qquad i = 1,2,3. \end{cases} \tag{1.57}$$

Here we are again using the indicial tensor notation in terms of the displacements u_1, u_2 and u_3.

The Cauchy-Navier equations can also be written as

$$\begin{aligned} \left(\frac{2-2\nu}{1-2\nu}\right)\frac{\partial^2 u_1}{\partial x_1^2} &+ \frac{\partial^2 u_1}{\partial x_2^2} + \frac{\partial^2 u_1}{\partial x_3^2} \\ &+ \left(\frac{1}{1-2\nu}\right)\frac{\partial^2 u_2}{\partial x_1 \partial x_2} + \left(\frac{1}{1-2\nu}\right)\frac{\partial^2 u_3}{\partial x_1 \partial x_3} = 0, \end{aligned} \tag{1.58}$$

$$\begin{aligned} \left(\frac{1}{1-2\nu}\right)\frac{\partial^2 u_1}{\partial x_1 \partial x_2} &+ \frac{\partial^2 u_2}{\partial x_1^2} + \left(\frac{2-2\nu}{1-2\nu}\right)\frac{\partial^2 u_2}{\partial x_2^2} \\ &+ \frac{\partial^2 u_2}{\partial x_3^2} + \left(\frac{1}{1-2\nu}\right)\frac{\partial^2 u_3}{\partial x_2 \partial x_3} = 0, \end{aligned} \tag{1.59}$$

$$\begin{aligned} \left(\frac{1}{1-2\nu}\right)\frac{\partial^2 u_1}{\partial x_1 \partial x_3} &+ \left(\frac{1}{1-2\nu}\right)\frac{\partial^2 u_2}{\partial x_2 \partial x_3} + \frac{\partial^2 u_3}{\partial x_1^2} \\ &+ \frac{\partial^2 u_3}{\partial x_2^2} + \left(\frac{2-2\nu}{1-2\nu}\right)\frac{\partial^2 u_3}{\partial x_3^2} = 0, \qquad \text{in} \;\; \Omega. \end{aligned} \tag{1.60}$$

In the MFS [64] the displacements are approximated by

$$\begin{aligned} u_{1_N}(\mathbf{a},\mathbf{b},\mathbf{c},\mathbf{Q};P) &= \sum_{n=1}^{N} a_n G_{11}(P,Q_n) \\ &+ \sum_{n=1}^{N} b_n G_{12}(P,Q_n) + \sum_{n=1}^{N} c_n G_{13}(P,Q_n), \end{aligned} \tag{1.61}$$

$$\begin{aligned} u_{2_N}(\mathbf{a},\mathbf{b},\mathbf{c},\mathbf{Q};P) &= \sum_{n=1}^{N} a_n G_{21}(P,Q_n) \\ &+ \sum_{n=1}^{N} b_n G_{22}(P,Q_n) + \sum_{n=1}^{N} c_n G_{23}(P,Q_n), \end{aligned} \tag{1.62}$$

$$\begin{aligned} u_{3_N}(\mathbf{a},\mathbf{b},\mathbf{c},\mathbf{Q};P) &= \sum_{n=1}^{N} a_n G_{31}(P,Q_n) \\ &+ \sum_{n=1}^{N} b_n G_{32}(P,Q_n) + \sum_{n=1}^{N} c_n G_{33}(P,Q_n)\,, \end{aligned} \tag{1.63}$$

where $\boldsymbol{a} = (a_1, a_2, \ldots, a_N)^T$, $\boldsymbol{b} = (b_1, b_2, \ldots, b_N)^T$, $\boldsymbol{c} = (c_1, c_2, \ldots, c_N)^T$, and $\mathbf{Q}$ is a $3N$-vector containing the coordinates of the singularities Q_n, $n = 1, \ldots, N$, which lie outside $\overline{\Omega}$.

The functions $G_{ij}, i, j = 1, 2, 3$ are the fundamental solutions of the system (1.60) and are given by

$$
\begin{aligned}
G_{11}(P,Q) &= \frac{1}{16\pi\mu(1-\nu)} \left[\frac{(3-4\nu)r_{PQ}^2 + (x_{1_P} - x_{1_Q})^2}{r_{PQ}^3} \right], \\
G_{12}(P,Q) &= G_{21}(P,Q) = \frac{1}{16\pi\mu(1-\nu)} \left[\frac{(x_{1_P} - x_{1_Q})(x_{2_P} - x_{2_Q})}{r_{PQ}^3} \right], \\
G_{13}(P,Q) &= G_{31}(P,Q) = \frac{1}{16\pi\mu(1-\nu)} \left[\frac{(x_{1_P} - x_{1_Q})(x_{3_P} - x_{3_Q})}{r_{PQ}^3} \right], \\
G_{22}(P,Q) &= \frac{1}{16\pi\mu(1-\nu)} \left[\frac{(3-4\nu)r_{PQ}^2 + (x_{2_P} - x_{2_Q})^2}{r_{PQ}^3} \right], \\
G_{23}(P,Q) &= G_{32}(P,Q) = \frac{1}{16\pi\mu(1-\nu)} \left[\frac{(x_{2_P} - x_{2_Q})(x_{3_P} - x_{3_Q})}{r_{PQ}^3} \right], \\
G_{33}(P,Q) &= \frac{1}{16\pi\mu(1-\nu)} \left[\frac{(3-4\nu)r_{PQ}^2 + (x_{3_P} - x_{3_Q})^2}{r_{PQ}^3} \right],
\end{aligned}
$$

where

$$r_{PQ} = \sqrt{(x_{1_P} - x_{1_Q})^2 + (x_{2_P} - x_{2_Q})^2 + (x_{3_P} - x_{3_Q})^2}.$$

In the case of moving singularities the locations of the singularities $\boldsymbol{Q}$ are determined by minimizing the functional

$$F(\boldsymbol{a}, \boldsymbol{b}, \boldsymbol{c}, \boldsymbol{Q}) = \sum_{i=1}^{M} \left[|\mathcal{B}\, u_{1N}(\boldsymbol{a}, \boldsymbol{b}, \boldsymbol{c}, \boldsymbol{Q}; P_i)|^2 + |\mathcal{B}\, u_{2N}(\boldsymbol{a}, \boldsymbol{b}, \boldsymbol{c}, \boldsymbol{Q}; P_i)|^2 + |\mathcal{B}\, u_{3N}(\boldsymbol{a}, \boldsymbol{b}, \boldsymbol{c}, \boldsymbol{Q}; P_i)|^2 \right],$$

When the singularities Q_n are fixed on the boundary $\partial\tilde{\Omega}$ of a solid $\tilde{\Omega}$ surrounding Ω, the coefficients $\boldsymbol{a}, \boldsymbol{b}$ and $\boldsymbol{c}$ are determined so that the boundary conditions are satisfied at the boundary points $\{P_i\}_{i=1}^N$:

$$\mathcal{B}u_{1_N}(\mathbf{a}, \mathbf{b}, \mathbf{c}, \mathbf{Q}; P_i) = 0,$$

$$\mathcal{B}u_{2_N}(\mathbf{a}, \mathbf{b}, \mathbf{c}, \mathbf{Q}; P_i) = 0,$$

and

$$\mathcal{B}u_{3_N}(\mathbf{a}, \mathbf{b}, \mathbf{c}, \mathbf{Q}; P_i) = 0, \quad i = 1, \ldots, N.$$

In the case of Dirichlet boundary conditions, yields a $3N \times 3N$ linear system of the form

$$\left(\begin{array}{c|c|c} H_{11} & H_{12} & H_{13} \\ \hline H_{21} & H_{22} & H_{23} \\ \hline H_{31} & H_{32} & H_{33} \end{array}\right)\left(\begin{array}{c} \boldsymbol{a} \\ \hline \boldsymbol{b} \\ \hline \boldsymbol{c} \end{array}\right) = \left(\begin{array}{c} \boldsymbol{f_1} \\ \hline \boldsymbol{f_2} \\ \hline \boldsymbol{f_3} \end{array}\right), \tag{1.64}$$

where the $N \times N$ matrices are now given, with the obvious notation, by

$$H_{k\ell_{i,j}} = G_{k\ell}(P_i, Q_j), \quad i,\, j = 1, \dots, N, \tag{1.65}$$

for $k, \ell = 1, 2, 3$.

1.4 Recent developments

1.4.1 Inhomogeneous problems

The MFS has been extended to problems including nonhomogeneous terms using particular solutions [24].

In the cases where the nonhomogeneous term is a known function, a particular solution can often be obtained. For example consider the Poisson equation

$$\Delta u(x) = f(x), \quad x \in \Omega, \tag{1.66}$$

where $\Omega \subset \mathbb{R}^n$ is bounded. As suggested in [3], a particular solution of (1.66) can be obtained by constructing the associated Newton potential

$$u_P(x) = \int_\Omega \Phi_0(x-y) f(y) dy. \tag{1.67}$$

Once we have a particular solution u_P of (1.66) and u is the solution of the boundary value problem

$$\begin{cases} \Delta u = f & \text{in} \quad \Omega, \\ u = g & \text{on} \quad \partial\Omega, \end{cases}$$

and set $v = u - u_P$ then

$$\Delta v(x) = 0, \quad x \in \Omega,$$

with the boundary condition

$$v(x) = g(x) - u_P(x), \quad x \in \partial\Omega,$$

which may be solved by the MFS [63]. An important task is therefore the determination of a particular solution of the Poisson equation.

In the cases where the nonhomogeneous term is an unknown function, an approximate particular solution can be obtained using the Dual Reciprocity Method (DRM). The DRM was originally developed for taking domain integrals to the boundary in the BEM [60], and is applied with the MFS in a very similar way. In the DRM the function f in (1.66) is approximated by a linear combination of basis functions $\{\varphi_j\}_{j=1}^n$,

$$f(x) \simeq \hat{f}(x) = \sum_{j=1}^{n} c_j \, \varphi_j(x)$$

where $\{c_j\}_{j=1}^n$ are undetermined coefficients which can be computed by collocation, i.e.,

$$\sum_{j=1}^{n} c_j \, \varphi_j(x_k) = f(x_k), \quad 1 \leq k \leq n,$$

where $\{x_k\}_{k=1}^n$ are n collocation points in $\mathbb{R}^n$. Since the particular solution does not in general have to satisfy the boundary condition, the collocation points $\{x_k\}_{k=1}^n$ can be selected inside and outside the domain Ω. Nevertheless, for the traditional DRM, $\{x_k\}_{k=1}^n$ are chosen inside the domain Ω. After the computation of $\{c_j\}_{j=1}^n$, we have an approximation of the particular solution $\hat{u}_P$ ginen by

$$\hat{u}_P(x) = \sum_{j=1}^{n} c_j \, \Psi_j(x)$$

where

$$\Delta \Psi_j = \varphi_j, \quad j = 1, \ldots, n, \tag{1.68}$$

because

$$\Delta u_P = f.$$

In [57] the MFS is used to solve some linear elastic problems, employing the DRM in cases involving inhomogeneous terms.

The most popular choice of basis functions is the set of Radial Basis Functions (RBFs), in particular thin plate and higher order radial splines, multiquadrics and Gaussians [10, 13, 14, 36]. These globally supported basis functions, however, lead to dense systems which can be highly ill-conditioned and thus compactly supported RBFs (CS-RBFs) have also become popular [14]. Another choice of basis functions is the set of polynomials and trigonometric functions [51]. It should be noted that a technique which is simpler than the DRM and has been used extensively is the so–called Kansa's method [34, 35].

In [4], Alves and Chen propose a new application of the method of fundamental solutions for nonhomogeneous elliptic problems. In particular, they present an extension of the MFS for the direct approximation of Poisson and nonhomogeneous Helmholtz problems. They do this by using the fundamental solutions of the associated eigenvalue equations as a basis to approximate the nonhomogeneous term.
In particular, Alves and Chen obtained $\hat{u}_P$ by considering the Ψ_j to be the fundamental solutions of the associated eigenvalue equations

$$\Delta\Psi_j = \lambda\Psi_j, \quad (\lambda \neq 0)$$

instead of solving (1.68) analytically.

A class of Poisson problems of particular interest is that in which the right hand side f is harmonic [18]. When f is an elementary harmonic function such as a constant or a polynomial, it is easy to construct a particular solution $\hat{u}$. The general case was addressed in [3], in which it is assumed that a particular solution is of the form $\hat{u}(x, y) = xH(x, y)/2$, with H harmonic. From the satisfaction of Poisson's equation, we obtain $\partial H/\partial x = f$. Integration yields

$$H(x, y) = \int_{x_0}^{x} f(s, y)ds + h(y), \tag{1.69}$$

where the point x_0 and the function $h(y)$ are arbitrary. From the fact that H is harmonic, it follows that

$$h''(y) = -\frac{\partial f}{\partial x}(x_0, y).$$

Integrating this differential equation gives

$$h(y) = -\int_{y_0}^{y} (y - t)\frac{\partial f}{\partial x}(x_0, t)dt,$$

from which, together with (1.69), one obtains the desired particular solution. This construction is considerably easier than the construction of a particular solution via the Newton potential as it only involves single integrals. Applications of this technique in combination with the MFS can be found in [63, 64].

1.4.2 Nonlinear inhomogeneous problems

In [12], Chen considers the problem

$$\begin{cases} \Delta u(P) + \delta f(u(P)) = 0 & P \in \Omega, \\ u(P) = 0 & P \in \partial\Omega, \end{cases} \tag{1.70}$$

where δ is the Frank–Kamenetskii parameter. The idea is to use a Picard-type iteration and solve the sequence of Poisson problems for $n = 1, 2, ...,$

$$\begin{cases} \Delta u_{n+1}(P) = -\delta f(u_n(P)), & P \in \Omega, \\ u_{n+1}(P) = 0 & P \in \partial\Omega. \end{cases} \tag{1.71}$$

Each of these problems may be solved using the methods described in section 4.1. In [12], at each iteration, Chen uses a combination of the dual reciprocity method to evaluate a particular solution of the inhomogeneous Poisson problem and an MFS-type method for the solution of the homogeneous problem.

1.4.3 Inverse Problems

In [54] Marin and Lesnic investigate the application of the MFS to boundary value problems associated with two-dimensional Helmholtz-type equations.
In particular they consider an open bounded domain $\Omega \subset \mathbb{R}^2$ and they assume that Ω is bounded by a smooth boundary $\Gamma \equiv \partial\Omega$, such that $\Gamma = \overline{\Gamma}_1 \cup \overline{\Gamma}_2$, where $\Gamma_1, \Gamma_2 \neq \emptyset$ and $\Gamma_1 \cap \Gamma_2 = \emptyset$. The function $u(x)$ satisfies the Helmholtz-type equation in the domain Ω, namely

$$(\Delta + k^2)u(x) = 0, \quad x \in \Omega \tag{1.72}$$

where $k = \alpha + \mathrm{i}\beta \in \mathbb{C}$. Let $\boldsymbol{n}(x)$ be the outward unit normal at $\partial\Omega$ and $v(x) \equiv (\nabla u \cdot \boldsymbol{n})(x), \quad x \in \partial\Omega$. The knowledge of u and/or v on the whole boundary Γ gives the corresponding Dirichlet, Neumann, or mixed boundary conditions which enable us to to determine u in the domain Ω. If it is possible to have both u and v on a part of the boundary Γ, say Γ_1, then this leads to the mathematical formulation of an inverse problem consisting of equation (1.72) and the boundary conditions

$$u(\boldsymbol{x}) = f(\boldsymbol{x}), \tag{1.73}$$

$$v(\boldsymbol{x}) = g(\boldsymbol{x}), \tag{1.74}$$

where $\boldsymbol{x} \in \Gamma_1 \subset \Gamma$ and f and g are prescribed functions.

In the MFS [41], the solution u is approximated by

$$u_N(\boldsymbol{c}, \boldsymbol{Q}; P) \;=\; \sum_{j=1}^{N} c_j \, k_3(P, Q_j), \qquad P \in \overline{\Omega}, \tag{1.75}$$

where $\boldsymbol{c} = (c_1, c_2, \ldots, c_N)^T \in \mathbb{C}^N$ and $\boldsymbol{Q}$ is a $N-$vector containing the coordinates of the singularities Q_j, $j = 1, \ldots, N$, which lie outside $\overline{\Omega}$. The function $k_3(P, Q)$ is a fundamental solution of the Helmholtz equation given by (2.2). On the boundary $\partial\Omega$

$$v_N(\boldsymbol{c}, \boldsymbol{Q}, \boldsymbol{n}; P) \;=\; \sum_{j=1}^{N} c_j \, \ell(P, Q_j; \boldsymbol{n}), \qquad P \in \partial\Omega \tag{1.76}$$

where

$$\ell(P, Q_j; \boldsymbol{n}) = \nabla_x k_3(P, Q) \cdot \boldsymbol{n}(x).$$

If a set of observation points $\{P_i\}_{i=1}^{M}$ is chosen on Γ_1 and the locations of the singularities $\{Q_j\}_{j=1}^{N}$ are set, then the application of approximations (1.75) and (1.76) to the boundary conditions (1.73) and (1.74) on Γ_1 yield a system of $2M$ linear algebraic equations in N unknowns which can be written as

$$A\,\boldsymbol{c} = f, \tag{1.77}$$

where

$$A_{i,j} = k_3(P_i, Q_j), \quad A_{N+i,j} = \ell(P_i, Q_j), \quad i = 1, 2, \ldots, M, \;\; j = 1, 2, \ldots, N,$$

and

$$f_i = u(P_i), \quad f_{M+i} = v(P_i), \quad i = 1, 2, \ldots, M.$$

It should be noted that in order to uniquely determine the solution $\boldsymbol{c}$ of system (1.77), the number M of the boundary collocation points and the number N of the singularities must satisfy the inequality $N \leq 2M$. System (1.77) cannot be solved by direct methods, such as the least–squares method, since such an approach would produce a highly unstable solution due to the large value of the condition number of the matrix A which increases dramatically as the number of boundary collocation points and source points increases. Marin and Lesnic used the Tikhonov regularization method to solve such ill–conditioned systems.

The Tikhonov regularized solution [52, 53, 54, 55] to the system of linear algebraic equations (1.77) is sought as

$$\boldsymbol{c}_\lambda \, : \, T_\lambda(\boldsymbol{c}_\lambda) = \min_{\boldsymbol{c} \in \mathbb{R}^N} T_\lambda(\boldsymbol{c}) \tag{1.78}$$

where T_λ represents the s^{th} order Tikhonov functional given by

$$T_\lambda(\cdot) \, : \, \mathbb{R}^N \to [0, \infty), \quad T_\lambda(\boldsymbol{c}) = \|A\boldsymbol{c} - \boldsymbol{f}\|_2^2 + \lambda^2 \|\mathbb{R}^{(s)}\boldsymbol{c}\|_2^2,$$

the matrix $\mathbb{R}^{(s)} \in \mathbb{R}^{(N-s)\times N}$ induces a C^s- constraint on the solution $\boldsymbol{c}$ and $\lambda > 0$ is the regularization parameter to be chosen. Formally, the Tikhonov regularized solution $\boldsymbol{c}_\lambda$ of the problem (1.78) is given as the solution of the regularized equation

$$(A^T A + \lambda^2 \mathbb{R}^{(s)^T} \mathbb{R}^{(s)})\boldsymbol{c} = A^T \boldsymbol{f}.$$

Regularization is necessary when solving ill-conditioned systems of linear equations because the simple least squares solution, i.e. $\lambda = 0$, is completely dominated by contributions from data errors and rounding errors. By adding regularization one is able to dampen out these contributions and maintain the norm $\|\mathbb{R}^{(s)}\boldsymbol{c}\|_2$ to be of reasonable size. The choice of regularization parameter λ is based on the L–curve method [52, 53, 54, 55].

In [52] Marin investigate the application of fundamental solutions to the Cauchy problem associated with the three–dimensional Helmholtz–type equations. The analysis he presents is analogous to the two-dimensional case we describe above. A similar approach is used in [53] to investigate the application of the method of fundamental solutions to the Cauchy problem for steady-state heat conduction in two dimensional functionally graded materials .

In [55] Marin and Lesnic present another application of the method of fundamental solutions to the Cauchy problem in two–dimensional isotropic linear elasticity. The resulting system of linear algebraic equations is again ill–conditioned and therefore its solution is regularized by employing the first–order Tikhonov functional, while the choice of the regularization parameter is based on the L–curve method.

1.4.4 Time dependent problems

Traditional boundary element methods have been used for some time for the numerical solution of transient problems; see, for example, [5, 18, 26]. The time dependence is handled using one of three methods. Firstly, one may use Laplace transforms to remove the time variable. Secondly, finite differences in time may be used, or lastly one could use time–dependent fundamental solutions [76]. This third approach was introduced by Kupradze [48] in the case of the heat equation.

Chen and Golberg [11] applied an MFS–type method for the solution of a time–dependent diffusion problem. The time variable is removed by taking Laplace transforms and the problem is transformed into one governed by the modified Helmholtz equation. In particular, they considered the diffusion equation

$$\frac{1}{k}\frac{\partial u}{\partial t}(P,t) = \Delta u(P,t), \quad P \in \Omega, \quad t > 0,$$

subject to the boundary conditions

$$u(P,t) = f_1(P,t), \quad P \in \partial\Omega_1, \quad t > 0,$$

$$\frac{\partial u}{\partial n}(P,t) = f_2(P,t), \quad P \in \partial\Omega_2, \quad t > 0,$$

where $\partial\Omega = \partial\Omega_1 \cup \partial\Omega_2$, and the initial condition

$$u(P,0) = u_0(P), \;\; P \in \Omega.$$

By taking the Laplace transform

$$Ł[u(P,t)] = U(P;s) = \int_0^\infty u(P,t)\,\mathrm{e}^{-st}dt,$$

the problem becomes

$$\left(\Delta - \frac{s}{k}\right) U(P;s) = -\frac{u_0(P)}{k}, \quad P \in \Omega,$$

$$U(P;s) = F_1(P;s), \;\; P \in \partial\Omega_1,$$

$$\frac{\partial U}{\partial n}(P;s) = F_2(P;s), \quad \in \partial\Omega_2,$$

where F_1 and F_2 are the Laplace transforms of f_1 and f_2, respectively. This boundary value problem is subsequently solved by determining a particular solution of the inhomogeneous problem using the associated Newton potential and then solving the homogeneous problem using an MFS–type method with the appropriate fundamental solution. The solution in the real-time space can be obtained by a numerical inverse Laplace transform scheme; see [11] for details.

1.4.5 Crack Problems

A variety of methods are currently available for computing stress intensity factors (SIFs) for elastic crack problems. The SIF is a measure of the strength of the stress singularity at a crack tip, and is useful from a mechanics perspective as it characterizes the displacement, stress and strain in the near field around the tip. Additionally, the stress intensity concept is important in terms of the crack extension as critical values of the SIF govern crack initiation.

In [73], Poullikas et al. studied the application of the method of fundamental solutions to the computation of SIF in linear elastic fracture mechanics. The displacements are approximated by linear combinations of the fundamental solutions of the Cauchy–Navier equations of elasticity and the leading terms for the displacement near the crack tip. They propose a linear least-squares MFS in which the singularities are fixed and a nonlinear least–squares MFS in which the singularities are free. The applicability of the two formulations of the method is demonstrated on two mode I crack problems. Both the proposed formulations are very easy to implement, require little data preparation, and, unlike boundary integral equation-type methods, avoid integrations on the boundary. It is shown that accurate approximations for the SIFs can be obtained with relatively few degrees of freedom.

In [7], Berger et al. studied mixed mode problems and they solved them using the MFS in two different formulations. The first formulation follows an idea presented in [73] of appending the usual MFS displacement field expansions with the elastic crack tip expansions. Numerical results using this approach indicate some difficulties with deeper cracks. They also develop a second formulation using a domain decomposition approach similar to that used in [6] for bimaterial problems. Then they used the developed method to calculate SIFs for a variety of crack lengths under mixed mode loading conditions.

Chapter 2

Numerical Analysis of the MFS for Harmonic Problems in Annular Domains

2.1 Method of fundamental solutions formulation

We consider the boundary value problem

$$\begin{cases} \Delta u = 0 & \text{in} \quad \Omega, \\ u = f_1 & \text{on} \quad \partial\Omega_1, \\ u = f_2 & \text{on} \quad \partial\Omega_2, \end{cases} \tag{2.1}$$

where Δ denotes the Laplace operator, the domain Ω is the annulus of radii ϱ_1 and ϱ_2, i.e., $\Omega = \{\boldsymbol{x} \in \mathbb{R}^2 \,:\, \varrho_1 < |\boldsymbol{x}| < \varrho_2\}$, and f_1 and f_2 are given functions. The boundary of Ω is $\partial\Omega = \partial\Omega_1 \cup \partial\Omega_2$ where $\partial\Omega_1$ and $\partial\Omega_2$ are the circles with radii ϱ_1 and ϱ_2, respectively. Let the function $k(P, Q)$ be a fundamental solution of Laplace's equation given by

$$k(P, Q) = -\frac{1}{2\pi} \log |P - Q|, \tag{2.2}$$

with $|P-Q|$ denoting the distance between the points P and Q. In the Method of Fundamental Solutions (MFS), the solution u is approximated by

$$u_N(\boldsymbol{c}, \boldsymbol{Q}; P) = \sum_{j=1}^{2N} c_j \, k(P, Q_j), \qquad P \in \overline{\Omega}, \tag{2.3}$$

where $\boldsymbol{c} = (c_1, c_2, \ldots, c_{2N})^T$ and $\boldsymbol{Q}$ is a $4N$-vector containing the coordinates of the singularities Q_j, $j = 1, \ldots, 2N$, which lie outside $\overline{\Omega}$. The singularities Q_j are fixed on the boundary $\partial\tilde{\Omega} = \partial\tilde{\Omega}_1 \cup \partial\tilde{\Omega}_2$ of an annulus $\tilde{\Omega}$ concentric to Ω and defined by $\tilde{\Omega} = \{\boldsymbol{x} \in \mathbb{R}^2 : R_1 < |\boldsymbol{x}| < R_2\}$, where $R_2 > \varrho_2 > \varrho_1 > R_1$. A set of collocation points $\{P_i\}_{i=1}^{2N}$ is placed on $\partial\Omega$. If $P_i = (x_{P_i}, y_{P_i})$, then we take

$$x_{P_i} = \varrho_1 \cos \frac{2(i-1)\pi}{N}, \quad y_{P_i} = \varrho_1 \sin \frac{2(i-1)\pi}{N}, \quad i = 1, \ldots, N, \tag{2.4}$$

and

$$x_{P_{N+i}} = \varrho_2 \cos \frac{2(i-1)\pi}{N}, \quad y_{P_{N+i}} = \varrho_2 \sin \frac{2(i-1)\pi}{N}, \quad i = 1, \ldots, N. \tag{2.5}$$

If $Q_j = (x_{Q_j}, y_{Q_j})$, then

$$x_{Q_j} = R_1 \cos \frac{2(j-1+\alpha)\pi}{N}, \quad y_{Q_j} = R_1 \sin \frac{2(j-1+\alpha)\pi}{N}, \quad j = 1, \ldots, N, \tag{2.6}$$

and

$$x_{Q_{N+j}} = R_2 \cos \frac{2(j-1+\alpha)\pi}{N}, \quad y_{Q_{N+j}} = R_2 \sin \frac{2(j-1+\alpha)\pi}{N}, \quad j = 1, \ldots, N. \tag{2.7}$$

The presence of the angular parameter $\alpha \in [0, 1)$ indicates that the sources are rotated by an angle $2\pi\alpha/N$ from the boundary points (see [67]). In the MFS with boundary collocation, the coefficients $\boldsymbol{c}$ are determined so that the boundary condition is satisfied at the boundary points $\{P_i\}_{i=1}^{2N}$:

$$u_N(\boldsymbol{c}, \boldsymbol{Q}; P_i) = f_1(P_i), \quad u_N(\boldsymbol{c}, \boldsymbol{Q}; P_{N+i}) = f_2(P_{N+i}), \quad i = 1, \ldots, N.$$

This yields a linear system of the form

$$\left(\begin{array}{c|c} A_{11} & A_{12} \\ \hline A_{21} & A_{22} \end{array}\right) \left(\begin{array}{c} \boldsymbol{d_1} \\ \hline \boldsymbol{d_2} \end{array}\right) = \left(\begin{array}{c} \boldsymbol{f_1} \\ \hline \boldsymbol{f_2} \end{array}\right), \tag{2.8}$$

where

$$\begin{aligned} \boldsymbol{f_1} &= (f_1(P_1), f_1(P_2), \ldots, f_1(P_N))^T, & \boldsymbol{f_2} &= (f_2(P_{N+1}), f_2(P_{N+2}), \ldots, f_2(P_{2N}))^T, \\ \boldsymbol{d_1} &= (c_1, c_2, \ldots, c_N)^T, & \boldsymbol{d_2} &= (c_{N+1}, c_{N+2}, \ldots, c_{2N})^T. \end{aligned}$$

The elements of the $N \times N$ submatrices A_{11}, A_{12}, A_{21} and A_{22} are given by

$$\begin{aligned} (A_{11})_{i,j} &= -\frac{1}{2\pi} \log |P_i - Q_j|, & (A_{12})_{i,j} &= -\frac{1}{2\pi} \log |P_i - Q_{N+j}|, \\ (A_{21})_{i,j} &= -\frac{1}{2\pi} \log |P_{N+i} - Q_j|, & (A_{22})_{i,j} &= -\frac{1}{2\pi} \log |P_{N+i} - Q_{N+j}|, \end{aligned}$$

respectively, for $i, j = 1, \ldots, N$. The matrices A_{11}, A_{12}, A_{21} and A_{22} are circulant. An extensive account of the properties of circulant matrices can be found in [15]. Details on the MFS and its applications can be found in the survey articles [18, 19, 25]. The convergence of the MFS for harmonic problems in the disk subject to Dirichlet boundary conditions has been studied in [42, 43, 68]. The convergence of a modified MFS for annular domains was studied by Katsurada [42] using Green's functions instead of the usual fundamental solutions, and considering two different circular problems. Our approach is different as it uses the standard fundamental solutions directly in the annulus and is based on the study of the eigenvalues of the coefficient matrix.

The chapter is structured as follows: In Section 2.2, we formulate the matrix decomposition algorithm for the solution of the linear system (2.8). In Section 3, we develop the properties of the eigenvalues of the coefficient matrix and study its invertibility. We also provide an explicit expression for the MFS approximation. The convergence of the method for analytic boundary data is proved in Section 4. Numerical experiments which enable us to confirm the theoretical predictions are given in Section 5. Finally, some conclusions are presented in Section 6.

2.2 Matrix decomposition algorithm

In order to develop a matrix decomposition algorithm, we need the following fact [15]. If a matrix A is circulant, written as $A = \text{circ}(a_1, \ldots, a_N)$, then it can be diagonalized as $A = U^* D U$, where U is the unitary $N \times N$ Fourier matrix with conjugate

$$U^* = \frac{1}{N^{1/2}} \begin{pmatrix} 1 & 1 & 1 & \cdots & 1 \\ 1 & \omega & \omega^2 & \cdots & \omega^{N-1} \\ 1 & \omega^2 & \omega^4 & \cdots & \omega^{2(N-1)} \\ \vdots & \vdots & \vdots & & \vdots \\ 1 & \omega^{N-1} & \omega^{2(N-1)} & \cdots & \omega^{(N-1)(N-1)} \end{pmatrix},$$

where $\omega = \mathrm{e}^{2\pi \mathrm{i}/N}$, $\mathrm{i} = \sqrt{-1}$, $D = \text{diag}(\lambda_1, \ldots, \lambda_N)$, and

$$\lambda_j = \sum_{k=1}^{N} a_k \, \omega^{(k-1)(j-1)}, \quad j = 1, \ldots, N, \tag{2.9}$$

are the eigenvalues of A. The orthogonal eigenvector corresponding to λ_j is

$$\boldsymbol{\xi}_j = \frac{1}{N^{1/2}} \left(1, \omega^{(j-1)}, \ldots, \omega^{(N-1)(j-1)}\right)^T.$$

Let $\langle \boldsymbol{z}, \boldsymbol{w} \rangle = \sum_{k=1}^{N} z_k \bar{w}_k$ be the inner product of $\boldsymbol{z}$, $\boldsymbol{w} \in \mathbb{C}^N$. Since $\{\boldsymbol{\xi}_j\}_{j=1,\ldots,N}$ forms an orthonormal basis of $\mathbb{C}^N$, any vector $\boldsymbol{v} \in \mathbb{C}^N$ can be expressed as $\boldsymbol{v} = \sum_{k=1}^{N} \langle \boldsymbol{v}, \boldsymbol{\xi}_k \rangle \boldsymbol{\xi}_k$ and hence $A\boldsymbol{v} = \sum_{k=1}^{N} d_k \langle \boldsymbol{v}, \boldsymbol{\xi}_k \rangle \boldsymbol{\xi}_k$. When A is nonsingular

$$A^{-1}\boldsymbol{v} = \sum_{k=1}^{N} \frac{1}{d_k} \langle \boldsymbol{v}, \boldsymbol{\xi}_k \rangle \boldsymbol{\xi}_k. \tag{2.10}$$

The system (2.8) can therefore be written as

$$\left(\begin{array}{c|c} U & 0 \\ \hline 0 & U \end{array}\right) \left(\begin{array}{c|c} A_{11} & A_{12} \\ \hline A_{21} & A_{22} \end{array}\right) \left(\begin{array}{c|c} U^* & 0 \\ \hline 0 & U^* \end{array}\right) \left(\begin{array}{c|c} U & 0 \\ \hline 0 & U \end{array}\right) \left(\begin{array}{c} \boldsymbol{d_1} \\ \hline \boldsymbol{d_2} \end{array}\right) = \left(\begin{array}{c|c} U & 0 \\ \hline 0 & U \end{array}\right) \left(\begin{array}{c} \boldsymbol{f_1} \\ \hline \boldsymbol{f_2} \end{array}\right) \tag{2.11}$$

or

$$\left(\begin{array}{c|c} UA_{11}U^* & UA_{12}U^* \\ \hline UA_{21}U^* & UA_{22}U^* \end{array}\right) \left(\begin{array}{c} U\boldsymbol{d_1} \\ \hline U\boldsymbol{d_2} \end{array}\right) = \left(\begin{array}{c} U\boldsymbol{f_1} \\ \hline U\boldsymbol{f_2} \end{array}\right) \tag{2.12}$$

or

$$\left(\begin{array}{c|c} D_{11} & D_{12} \\ \hline D_{21} & D_{22} \end{array}\right) \left(\begin{array}{c} \hat{\boldsymbol{d}}_{\boldsymbol{1}} \\ \hline \hat{\boldsymbol{d}}_{\boldsymbol{2}} \end{array}\right) = \left(\begin{array}{c} \hat{\boldsymbol{f}}_{\boldsymbol{1}} \\ \hline \hat{\boldsymbol{f}}_{\boldsymbol{2}} \end{array}\right), \tag{2.13}$$

where

$$\hat{\boldsymbol{d}}_{\boldsymbol{1}} = U\boldsymbol{d_1}, \quad \hat{\boldsymbol{d}}_{\boldsymbol{2}} = U\boldsymbol{d_2}, \quad \hat{\boldsymbol{f}}_{\boldsymbol{1}} = U\boldsymbol{f_1}, \quad \hat{\boldsymbol{f}}_{\boldsymbol{2}} = U\boldsymbol{f_2},$$

and

$$D_{ij} = \mathrm{diag}(\lambda_1^{ij}, \ldots, \lambda_N^{ij}), \qquad i, j = 1, 2$$

is the diagonal matrix whose diagonal elements are the eigenvalues of the submatrix A_{ij}, $i, j = 1, 2$. The solution of system (2.13) can thus be reduced to the solution of the N independent 2×2 systems

$$\left(\begin{array}{c|c} \lambda_k^{11} & \lambda_k^{12} \\ \hline \lambda_k^{21} & \lambda_k^{22} \end{array}\right) \left(\begin{array}{c} \hat{d}_k^1 \\ \hline \hat{d}_k^2 \end{array}\right) = \left(\begin{array}{c} \hat{f}_k^1 \\ \hline \hat{f}_k^2 \end{array}\right), \quad k = 1, 2, \cdots N,$$

from which it follows that

$$\hat{d}_k^1 = \frac{\lambda_k^{22} \hat{f}_k^1 - \lambda_k^{12} \hat{f}_k^2}{\lambda_k^{11}\lambda_k^{22} - \lambda_k^{12}\lambda_k^{21}}, \quad \hat{d}_k^2 = \frac{-\lambda_k^{21} \hat{f}_k^1 + \lambda_k^{11} \hat{f}_k^2}{\lambda_k^{11}\lambda_k^{22} - \lambda_k^{12}\lambda_k^{21}} \quad k = 1, \cdots, N.$$

Having obtained $\hat{\boldsymbol{d}}_{\boldsymbol{1}}$ and $\hat{\boldsymbol{d}}_{\boldsymbol{2}}$, we can determine $\boldsymbol{d_1}$ and $\boldsymbol{d_2}$ (and hence $\boldsymbol{c}$) from

$$\boldsymbol{d_1} = U^* \hat{\boldsymbol{d}}_{\boldsymbol{1}}, \quad \boldsymbol{d_2} = U^* \hat{\boldsymbol{d}}_{\boldsymbol{2}}. \tag{2.14}$$

We thus have the following matrix decomposition algorithm for solving (2.8):

Algorithm

Step 1. `Compute` $\hat{\boldsymbol{f}}_{\mathbf{1}} = U\boldsymbol{f}_{\mathbf{1}}$ `and` $\hat{\boldsymbol{f}}_{\mathbf{2}} = U\boldsymbol{f}_{\mathbf{2}}$.

Step 2. `Construct the diagonal matrices` D_{ij}, $i, j = 1, 2$.

Step 3. `Evaluate` $\hat{\boldsymbol{d}}_{\mathbf{1}}$ `and` $\hat{\boldsymbol{d}}_{\mathbf{2}}$.

Step 4. `Compute` $\boldsymbol{d}_{\mathbf{1}} = U^*\hat{\boldsymbol{d}}_{\mathbf{1}}, \quad \boldsymbol{d}_{\mathbf{2}} = U^*\hat{\boldsymbol{d}}_{\mathbf{2}}$.

Remarks

(i) In ***Step* 1** and ***Step* 4**, because of the form of the matrices U and U^*, the operations can be carried out via Fast Fourier Transforms (FFTs) at a cost of $O(N \log N)$ operations.

(ii) FFTs can also be used for the evaluation of the diagonal matrices in ***Step* 2**.

(iii) The same algorithm is also applicable when, instead of the boundary conditions of (2.1), we have

$$u = f_1 \quad \text{on} \quad \partial\Omega_1, \qquad \frac{\partial u}{\partial n} = g_2 \quad \text{on} \quad \partial\Omega_2\,,$$

or

$$\frac{\partial u}{\partial n} = g_1 \quad \text{on} \quad \partial\Omega_1, \qquad u = f_2 \quad \text{on} \quad \partial\Omega_2.$$

2.3 Properties of the eigenvalues

Since our aim is to solve (2.8), we investigate the properties of the eigenvalues of the matrix

$$G = \left(\begin{array}{c|c} A_{11} & A_{12} \\ \hline A_{21} & A_{22} \end{array} \right).$$

In particular, we are interested in the cases where these eigenvalues vanish. We first consider the eigenvalues of the submatrices A_{11}, A_{12}, A_{21}, A_{22}. In the following, we denote by A each of the matrices A_{ij}, $i, j = 1, 2$, and by λ_k each of the eigenvalues λ_k^{ij}, $i, j = 1, 2$. Thus we shall denote by $(a_1, \ldots, a_N)$ the vector $(a_1^{ij}, \ldots, a_N^{ij})$, which generates the circulant matrix A_{ij},

$i, j = 1, 2$. Since each of the A_{ij}'s involves the distances between points on two concentric circles, we shall denote the radii of these circles by R and ϱ.

We divide these eigenvalues into three groups:

(i) the 'first' eigenvalue λ_1;

(ii) when N is even, the eigenvalue $\lambda_{N/2+1}$;

(iii) the remaining eigenvalues.

2.3.1 The first eigenvalue

An exact expression for the first eigenvalue is given in the following theorem.

Theorem 2.3.1. *The eigenvalue* λ_1 *is given by*

$$\lambda_1 = -\frac{1}{4\pi} \log\left(R^{2N} - 2R^N \varrho^N \cos(2\pi\alpha) + \varrho^{2N}\right). \tag{2.15}$$

PROOF. Since A is circulant, from (2.9), we have

$$\lambda_1 = \sum_{k=1}^{N} a_k. \tag{2.16}$$

Since

$$a_k = -\frac{1}{4\pi} \log\left(R^2 - 2R\varrho\cos\left(\frac{2\pi(k+\alpha-1)}{N}\right) + \varrho^2\right), \tag{2.17}$$

it follows that

$$\lambda_1 = -\frac{1}{4\pi} \log\left\{\prod_{k=1}^{N}\left(R^2 - 2R\varrho\cos\left(\frac{2\pi(k+\alpha-1)}{N}\right) + \varrho^2\right)\right\}.$$

From the identity [29, p. 40]

$$\prod_{k=0}^{n-1}\left\{x^2 - 2xy\cos\left(\alpha + \frac{2k\pi}{n}\right) + y^2\right\} = x^{2n} - 2x^n y^n \cos n\alpha + y^{2n}, \tag{2.18}$$

(2.15) follows. □

We have the following corollary:

Corollary 2.3.2. *For* $\alpha = 0$, $\lambda_1 \neq 0$ (*i.e., the matrix* A *is nonsingular*) *if and only if* $R^N - \varrho^N \neq 1$. □

2.3.2 The eigenvalue $\lambda_{N/2+1}$ when N is even

We next investigate the behaviour of the eigenvalue $\lambda_{N/2+1}$ in the case N is even. We have the exact expression:

Proposition 2.3.3. *If N is even, then*

$$\lambda_{N/2+1} \;=\; -\frac{1}{4\pi}\log\frac{R^N - 2R^{N/2}\varrho^{N/2}\cos\alpha\pi + \varrho^N}{R^N - 2R^{N/2}\varrho^{N/2}\cos(\alpha{+}1)\pi + \varrho^N}\;. \tag{2.19}$$

Proof. From (2.9), we have

$$\begin{aligned}
\lambda_{N/2+1} \;&=\; -\frac{1}{4\pi}\sum_{k=1}^{N}(-1)^{k-1}\log\left(R^2 - 2R\varrho\cos\frac{2\pi(k+\alpha-1)}{N} + \varrho^2\right)\\
&=\; -\frac{1}{4\pi}\sum_{n=1}^{N/2}\log\left(R^2 - 2R\varrho\cos\left(2\pi\frac{n-1}{M} + \frac{\alpha\pi}{M}\right) + \varrho^2\right)\\
&\quad\; +\frac{1}{4\pi}\sum_{n=1}^{N/2}\log\left(R^2 - 2R\varrho\cos\left(2\pi\frac{n-1}{M} + \frac{(\alpha+1)\pi}{M}\right) + \varrho^2\right).
\end{aligned}$$

From (2.18) we obtain

$$\begin{aligned}
\lambda_{N/2+1} =& -\frac{1}{4\pi}\log\left(R^{2M} - 2R^M\varrho^M\cos\alpha\pi + \varrho^{2M}\right)\\
&+\frac{1}{4\pi}\log\left(R^{2M} - 2R^M\varrho^M\cos(\alpha+1)\pi + \varrho^{2M}\right)\\
=& -\frac{1}{4\pi}\log\frac{R^N - 2R^{N/2}\varrho^{N/2}\cos\alpha\pi + \varrho^N}{R^N - 2R^{N/2}\varrho^{N/2}\cos(\alpha{+}1)\pi + \varrho^N}\;.
\end{aligned}$$

□

A direct application of this proposition yields the following corollary:

Corollary 2.3.4. *For N even, the eigenvalue $\lambda_{N/2+1} = 0$ if and only if $\alpha = \frac{1}{2}$.*

Proof. Taking $\alpha = \frac{1}{2}$ in (2.19) yields that $\lambda_{N/2+1} = 0$. For $\alpha \in [0, \frac{1}{2})$, it is clear that $\cos\alpha\pi > 0$ whereas $\cos(\alpha+1)\pi < 0$, and (2.19) yields that in this case $\lambda_{N/2+1} \neq 0$. □

2.3.3 The eigenvalues λ_j, $j \neq 1, N/2+1$, when N is even

In this case we have the expression:

Proposition 2.3.5. *For* $\alpha \in [0, \frac{1}{2}]$ *and* $j \neq 1$, *we have*

$$\lambda_j = \frac{N}{4\pi} \sum_{m \geq 0} \left\{ \frac{e^{-\mathrm{i}\frac{2\pi}{N}(mN+j-1)\alpha} \varrho^{mN+j-1}}{(mN+j-1)R^{mN+j-1}} + \frac{e^{\mathrm{i}\frac{2\pi}{N}((m+1)N-j+1)\alpha} \varrho^{(m+1)N-j+1}}{((m+1)N-j+1)R^{(m+1)N-j+1}} \right\}. \tag{2.20}$$

In particular when N *is even*

$$\lambda_{N/2+1} = \frac{N}{2\pi} \sum_{m \geq 0} \frac{\cos\big((2m+1)\alpha\pi\big) \varrho^{mN+N/2}}{(mN+N/2)\, R^{mN+N/2}}. \tag{2.21}$$

Proof. We define the function

$$F(R, \varrho, \vartheta) \;=\; -\frac{1}{4\pi} \log(R^2 - 2R\varrho\cos\vartheta + \varrho^2).$$

From [29, p. 52], we have that

$$F(R, \varrho, \vartheta) = -\frac{1}{2\pi} \log R + \frac{1}{2\pi} \sum_{n \geq 1} \frac{\varrho^n \cos n\vartheta}{nR^n},$$

where $R > \varrho$. This is true in the cases where $R = R_2, \varrho = \varrho_1$ and $R = R_2, \varrho = \varrho_2$. When $R < \varrho$, i.e., when $R = R_1, \varrho = \varrho_1$ and $R = R_1, \varrho = \varrho_2$, in a similar way, we have

$$F(\varrho, R, \vartheta) \;=\; -\frac{1}{4\pi} \log(R^2 - 2R\varrho\cos\vartheta + \varrho^2) \;=\; -\frac{1}{2\pi} \log\varrho + \frac{1}{2\pi} \sum_{n \geq 1} \frac{R^n \cos n\vartheta}{n\varrho^n}.$$

Then, from (2.9), for $j = 2, \ldots, N$,

$$\begin{aligned}
\lambda_j \;&=\; \sum_{k=1}^{N} \mathrm{e}^{\mathrm{i}\frac{2\pi}{N}(j-1)(k-1)} F\left(R, \varrho, \frac{2\pi}{N}(k-1+\alpha)\right) \\
&=\; \frac{1}{2\pi} \sum_{k=1}^{N} \cos\left(\frac{2\pi}{N}(j-1)(k-1)\right) \left\{ \sum_{n \geq 1} \frac{\varrho^n \cos\left(\frac{2\pi}{N} n(k-1+\alpha)\right)}{nR^n} \right\} \\
&\quad + \mathrm{i}\frac{1}{2\pi} \sum_{k=1}^{N} \sin\left(\frac{2\pi}{N}(j-1)(k-1)\right) \left\{ \sum_{n \geq 1} \frac{\varrho^n \cos\left(\frac{2\pi}{N} n(k-1+\alpha)\right)}{nR^n} \right\} \\
&=\; \frac{1}{2\pi} \sum_{n \geq 1} \frac{\varrho^n}{nR^n} \left\{ \sum_{k=1}^{N} \cos\left(\frac{2\pi}{N}(j-1)(k-1)\right) \cos\left(\frac{2\pi}{N} n(k-1+\alpha)\right) \right\} \\
&\quad + \mathrm{i}\frac{1}{2\pi} \sum_{n \geq 1} \frac{\varrho^n}{nR^n} \left\{ \sum_{k=1}^{N} \sin\left(\frac{2\pi}{N}(j-1)(k-1)\right) \cos\left(\frac{2\pi}{N} n(k-1+\alpha)\right) \right\}.
\end{aligned} \tag{2.22}$$

For the first sum, we have from [68],

$$\sum_{k=1}^{N}\cos\left(\frac{2\pi}{N}k(j-1)\right)\cos\left(\frac{2\pi}{N}n(k-1+\alpha)\right)=\frac{1}{2}\cos\left(\frac{2\pi}{N}n\alpha\right)\left\{C_{n-j+1}^{N}+C_{n+j-1}^{N}\right\}, \quad (2.23)$$

$$\sum_{k=1}^{N}\sin\left(\frac{2\pi}{N}k(j-1)\right)\cos\left(\frac{2\pi}{N}n(k-1+\alpha)\right)=\frac{1}{2}\sin\left(\frac{2\pi}{N}n\alpha\right)\left\{C_{n-j+1}^{N}-C_{n+j-1}^{N}\right\}, \quad (2.24)$$

where

$$C_{\kappa}^{N} \;=\; \sum_{j=1}^{N}\cos\left(\frac{2\pi}{N}\kappa j\right) \;=\; \begin{cases} N & \text{if} \quad \kappa = 0\,(\mathrm{mod}\,N), \\ 0 & \text{if} \quad \kappa \neq 0\,(\mathrm{mod}\,N.) \end{cases} \quad (2.25)$$

Combining (2.22), (2.23) and (2.24), we obtain

$$\begin{aligned}\lambda_j &= \frac{1}{4\pi}\sum_{n\geq 1}\frac{\varrho^n\cos\left(\frac{2\pi}{N}n\alpha\right)}{nR^n}\left\{C_{n-j+1}^{N}+C_{n+j-1}^{N}\right\}-\frac{\mathrm{i}}{4\pi}\sum_{n\geq 1}\frac{\varrho^n\sin\left(\frac{2\pi}{N}n\alpha\right)}{nR^n}\left\{C_{n-j+1}^{N}-C_{n+j-1}^{N}\right\}\\ &= \frac{N}{4\pi}\sum_{m\geq 0}\left\{\frac{\varrho^{mN+j-1}\mathrm{e}^{-\mathrm{i}\frac{2\pi}{N}(mN+j-1)\alpha}}{(mN+j-1)R^{mN+j-1}}+\frac{\mathrm{e}^{\mathrm{i}\frac{2\pi}{N}(mN+N-j+1)\alpha}\varrho^{mN+N-j+1}}{(mN+N-j+1)R^{mN+N-j+1}}\right\}\end{aligned}$$

which proves (2.20). Formula (2.21) is an immediate consequence of (2.20). □

We also have the following two corollaries when $\alpha = 0$:

Corollary 2.3.6. *For $\alpha = 0$ and $j \neq 1$, we have*

$$\lambda_j \;=\; \frac{N}{4\pi}\sum_{m\geq 0}\left(\frac{1}{j-1+mN}\cdot\frac{\varrho^{j-1+mN}}{R^{j-1+mN}}+\frac{1}{N-j+1+mN}\cdot\frac{\varrho^{N-j+1+mN}}{R^{N-j+1+mN}}\right). \quad (2.26)$$

In particular, for N even and $j = N/2+1$,

$$\lambda_{N/2+1} \;=\; \frac{N}{2\pi}\sum_{m\geq 0}\frac{1}{N/2+mN}\cdot\frac{\varrho^{N/2+mN}}{R^{N/2+mN}}. \quad (2.27)$$

Also, for $j = [N/2]+1,\ldots,N$, we have $\lambda_j = \lambda_{N-j+2}$.

Since, the λ_j are sums of positive numbers, we have:

Corollary 2.3.7. *For $\alpha = 0$ and $j = 2,\ldots,N$, we have $\lambda_j > 0$.* □

2.3.4 Invertibility of the matrix G

Since

$$G \;=\; \left(\begin{array}{c|c} A_{11} & A_{12} \\ \hline A_{21} & A_{22} \end{array}\right) \;=\; \left(\begin{array}{c|c} U^* & 0 \\ \hline 0 & U^* \end{array}\right)\left(\begin{array}{c|c} D_{11} & D_{12} \\ \hline D_{21} & D_{22} \end{array}\right)\left(\begin{array}{c|c} U & 0 \\ \hline 0 & U \end{array}\right),$$

it is sufficient to examine the matrix $D = \left(\begin{array}{c|c} D_{11} & D_{12} \\ \hline D_{21} & D_{22} \end{array}\right)$. The following lemma can be easily proved.

Lemma 2.3.8. *If* $\det D$ *denotes the determinant of* D*, then*

$$\det D = \det \left(\begin{array}{ccccc|ccccc}
\lambda_1^{11} & 0 & 0 & \cdots & 0 & \lambda_1^{12} & 0 & 0 & \cdots & 0 \\
0 & \lambda_2^{11} & 0 & \cdots & 0 & 0 & \lambda_2^{12} & 0 & \cdots & 0 \\
0 & 0 & \lambda_3^{11} & \cdots & 0 & 0 & 0 & \lambda_3^{12} & \cdots & 0 \\
\vdots & \vdots & \vdots & & \vdots & \vdots & \vdots & \vdots & & \vdots \\
0 & 0 & 0 & \cdots & \lambda_N^{11} & 0 & 0 & 0 & \cdots & \lambda_N^{12} \\
\hline
\lambda_1^{21} & 0 & 0 & \cdots & 0 & \lambda_1^{22} & 0 & 0 & \cdots & 0 \\
0 & \lambda_2^{21} & 0 & \cdots & 0 & 0 & \lambda_2^{22} & 0 & \cdots & 0 \\
0 & 0 & \lambda_3^{21} & \cdots & 0 & 0 & 0 & \lambda_3^{22} & \cdots & 0 \\
\vdots & \vdots & \vdots & & \vdots & \vdots & \vdots & \vdots & & \vdots \\
0 & 0 & 0 & \cdots & \lambda_N^{21} & 0 & 0 & 0 & \cdots & \lambda_N^{22}
\end{array}\right) = \prod_{k=1}^{N} (\lambda_k^{11}\lambda_k^{22} - \lambda_k^{12}\lambda_k^{21}).$$

Therefore, the matrix D *is nonsingular if and only if*

$$\lambda_k^{11}\lambda_k^{22} - \lambda_k^{12}\lambda_k^{21} \neq 0, \quad k = 1, \ldots, N. \qquad \square$$

When $\alpha = 0$ we have the following proposition.

Proposition 2.3.9. *For* $\alpha = 0$*, the matrix* G *is singular if and only if*

$$\lambda_1^{11}\lambda_1^{22} - \lambda_1^{12}\lambda_1^{21} = 0.$$

PROOF. Let

$$F_{N,j}(\omega) = \frac{N}{4\pi} \sum_{m \geq 0} \left(\frac{\omega^{j-1+mN}}{j-1+mN} + \frac{\omega^{N-j+1+mN}}{N-j+1+mN} \right).$$

Clearly $F_{N,j}(\omega)$, $\omega \in (0, 1)$, is positive and strictly increasing. For $j \neq 1$, we have (see Corollary 2.3.6)

$$\lambda_j^{11} = F_{N,j}(R_1/\varrho_1), \ \lambda_j^{12} = F_{N,j}(\varrho_1/R_2), \ \lambda_j^{21} = F_{N,j}(R_1/\varrho_2) \ \text{and} \ \lambda_j^{22} = F_{N,j}(\varrho_2/R_2).$$

Since $R_1 < \varrho_1 < \varrho_2 < R_2$, we have

$$0 < \frac{R_1}{\varrho_2} < \frac{R_1}{\varrho_1}, \quad \text{so that} \quad \lambda_j^{21} < \lambda_j^{11},$$

and

$$0 < \frac{\varrho_1}{R_2} < \frac{\varrho_2}{R_2}, \quad \text{so that} \quad \lambda_j^{12} < \lambda_j^{22}.$$

Thus,

$$\lambda_k^{11}\lambda_k^{22} - \lambda_k^{12}\lambda_k^{21} > 0, \qquad k = 2, 3, \ldots, N.$$

Therefore, the only case in which G can be singular is when $\lambda_1^{11}\lambda_1^{22} - \lambda_1^{12}\lambda_1^{21} = 0$. □

2.3.5 The approximate solution in terms of eigenvalues and eigenvectors.

Denoting the approximation $u_N(\boldsymbol{c}, \boldsymbol{Q}; P)$ in (2.3) by $u_N(P)$, we have

$$u_N(P) \ = \sum_{k=1}^{N} d_k^1 \log|P - Q_k| + \sum_{k=1}^{N} d_k^2 \log|P - Q_{N+k}| \ = \langle \boldsymbol{d}_1, \boldsymbol{l_1} \rangle + \langle \boldsymbol{d}_2, \boldsymbol{l_2} \rangle, \tag{2.28}$$

where

$$\boldsymbol{l}_1 = (\log|P - Q_1|, \ldots, \log|P - Q_N|)^T, \ \boldsymbol{l}_2 = (\log|P - Q_{N+1}|, \ldots, \log|P - Q_{2N}|)^T$$

and $\boldsymbol{d}_1$, $\boldsymbol{d}_2$ satisfy (2.8). Thus

$$\begin{aligned} \boldsymbol{d}_1 &= \left(A_{12}^{-1}A_{11} - A_{22}^{-1}A_{21}\right)^{-1}\left(A_{12}^{-1}\boldsymbol{f_1} - A_{22}^{-1}\boldsymbol{f_2}\right), \\ \boldsymbol{d}_2 &= \left(A_{11}^{-1}A_{12} - A_{21}^{-1}A_{22}\right)^{-1}\left(A_{11}^{-1}\boldsymbol{f_1} - A_{21}^{-1}\boldsymbol{f_2}\right), \end{aligned}$$

so that

$$\begin{aligned} \langle \boldsymbol{d}_2, \boldsymbol{l_2} \rangle &= \left\langle \left(A_{11}^{-1}A_{12} - A_{21}^{-1}A_{22}\right)^{-1}\left(A_{11}^{-1}\sum_{k=1}^{N}\langle \boldsymbol{f_1}, \boldsymbol{\xi_k}\rangle\boldsymbol{\xi_k} - A_{21}^{-1}\sum_{k=1}^{N}\langle \boldsymbol{f_2}, \boldsymbol{\xi_k}\rangle\boldsymbol{\xi_k}\right), \boldsymbol{l}_2 \right\rangle \\ &= \sum_{k=1}^{N}\frac{\lambda_k^{11}}{\Delta_k}\langle \boldsymbol{f_2}, \boldsymbol{\xi}_k\rangle\overline{\langle \boldsymbol{l_2}, \boldsymbol{\xi}_k\rangle} - \sum_{k=1}^{N}\frac{\lambda_k^{21}}{\Delta_k}\langle \boldsymbol{f_1}, \boldsymbol{\xi}_k\rangle\overline{\langle \boldsymbol{l_2}, \boldsymbol{\xi}_k\rangle} \end{aligned}$$

where $\Delta_k = \lambda_k^{11}\lambda_k^{22} - \lambda_k^{12}\lambda_k^{21}$, assuming that all matrix inverses indicated exist. Analogously,

$$\langle \boldsymbol{d}_1, \boldsymbol{l_1} \rangle = \sum_{k=1}^{N}\frac{\lambda_k^{22}}{\Delta_k}\langle \boldsymbol{f_1}, \boldsymbol{\xi}_k\rangle\overline{\langle \boldsymbol{l_1}, \boldsymbol{\xi}_k\rangle} - \sum_{k=1}^{N}\frac{\lambda_k^{12}}{\Delta_k}\langle \boldsymbol{f_2}, \boldsymbol{\xi}_k\rangle\overline{\langle \boldsymbol{l_1}, \boldsymbol{\xi}_k\rangle}.$$

Therefore, we obtain the explicit expression for the MFS approximation,

$$\begin{aligned} u_N(P) = &\sum_{k=1}^{N}\frac{\lambda_k^{11}}{\Delta_k}\langle \boldsymbol{f_2}, \boldsymbol{\xi}_k\rangle\overline{\langle \boldsymbol{l_2}, \boldsymbol{\xi}_k\rangle} - \sum_{k=1}^{N}\frac{\lambda_k^{21}}{\Delta_k}\langle \boldsymbol{f_1}, \boldsymbol{\xi}_k\rangle\overline{\langle \boldsymbol{l_2}, \boldsymbol{\xi}_k\rangle} \\ &- \sum_{k=1}^{N}\frac{\lambda_k^{12}}{\Delta_k}\langle \boldsymbol{f_2}, \boldsymbol{\xi}_k\rangle\overline{\langle \boldsymbol{l_1}, \boldsymbol{\xi}_k\rangle} + \sum_{k=1}^{N}\frac{\lambda_k^{22}}{\Delta_k}\langle \boldsymbol{f_1}, \boldsymbol{\xi}_k\rangle\overline{\langle \boldsymbol{l_1}, \boldsymbol{\xi}_k\rangle}. \end{aligned} \tag{2.29}$$

Note that the evaluation of the approximate solution via equation (2.29) is equivalent to applying the matrix decomposition algorithm described in Section 2.2. This form is useful for the derivation of the theoretical results which follow.

2.4 Convergence of the MFS for analytic boundary data

In this section, we show that the MFS approximation u_N converges exponentially with respect to N to the exact solution u of (2.1) in the $\|\cdot\|_\infty$−norm, provided the boundary data f_1, f_2 are analytic, or, equivalently, u can be extended as a harmonic function in an open region V containing the annulus.

The analyticity of the boundary data yields that there exists a constant $\beta > 0$, such that

$$\overline{\Omega}_\beta \;=\; \left\{ \boldsymbol{x} \in \mathbb{R}^2 \mid \varrho_1 - \beta \le |\boldsymbol{x}| \le \varrho_2 + \beta \right\} \,\subset\, V. \tag{2.30}$$

The analytic solution u, expressed in polar coordinates, is of the form [72]

$$u(r,\vartheta) \;=\; \sum_{k\in\mathbb{Z}} \zeta_k\, r^k\, \mathrm{e}^{\mathrm{i}k\vartheta} + \sum_{k\in\mathbb{Z}\smallsetminus\{0\}} \eta_k\, r^k\, \mathrm{e}^{-\mathrm{i}k\vartheta} + \eta_0\, \log r. \tag{2.31}$$

Thus (2.31) implies that the boundary data can be expressed as

$$f_j(\vartheta) \;=\; \sum_{k\in\mathbb{Z}} \zeta_k\, \varrho_j^k\, \mathrm{e}^{\mathrm{i}k\vartheta} + \sum_{k\in\mathbb{Z}\smallsetminus\{0\}} \eta_k\, \varrho_j^k\, \mathrm{e}^{-\mathrm{i}k\vartheta} + \eta_0\, \log \varrho_j, \quad j = 1, 2.$$

The analyticity assumption also implies that there exists a positive constant M_β such that

$$|\zeta_k|,\, |\eta_k| \;\le\; M_\beta\, (\varrho_2 + \beta)^{-k} \;\text{ for } k \ge 0, \tag{2.32}$$

$$|\zeta_k|,\, |\eta_k| \;\le\; M_\beta\, (\varrho_1 - \beta)^{k} \;\text{ for }\; k < 0. \tag{2.33}$$

For simplicity, we prove the convergence of the MFS approximation to the exact solution in the case when $\alpha = 0$. The proof for $\alpha \ne 0$ is analogous but much more tedious.

2.4.1 The discrete Fourier interpolant

We assume that N is even. (The case when N is odd can be treated analogously.) We define the *discrete Fourier interpolant* $\tilde{u}_N$ (which interpolates the boundary data), to be

$$\tilde{u}_N(r,\vartheta) \;=\; \sum_{k=-N/2+1}^{N/2} \mu_k\, r^k\, \mathrm{e}^{\mathrm{i}k\vartheta} + \sum_{\substack{k=-N/2+1\\ k\ne 0}}^{N/2} \nu_k\, r^{-k}\, \mathrm{e}^{\mathrm{i}k\vartheta} + \nu_0 \log r. \tag{2.34}$$

We also define

$$f_{1,N}(\vartheta) = \tilde{u}_N(\varrho_1, \vartheta), \quad f_{2,N}(\vartheta) = \tilde{u}_N(\varrho_2, \vartheta).$$

The coefficients $\mu_k, \nu_k \in \mathbb{C}$, $k = -N/2+1, \ldots, N/2$, are chosen so that $\tilde{u}_N$ agrees with the boundary data f_1, f_2 at the points $\varrho_1 \,\mathrm{e}^{\mathrm{i}\vartheta_j}$, $\varrho_2 \,\mathrm{e}^{\mathrm{i}\vartheta_j}$, where $\vartheta_j = 2\pi(j-1)/N$ $j = 1, \ldots, N$. Thus for $k = -N/2+1, \ldots, N/2$ with $k \neq 0$, by equating the coefficients of $\mathrm{e}^{\mathrm{i}k\vartheta}$, the μ_k, ν_k satisfy

$$\mu_k \varrho_1^k + \nu_k \varrho_1^{-k} = \sum_{m\in\mathbb{Z}} \left(\zeta_{k+mN} \varrho_1^{k+mN} + \eta_{-k-mN} \varrho_1^{-k-mN} \right),$$

$$\mu_k \varrho_2^k + \nu_k \varrho_2^{-k} = \sum_{m\in\mathbb{Z}} \left(\zeta_{k+mN} \varrho_2^{k+mN} + \eta_{-k-mN} \varrho_2^{-k-mN} \right),$$

from which it follows that, with $\delta_k = \varrho_1^k \varrho_2^{-k} - \varrho_1^{-k} \varrho_2^k$,

$$\mu_k = \frac{\varrho_2^{-k} \sum_{m\in\mathbb{Z}} \left(\zeta_{k+mN} \varrho_1^{k+mN} + \eta_{-k-mN} \varrho_1^{-k-mN} \right)}{\delta_k} - \frac{\varrho_1^{-k} \sum_{m\in\mathbb{Z}} \left(\zeta_{k+mN} \varrho_2^{k+mN} + \eta_{-k-mN} \varrho_2^{-k-mN} \right)}{\delta_k} \tag{2.35}$$

$$\nu_k = \frac{\varrho_1^{k} \sum_{m\in Z} \left(\zeta_{k+mN} \varrho_2^{k+mN} + \eta_{-k-mN} \varrho_2^{-k-mN} \right)}{\delta_k} - \frac{\varrho_2^{k} \sum_{m\in Z} \left(\zeta_{k+mN} \varrho_1^{k+mN} + \eta_{-k-mN} \varrho_1^{-k-mN} \right)}{\delta_k} \tag{2.36}$$

For $k = 0$, we have

$$\mu_0 + \nu_0 \log \varrho_1 = \sum_{m\in\mathbb{Z}} \zeta_{mN} \varrho_1^{mN} + \sum_{m\in\mathbb{Z}\smallsetminus\{0\}} \eta_{mN} \varrho_1^{mN} + \eta_0 \log \varrho_1,$$

$$\mu_0 + \nu_0 \log \varrho_2 = \sum_{m\in\mathbb{Z}} \zeta_{mN} \varrho_2^{mN} + \sum_{m\in\mathbb{Z}\smallsetminus\{0\}} \eta_{mN} \varrho_2^{mN} + \eta_0 \log \varrho_2,$$

and therefore

$$\begin{aligned} \mu_0 = \frac{1}{\log \varrho_2/\varrho_1} \Bigg\{ & \log \varrho_2 \left[\sum_{m\in\mathbb{Z}} \zeta_{mN} \varrho_1^{mN} + \sum_{m\in\mathbb{Z}\smallsetminus\{0\}} \eta_{mN} \varrho_1^{mN} \right] \\ & - \log \varrho_1 \left[\sum_{m\in\mathbb{Z}} \zeta_{mN} \varrho_2^{mN} + \sum_{m\in\mathbb{Z}\smallsetminus\{0\}} \eta_{mN} \varrho_2^{mN} \right] \Bigg\}, \end{aligned} \tag{2.37}$$

$$\begin{aligned} \nu_0 = \frac{1}{\log \varrho_2/\varrho_1} \Bigg\{ & \sum_{m\in\mathbb{Z}} \zeta_{mN} \varrho_2^{mN} + \sum_{m\in\mathbb{Z}\smallsetminus\{0\}} \eta_{mN} \varrho_2^{mN} \\ & - \left[\sum_{m\in\mathbb{Z}} \zeta_{mN} \varrho_1^{mN} + \sum_{m\in\mathbb{Z}\smallsetminus\{0\}} \eta_{mN} \varrho_1^{mN} \right] \Bigg\} + \eta_0. \end{aligned} \tag{2.38}$$

Next we bound the coefficients $\mu_k, \;\; k = -N/2+1, \ldots, N/2$. We consider three cases: Case I: $k > 0$, Case II: $k < 0$ and Case III: $k = 0$.

Case I. $k > 0$. First, from (2.32) and (2.33) we have

$$\left| \sum_{m \in \mathbb{Z}} \zeta_{k+mN} \varrho_1^{k+mN} \right| \leq \sum_{m \geq 0} |\zeta_{k+mN}| \varrho_1^{k+mN} + \sum_{m<0} |\zeta_{k+mN}| \varrho_1^{k+mN}$$
$$\leq \sum_{m \geq 0} M_\beta \, (\varrho_2 + \beta)^{-(k+mN)} \, \varrho_1^{k+mN} + \sum_{m<0} M_\beta \, (\varrho_1 - \beta)^{-(k+mN)} \, \varrho_1^{k+mN}.$$

By taking $\gamma_1 = \max\left\{ \frac{\varrho_1}{\varrho_2+\beta}, \frac{\varrho_1-\beta}{\varrho_1} \right\} < 1$, we get

$$\left| \sum_{m \in \mathbb{Z}} \zeta_{k+mN} \varrho_1^{k+mN} \right| \leq M_\beta \; \gamma_1^k \sum_{m \geq 0} \gamma_1^{mN} + M_\beta \; \gamma_1^{N-k} \sum_{m \geq 0} \gamma_1^{Nm}$$

by observing that $k \leq N-k$, since $k \leq N/2$, we finally have

$$\left| \sum_{m \in \mathbb{Z}} \zeta_{k+mN} \varrho_1^{k+mN} \right| \leq 2M_\beta \; \gamma_1^k \sum_{m \geq 0} \gamma_1^{mN} = 2M_\beta \gamma_1^k (1-\gamma_1^N)^{-1} \leq M_1 \; \gamma_1^k,$$

where $M_1 = \frac{2M_\beta}{1-\gamma_1}$. Following an identical argument, we get

$$\left| \sum_{\substack{m \in \mathbb{Z} \\ k \neq 0}} \eta_{k+mN} \varrho_1^{k+mN} \right| \leq \; M_1 \; \gamma_1^k.$$

Similarly, taking $\gamma_2 = \max\left\{ \frac{\varrho_2}{\varrho_2+\beta}, \frac{\varrho_1-\beta}{\varrho_2} \right\} < 1,$ and using the fact that $\gamma_2^k < \gamma_2^{N-k}$, we obtain

$$\left| \sum_{m \in \mathbb{Z}} \zeta_{k+mN} \varrho_2^{k+mN} \right|, \; \left| \sum_{\substack{m \in \mathbb{Z} \\ k \neq 0}} \eta_{k+mN} \varrho_2^{k+mN} \right| \leq \; M_2 \; \gamma_2^k,$$

where $M_2 = 2M_\beta \; \gamma_2^k (1-\gamma_2)^{-1}$.

Cases II - III. Following the arguments used in Case I, we obtain for Case II ($k < 0$)

$$\left| \sum_{m \in \mathbb{Z}} \zeta_{k+mN} \varrho_i^{k+mN} \right|, \; \left| \sum_{m \in \mathbb{Z}} \eta_{k+mN} \varrho_i^{k+mN} \right| \leq M_i \; \gamma_i^{-k}, \quad i = 1, 2$$

and similarly for Case III ($k = 0$), we obtain

$$\left| \sum_{m \in \mathbb{Z}} \zeta_{mN} \varrho_1^{mN} \right|, \; \left| \sum_{m \in \mathbb{Z}} \eta_{-mN} \varrho_1^{-mN} \right| \leq M_i, \quad i = 1, 2.$$

We define γ_3 such that $\gamma_1, \gamma_2 \leq \gamma_3 = \max\left\{ \frac{\varrho_2}{\varrho_2+\beta}, \frac{\varrho_1-\beta}{\varrho_1} \right\} < 1$, and we take $M_3 = \max\{M_1, M_2\}$. Therefore, for $k \in \mathbb{Z}$, we have

$$|\mu_k| \leq \frac{2M_3 \; \gamma_3^{|k|} \left(\varrho_2^{-k} + \varrho_1^{-k} \right)}{|\delta_k|}.$$

In particular, when $k > 0$ we have that

$$|\mu_k| \le \frac{2M_3\gamma_3^k}{\varrho_2^k}\left(1-\left(\frac{\varrho_1}{\varrho_2}\right)^k\right)^{-1} \le \frac{2M_3\gamma_3^k}{\varrho_2^k}\left(1-\frac{\varrho_1}{\varrho_2}\right)^{-1} \le \frac{M_4\,\gamma_3^k}{\varrho_2^k},$$

where $M_4 = 2M_3\left(1-\frac{\varrho_1}{\varrho_2}\right)^{-1}$.

When $k < 0$,

$$|\mu_k| \le M_4\,\gamma_3^{-k}\varrho_1^{-k}, \tag{2.39}$$

and, when $k = 0$, we have that

$$\begin{aligned}|\mu_0| <& \frac{\log\varrho_2\,(2M_3 + M_3\log\varrho_1) + \log\varrho_1\,(2M_3 + M_3\log\varrho_2)}{\log(\varrho_2/\varrho_1)}\\ \le& \frac{2M_3\,(\log\varrho_2 + \log\varrho_1 + \log\varrho_2\log\varrho_1)}{\log(\varrho_2/\varrho_1)}.\end{aligned}$$

Similarly, for the coefficients ν_k, $k > 0$, we have that $|\nu_k| \le M_4\gamma_3^k\varrho_1^k$, for $k < 0$, $|\nu_k| \le M_4\gamma_3^{-k}\varrho_2^k$, and for $k = 0$, $|\nu_0| \le \dfrac{M_3\,(4 + \log\varrho_2 + \log\varrho_1)}{\log(\varrho_2/\varrho_1)}$. If we take

$$M = \max\left\{M_4, \frac{2M_3\,(\log\varrho_2 + \log\varrho_1 + \log\varrho_2\log\varrho_1)}{\log(\varrho_2/\varrho_1)}, \frac{M_3\,(4+\log\varrho_2+\log\varrho_1)}{\log(\varrho_2/\varrho_1)}\right\},$$

then

$$|\mu_k| \le \begin{cases} M\gamma_3^k\varrho_2^{-k}, & k > 0,\\ M\gamma_3^{-k}\varrho_1^{-k}, & k < 0,\\ M, & k = 0,\end{cases} \qquad |\nu_k| \le \begin{cases} M\gamma_3^k\varrho_1^k, & k > 0,\\ M\gamma_3^{-k}\varrho_2^k, & k < 0,\\ M, & k = 0.\end{cases}$$

This leads to the following theorem with a uniform bound (covering all cases)

Theorem 2.4.1. *The coefficients μ_k,ν_k in (2.34) are bounded by:*

$$|\mu_k|, |\nu_k| \le M\gamma_4^{|k|}, \tag{2.40}$$

where $\gamma_4 = \max\left\{\gamma_3\varrho_1, \frac{\gamma_3}{\varrho_2}\right\} < 1$. □

2.4.2 The error bound

Let us denote by $u(\cdot;\boldsymbol{h})$ the solution of the boundary value problem

$$\begin{cases}\Delta u = 0 & \text{in} \quad \Omega,\\ u = h_1 & \text{on} \quad \partial\Omega_1,\\ u = h_2 & \text{on} \quad \partial\Omega_2,\end{cases}$$

where $\boldsymbol{h} = (h_1, h_2)^T$ and by $u_N(\cdot;\boldsymbol{h})$ its MFS approximation. Note that u_N depends also on R_1, R_2. Since both $u(\cdot;\boldsymbol{h})$ and $u_N(\cdot;\boldsymbol{h})$ depend linearly on h_1 and h_2 we have, with $\boldsymbol{f}_N = (f_{1_N}, f_{2_N})^T$, and $\boldsymbol{f} = (f_1, f_2)^T$,

$$\|u_N(\cdot;\boldsymbol{f}) - u(\cdot;\boldsymbol{f})\|_\infty \le \|u(\cdot;\boldsymbol{f}-\boldsymbol{f}_N)\|_\infty + \|u_N(\cdot;\boldsymbol{f}-\boldsymbol{f}_N)\|_\infty + \|u_N(\cdot;\boldsymbol{f}_N) - u(\cdot;\boldsymbol{f}_N)\|_\infty$$

$$= \|u(\cdot;\boldsymbol{f}-\boldsymbol{f}_N)\|_\infty + \|u_N(\cdot;\boldsymbol{f}_N) - u(\cdot;\boldsymbol{f}_N)\|_\infty, \tag{2.41}$$

since $\boldsymbol{f}$ and $\boldsymbol{f}_N$ agree at the boundary points. In the following, we show, using the maximum principle, that each term on the right hand side of (2.41) decays exponentially fast as $N \to \infty$.

The term $\|u(\cdot, \boldsymbol{f} - \boldsymbol{f}_N)\|_\infty$

From (2.31) and (2.34), we have

$$\begin{aligned} u - \tilde{u}_N = & \sum_{k \le -N/2} \left(\zeta_k r^k \mathrm{e}^{\mathrm{i}k\vartheta} + \eta_k r^k \mathrm{e}^{-\mathrm{i}k\vartheta} \right) + \sum_{k > N/2} \left(\zeta_k r^k \mathrm{e}^{\mathrm{i}k\vartheta} + \eta_k r^k \mathrm{e}^{-\mathrm{i}k\vartheta} \right) \\ & + \sum_{k=-N/2+1}^{N/2} (\zeta_k - \mu_k)\, r^k \mathrm{e}^{\mathrm{i}k\vartheta} + \sum_{k=-N/2+1}^{-1} (\eta_k - \nu_k)\, r^{-k} \mathrm{e}^{\mathrm{i}k\vartheta} \\ & + \sum_{k=1}^{N/2} (\eta_k - \nu_k)\, r^{-k} \mathrm{e}^{\mathrm{i}k\vartheta} + (\eta_0 - \nu_0) \log r. \end{aligned} \tag{2.42}$$

By observing that the term corresponding to $m = 0$ in (2.35) vanishes, i.e.

$$\frac{\varrho_2^{-k} \left(\zeta_k \varrho_1^k + \eta_{-k} \varrho_1^{-k} \right) - \varrho_1^{-k} \left(\zeta_k \varrho_2^k + \eta_{-k} \varrho_2^{-k} \right)}{\delta_k} - \zeta_k = 0,$$

we have that (2.35) reduces to

$$\begin{aligned} \mu_k - \zeta_k = & \frac{1}{\delta_k} \left\{ \varrho_2^{-k} \sum_{m \in \mathbb{Z} \setminus \{0\}} \left(\zeta_{k+mN} \varrho_1^{k+mN} + \eta_{-k-mN} \varrho_1^{-k-mN} \right) \right. \\ & \left. - \varrho_1^{-k} \sum_{m \in \mathbb{Z} \setminus \{0\}} \left(\zeta_{k+mN} \varrho_2^{k+mN} + \eta_{-k-mN} \varrho_2^{-k-mN} \right) \right\}. \end{aligned}$$

Thus,

$$
\begin{aligned}
|\mu_k-\zeta_k| \leq & \frac{\varrho_2^{-k}}{|\delta_k|}\left\{\sum_{m>0}|\zeta_{k+mN}|\varrho_1^{k+mN}+\sum_{m>0}|\eta_{-k-mN}|\varrho_1^{-k-mN}+\sum_{m<0}|\zeta_{k+mN}|\varrho_1^{k+mN}\right.\\
&\left.+\sum_{m<0}|\eta_{-k-mN}|\varrho_1^{-k-mN}\right\}\\
&+\frac{\varrho_1^{-k}}{|\delta_k|}\left\{\sum_{m>0}|\zeta_{k+mN}|\varrho_2^{k+mN}+\sum_{m>0}|\eta_{-k-mN}|\varrho_2^{-k-mN}+\sum_{m<0}|\zeta_{k+mN}|\varrho_2^{k+mN}\right.\\
&\left.+\sum_{m<0}|\eta_{-k-mN}|\varrho_2^{-k-mN}\right\}\\
\leq & \frac{\varrho_2^{-k}}{|\delta_k|}\left\{\sum_{m>0}M_\beta\left(\varrho_2+\beta\right)^{-(k+mN)}\varrho_1^{k+mN}+\sum_{m<0}M_\beta\left(\varrho_1-\beta\right)^{-(k+mN)}\varrho_1^{k+mN}\right.\\
&\left.+\sum_{m>0}M_\beta\left(\varrho_1-\beta\right)^{k+mN}\varrho_1^{-(k+mN)}+\sum_{m<0}M_\beta\left(\varrho_2+\beta\right)^{k+mN}\varrho_1^{-(k+mN)}\right\}\\
&+\frac{\varrho_1^{-k}}{|\delta_k|}\left\{\sum_{m>0}M_\beta\left(\varrho_2+\beta\right)^{-(k+mN)}\varrho_2^{k+mN}+\sum_{m<0}M_\beta\left(\varrho_1-\beta\right)^{-(k+mN)}\varrho_2^{k+mN}\right.\\
&\left.+\sum_{m>0}M_\beta\left(\varrho_1-\beta\right)^{k+mN}\varrho_2^{-(k+mN)}+\sum_{m<0}M_\beta\left(\varrho_2+\beta\right)^{k+mN}\varrho_2^{-(k+mN)}\right\}\\
\leq & \frac{M_\beta\ \varrho_2^{-k}}{|\delta_k|}\left\{\gamma_3^{k+N}\sum_{m\geq 0}\gamma_3^{Nm}+\gamma_3^{N-k}\sum_{m\geq 0}\gamma_3^{Nm}+\gamma_3^{N+k}\sum_{m\geq 0}\gamma_3^{Nm}+\gamma_3^{N-k}\sum_{m\geq 0}\gamma_3^{Nm}\right\}\\
&+\frac{M_\beta\ \varrho_1^{-k}}{|\delta_k|}\left\{\gamma_3^{k+N}\sum_{m\geq 0}\gamma_3^{Nm}+\gamma_3^{N-k}\sum_{m\geq 0}\gamma_3^{Nm}+\gamma_3^{N+k}\sum_{m\geq 0}\gamma_3^{Nm}+\gamma_3^{N-k}\sum_{m\geq 0}\gamma_3^{Nm}\right\},
\end{aligned}
$$

If $k>0$, then $k+N>N-k$, and

$$
|\mu_k-\zeta_k| \leq \frac{8M_\beta\ \varrho_2^k\gamma_3^{N-k}}{\varrho_2^{2k}-\varrho_1^{2k}}\ \sum_{m\geq 0}\gamma_3^{Nm} \leq \frac{8M_\beta\gamma_3^{N-k}}{\varrho_2^k\left(1-\frac{\varrho_1^2}{\varrho_2^2}\right)(1-\gamma_3)}\ \leq \frac{M_5\ \gamma_3^{N-k}}{\varrho_2^k}
$$

where $M_5=\frac{8M_\beta}{(1-\gamma_3)}\left(1-\frac{\varrho_1^2}{\varrho_2^2}\right)^{-1}$. If $k<0$ then $k+N<N-k$, and

$$
\begin{aligned}
|\mu_k-\zeta_k| \leq & \frac{4M_\beta\varrho_2^{-k}\gamma_3^{k+N}}{|\delta_k|}\ \sum_{m\geq 0}\gamma_3^{Nm}+\frac{4M_\beta\varrho_1^{-k}\gamma_3^{k+N}}{|\delta_k|}\ \sum_{m\geq 0}\gamma_3^{Nm}\\
\leq & \frac{8M_\beta\varrho_1^{-k}\gamma_3^{k+N}}{\left(1-\frac{\varrho_1^2}{\varrho_2^2}\right)(1-\gamma_3)}\ \leq M_5\ \gamma_3^{N+k}\varrho_1^{-k}.
\end{aligned}
$$

When $k=0$, from (2.37) and by observing that

$$
\frac{\log\varrho_2\ \zeta_0-\log\varrho_1\ \zeta_0}{\log\varrho_2/\varrho_1}-\zeta_0=0,
$$

we have

$$\mu_0-\zeta_0=\frac{1}{\log\varrho_2/\varrho_1}\left\{\log\varrho_2\left[\sum_{m\in\mathbb{Z}}\zeta_{mN}\varrho_1^{mN}+\sum_{m\in\mathbb{Z}\smallsetminus\{0\}}\eta_{-mN}\varrho_1^{-mN}+\eta_0\log\varrho_1\right]\right.$$
$$\left.-\log\varrho_1\left[\sum_{m\in\mathbb{Z}}\zeta_{mN}\varrho_2^{mN}+\sum_{m\in\mathbb{Z}\smallsetminus\{0\}}\eta_{-mN}\varrho_2^{-mN}+\eta_0\log\varrho_2\right]\right\}-\zeta_0.$$

Thus,

$$\begin{aligned}
|\mu_0-\zeta_0| =&\frac{1}{\log\varrho_2/\varrho_1}\left|\log\varrho_2\sum_{m\in\mathbb{Z}\smallsetminus\{0\}}\left(\zeta_{mN}\varrho_1^{mN}+\eta_{-mN}\varrho_1^{-mN}\right)\right.\\
&\left.-\log\varrho_1\sum_{m\in\mathbb{Z}\smallsetminus\{0\}}\left(\zeta_{mN}\varrho_2^{mN}+\eta_{-mN}\varrho_2^{-mN}\right)\right|\\
=&\frac{1}{\log\varrho_2/\varrho_1}\left|\left\{\log\varrho_2\left[\sum_{m>0}\left(\zeta_{mN}\varrho_1^{mN}+\eta_{-mN}\varrho_1^{-mN}\right)+\sum_{m<0}\left(\zeta_{mN}\varrho_1^{mN}+\eta_{-mN}\varrho_1^{-mN}\right)\right]\right.\right.\\
&\left.\left.+\log\varrho_1\left[\sum_{m>0}\left(\zeta_{mN}\varrho_2^{mN}+\eta_{-mN}\varrho_2^{-mN}\right)+\sum_{m<0}\left(\zeta_{mN}\varrho_2^{mN}+\eta_{-mN}\varrho_2^{-mN}\right)\right]\right\}\right|\\
\leq&\frac{\log\varrho_2}{\log\varrho_2/\varrho_1}\left\{\sum_{m>0}M_\beta\left(\varrho_2+\beta\right)^{-mN}\varrho_1^{mN}+\sum_{m<0}M_\beta\left(\varrho_1-\beta\right)^{-mN}\varrho_1^{mN}\right.\\
&\left.+\sum_{m>0}M_\beta\left(\varrho_1-\beta\right)^{mN}\varrho_1^{-mN}+\sum_{m<0}M_\beta\left(\varrho_2+\beta\right)^{mN}\varrho_1^{-mN}\right\}\\
&+\frac{1}{\log\varrho_2/\varrho_1}\left\{\sum_{m>0}M_\beta\left(\varrho_2+\beta\right)^{-mN}\varrho_2^{mN}+\sum_{m<0}M_\beta\left(\varrho_1-\beta\right)^{-mN}\varrho_2^{mN}\right.\\
&\left.+\sum_{m>0}M_\beta\left(\varrho_1-\beta\right)^{mN}\varrho_2^{-mN}+\sum_{m<0}M_\beta\left(\varrho_2+\beta\right)^{mN}\varrho_2^{-mN}\right\}\\
\leq&\frac{8M_\beta\log\varrho_2}{\log\varrho_2/\varrho_1}\gamma_3^N\sum_{m\geq0}\gamma_3^{Nm}\leq\frac{8M_\beta\log\varrho_2}{\log\varrho_2/\varrho_1}\frac{\gamma_3^N}{1-\gamma_3}=M_6\,\gamma_3^N,
\end{aligned}$$

where $M_6=\dfrac{8M_\beta\ \log\varrho_2}{(1-\gamma_3)\log\varrho_2/\varrho_1}$. Following similar arguments we have that

$$|\nu_k-\eta_k|\leq\begin{cases}M_5\ \gamma_3^{N-k}\varrho_1^k, & k>0\\[2ex] M_5\ \gamma_3^{N+k}\varrho_2^k, & k<0\\[2ex] M_6\ \gamma_3^N & k=0.\end{cases}$$

If we take $M_7=\max\{M_5,M_6\}$ we obtain the lemma

Lemma 2.4.2. *The terms $\mu_k - \zeta_k$ and $\nu_k - \eta_k$ in equation* (2.42) *are bounded by:*

$$|\mu_k - \zeta_k| \le \begin{cases} M_7\,\gamma_3^{N-k}\varrho_2^{-k}, & k>0,\\[2ex] M_7\,\gamma_3^{N+k}\varrho_1^{-k}, & k<0,\\[2ex] M_7\,\gamma_3^{N}, & k=0,\end{cases} \qquad |\nu_k - \eta_k| \le \begin{cases} M_7\,\gamma_3^{N-k}\varrho_1^{k}, & k>0,\\[2ex] M_7\,\gamma_3^{N+k}\varrho_2^{k}, & k<0,\\[2ex] M_7\,\gamma_3^{N}, & k=0.\end{cases}$$

□

We are now in a position to bound the following terms appearing in equation (2.42)

$$\sum_{k=-N/2+1}^{N/2} (\zeta_k - \mu_k)\, r^k \mathrm{e}^{\mathrm{i}k\vartheta} + \sum_{k=-N/2+1}^{-1} (\eta_k - \nu_k)\, r^{-k}\mathrm{e}^{\mathrm{i}k\vartheta} + \sum_{k=1}^{N/2} (\eta_k - \nu_k)\, r^{-k}\mathrm{e}^{\mathrm{i}k\vartheta} + (\eta_0 - \nu_0)\log r.$$

In the case when the error attains its maximum value on the inner circle $r = \varrho_1$, we have, using Lemma 2.4.2,

$$\begin{aligned} &\left| \sum_{k=-N/2+1}^{N/2} (\zeta_k - \mu_k)\, \varrho_1^k \mathrm{e}^{\mathrm{i}k\vartheta} + \sum_{k=-N/2+1}^{-1} (\eta_k - \nu_k)\, \varrho_1^{-k}\mathrm{e}^{\mathrm{i}k\vartheta} + \sum_{k=1}^{N/2} (\eta_k - \nu_k)\, \varrho_1^{-k}\mathrm{e}^{\mathrm{i}k\vartheta} + (\eta_0 - \nu_0)\log \varrho_1 \right| \\[2ex] &\le \sum_{k=1}^{N/2} |\mu_k - \zeta_k| \varrho_1^k + \sum_{k=-N/2+1}^{-1} |\mu_k - \zeta_k| \varrho_1^k + |\mu_0 - \zeta_0| \\ &\quad + \sum_{k=1}^{N/2} |\nu_k - \eta_k| \varrho_1^{-k} + \sum_{k=-N/2+1}^{-1} |\nu_k - \eta_k| \varrho_1^{-k} + |\nu_0 - \eta_0| \log \varrho_1 \\ &\le M_8 \Bigg\{ \sum_{k=1}^{N/2} \gamma_3^{N-k} \left(\frac{\varrho_1}{\varrho_2}\right)^k + \sum_{k=-N/2+1}^{-1} \gamma_3^{N+k} \varrho_1^{-k}\varrho_1^k + \gamma_3^N + \sum_{k=1}^{N/2} \gamma_3^{N-k}\varrho_1^k\varrho_1^{-k} + \sum_{k=-N/2+1}^{-1} \gamma_3^{N+k} \left(\frac{\varrho_1}{\varrho_2}\right)^{-k} + \gamma_3^N \Bigg\} \\ &\le M_8 \Bigg\{ \sum_{k=1}^{N/2} \gamma_3^{N-k} + \sum_{k=1}^{N/2} \gamma_3^{N-k} + \gamma_3^N + \sum_{k=1}^{N/2} \gamma_3^{N-k} + \sum_{k=1}^{N/2} \gamma_3^{N-k} + \gamma_3^N \Bigg\} \\ &\le 4M_8 \Big\{ \gamma_3^{N/2} + \gamma_3^N \Big\} \le 8M_8\, \gamma_3^{N/2}, \end{aligned} \tag{2.43}$$

where $M_8 = \max\{M_7, \log\varrho_1, \log\varrho_2\}$. Similarly, when the maximum is attained on the outer circle $r = \varrho_2$, we have

$$\left| \sum_{k=-N/2+1}^{-1} (\zeta_k - \mu_k)\, \varrho_2^k \mathrm{e}^{\mathrm{i}k\vartheta} + \sum_{k=-N/2+1}^{-1} (\eta_k - \nu_k)\, \varrho_2^{-k}\mathrm{e}^{\mathrm{i}k\vartheta} + \sum_{k=1}^{N/2} (\eta_k - \nu_k)\, \varrho_2^{-k}\mathrm{e}^{\mathrm{i}k\vartheta} + (\eta_0 - \nu_0)\log \varrho_2 \right|$$

$$\leq \quad 4M_8 \left\{ \gamma_3^{N/2} + \gamma_3^N \right\} \leq 8M_8 \ \gamma_3^{N/2}. \tag{2.44}$$

The remaining term in (2.42) can be bounded in the following way:

$$\left| \sum_{k>N/2} \left(\zeta_k r^k \mathrm{e}^{\mathrm{i}k\vartheta} + \eta_k r^k \mathrm{e}^{-\mathrm{i}k\vartheta} \right) + \sum_{k\leq N/2} \left(\zeta_k r^k \mathrm{e}^{\mathrm{i}k\vartheta} + \eta_k r^k \mathrm{e}^{-\mathrm{i}k\vartheta} \right) \right|$$

$$\leq \sum_{k>N/2} |\zeta_k| r^k + \sum_{k>N/2} |\eta_k| r^k + \sum_{k\leq -N/2} |\zeta_k| r^k + \sum_{k\leq -N/2} |\eta_k| r^k$$

$$\leq \sum_{k=N/2+1}^{\infty} M_\beta \left(\frac{r}{\varrho_2+\beta} \right)^k + \sum_{k=N/2+1}^{\infty} M_\beta \left(\frac{r}{\varrho_2+\beta} \right)^k + \sum_{k\leq -N/2} M_\beta \left(\frac{r}{\varrho_1-\beta} \right)^k + \sum_{k\leq -N/2} M_\beta \left(\frac{r}{\varrho_1-\beta} \right)^k$$

$$\leq 2M_\beta \left\{ \sum_{k=N/2+1}^{\infty} \left(\frac{r}{\varrho_2+\beta} \right)^k + \sum_{k=N/2}^{\infty} \left(\frac{\varrho_1-\beta}{r} \right)^k \right\}$$

$$\leq 2M_\beta \left\{ \sum_{k=N/2}^{\infty} \left(\frac{r}{\varrho_2+\beta} \right)^k + \sum_{k=N/2}^{\infty} \left(\frac{\varrho_1-\beta}{r} \right)^k \right\}$$

$$= 2M_\beta \left\{ \left(\frac{r}{\varrho_2+\beta} \right)^{N/2} \sum_{k\geq 0} \left(\frac{r}{\varrho_2+\beta} \right)^k + \left(\frac{\varrho_1-\beta}{r} \right)^{N/2} \sum_{k\geq 0} \left(\frac{\varrho_1-\beta}{r} \right)^k \right\}$$

$$= 2M_\beta \left\{ \left(\frac{r}{\varrho_2+\beta} \right)^{N/2} \left(1 - \frac{r}{\varrho_2+\beta} \right)^{-1} + \left(\frac{\varrho_1-\beta}{r} \right)^{N/2} \left(1 - \frac{\varrho_1-\beta}{r} \right)^{-1} \right\}.$$

Therefore, when the maximum is attained on the inner circle $r = \varrho_1$, we have

$$\left| \sum_{k>N/2} \left(\zeta_k \varrho_1^k \mathrm{e}^{\mathrm{i}k\vartheta} + \eta_k \varrho_1^k \mathrm{e}^{-\mathrm{i}k\vartheta} \right) + \sum_{k\leq N/2} \left(\zeta_k \varrho_1^k \mathrm{e}^{\mathrm{i}k\vartheta} + \eta_k \varrho_1^k \mathrm{e}^{-\mathrm{i}k\vartheta} \right) \right|$$

$$\leq 2M_\beta \left\{ \left(1 - \frac{\varrho_1}{\varrho_2+\beta} \right)^{-1} + \left(1 - \frac{\varrho_1-\beta}{\varrho_1} \right)^{-1} \right\} \gamma_3^{N/2} = M_1 \gamma_3^{N/2} \leq M_8 \ \gamma_3^{N/2}. \tag{2.45}$$

Similarly, when the maximum is obtained on the external circle $r = \varrho_2$, we have

$$\left| \sum_{k>N/2} \left(\zeta_k \varrho_2^k \mathrm{e}^{\mathrm{i}k\vartheta} + \eta_k \varrho_2^k \mathrm{e}^{-\mathrm{i}k\vartheta} \right) + \sum_{k\leq N/2} \left(\zeta_k \varrho_2^k \mathrm{e}^{\mathrm{i}k\vartheta} + \eta_k \varrho_2^k \mathrm{e}^{-\mathrm{i}k\vartheta} \right) \right|$$

$$\leq 2M_1 \left\{ \left(1 - \frac{\varrho_2}{\varrho_2+\beta} \right)^{-1} + \left(1 - \frac{\varrho_1-\beta}{\varrho_2} \right)^{-1} \right\} \gamma_3^{N/2} = M_2 \gamma_3^{N/2} \leq M_8 \ \gamma_3^{N/2}. \tag{2.46}$$

Therefore, we have the following result:

Lemma 2.4.3.

$$\| u(\cdot, \boldsymbol{f} - \boldsymbol{f}_N) \|_\infty \leq 9M_8 \ \gamma_3^{N/2}. \tag{2.47}$$

□

The term $\|u_N(\cdot;\boldsymbol{f}_N)-u(\cdot;\boldsymbol{f}_N)\|_\infty$

To bound this term, we need to investigate how well the MFS approximates problems corresponding to exact solutions of the form $z^k, k=\frac{-N}{2},\ldots,N/2,$ and $\log|z|$ which in polar coordinates take the form $r^k\mathrm{e}^{\mathrm{i}k\varphi}$ and $\log r$, respectively, $r\in[\varrho_1,\varrho_2]$, and $\varphi\in[0,2\pi]$. For simplicity we denote this solution by $u(\cdot;r^k\mathrm{e}^{\mathrm{i}k\varphi})$ and its MFS approximation by $u_N(\cdot;r^k\mathrm{e}^{\mathrm{i}k\varphi})$. Thus we need to bound

$$\|u_N(\cdot;r^k\mathrm{e}^{\mathrm{i}k\varphi})-u(\cdot;r^k\mathrm{e}^{\mathrm{i}k\varphi})\|_\infty,\ \ k=-N/2+1,\ldots,N/2,\text{and}$$
$$\|u_N(\cdot;\log r)-u(\cdot;\log r)\|_\infty.$$

Without loss of generality, we assume that $\varrho_1=1$. We shall prove the following lemma:

Lemma 2.4.4. *We have the following estimates:*

$$\|u_N(\cdot;r^k e^{\mathrm{i}k\varphi})-u(\cdot;r^k e^{\mathrm{i}k\varphi})\|_\infty\le CN^4\sigma^{N-2|k|},\tag{2.48}$$

where $k=-N/2+1,\ldots,N/2,$ $\sigma=\max\left\{R_1,\frac{1}{R_2},\frac{\varrho_2}{R_2}\right\}<1$ *and* C *is a constant independent of* k *and* N*.*

PROOF. Since u and u_N are harmonic in the annulus, from the maximum principle

$$||u_N-u||_\infty=\max\{\sup_{r=\varrho_1}|u_N-u|,\sup_{r=\varrho_2}|u_N-u|\}\,.$$

First, we bound the term $u_N(\cdot;r^ke^{ik\varphi})-u(\cdot;r^ke^{ik\varphi})$ on the circle $r=\varrho_1=1$.

Case I. $k=0$.

In this case, the exact solution is $u\equiv1$, i.e., $f_1,f_2\equiv1$, and thus $\boldsymbol{f_1}=\boldsymbol{f_2}=(1,1,\ldots,1)$, and

$$\langle\boldsymbol{f_1},\boldsymbol{\xi}_j\rangle=\begin{cases}\sqrt{N}&\text{if }j=1,\\0&\text{otherwise,}\end{cases}\qquad\langle\boldsymbol{f_2},\boldsymbol{\xi}_j\rangle=\begin{cases}\sqrt{N}&\text{if }j=1\\0&\text{otherwise.}\end{cases}$$

Thus, from expression (2.29), we have

$$u_N(\cdot;1)=\frac{\sqrt{N}}{\lambda_1^{11}\lambda_1^{22}-\lambda_1^{12}\lambda_1^{21}}\{(\lambda_1^{11}-\lambda_1^{21})\langle\overline{\boldsymbol{l_2},\boldsymbol{\xi}_1}\rangle+(\lambda_1^{22}-\lambda_1^{12})\langle\overline{\boldsymbol{l_1},\boldsymbol{\xi}_1}\rangle\},$$

where

$$\lambda_1^{11}=\frac{N}{2\pi}\sum_{m=1}^\infty\frac{1}{mN}R_1^{mN},\qquad\lambda_1^{12}=\frac{N}{2\pi}\left\{\sum_{m=1}^\infty\frac{1}{mN}\left(\frac{1}{R_2}\right)^{mN}-\log R_2\right\},$$
$$\lambda_1^{21}=\frac{N}{2\pi}\left\{\sum_{m=1}^\infty\frac{1}{mN}\left(\frac{R_1}{\varrho_2}\right)^{mN}-\log\varrho_2\right\},\qquad\lambda_1^{22}=\frac{N}{2\pi}\left\{\sum_{m=1}^\infty\frac{1}{mN}\left(\frac{\varrho_2}{R_2}\right)^{mN}-\log R_2\right\},$$

and

$$\langle \overline{\boldsymbol{l_1}, \boldsymbol{\xi}_1} \rangle = \frac{\sqrt{N}}{2\pi} \sum_{m=1}^{\infty} \frac{1}{mN} R_1^{mN} \cos(mN\vartheta), \quad \langle \overline{\boldsymbol{l_2}, \boldsymbol{\xi}_1} \rangle = \frac{\sqrt{N}}{2\pi} \left\{ \sum_{m=1}^{\infty} \frac{1}{mN} \left(\frac{1}{R_2} \right)^{mN} \cos(mN\vartheta) - \log R_2 \right\}.$$

Therefore,

$$||u_N(\cdot, ; 1) - u(\cdot, ; 1)||_\infty = \max_{\vartheta \in [0, 2\pi]} |u_N(\cos\vartheta, \sin\vartheta ; 1) - 1| = |\frac{A - B}{B}|$$

where

$$\begin{aligned} A = & \frac{N}{2\pi} \left\{ (\lambda_1^{11} - \lambda_1^{21}) \left\{ \sum_{m=1}^{\infty} \frac{1}{mN} \left(\frac{1}{R_2} \right)^{mN} \cos(mN\vartheta) - \log R_2 \right\} \right. \\ & \left. + (\lambda_1^{22} - \lambda_1^{12}) \sum_{m=1}^{\infty} \frac{1}{mN} R_1^{mN} \cos(mN\vartheta) \right\}, \end{aligned}$$

and $B = \lambda_1^{11}\lambda_1^{22} - \lambda_1^{12}\lambda_1^{21}$. We thus have

$$\begin{aligned} |B| = & \frac{1}{4\pi^2} \sum_{m=1}^{\infty} \frac{1}{m} R_1^{mN} \left\{ N \log R_2 - \sum_{m=1}^{\infty} \frac{1}{m} \left(\frac{\varrho_2}{R_2} \right)^{mN} \right\} \\ & + \left\{ N \log R_2 - \sum_{m=1}^{\infty} \frac{1}{m} \left(\frac{1}{R_2} \right)^{mN} \right\} \left\{ N \log \varrho_2 - \sum_{m=1}^{\infty} \frac{1}{m} \left(\frac{R_1}{\varrho_2} \right)^{mN} \right\} \geq N^2 \log R_2 \log \varrho_2 \, , \end{aligned}$$

and

$$\begin{aligned} |A - B| = & \left| \frac{N}{2\pi} \left\{ (\lambda_1^{11} - \lambda_1^{21}) \left\{ \sum_{m=1}^{\infty} \frac{1}{mN} \left(\frac{1}{R_2} \right)^{mN} \cos(mN\vartheta) - \log R_2 \right\} \right. \right. \\ & \left. \left. + (\lambda_1^{22} - \lambda_1^{12}) \sum_{m=1}^{\infty} \frac{1}{mN} R_1^{mN} \cos(mN\vartheta) \right\} - (\lambda_1^{11}\lambda_1^{22} - \lambda_1^{12}\lambda_1^{21}) \right| \end{aligned}$$

$$
\begin{aligned}
&= \Bigg| \frac{N}{2\pi} \Bigg\{ \Bigg(\frac{1}{2\pi} \sum_{m=1}^{\infty} \frac{1}{m} R_1^{mN} + \frac{1}{2\pi} \Bigg[N \log \varrho_2 - \sum_{m=1}^{\infty} \frac{1}{m} \left(\frac{R_1}{\varrho_2} \right)^{mN} \Bigg] \Bigg) \\
&\quad \times \Bigg(\sum_{m=1}^{\infty} \frac{1}{mN} \left(\frac{1}{R_2} \right)^{mN} \cos(mN\vartheta) - \log R_2 \Bigg) \\
&\quad + \Bigg(\frac{1}{2\pi} \Bigg[\sum_{m=1}^{\infty} \frac{1}{m} \left(\frac{\varrho_2}{R_2} \right)^{mN} - N \log R_2 \Bigg] - \frac{1}{2\pi} \Bigg[\sum_{m=1}^{\infty} \frac{1}{m} \left(\frac{1}{R_2} \right)^{mN} - N \log R_2 \Bigg] \Bigg) \\
&\quad \times \sum_{m=1}^{\infty} \frac{1}{mN} {R_1}^{mN} \cos(mN\vartheta) \Bigg\} \\
&\quad + \frac{1}{4\pi^2} \Bigg\{ \sum_{m=1}^{\infty} \frac{1}{m} R_1^{mN} \Bigg[N \log R_2 - \sum_{m=1}^{\infty} \frac{1}{m} \left(\frac{\varrho_2}{R_2} \right)^{mN} \Bigg] \\
&\quad + \Bigg[N \log R_2 - \sum_{m=1}^{\infty} \frac{1}{m} \left(\frac{1}{R_2} \right)^{mN} \Bigg] \Bigg[N \log \varrho_2 - \sum_{m=1}^{\infty} \frac{1}{m} \left(\frac{R_1}{\varrho_2} \right)^{mN} \Bigg] \Bigg\} \Bigg| \\
&= \Bigg| \frac{N}{4\pi^2} \Bigg\{ \Bigg(\sum_{m=1}^{\infty} \frac{1}{m} R_1^{mN} + N \log \varrho_2 - \sum_{m=1}^{\infty} \frac{1}{m} \left(\frac{R_1}{\varrho_2} \right)^{mN} \Bigg) \Bigg(\sum_{m=1}^{\infty} \frac{1}{mN} \frac{1}{R_2^{mN}} \cos(mN\vartheta) \Bigg) \\
&\quad + \Bigg(\sum_{m=1}^{\infty} \frac{1}{m} \left(\frac{\varrho_2}{R_2} \right)^{mN} - \sum_{m=1}^{\infty} \frac{1}{m} \frac{1}{R_2^{mN}} \Bigg) \sum_{m=1}^{\infty} \frac{1}{mN} R_1^{mN} \cos(mN\vartheta) \Bigg\} \\
&\quad + \frac{1}{4\pi^2} \Bigg\{ \sum_{m=1}^{\infty} \frac{1}{m} R_1^{mN} \Bigg[N \log R_2 - \sum_{m=1}^{\infty} \frac{1}{m} \left(\frac{\varrho_2}{R_2} \right)^{mN} \Bigg] \\
&\quad + \Bigg[N \log R_2 - \sum_{m=1}^{\infty} \frac{1}{m} \left(\frac{1}{R_2} \right)^{mN} \Bigg] \Bigg[N \log \varrho_2 - \sum_{m=1}^{\infty} \frac{1}{m} \left(\frac{R_1}{\varrho_2} \right)^{mN} \Bigg] \Bigg\} \Bigg| \\
&= \frac{1}{4\pi^2} \Bigg| \Bigg\{ N \sum_{m=1}^{\infty} \frac{1}{m} R_1^{mN} \sum_{m=1}^{\infty} \frac{1}{mN} \frac{1}{R_2^{mN}} \cos(mN\vartheta) - N \log R_2 \sum_{m=1}^{\infty} \frac{1}{m} R_1^{mN} \\
&\quad + N^2 \log \varrho_2 \sum_{m=1}^{\infty} \frac{1}{mN} \frac{1}{R_2^{mN}} \cos(mN\vartheta) - N^2 \log \varrho_2 \log R_2 \\
&\quad - \sum_{m=1}^{\infty} \frac{1}{m} \left(\frac{R_1}{\varrho_2} \right)^{mN} \sum_{m=1}^{\infty} \frac{1}{m} \frac{1}{R_2^{mN}} \cos(mN\vartheta) + N \sum_{m=1}^{\infty} \frac{1}{m} \left(\frac{R_1}{\varrho_2} \right)^{mN} \log R_2 \\
&\quad + N \sum_{m=1}^{\infty} \frac{1}{m} \left(\frac{\varrho_2}{R_2} \right)^{mN} \sum_{m=1}^{\infty} \frac{1}{mN} R_1^{mN} \cos(mN\vartheta) \\
&\quad - N \sum_{m=1}^{\infty} \frac{1}{m} \frac{1}{R_2^{mN}} \sum_{m=1}^{\infty} \frac{1}{mN} R_1^{mN} \cos(mN\vartheta) \\
&\quad + N \log R_2 \sum_{m=1}^{\infty} \frac{1}{m} R_1^{mN} - \sum_{m=1}^{\infty} \frac{1}{m} R_1^{mN} \sum_{m=1}^{\infty} \frac{1}{m} \left(\frac{\varrho_2}{R_2} \right)^{mN} \\
&\quad + N^2 \log \varrho_2 \log R_2 - N \log R_2 \sum_{m=1}^{\infty} \frac{1}{m} \left(\frac{R_1}{\varrho_2} \right)^{mN} \\
&\quad - N \log \varrho_2 \sum_{m=1}^{\infty} \frac{1}{m} \frac{1}{R_2^{mN}} + \sum_{m=1}^{\infty} \frac{1}{m} \frac{1}{R_2^{mN}} \sum_{m=1}^{\infty} \frac{1}{m} \left(\frac{R_1}{\varrho_2} \right)^{mN} \Bigg\} \Bigg|
\end{aligned}
$$

$$
\begin{aligned}
&\leq \sum_{m=1}^{\infty} R_1^{mN} \sum_{m=1}^{\infty} \frac{1}{R_2^{mN}} + N \log R_2 \sum_{m=1}^{\infty} R_1^{mN} + N^2 \log \varrho_2 \sum_{m=1}^{\infty} \frac{1}{R_2^{mN}} \\
&\quad + \sum_{m=1}^{\infty} \left(\frac{R_1}{\varrho_2}\right)^{mN} \sum_{m=1}^{\infty} \frac{1}{R_2^{mN}} + N \log R_2 \sum_{m=1}^{\infty} \left(\frac{R_1}{\varrho_2}\right)^{mN} \\
&\quad + \sum_{m=1}^{\infty} \left(\frac{\varrho_2}{R_2}\right)^{mN} \sum_{m=1}^{\infty} R_1^{mN} + \sum_{m=1}^{\infty} \frac{1}{R_2^{mN}} \sum_{m=1}^{\infty} R_1^{mN} + \\
&\quad + N \log R_2 \sum_{m=1}^{\infty} R_1^{mN} + \sum_{m=1}^{\infty} R_1^{mN} \sum_{m=1}^{\infty} \left(\frac{\varrho_2}{R_2}\right)^{mN} + N \log R_2 \sum_{m=1}^{\infty} \left(\frac{R_1}{\varrho_2}\right)^{mN} \\
&\quad + N \log \varrho_2 \sum_{m=1}^{\infty} \frac{1}{R_2^{mN}} + \sum_{m=1}^{\infty} \frac{1}{R_2^{mN}} \sum_{m=1}^{\infty} \left(\frac{R_1}{\varrho_2}\right)^{mN} \\
&\leq 2R_1^N \frac{2}{R_2^N} + N \log R_2 2R_1^N + N^2 \log \varrho_2 \frac{2}{R_2^N} + 2\left(\frac{R_1}{\varrho_2}\right)^N \frac{2}{R_2^N} \\
&\quad + N \log R_2 2 \left(\frac{R_1}{\varrho_2}\right)^N + 4\left(\frac{\varrho_2}{R_2}\right)^N R_1^N + \frac{2}{R_2^N} 2R_1^N \\
&\quad + 2N \log R_2 R_1^N + 4R_1^N \left(\frac{\varrho_2}{R_2}\right)^N + 2N \log R_2 \left(\frac{R_1}{\varrho_2}\right)^N + 2N \log \varrho_2 \frac{1}{R_2^N} + 4\frac{1}{R_2^N}\left(\frac{R_1}{\varrho_2}\right)^N .
\end{aligned}
$$

Therefore:

$$
\begin{aligned}
|A-B| \; &\leq 4\sigma^{2N} + 2N \log R_2 \sigma^N + 2N^2 \log \varrho_2 \sigma^N + 4\sigma^{2N} + 2N \log R_2 \sigma^{2N} + 4\sigma^{2N} \\
&\quad + 4\sigma^{2N} + 2N \log R_2 \sigma^N + 4\sigma^{2N} + 2N \log R_2 \sigma^N + 2N \log R_2 \sigma^N + 4\sigma^{2N} \\
&\leq 4\sigma^N + 2N \log R_2 \sigma^N + 2N^2 \log R_2 \sigma^N + 4\sigma^N + 2N \log R_2 \sigma^N + 4\sigma^N + 4\sigma^N + 2N \log R_2 \sigma^N + 4\sigma^N \\
&\quad + 2N \log R_2 \sigma^N + 2N \log R_2 \sigma^N + 4\sigma^N \leq 24\sigma^N + 12N^2 \log R_2 \sigma^N .
\end{aligned}
$$

Thus if $\log R_2 > 1$ we have:

$$
\frac{|A-B|}{|B|} \leq \frac{24\sigma^N + 12N^2 \log R_2 \sigma^N}{N^2 \log R_2 \log \varrho_2} \leq \frac{24N^2 \log R_2 \sigma^N + 12N^2 \log R_2 \sigma^N}{N^2 \log R_2 \log \varrho_2} \leq \frac{36N^2 \log R_2 \sigma^N}{N^2 \log R_2 \log \varrho_2}
$$

$$
= \frac{36\sigma^N}{\log \varrho_2}
$$

If $\log R_2 < 1$ we have:

$$
\frac{|A-B|}{|B|} \leq \frac{24\sigma^N + 12N^2 \log R_2 \sigma^N}{N^2 \log R_2 \log \varrho_2} \leq \frac{24N^2\sigma^N + 12N^2\sigma^N}{N^2 \log R_2 \log \varrho_2} = \frac{36\sigma^N}{\log R_2 \log \varrho_2} = \frac{36\sigma^N}{\log \varrho_2 \log R_2}
$$

Case II, $0 < k \le N/2$: From (2.29) we have:

$$u_N = \sum_{j=1}^{N} \frac{\lambda_j^{11}}{\lambda_j^{11}\lambda_j^{22} - \lambda_j^{12}\lambda_j^{21}} \langle \boldsymbol{f_2}, \boldsymbol{\xi}_j\rangle \overline{\langle \boldsymbol{l_2}, \boldsymbol{\xi}_j\rangle} - \sum_{j=1}^{N} \frac{\lambda_j^{21}}{\lambda_j^{11}\lambda_j^{22} - \lambda_j^{12}\lambda_j^{21}} \langle \boldsymbol{f_1}, \boldsymbol{\xi}_j\rangle \overline{\langle \boldsymbol{l_2}, \boldsymbol{\xi}_j\rangle}$$
$$- \sum_{j=1}^{N} \frac{\lambda_j^{12}}{\lambda_j^{11}\lambda_j^{22} - \lambda_j^{12}\lambda_j^{21}} \langle \boldsymbol{f_2}, \boldsymbol{\xi}_j\rangle \overline{\langle \boldsymbol{l_1}, \boldsymbol{\xi}_j\rangle} + \sum_{j=1}^{N} \frac{\lambda_j^{22}}{\lambda_j^{11}\lambda_j^{22} - \lambda_j^{12}\lambda_j^{21}} \langle \boldsymbol{f_1}, \boldsymbol{\xi}_j\rangle \overline{\langle \boldsymbol{l_1}, \boldsymbol{\xi}_j\rangle},$$

where

$$\langle \boldsymbol{f_1}, \boldsymbol{\xi}_j\rangle = \begin{cases} \sqrt{N} & \text{if } j = k+1 \\ 0 & \text{otherwise}. \end{cases} \quad \text{and} \quad \langle \boldsymbol{f_2}, \boldsymbol{\xi}_j\rangle = \begin{cases} \sqrt{N}\varrho_2^k & \text{if } j = k+1 \\ 0 & \text{otherwise}. \end{cases}$$

Thus,

$$u_N = \frac{\sqrt{N}}{\lambda_{k+1}^{11}\lambda_{k+1}^{22} - \lambda_{k+1}^{12}\lambda_{k+1}^{21}} \{(\varrho_2^k\lambda_{k+1}^{11} - \lambda_{k+1}^{21})\overline{\langle \boldsymbol{l_2}, \boldsymbol{\xi}_{k+1}\rangle} + (\lambda_{k+1}^{22} - \varrho_2^k\lambda_{k+1}^{12})\overline{\langle \boldsymbol{l_1}, \boldsymbol{\xi}_{k+1}\rangle}\}$$

We can therefore write

$$|\frac{A}{B} - e^{ik\theta}| = \frac{|A - e^{ik\theta}B|}{|B|}$$

where

$$A = \sqrt{N}\{(\varrho_2^k\lambda_{k+1}^{11} - \lambda_{k+1}^{21})\overline{\langle \boldsymbol{l_2}, \boldsymbol{\xi}_{k+1}\rangle} + (\lambda_{k+1}^{22} - \varrho_2^k\lambda_{k+1}^{12})\overline{\langle \boldsymbol{l_1}, \boldsymbol{\xi}_{k+1}\rangle}\}$$

and

$$B = \lambda_{k+1}^{11}\lambda_{k+1}^{22} - \lambda_{k+1}^{12}\lambda_{k+1}^{21}.$$

Since $\varrho_1 = 1$, we have

$$\lambda_{k+1}^{11} = \frac{N}{4\pi}\sum_{m=0}^{\infty}\left\{R_1^{k+mN}\frac{1}{k+mN} + R_1^{N-k+mN}\frac{1}{N-k+mN}\right\}$$
$$\lambda_{k+1}^{12} = \frac{N}{4\pi}\sum_{m=0}^{\infty}\left\{\left(\frac{1}{R_2}\right)^{k+mN}\frac{1}{k+mN} + \left(\frac{1}{R_2}\right)^{N-k+mN}\frac{1}{N-k+mN}\right\}$$
$$\lambda_{k+1}^{21} = \frac{N}{4\pi}\sum_{m=0}^{\infty}\left\{\left(\frac{R_1}{\varrho_2}\right)^{k+mN}\frac{1}{k+mN} + \left(\frac{R_1}{\varrho_2}\right)^{N-k+mN}\frac{1}{N-k+mN}\right\}$$
$$\lambda_{k+1}^{22} = \frac{N}{4\pi}\sum_{m=0}^{\infty}\left\{\left(\frac{\varrho_2}{R_2}\right)^{k+mN}\frac{1}{k+mN} + \left(\frac{\varrho_2}{R_2}\right)^{N-k+mN}\frac{1}{N-k+mN}\right\}$$

and

$$\overline{\langle \boldsymbol{l_1}, \boldsymbol{\xi}_{k+1}\rangle} = \frac{\sqrt{N}}{4\pi}\sum_{m=1}^{\infty}\left\{R_1^{k+mN}\frac{e^{i(k+mN)\vartheta}}{k+mN} + R_1^{N-k+mN}\frac{e^{-i(N-k+mN)\vartheta}}{N-k+mN}\right\}$$

$$\overline{\langle \boldsymbol{l_2}, \boldsymbol{\xi}_{k+1}\rangle} = \frac{\sqrt{N}}{4\pi}\sum_{m=1}^{\infty}\left\{\left(\frac{1}{R_2}\right)^{k+mN}\frac{e^{i(k+mN)\vartheta}}{k+mN} + \left(\frac{1}{R_2}\right)^{N-k+mN}\frac{e^{-i(N-k+mN)\vartheta}}{N-k+mN}\right\}.$$

Next, we obtain a lower bound for $|B|$.

$$
\begin{aligned}
B =& \sum_{m=0}^{\infty} \left\{ \frac{R_1^{k+mN}}{k+mN} + \frac{R_1^{N-k+mN}}{N-k+mN} \right\} \sum_{m=0}^{\infty} \left\{ \left(\frac{\varrho_2}{R_2}\right)^{k+mN} \frac{1}{k+mN} \right. \\
& \left. + \left(\frac{\varrho_2}{R_2}\right)^{N-k+mN} \frac{1}{N-k+mN} \right\} \\
& - \sum_{m=0}^{\infty} \left\{ \left(\frac{1}{R_2}\right)^{k+mN} \frac{1}{k+mN} + \left(\frac{1}{R_2}\right)^{N-k+mN} \frac{1}{N-k+mN} \right\} \\
& \times \sum_{m=0}^{\infty} \left\{ \left(\frac{R_1}{\varrho_2}\right)^{k+mN} \frac{1}{k+mN} + \left(\frac{R_1}{\varrho_2}\right)^{N-k+mN} \frac{1}{N-k+mN} \right\} \\
=& \left\{ \frac{R_1}{k} + \frac{R_1^{N-k}}{N-k} + \sum_{m=1}^{\infty} \frac{R_1^{k+mN}}{k+mN} + \sum_{m=1}^{\infty} \frac{R_1^{N-k+mN}}{N-k+mN} \right\} \\
& \times \left\{ \frac{1}{k} \left(\frac{\varrho_2}{R_2}\right)^{k} + \frac{1}{N-k} \left(\frac{\varrho_2}{R_2}\right)^{N-k} \right. \\
& \left. + \sum_{m=1}^{\infty} \left(\frac{\varrho_2}{R_2}\right)^{k+mN} \frac{1}{k+mN} + \sum_{m=1}^{\infty} \left(\frac{\varrho_2}{R_2}\right)^{N-k+mN} \frac{1}{N-k+mN} \right\} \\
& - \left\{ \frac{1}{kR_2^k} + \frac{1}{(N-k)R_2^{N-k}} + \sum_{m=1}^{\infty} \left(\frac{1}{R_2}\right)^{k+mN} \frac{1}{k+mN} + \sum_{m=1}^{\infty} \left(\frac{1}{R_2}\right)^{N-k+mN} \frac{1}{N-k+mN} \right\} \\
& \times \left\{ \frac{1}{k} \left(\frac{R_1}{\varrho_2}\right)^{k} + \frac{1}{N-k} \left(\frac{R_1}{\varrho_2}\right)^{N-k} + \sum_{m=1}^{\infty} \left(\frac{R_1}{\varrho_2}\right)^{k+mN} \frac{1}{k+mN} + \sum_{m=1}^{\infty} \left(\frac{R_1}{\varrho_2}\right)^{N-k+mN} \frac{1}{N-k+mN} \right\} \\
=& \frac{1}{k^2} \frac{R_1^k \varrho_2^k}{R_2^k} + \frac{1}{k(N-k)} \frac{R_1^k \varrho_2^{N-k}}{R_2^{N-k}} + \frac{R_1^k}{k} \sum_{m=1}^{\infty} \left(\frac{\varrho_2}{R_2}\right)^{k+mN} \frac{1}{k+mN} \\
& + \frac{R_1^k}{k} \sum_{m=1}^{\infty} \left(\frac{\varrho_2}{R_2}\right)^{N-k+mN} \frac{1}{N-k+mN} \\
& + \frac{1}{k(N-k)} \frac{R_1^{N-k} \varrho_2^k}{R_2^k} + \frac{1}{(N-k)^2} \left(\frac{R_1 \varrho_2}{R_2}\right)^{N-k} + \frac{R_1^{N-k}}{N-k} \sum_{m=1}^{\infty} \left(\frac{\varrho_2}{R_2}\right)^{k+mN} \frac{1}{k+mN} \\
& + \frac{R_1^{N-k}}{N-k} \sum_{m=1}^{\infty} \left(\frac{\varrho_2}{R_2}\right)^{N-k+mN} \frac{1}{N-k+mN} \\
& + \frac{1}{k} \left(\frac{\varrho_2}{R_2}\right)^{k} \sum_{m=1}^{\infty} \frac{R_1^{k+mN}}{k+mN} + \frac{1}{N-k} \left(\frac{\varrho_2}{R_2}\right)^{N-k} \sum_{m=1}^{\infty} \frac{R_1^{k+mN}}{k+mN} \\
& + \sum_{m=1}^{\infty} \frac{R_1^{k+mN}}{k+mN} \sum_{m=1}^{\infty} \left(\frac{\varrho_2}{R_2}\right)^{k+mN} \frac{1}{k+mN} \\
& + \sum_{m=1}^{\infty} \frac{R_1^{k+mN}}{k+mN} \sum_{m=1}^{\infty} \left(\frac{\varrho_2}{R_2}\right)^{N-k+mN} \frac{1}{N-k+mN} \\
& + \frac{1}{k} \left(\frac{\varrho_2}{R_2}\right)^{k} \sum_{m=1}^{\infty} \frac{R_1^{N-k+mN}}{N-k+mN} + \frac{1}{N-k} \left(\frac{\varrho_2}{R_2}\right)^{N-k} \sum_{m=1}^{\infty} \frac{R_1^{N-k+mN}}{N-k+mN} \\
& + \sum_{m=1}^{\infty} \frac{R_1^{N-k+mN}}{N-k+mN} \sum_{m=1}^{\infty} \left(\frac{\varrho_2}{R_2}\right)^{k+mN} \frac{1}{k+mN}
\end{aligned}
$$

$$
\begin{aligned}
&+\sum_{m=1}^{\infty}\frac{R_1^{N-k+mN}}{N-k+mN}\sum_{m=1}^{\infty}\left(\frac{\varrho_2}{R_2}\right)^{N-k+mN}\frac{1}{N-k+mN}\\
&-\frac{1}{k^2}\frac{R_1^k}{\varrho_2^k R_2^k}-\frac{1}{k(N-k)}\frac{R_1^{N-k}}{\varrho_2^{N-k}R_2^k}-\frac{1}{kR_2^k}\sum_{m=1}^{\infty}\left(\frac{R_1}{\varrho_2}\right)^{k+mN}\frac{1}{k+mN}\\
&-\frac{1}{kR_2^k}\sum_{m=1}^{\infty}\left(\frac{R_1}{\varrho_2}\right)^{N-k+mN}\frac{1}{N-k+mN}\\
&-\frac{1}{k(N-k)}\frac{R_1^k}{\varrho_2^k R_2^{N-k}}-\frac{1}{(N-k)^2}\left(\frac{R_1}{\varrho_2 R_2}\right)^{N-k}-\frac{1}{(N-k)R_2^{N-k}}\sum_{m=1}^{\infty}\left(\frac{R_1}{\varrho_2}\right)^{k+mN}\frac{1}{k+mN}\\
&-\frac{1}{(N-k)R_2^{N-k}}\sum_{m=1}^{\infty}\left(\frac{R_1}{\varrho_2}\right)^{N-k+mN}\frac{1}{N-k+mN}\\
&-\frac{1}{k}\left(\frac{R_1}{\varrho_2}\right)^{k}\sum_{m=1}^{\infty}\left(\frac{1}{R_2}\right)^{k+mN}\frac{1}{k+mN}-\frac{1}{N-k}\left(\frac{R_1}{\varrho_2}\right)^{N-k}\sum_{m=1}^{\infty}\left(\frac{1}{R_2}\right)^{k+mN}\frac{1}{k+mN}\\
&-\sum_{m=1}^{\infty}\left(\frac{1}{R_2}\right)^{k+mN}\frac{1}{k+mN}\sum_{m=1}^{\infty}\left(\frac{R_1}{\varrho_2}\right)^{k+mN}\frac{1}{k+mN}\\
&-\sum_{m=1}^{\infty}\left(\frac{1}{R_2}\right)^{k+mN}\frac{1}{k+mN}\sum_{m=1}^{\infty}\left(\frac{R_1}{\varrho_2}\right)^{N-k+mN}\frac{1}{N-k+mN}\\
&-\frac{1}{k}\left(\frac{R_1}{\varrho_2}\right)^{k}\sum_{m=1}^{\infty}\left(\frac{1}{R_2}\right)^{N-k+mN}\frac{1}{N-k+mN}-\frac{1}{N-k}\left(\frac{R_1}{\varrho_2}\right)^{N-k}\sum_{m=1}^{\infty}\left(\frac{1}{R_2}\right)^{N-k+mN}\frac{1}{N-k+mN}\\
&-\sum_{m=1}^{\infty}\left(\frac{1}{R_2}\right)^{N-k+mN}\frac{1}{N-k+mN}\sum_{m=1}^{\infty}\left(\frac{R_1}{\varrho_2}\right)^{k+mN}\frac{1}{k+mN}\\
&-\sum_{m=1}^{\infty}\left(\frac{1}{R_2}\right)^{N-k+mN}\frac{1}{N-k+mN}\sum_{m=1}^{\infty}\left(\frac{R_1}{\varrho_2}\right)^{N-k+mN}\frac{1}{N-k+mN}\\
=&\frac{1}{k^2}\frac{R_1^k}{R_2^k}\left(\varrho_2^k-\frac{1}{\varrho_2^k}\right)+\frac{1}{k(N-k)}\left(\frac{R_1^k\varrho_2^{N-k}}{R_2^{N-k}}-\frac{R_1^k}{\varrho_2^k R_2^{N-k}}\right)\\
&+\frac{1}{k(N-k)}\left(\frac{R_1^{N-k}\varrho_2^k}{R_2^k}-\frac{R_1^{N-k}}{\varrho_2^{N-k}R_2^k}\right)\\
&+\frac{1}{k}\sum_{m=1}^{\infty}\left\{\frac{R_1^k\varrho_2^{k+mN}}{R_2^{k+mN}}-\frac{R_1^k}{\varrho_2^k R_2^{k+mN}}\right\}\frac{1}{k+mN}\\
&+\frac{1}{k}\sum_{m=1}^{\infty}\left\{\frac{R_1^{k+mN}\varrho_2^k}{R_2^k}-\frac{R_1^{k+mN}}{\varrho_2^{k+mN}R_2^k}\right\}\frac{1}{k+mN}\\
&+\frac{1}{k}\sum_{m=1}^{\infty}\left\{\frac{R_1^k\varrho_2^{N-k+mN}}{R_2^{N-k+mN}}-\frac{R_1^k}{\varrho_2^k R_2^{N-k+mN}}\right\}\frac{1}{N-k+mN}\\
&+\frac{1}{k}\sum_{m=1}^{\infty}\left\{\frac{R_1^{N-k+mN}\varrho_2^k}{R_2^k}-\frac{R_1^{N-k+mN}}{\varrho_2^{N-k+mN}R_2^k}\right\}\frac{1}{N-k+mN}\\
&+\frac{1}{(N-k)^2}\left\{\left(\frac{R_1\varrho_2}{R_2}\right)^{N-k}-\left(\frac{R_1}{\varrho_2 R_2}\right)^{N-k}\right\}\\
&+\frac{1}{N-k}\sum_{m=1}^{\infty}\left\{\frac{R_1^{N-k}\varrho_2^{k+mN}}{R_2^{k+mN}}-\frac{R_1^{N-k}}{\varrho_2^{N-k}R_2^{k+mN}}\right\}\frac{1}{k+mN}
\end{aligned}
$$

$$
\begin{aligned}
&+ \frac{1}{N-k}\sum_{m=1}^{\infty}\left\{\frac{\varrho_2^{N-k}R_1^{k+mN}}{R_2^{N-k}} - \frac{R_1^{k+mN}}{\varrho_2^{k+mN}R_2^{N-k}}\right\}\frac{1}{k+mN} + \\
&\frac{1}{N-k}\sum_{m=1}^{\infty}\left\{\frac{R_1^{N-k}\varrho_2^{N-k+mN}}{R_2^{N-k+mN}} - \frac{R_1^{N-k}}{\varrho_2^{N-k}R_2^{N-k+mN}}\right\}\frac{1}{N-k+mN} \\
&+ \frac{1}{N-k}\sum_{m=1}^{\infty}\left\{\frac{\varrho_2^{N-k}R_1^{N-k+mN}}{R_2^{N-k}} - \frac{R_1^{N-k+mN}}{\varrho_2^{N-k+mN}R_2^{N-k}}\right\}\frac{1}{N-k+mN} \\
&\left\{\sum_{m=1}^{\infty}\frac{R_1^{k+mN}}{k+mN}\sum_{m=1}^{\infty}\left(\frac{\varrho_2}{R_2}\right)^{k+mN}\frac{1}{k+mN}\right. \\
&\left.-\sum_{m=1}^{\infty}\left(\frac{1}{R_2}\right)^{k+mN}\frac{1}{k+mN}\sum_{m=1}^{\infty}\left(\frac{R_1}{\varrho_2}\right)^{k+mN}\frac{1}{k+mN}\right\} \\
&+\left\{\sum_{m=1}^{\infty}\frac{R_1^{k+mN}}{k+mN}\sum_{m=1}^{\infty}\left(\frac{\varrho_2}{R_2}\right)^{N-k+mN}\frac{1}{N-k+mN}\right. \\
&\left.-\sum_{m=1}^{\infty}\left(\frac{1}{R_2}\right)^{N-k+mN}\frac{1}{N-k+mN}\sum_{m=1}^{\infty}\left(\frac{R_1}{\varrho_2}\right)^{k+mN}\frac{1}{k+mN}\right\} \\
&\left\{\sum_{m=1}^{\infty}\frac{R_1^{N-k+mN}}{N-k+mN}\sum_{m=1}^{\infty}\left(\frac{\varrho_2}{R_2}\right)^{k+mN}\frac{1}{k+mN}\right. \\
&\left.-\sum_{m=1}^{\infty}\left(\frac{1}{R_2}\right)^{k+mN}\frac{1}{k+mN}\sum_{m=1}^{\infty}\left(\frac{R_1}{\varrho_2}\right)^{N-k+mN}\frac{1}{N-k+mN}\right\} \\
&+\left\{\sum_{m=1}^{\infty}\frac{R_1^{N-k+mN}}{N-k+mN}\sum_{m=1}^{\infty}\left(\frac{\varrho_2}{R_2}\right)^{N-k+mN}\frac{1}{N-k+mN}\right. \\
&\left.-\sum_{m=1}^{\infty}\left(\frac{1}{R_2}\right)^{N-k+mN}\frac{1}{N-k+mN}\sum_{m=1}^{\infty}\left(\frac{R_1}{\varrho_2}\right)^{N-k+mN}\frac{1}{N-k+mN}\right\}.
\end{aligned}
$$

Since each term is positive we have that

$$
B \geq \frac{1}{k^2}\frac{R_1^k}{R_2^k}\left(\varrho_2^k - \frac{1}{\varrho_2^k}\right). \tag{2.49}
$$

On the other hand we have:

$$
\begin{aligned}
\left|A - e^{ik\vartheta}B\right| = \; &\Big|\sqrt{N}\{(\varrho_2^k\lambda_{k+1}^{11} - \lambda_{k+1}^{21})\langle\overline{\boldsymbol{l_2}, \boldsymbol{\xi}_{k+1}}\rangle + (\lambda_{k+1}^{22} - \varrho_2^k\lambda_{k+1}^{12})\langle\overline{\boldsymbol{l_1}, \boldsymbol{\xi}_{k+1}}\rangle\} \\
&- \{e^{ik\vartheta}(\lambda_{k+1}^{11}\lambda_{k+1}^{22} - \lambda_{k+1}^{12}\lambda_{k+1}^{21})\}\Big|
\end{aligned} \tag{2.50}
$$

$$
\begin{aligned}
=&\frac{N^2}{16\pi^2}\Bigg|\varrho_2^k \sum_{m=0}^{\infty}\left\{\frac{R_1^{k+mN}}{k+mN}+\frac{R_1^{N-k+mN}}{N-k+mN}\right\} \\
&\times \sum_{m=0}^{\infty}\left\{\left(\frac{1}{R_2}\right)^{k+mN}\frac{e^{i(k+mN)\vartheta}}{k+mN}+\left(\frac{1}{R_2}\right)^{N-k+mN}\frac{e^{-i(N-k+mN)\vartheta}}{N-k+mN}\right\} \\
&-\sum_{m=0}^{\infty}\left\{\left(\frac{R_1}{\varrho_2}\right)^{k+mN}\frac{1}{k+mN}+\left(\frac{R_1}{\varrho_2}\right)^{N-k+mN}\frac{1}{N-k+mN}\right\} \\
&\times \sum_{m=0}^{\infty}\left\{\left(\frac{1}{R_2}\right)^{k+mN}\frac{e^{i(k+mN)\vartheta}}{k+mN}+\left(\frac{1}{R_2}\right)^{N-k+mN}\frac{e^{-i(N-k+mN)\vartheta}}{N-k+mN}\right\} \\
&+\sum_{m=0}^{\infty}\left\{\left(\frac{\varrho_2}{R_2}\right)^{k+mN}\frac{1}{k+mN}+\left(\frac{\varrho_2}{R_2}\right)^{N-k+mN}\frac{1}{N-k+mN}\right\} \\
&\times \sum_{m=0}^{\infty}\left\{R_1^{k+mN}\frac{e^{i(k+mN)\vartheta}}{k+mN}+R_1^{N-k+mN}\frac{e^{-i(N-k+mN)\vartheta}}{N-k+mN}\right\} \\
&-\varrho_2^k\sum_{m=0}^{\infty}\left\{\left(\frac{1}{R_2}\right)^{k+mN}\frac{1}{k+mN}+\left(\frac{1}{R_2}\right)^{N-k+mN}\frac{1}{N-k+mN}\right\} \\
&\times \sum_{m=0}^{\infty}\left\{R_1^{k+mN}\frac{e^{i(k+mN)\vartheta}}{k+mN}+R_1^{N-k+mN}\frac{e^{-i(N-k+mN)\vartheta}}{N-k+mN}\right\} \\
&-e^{ik\vartheta}\sum_{m=0}^{\infty}\left\{\frac{R_1^{k+mN}}{k+mN}+\frac{R_1^{N-k+mN}}{N-k+mN}\right\} \\
&\times \sum_{m=0}^{\infty}\left\{\left(\frac{\varrho_2}{R_2}\right)^{k+mN}\frac{1}{k+mN}+\left(\frac{\varrho_2}{R_2}\right)^{N-k+mN}\frac{1}{N-k+mN}\right\} \\
&+e^{ik\vartheta}\sum_{m=0}^{\infty}\left\{\left(\frac{1}{R_2}\right)^{k+mN}\frac{1}{k+mN}+\left(\frac{1}{R_2}\right)^{N-k+mN}\frac{1}{N-k+mN}\right\}
\end{aligned}
$$

$$
\times \sum_{m=0}^{\infty}\left\{\left(\frac{R_1}{\varrho_2}\right)^{k+mN}\frac{1}{k+mN}+\left(\frac{R_1}{\varrho_2}\right)^{N-k+mN}\frac{1}{N-k+mN}\right\}\Bigg| \tag{2.51}
$$

$$
\begin{aligned}
=&\frac{N^2}{16\pi^2}\Bigg|\varrho_2^k\left\{\frac{R_1^k}{k}+\frac{R_1^{N-k}}{N-k}+\sum_{m=1}^{\infty}\frac{R_1^{k+mN}}{k+mN}+\sum_{m=1}^{\infty}\frac{R_1^{N-k+mN}}{N-k+mN}\right\}\\
&\times\left\{\frac{1}{R_2^k}\frac{e^{ik\vartheta}}{k}+\frac{1}{R_2^{N-k}}\frac{e^{-i(N-k)\vartheta}}{N-k}+\sum_{m=1}^{\infty}\frac{1}{R_2^{k+mN}}\frac{e^{i(k+mN)\vartheta}}{k+mN}+\sum_{m=1}^{\infty}\frac{1}{R_2^{N-k+mN}}\frac{e^{-i(N-k+mN)\vartheta}}{N-k+mN}\right\}\\
&-\varrho_2^k\left\{R_1^k\frac{e^{ik\vartheta}}{k}+R_1^{N-k}\frac{e^{-i(N-k)\vartheta}}{N-k}+\sum_{m=1}^{\infty}R_1^{k+mN}\frac{e^{i(k+mN)\vartheta}}{k+mN}+\sum_{m=1}^{\infty}R_1^{N-k+mN}\frac{e^{-i(N-k+mN)\vartheta}}{N-k+mN}\right\}\\
&\times\left\{\frac{1}{R_2^k}\frac{1}{k}+\frac{1}{R_2^{N-k}}\frac{1}{N-k}+\sum_{m=1}^{\infty}\frac{1}{R_2^{k+mN}}\frac{1}{k+mN}+\sum_{m=1}^{\infty}\frac{1}{R_2^{N-k+mN}}\frac{1}{N-k+mN}\right\}\\
&+\left\{\left(\frac{R_1}{\varrho_2}\right)^k\frac{1}{k}+\left(\frac{R_1}{\varrho_2}\right)^{N-k}\frac{1}{N-k}+\sum_{m=1}^{\infty}\left(\frac{R_1}{\varrho_2}\right)^{k+mN}\frac{1}{k+mN}+\sum_{m=1}^{\infty}\left(\frac{R_1}{\varrho_2}\right)^{N-k+mN}\frac{1}{N-k+mN}\right\}\\
&\times\left\{\frac{1}{R_2^k}\frac{e^{ik\vartheta}}{k}+\frac{1}{R_2^{N-k}}\frac{e^{ik\vartheta}}{N-k}+\sum_{m=1}^{\infty}\frac{1}{R_2^{k+mN}}\frac{e^{ik\vartheta}}{k+mN}+\sum_{m=1}^{\infty}\frac{1}{R_2^{N-k+mN}}\frac{e^{ik\vartheta}}{N-k+mN}\right\}\\
&-\left\{\left(\frac{R_1}{\varrho_2}\right)^k\frac{1}{k}+\left(\frac{R_1}{\varrho_2}\right)^{N-k}\frac{1}{N-k}+\sum_{m=1}^{\infty}\left(\frac{R_1}{\varrho_2}\right)^{k+mN}\frac{1}{k+mN}+\sum_{m=1}^{\infty}\left(\frac{R_1}{\varrho_2}\right)^{N-k+mN}\frac{1}{N-k+mN}\right\}\\
&\times\left\{\frac{1}{R_2^k}\frac{e^{ik\vartheta}}{k}+\frac{1}{R_2^{N-k}}\frac{e^{-i(N-k)\vartheta}}{N-k}+\sum_{m=1}^{\infty}\frac{1}{R_2^{k+mN}}\frac{e^{i(k+mN)\vartheta}}{k+mN}+\sum_{m=1}^{\infty}\frac{1}{R_2^{N-k+mN}}\frac{e^{-i(N-k+mN)\vartheta}}{N-k+mN}\right\}\\
&+\left\{R_1^k\frac{e^{ik\vartheta}}{k}+R_1^{N-k}\frac{e^{-i(N-k)\vartheta}}{N-k}+\sum_{m=1}^{\infty}R_1^{k+mN}\frac{e^{i(k+mN)\vartheta}}{k+mN}+\sum_{m=1}^{\infty}R_1^{N-k+mN}\frac{e^{-i(N-k+mN)\vartheta}}{N-k+mN}\right\}\\
&\times\left\{\left(\frac{\varrho_2}{R_2}\right)^k\frac{1}{k}+\left(\frac{\varrho_2}{R_2}\right)^{N-k}\frac{1}{N-k}+\sum_{m=1}^{\infty}\left(\frac{\varrho_2}{R_2}\right)^{k+mN}\frac{1}{k+mN}+\sum_{m=1}^{\infty}\left(\frac{\varrho_2}{R_2}\right)^{N-k+mN}\frac{1}{N-k+mN}\right\}\\
&-\left\{R_1^k\frac{e^{ik\vartheta}}{k}+R_1^{N-k}\frac{e^{ik\vartheta}}{N-k}+\sum_{m=1}^{\infty}R_1^{k+mN}\frac{e^{ik\vartheta}}{k+mN}+\sum_{m=1}^{\infty}R_1^{N-k+mN}\frac{e^{ik\vartheta}}{N-k+mN}\right\}\\
&\times\left\{\left(\frac{\varrho_2}{R_2}\right)^k\frac{1}{k}+\left(\frac{\varrho_2}{R_2}\right)^{N-k}\frac{1}{N-k}+\sum_{m=1}^{\infty}\left(\frac{\varrho_2}{R_2}\right)^{k+mN}\frac{1}{k+mN}+\sum_{m=1}^{\infty}\left(\frac{\varrho_2}{R_2}\right)^{N-k+mN}\frac{1}{N-k+mN}\right\}\Bigg|_{\infty}\\
=&\frac{N^2}{16\pi^2}\Bigg|\varrho_2^k\left\{\frac{R_1^k}{R_2^k}\frac{e^{ik\vartheta}}{k^2}+\frac{R_1^k}{R_2^{N-k}}\frac{e^{-i(N-k)\vartheta}}{k(N-k)}+\frac{R_1^k}{k}\sum_{m=1}^{\infty}\frac{1}{R_2^{k+mN}}\frac{e^{i(k+mN)\vartheta}}{k+mN}+\frac{R_1^k}{k}\sum_{m=1}^{\infty}\frac{1}{R_2^{N-k+mN}}\frac{e^{-i(N-k+mN)\vartheta}}{N-k+mN}\right\}\\
&+\varrho_2^k\left\{\frac{R_1^{N-k}}{R_2^k}\frac{e^{ik\vartheta}}{k(N-k)}+\frac{R_1^{N-k}}{R_2^{N-k}}\frac{e^{-i(N-k)\vartheta}}{(N-k)^2}+\frac{R_1^{N-k}}{N-k}\sum_{m=1}^{\infty}\frac{1}{R_2^{k+mN}}\frac{e^{i(k+mN)\vartheta}}{k+mN}\right.\\
&\left.+\frac{R_1^{N-k}}{N-k}\sum_{m=1}^{\infty}\frac{1}{R_2^{N-k+mN}}\frac{e^{-i(N-k+mN)\vartheta}}{N-k+mN}\right\}\\
&+\varrho_2^k\left\{\frac{1}{R_2^k}\frac{e^{ik\vartheta}}{k}\sum_{m=1}^{\infty}\frac{R_1^{k+mN}}{k+mN}+\frac{1}{R_2^{N-k}}\frac{e^{-i(N-k)\vartheta}}{N-k}\sum_{m=1}^{\infty}\frac{R_1^{k+mN}}{k+mN}+\sum_{m=1}^{\infty}\frac{R_1^{k+mN}}{k+mN}\sum_{m=1}^{\infty}\frac{1}{R_2^{k+mN}}\frac{e^{i(k+mN)\vartheta}}{k+mN}\right.\\
&\left.+\sum_{m=1}^{\infty}\frac{R_1^{k+mN}}{k+mN}\sum_{m=1}^{\infty}\frac{1}{R_2^{N-k+mN}}\frac{e^{-i(N-k+mN)\vartheta}}{N-k+mN}\right\}\\
&+\varrho_2^k\left\{\frac{1}{R_2^k}\frac{e^{ik\vartheta}}{k}\sum_{m=1}^{\infty}\frac{R_1^{N-k+mN}}{N-k+mN}+\frac{1}{R_2^{N-k}}\frac{e^{-i(N-k)\vartheta}}{N-k}\sum_{m=1}^{\infty}\frac{R_1^{N-k+mN}}{N-k+mN}\right.
\end{aligned}
$$

$$+\sum_{m=1}^{\infty}\frac{R_1^{N-k+mN}}{N-k+mN}\sum_{m=1}^{\infty}\frac{1}{R_2^{k+mN}}\frac{e^{i(k+mN)\vartheta}}{k+mN}\sum_{m=1}^{\infty}\frac{R_1^{N-k+mN}}{N-k+mN}\sum_{m=1}^{\infty}\frac{1}{R_2^{N-k+mN}}\frac{e^{-i(N-k+mN)\vartheta}}{N-k+mN}\Bigg\}$$

$$-\varrho_2^k\Bigg\{\frac{R_1^k}{R_2^k}\frac{e^{ik\vartheta}}{k^2}+\frac{R_1^k}{R_2^{N-k}}\frac{e^{ik\vartheta}}{k(N-k)}+R_1^k\frac{e^{ik\vartheta}}{k}\sum_{m=1}^{\infty}\frac{1}{R_2^{k+mN}}\frac{1}{k+mN}+R_1^k\frac{e^{ik\vartheta}}{k}\sum_{m=1}^{\infty}\frac{1}{R_2^{N-k+mN}}\frac{1}{N-k+mN}\Bigg\}$$

$$-\varrho_2^k\Bigg\{\frac{R_1^{N-k}}{R_2^k}\frac{e^{-i(N-k)\vartheta}}{k(N-k)}+\frac{R_1^{N-k}}{R_2^{N-k}}\frac{e^{-i(N-k)\vartheta}}{(N-k)^2}+R_1^{N-k}\frac{e^{-i(N-k)\vartheta}}{N-k}\sum_{m=1}^{\infty}\frac{1}{R_2^{k+mN}}\frac{1}{k+mN}$$

$$+R_1^{N-k}\frac{e^{-i(N-k)\vartheta}}{N-k}\sum_{m=1}^{\infty}\frac{1}{R_2^{N-k+mN}}\frac{1}{N-k+mN}\Bigg\}$$

$$-\varrho_2^k\Bigg\{\frac{1}{R_2^k}\frac{1}{k}\sum_{m=1}^{\infty}R_1^{k+mN}\frac{e^{i(k+mN)\vartheta}}{k+mN}+\frac{1}{R_2^{N-k}}\frac{1}{N-k}\sum_{m=1}^{\infty}R_1^{k+mN}\frac{e^{i(k+mN)\vartheta}}{k+mN}$$

$$+\sum_{m=1}^{\infty}R_1^{k+mN}\frac{e^{i(k+mN)\vartheta}}{k+mN}\sum_{m=1}^{\infty}\frac{1}{R_2^{k+mN}}\frac{1}{k+mN}+\sum_{m=1}^{\infty}R_1^{k+mN}\frac{e^{i(k+mN)\vartheta}}{k+mN}\sum_{m=1}^{\infty}\frac{1}{R_2^{N-k+mN}}\frac{1}{N-k+mN}\Bigg\}$$

$$-\varrho_2^k\Bigg\{\frac{1}{R_2^k}\frac{1}{k}\sum_{m=1}^{\infty}R_1^{N-k+mN}\frac{e^{-i(N-k+mN)\vartheta}}{N-k+mN}+\frac{1}{R_2^{N-k}}\frac{1}{N-k}\sum_{m=1}^{\infty}R_1^{N-k+mN}\frac{e^{-i(N-k+mN)\vartheta}}{N-k+mN}$$

$$+\sum_{m=1}^{\infty}R_1^{N-k+mN}\frac{e^{-i(N-k+mN)\vartheta}}{N-k+mN}\sum_{m=1}^{\infty}\frac{1}{R_2^{k+mN}}\frac{1}{k+mN}$$

$$+\sum_{m=1}^{\infty}R_1^{N-k+mN}\frac{e^{-i(N-k+mN)\vartheta}}{N-k+mN}\sum_{m=1}^{\infty}\frac{1}{R_2^{N-k+mN}}\frac{1}{N-k+mN}\Bigg\}$$

$$+\Bigg\{\frac{R_1^k}{\varrho_2^kR_2^{N-k}}\frac{e^{ik\vartheta}}{k(N-k)}+\left(\frac{R_1}{\varrho_2}\right)^k\frac{1}{k}\sum_{m=1}^{\infty}\left(\frac{1}{R_2}\right)^{k+mN}\frac{e^{ik\vartheta}}{k+mN}$$

$$+\left(\frac{R_1}{\varrho_2}\right)^k\frac{1}{k}\sum_{m=1}^{\infty}\left(\frac{1}{R_2}\right)^{N-k+mN}\frac{e^{ik\vartheta}}{N-k+mN}\Bigg\}$$

$$+\Bigg\{\left(\frac{R_1}{\varrho_2R_2}\right)^{N-k}\frac{e^{ik\vartheta}}{(N-k)^2}+\left(\frac{R_1}{\varrho_2}\right)^{N-k}\frac{1}{N-k}\sum_{m=1}^{\infty}\left(\frac{1}{R_2}\right)^{k+mN}\frac{e^{ik\vartheta}}{k+mN}$$

$$+\left(\frac{R_1}{\varrho_2}\right)^{N-k}\frac{1}{N-k}\sum_{m=1}^{\infty}\left(\frac{1}{R_2}\right)^{N-k+mN}\frac{e^{ik\vartheta}}{N-k+mN}\Bigg\}$$

$$+\Bigg\{\frac{1}{R_2^{N-k}}\frac{e^{ik\vartheta}}{N-k}\sum_{m=1}^{\infty}\left(\frac{R_1}{\varrho_2}\right)^{k+mN}\frac{1}{k+mN}$$

$$+\sum_{m=1}^{\infty}\left(\frac{R_1}{\varrho_2}\right)^{k+mN}\frac{1}{k+mN}\sum_{m=1}^{\infty}\left(\frac{1}{R_2}\right)^{k+mN}\frac{e^{ik\vartheta}}{k+mN}$$

$$+\sum_{m=1}^{\infty}\left(\frac{R_1}{\varrho_2}\right)^{k+mN}\frac{1}{k+mN}\sum_{m=1}^{\infty}\left(\frac{1}{R_2}\right)^{N-k+mN}\frac{e^{ik\vartheta}}{N-k+mN}\Bigg\}$$

$$+\Bigg\{\frac{1}{R_2^{N-k}}\frac{e^{ik\vartheta}}{N-k}\sum_{m=1}^{\infty}\left(\frac{R_1}{\varrho_2}\right)^{N-k+mN}\frac{1}{N-k+mN}$$

$$+\sum_{m=1}^{\infty}\left(\frac{R_1}{\varrho_2}\right)^{N-k+mN}\frac{1}{N-k+mN}\sum_{m=1}^{\infty}\left(\frac{1}{R_2}\right)^{k+mN}\frac{e^{ik\vartheta}}{k+mN}$$

$$+\sum_{m=1}^{\infty}\left(\frac{R_1}{\varrho_2}\right)^{N-k+mN}\frac{1}{N-k+mN}\sum_{m=1}^{\infty}\left(\frac{1}{R_2}\right)^{N-k+mN}\frac{e^{ik\vartheta}}{N-k+mN}\Bigg\}$$

$$
\begin{aligned}
&- \Bigg\{ \frac{R_1^k}{\varrho_2^k R_2^{N-k}} \frac{e^{-i(N-k)\vartheta}}{k(N-k)} + \left(\frac{R_1}{\varrho_2}\right)^k \frac{1}{k} \sum_{m=1}^{\infty} \left(\frac{1}{R_2}\right)^{k+mN} \frac{e^{i(k+mN)\vartheta}}{k+mN} \\
&+ \left(\frac{R_1}{\varrho_2}\right)^k \frac{1}{k} \sum_{m=1}^{\infty} \left(\frac{1}{R_2}\right)^{N-k+mN} \frac{e^{-i(N-k+mN)\vartheta}}{N-k+mN} \Bigg\} \\
&- \Bigg\{ \left(\frac{R_1}{\varrho_2 R_2}\right)^{N-k} \frac{e^{-i(N-k)\vartheta}}{(N-k)^2} + \left(\frac{R_1}{\varrho_2}\right)^{N-k} \frac{1}{N-k} \sum_{m=1}^{\infty} \left(\frac{1}{R_2}\right)^{k+mN} \frac{e^{i(k+mN)\vartheta}}{k+mN} \\
&+ \left(\frac{R_1}{\varrho_2}\right)^{N-k} \frac{1}{N-k} \sum_{m=1}^{\infty} \left(\frac{1}{R_2}\right)^{N-k+mN} \frac{e^{-i(N-k+mN)\vartheta}}{N-k+mN} \Bigg\} \\
&- \Bigg\{ \frac{1}{R_2^{N-k}} \frac{e^{-i(N-k)\vartheta}}{N-k} \sum_{m=1}^{\infty} \left(\frac{R_1}{\varrho_2}\right)^{k+mN} \frac{1}{k+mN} \\
&+ \sum_{m=1}^{\infty} \left(\frac{R_1}{\varrho_2}\right)^{k+mN} \frac{1}{k+mN} \sum_{m=1}^{\infty} \left(\frac{1}{R_2}\right)^{k+mN} \frac{e^{i(k+mN)\vartheta}}{k+mN} \\
&+ \sum_{m=1}^{\infty} \left(\frac{R_1}{\varrho_2}\right)^{k+mN} \frac{1}{k+mN} \sum_{m=1}^{\infty} \left(\frac{1}{R_2}\right)^{N-k+mN} \frac{e^{-i(N-k+mN)\vartheta}}{N-k+mN} \Bigg\} \\
&- \Bigg\{ \frac{1}{R_2^{N-k}} \frac{e^{-i(N-k)\vartheta}}{N-k} \sum_{m=1}^{\infty} \left(\frac{R_1}{\varrho_2}\right)^{N-k+mN} \frac{1}{N-k+mN} \\
&+ \sum_{m=1}^{\infty} \left(\frac{R_1}{\varrho_2}\right)^{N-k+mN} \frac{1}{N-k+mN} \sum_{m=1}^{\infty} \left(\frac{1}{R_2}\right)^{k+mN} \frac{e^{i(k+mN)\vartheta}}{k+mN} \\
&+ \sum_{m=1}^{\infty} \left(\frac{R_1}{\varrho_2}\right)^{N-k+mN} \frac{1}{N-k+mN} \sum_{m=1}^{\infty} \left(\frac{1}{R_2}\right)^{N-k+mN} \frac{e^{-i(N-k+mN)\vartheta}}{N-k+mN} \Bigg\} \\
&+ \Bigg\{ \frac{R_1^{N-k} \varrho_2^k}{R_2^k} \frac{e^{-i(N-k)\vartheta}}{k(N-k)} + \left(\frac{R_1 \varrho_2}{R_2}\right)^{N-K} \frac{e^{-i(N-k)\vartheta}}{(N-k)^2} + R_1^{N-k} \frac{e^{-i(N-k)\vartheta}}{N-k} \sum_{m=1}^{\infty} \left(\frac{\varrho_2}{R_2}\right)^{k+mN} \frac{1}{k+mN} \\
&+ R_1^{N-k} \frac{e^{-i(N-k)\vartheta}}{N-k} \sum_{m=1}^{\infty} \left(\frac{\varrho_2}{R_2}\right)^{N-k+mN} \frac{1}{N-k+mN} \Bigg\} \\
&+ \Bigg\{ \left(\frac{\varrho_2}{R_2}\right)^k \frac{1}{k} \sum_{m=1}^{\infty} R_1^{k+mN} \frac{e^{i(k+mN)\vartheta}}{k+mN} + \left(\frac{\varrho_2}{R_2}\right)^{N-k} \frac{1}{N-k} \sum_{m=1}^{\infty} R_1^{k+mN} \frac{e^{i(k+mN)\vartheta}}{k+mN} \\
&+ \sum_{m=1}^{\infty} R_1^{k+mN} \frac{e^{i(k+mN)\vartheta}}{k+mN} \sum_{m=1}^{\infty} \left(\frac{\varrho_2}{R_2}\right)^{k+mN} \frac{1}{k+mN} \\
&+ \sum_{m=1}^{\infty} R_1^{k+mN} \frac{e^{i(k+mN)\vartheta}}{k+mN} \sum_{m=1}^{\infty} \left(\frac{\varrho_2}{R_2}\right)^{N-k+mN} \frac{1}{N-k+mN} \Bigg\} \\
&+ \Bigg\{ \left(\frac{\varrho_2}{R_2}\right)^k \frac{1}{k} \sum_{m=1}^{\infty} R_1^{N-k+mN} \frac{e^{-i(N-k+mN)\vartheta}}{k+mN} + \left(\frac{\varrho_2}{R_2}\right)^{N-k} \frac{1}{N-k} \sum_{m=1}^{\infty} R_1^{N-k+mN} \frac{e^{-i(N-k+mN)\vartheta}}{N-k+mN} \\
&+ \sum_{m=1}^{\infty} R_1^{N-k+mN} \frac{e^{-i(N-k+mN)\vartheta}}{N-k+mN} \sum_{m=1}^{\infty} \left(\frac{\varrho_2}{R_2}\right)^{k+mN} \frac{1}{k+mN} \\
&+ \sum_{m=1}^{\infty} R_1^{N-k+mN} \frac{e^{-i(N-k+mN)\vartheta}}{N-k+mN} \sum_{m=1}^{\infty} \left(\frac{\varrho_2}{R_2}\right)^{N-k+mN} \frac{1}{N-k+mN} \Bigg\} \\
&- \Bigg\{ \frac{R_1^{N-k} \varrho_2^k}{R_2^k} \frac{e^{ik\vartheta}}{k(N-k)} + \left(\frac{R_1 \varrho_2}{R_2}\right)^{N-K} \frac{e^{ik\vartheta}}{(N-k)^2} + R_1^{N-k} \frac{e^{ik\vartheta}}{N-k} \sum_{m=1}^{\infty} \left(\frac{\varrho_2}{R_2}\right)^{k+mN} \frac{1}{k+mN}
\end{aligned}
$$

$$
\begin{aligned}
&+ R_1^{N-k} \frac{e^{ik\vartheta}}{N-k} \sum_{m=1}^{\infty} \left(\frac{\varrho_2}{R_2}\right)^{N-k+mN} \frac{1}{N-k+mN} \Bigg\} \\
&- \Bigg\{ \left(\frac{\varrho_2}{R_2}\right)^{k} \frac{1}{k} \sum_{m=1}^{\infty} R_1^{k+mN} \frac{e^{ik\vartheta}}{k+mN} + \left(\frac{\varrho_2}{R_2}\right)^{N-k} \frac{1}{N-k} \sum_{m=1}^{\infty} R_1^{k+mN} \frac{e^{ik\vartheta}}{k+mN} \\
&+ \sum_{m=1}^{\infty} R_1^{k+mN} \frac{e^{ik\vartheta}}{k+mN} \sum_{m=1}^{\infty} \left(\frac{\varrho_2}{R_2}\right)^{k+mN} \frac{1}{k+mN} \\
&+ \sum_{m=1}^{\infty} R_1^{k+mN} \frac{e^{ik\vartheta}}{k+mN} \sum_{m=1}^{\infty} \left(\frac{\varrho_2}{R_2}\right)^{N-k+mN} \frac{1}{N-k+mN} \Bigg\} \\
&- \Bigg\{ \left(\frac{\varrho_2}{R_2}\right)^{k} \frac{1}{k} \sum_{m=1}^{\infty} R_1^{N-k+mN} \frac{e^{ik\vartheta}}{k+mN} + \left(\frac{\varrho_2}{R_2}\right)^{N-k} \frac{1}{N-k} \sum_{m=1}^{\infty} R_1^{N-k+mN} \frac{e^{ik\vartheta}}{N-k+mN} \\
&+ \sum_{m=1}^{\infty} R_1^{N-k+mN} \frac{e^{ik\vartheta}}{N-k+mN} \sum_{m=1}^{\infty} \left(\frac{\varrho_2}{R_2}\right)^{k+mN} \frac{1}{k+mN} \\
&+ \sum_{m=1}^{\infty} R_1^{N-k+mN} \frac{e^{ik\vartheta}}{N-k+mN} \sum_{m=1}^{\infty} \left(\frac{\varrho_2}{R_2}\right)^{N-k+mN} \frac{1}{N-k+mN} \Bigg\} \\
\le & \frac{2N^2}{16\pi^2} \Bigg\{ \varrho_2^k \Bigg\{ \frac{R_1^k}{R_2^{N-k}} + R_1^k \sum_{m=1}^{\infty} \left(\frac{1}{R_2}\right)^{k+mN} + R_1^k \sum_{m=1}^{\infty} \left(\frac{1}{R_2}\right)^{N-k+mN} + \frac{R_1^{N-k}}{R_2^k} + \left(\frac{R_1}{R_2}\right)^{N-k} \\
&+ R_1^{N-k} \sum_{m=1}^{\infty} \left(\frac{1}{R_2}\right)^{k+mN} + R_1^{N-k} \sum_{m=1}^{\infty} \left(\frac{1}{R_2}\right)^{N-k+mN} + \frac{1}{R_2^k} \sum_{m=1}^{\infty} R_1^{k+mN} + \frac{1}{R_2^{N-k}} \sum_{m=1}^{\infty} R_1^{k+mN} \\
&+ \sum_{m=1}^{\infty} R_1^{k+mN} \sum_{m=1}^{\infty} \left(\frac{1}{R_2}\right)^{k+mN} + \sum_{m=1}^{\infty} R_1^{k+mN} \sum_{m=1}^{\infty} \left(\frac{1}{R_2}\right)^{N-k+mN} + \frac{1}{R_2^k} \sum_{m=1}^{\infty} R_1^{N-k+mN} \\
&+ \frac{1}{R_2^{N-k}} \sum_{m=1}^{\infty} R_1^{N-k+mN} + \sum_{m=1}^{\infty} R_1^{N-k+mN} \sum_{m=1}^{\infty} \left(\frac{1}{R_2}\right)^{k+mN} + \sum_{m=1}^{\infty} R_1^{N-k+mN} \sum_{m=1}^{\infty} \left(\frac{1}{R_2}\right)^{N-k+mN} \Bigg\} \\
&+ \frac{R_1^k}{\varrho_2^k R_2^{N-k}} + \left(\frac{R_1}{\varrho_2}\right)^{k} \sum_{m=1}^{\infty} \left(\frac{1}{R_2}\right)^{k+mN} + \left(\frac{R_1}{\varrho_2}\right)^{k} \sum_{m=1}^{\infty} \left(\frac{1}{R_2}\right)^{N-k+mN} \\
&+ \left(\frac{R_1}{\varrho_2 R_2}\right)^{N-k} + \left(\frac{R_1}{\varrho_2}\right)^{N-k} \sum_{m=1}^{\infty} \left(\frac{1}{R_2}\right)^{k+mN} + \left(\frac{R_1}{\varrho_2}\right)^{N-k} \sum_{m=1}^{\infty} \left(\frac{1}{R_2}\right)^{N-k+mN} \\
&+ \frac{1}{R_2^{N-k}} \sum_{m=1}^{\infty} \left(\frac{R_1}{\varrho_2}\right)^{k+mN} + \sum_{m=1}^{\infty} \left(\frac{R_1}{\varrho_2}\right)^{k+mN} \sum_{m=1}^{\infty} \left(\frac{1}{R_2}\right)^{k+mN} + \sum_{m=1}^{\infty} \left(\frac{R_1}{\varrho_2}\right)^{k+mN} \sum_{m=1}^{\infty} \left(\frac{1}{R_2}\right)^{N-k+mN} \\
&+ \frac{1}{R_2^{N-k}} \sum_{m=1}^{\infty} \left(\frac{R_1}{\varrho_2}\right)^{N-k+mN} + \sum_{m=1}^{\infty} \left(\frac{R_1}{\varrho_2}\right)^{N-k+mN} \sum_{m=1}^{\infty} \left(\frac{1}{R_2}\right)^{k+mN} + \sum_{m=1}^{\infty} \left(\frac{R_1}{\varrho_2}\right)^{N-k+mN} \sum_{m=1}^{\infty} \left(\frac{1}{R_2}\right)^{N-k+mN} \\
&+ \frac{R_1^{N-k} \varrho_2^k}{R_2^k} + \left(\frac{R_1 \varrho_2}{R_2}\right)^{N-k} + R_1^{N-k} \sum_{m=1}^{\infty} \left(\frac{\varrho_2}{R_2}\right)^{k+mN} + R_1^{N-k} \sum_{m=1}^{\infty} \left(\frac{\varrho_2}{R_2}\right)^{N-k+mN} \\
&+ \left(\frac{\varrho_2}{R_2}\right)^{k} \sum_{m=1}^{\infty} R_1^{k+mN} + \left(\frac{\varrho_2}{R_2}\right)^{N-k} \sum_{m=1}^{\infty} R_1^{k+mN} + \sum_{m=1}^{\infty} R_1^{k+mN} \sum_{m=1}^{\infty} \left(\frac{\varrho_2}{R_2}\right)^{k+mN} \\
&+ \sum_{m=1}^{\infty} R_1^{k+mN} \sum_{m=1}^{\infty} \left(\frac{\varrho_2}{R_2}\right)^{N-k+mN} + \left(\frac{\varrho_2}{R_2}\right)^{k} \sum_{m=1}^{\infty} R_1^{N-k+mN} + \left(\frac{\varrho_2}{R_2}\right)^{N-k} \sum_{m=1}^{\infty} R_1^{N-k+mN} \\
&+ \sum_{m=1}^{\infty} R_1^{N-k+mN} \sum_{m=1}^{\infty} \left(\frac{\varrho_2}{R_2}\right)^{k+mN} + \sum_{m=1}^{\infty} R_1^{N-k+mN} \sum_{m=1}^{\infty} \left(\frac{\varrho_2}{R_2}\right)^{N-k+mN} \Bigg\}
\end{aligned}
$$

$$
\begin{aligned}
\leq & \frac{2N^2}{16\pi^2}\left\{\varrho_2^k\left\{\frac{R_1^k}{R_2^{N-k}}+2R_1^k\left(\frac{1}{R_2}\right)^{k+N}+2R_1^k\left(\frac{1}{R_2}\right)^{2N-k}+\frac{R_1^{N-k}}{R_2^k}+\left(\frac{R_1}{R_2}\right)^{N-k}+2R_1^{N-k}\left(\frac{1}{R_2}\right)^{k+N}\right.\right.\\
&+2R_1^{N-k}\left(\frac{1}{R_2}\right)^{2N-k}+2\frac{1}{R_2^k}R_1^{k+N}+2\frac{1}{R_2^{N-k}}R_1^{k+N}+4\left(\frac{R_1}{R_2}\right)^{k+N}+4R_1^{k+N}\left(\frac{1}{R_2}\right)^{2N-k}\\
&\left.+2\frac{1}{R_2^k}R_1^{2N-k}+2\frac{1}{R_2^{N-k}}R_1^{2N-k}+4R_1^{2N-k}\left(\frac{1}{R_2}\right)^{k+N}+4\left(\frac{R_1}{R_2}\right)^{2N-k}\right\}+\\
&+\frac{R_1^k}{\varrho_2^k R_2^{N-k}}+2\left(\frac{R_1}{\varrho_2}\right)^k\left(\frac{1}{R_2}\right)^{k+N}+2\left(\frac{R_1}{\varrho_2}\right)^k\left(\frac{1}{R_2}\right)^{2N-k}+\left(\frac{R_1}{\varrho_2 R_2}\right)^{N-k}\\
&+2\left(\frac{R_1}{\varrho_2}\right)^{N-k}\left(\frac{1}{R_2}\right)^{k+N}+2\left(\frac{R_1}{\varrho_2}\right)^{N-k}\left(\frac{1}{R_2}\right)^{2N-k}+2\left(\frac{R_1}{\varrho_2}\right)^{k+N}\left(\frac{1}{R_2}\right)^{N-k}+4\left(\frac{R_1}{\varrho_2}\right)^{k+N}\left(\frac{1}{R_2}\right)^{k+N}\\
&+4\left(\frac{R_1}{\varrho_2}\right)^{k+N}\left(\frac{1}{R_2}\right)^{2N-k}+2\left(\frac{R_1}{\varrho_2}\right)^{2N-k}\left(\frac{1}{R_2}\right)^{N-k}+4\left(\frac{R_1}{\varrho_2}\right)^{2N-k}\left(\frac{1}{R_2}\right)^{k+N}+4\left(\frac{R_1}{\varrho_2}\right)^{2N-k}\left(\frac{1}{R_2}\right)^{2N-k}\\
&+\frac{R_1^{N-k}\varrho_2^k}{R_2^k}+\left(\frac{R_1\varrho_2}{R_2}\right)^{N-k}+2R_1^{N-k}\left(\frac{\varrho_2}{R_2}\right)^{k+N}+2R_1^{N-k}\left(\frac{\varrho_2}{R_2}\right)^{2N-k}+2R_1^{k+N}\left(\frac{\varrho_2}{R_2}\right)^{k}\\
&+2R_1^{k+N}\left(\frac{\varrho_2}{R_2}\right)^{N-k}+4R_1^{k+N}\left(\frac{\varrho_2}{R_2}\right)^{k+N}+4R_1^{k+N}\left(\frac{\varrho_2}{R_2}\right)^{2N-k}+2R_1^{2N-k}\left(\frac{\varrho_2}{R_2}\right)^{k}+2R_1^{2N-k}\left(\frac{\varrho_2}{R_2}\right)^{N-k}\\
&+4R_1^{2N-k}\left(\frac{\varrho_2}{R_2}\right)^{k+N}+4R_1^{2N-k}\left(\frac{\varrho_2}{R_2}\right)^{2N-k},
\end{aligned}
$$

for sufficiently large N. Therefore

$$
\begin{aligned}
|A-e^{ik\vartheta}B| \leq & 2N^2\left\{\varrho_2^k\left\{5R_1^k\left(\frac{1}{R_2}\right)^{N-k}+10R_1^{N-k}\left(\frac{1}{R_2}\right)^{k}+22R_1^{N-k}\left(\frac{1}{R_2}\right)^{k}\right\}\right.\\
&\left.+28\left(\frac{R_1}{R_2}\right)^{k}\left(\frac{1}{R_2}\right)^{N-k}+27R_1^k\left(\frac{\varrho_2}{R_2}\right)^{N-k}+5R_1^{N-k}\left(\frac{\varrho_2}{R_2}\right)^{k}\right\}\\
= & 2N^2\left\{\varrho_2^k\left\{5R_1^k\left(\frac{1}{R_2}\right)^{N-k}+32R_1^{N-k}\left(\frac{1}{R_2}\right)^{k}\right\}\right.\\
&\left.+28\left(\frac{R_1}{R_2}\right)^{k}\left(\frac{1}{R_2}\right)^{N-k}+27R_1^k\left(\frac{\varrho_2}{R_2}\right)^{N-k}+5R_1^{N-k}\left(\frac{\varrho_2}{R_2}\right)^{k}\right\}.
\end{aligned}
$$

Since

$$
|B| \geq \frac{1}{k^2}\frac{R_1^k}{R_2^k}\left(\varrho_2^k-\frac{1}{\varrho_2^k}\right)=\frac{1}{k^2}\frac{R_1^k}{R_2^k}\beta\varrho_2^k
$$

where $1>\beta>1-\frac{1}{\varrho_2}$, we have

$$
\begin{aligned}
\frac{|A-e^{ik\vartheta}B|}{|B|} \leq & \frac{2N^2k^2}{\beta}\left\{\frac{\frac{5\varrho_2^kR_1^k}{R_2^{N-k}}}{\frac{\varrho_2^kR_1^k}{R_2^k}}+\frac{\frac{32\varrho_2^kR_1^{N-k}}{R_2^{N-k}}}{\frac{\varrho_2^kR_1^k}{R_2^k}}+\frac{\frac{28R_1^k}{R_2^kR_2^{N-k}}}{\frac{\varrho_2^kR_1^k}{R_2^k}}+\frac{\frac{27\varrho_2^{N-k}R_1^k}{R_2^{N-k}}}{\frac{\varrho_2^kR_1^k}{R_2^k}}+\frac{\frac{5\varrho_2^kR_1^{N-k}}{R_2^k}}{\frac{\varrho_2^kR_1^k}{R_2^k}}\right\} \\
= & \frac{2N^2k^2}{\beta}\left\{\frac{5}{R_2^{N-2k}}+32R_1^{N-2k}+\frac{28}{\varrho_2^kR_2^{N-k}}+27\left(\frac{\varrho_2}{R_2}\right)^{N-2k}+5R_1^{N-2k}\right\}
\end{aligned}
$$

Therefore we have

$$
\begin{aligned}
\frac{|A-e^{ik\vartheta}B|}{|B|} \leq & \frac{2N^2k^2}{\beta}\left\{5\sigma^{N-2k}+32\sigma^{N-2k}+28\sigma^{N-2k}+27\sigma^{N-2k}+5\sigma^{N-2k}\right\} \\
= & \frac{2N^2k^2}{\beta}97\sigma^{N-2k}=\frac{194N^2k^2}{\beta}\sigma^{N-2k},
\end{aligned}
$$

where $1>\beta>1-\frac{1}{\varrho_2}$.

Case III, $-N/2 \leq k < 0$: From 2.29 we have

$$
\begin{aligned}
u_N = & \sum_{j=1}^{N}\frac{\lambda_j^{11}}{\lambda_j^{11}\lambda_j^{22}-\lambda_j^{12}\lambda_j^{21}}\langle \boldsymbol{f_2},\boldsymbol{\xi}_j\rangle\overline{\langle \boldsymbol{l_2},\boldsymbol{\xi}_j\rangle}-\sum_{j=1}^{N}\frac{\lambda_j^{21}}{\lambda_j^{11}\lambda_j^{22}-\lambda_j^{12}\lambda_j^{21}}\langle \boldsymbol{f_1},\boldsymbol{\xi}_j\rangle\overline{\langle \boldsymbol{l_2},\boldsymbol{\xi}_j\rangle} \\
& -\sum_{j=1}^{N}\frac{\lambda_j^{12}}{\lambda_j^{11}\lambda_j^{22}-\lambda_j^{12}\lambda_j^{21}}\langle \boldsymbol{f_2},\boldsymbol{\xi}_j\rangle\overline{\langle \boldsymbol{l_1},\boldsymbol{\xi}_j\rangle}+\sum_{j=1}^{N}\frac{\lambda_j^{22}}{\lambda_j^{11}\lambda_j^{22}-\lambda_j^{12}\lambda_j^{21}}\langle \boldsymbol{f_1},\boldsymbol{\xi}_j\rangle\overline{\langle \boldsymbol{l_1},\boldsymbol{\xi}_j\rangle},
\end{aligned}
$$

$$
\langle \boldsymbol{f_1},\boldsymbol{\xi}_j\rangle = \begin{cases}\sqrt{N} & \text{if } j=k+1\\ 0 & \text{otherwise}.\end{cases} \quad \text{and} \quad \langle \boldsymbol{f_2},\boldsymbol{\xi}_j\rangle = \begin{cases}\sqrt{N}\frac{1}{\varrho_2^{|k|}} & \text{if } j=k+1\\ 0 & \text{otherwise}.\end{cases}
$$

Thus

$$
u_N=\frac{\sqrt{N}}{\lambda_{k+1}^{11}\lambda_{k+1}^{22}-\lambda_{k+1}^{12}\lambda_{k+1}^{21}}\{(\frac{1}{\varrho_2^{|k|}}\lambda_{k+1}^{11}-\lambda_{k+1}^{21})\overline{\langle \boldsymbol{l_2},\boldsymbol{\xi}_{k+1}\rangle}+(\lambda_{k+1}^{22}-\frac{1}{\varrho_2^{|k|}}\lambda_{k+1}^{12})\overline{\langle \boldsymbol{l_1},\boldsymbol{\xi}_{k+1}\rangle}\}
$$

Therefore, since $u(\cdot;\bar{h})=\overline{u(\cdot;h)}$ and $u_N(\cdot;\bar{h})=\overline{u_N(\cdot;h)}$, we have

$$
\left\|u_N(\cdot\,;\,e^{-i|k|\varphi})-u(\cdot\,;\,e^{-i|k|\varphi})\right\|_\infty=\max_{\vartheta\in[0,2\pi]}\left|\frac{A}{B}-e^{-i|k|\vartheta}\right|=\max_{\vartheta\in[0,2\pi]}\frac{\left|A-e^{-i|k|\vartheta}B\right|}{|B|}
$$

where

$$
A=\sqrt{N}\{(\frac{1}{\varrho_2^{|k|}}\lambda_{k+1}^{11}-\lambda_{k+1}^{21})\overline{\langle \boldsymbol{l_2},\boldsymbol{\xi}_{k+1}\rangle}+(\lambda_{k+1}^{22}-\frac{1}{\varrho_2^{|k|}}\lambda_{k+1}^{12})\overline{\langle \boldsymbol{l_1},\boldsymbol{\xi}_{k+1}\rangle}\}
$$

and

$$
B=\lambda_{k+1}^{11}\lambda_{k+1}^{22}-\lambda_{k+1}^{12}\lambda_{k+1}^{21}
$$

Following a similar proof as in case II with the following differences in $|A-e^{i|k|\theta}B|$:

- The coefficient $\varrho_2^{|k|}$ in equation (2.50) is replaced by $\frac{1}{\varrho_2^{|k|}}$,

- The angles in (2.51) have opposite signs,

we obtain

$$\frac{|A - e^{-i|k|\theta} B|}{|B|} \leq \frac{194 N^2 k^2}{\beta} \sigma^{N-2|k|}$$

where $1 > \beta > 1 - \frac{1}{\varrho_2}$.

Next, we bound the term $u_N(\cdot; r^k e^{ik\varphi}) - u(\cdot; r^k e^{ik\varphi})$ on the circle $r = \varrho_2$.

Case I. $k = 0$. In this case, $f_1 = f_2 = 1$, $\boldsymbol{f_1} = \boldsymbol{f_2} = (1, 1, \ldots, 1)$, $u \equiv 1$ and

$$\langle \boldsymbol{f_1}, \boldsymbol{\xi}_j \rangle = \begin{cases} \sqrt{N} & \text{if } j = 1 \\ 0 & \text{otherwise}. \end{cases} \quad \text{and} \quad \langle \boldsymbol{f_2}, \boldsymbol{\xi}_j \rangle = \begin{cases} \sqrt{N} & \text{if } j = 1 \\ 0 & \text{otherwise}. \end{cases}$$

Thus from expression (2.29) we have

$$u_N(\cdot; 1) = \frac{\sqrt{N}}{\lambda_1^{11}\lambda_1^{22} - \lambda_1^{12}\lambda_1^{21}} \{ (\lambda_1^{11} - \lambda_1^{21}) \langle \overline{\boldsymbol{l_2}, \boldsymbol{\xi}_1} \rangle + (\lambda_1^{22} - \lambda_1^{12}) \langle \overline{\boldsymbol{l_1}, \boldsymbol{\xi}_1} \rangle \}$$

where the eigenvalues take the form:

$$\lambda_1^{11} = \frac{N}{2\pi} \sum_{m=1}^{\infty} \frac{1}{mN} R_1^{mN}, \quad \lambda_1^{12} = \frac{N}{2\pi} \left\{ \sum_{m=1}^{\infty} \frac{1}{mN} \left(\frac{1}{R_2} \right)^{mN} - \log R_2 \right\}$$

$$\lambda_1^{21} = \frac{N}{2\pi} \left\{ \sum_{m=1}^{\infty} \frac{1}{mN} \left(\frac{R_1}{\varrho_2} \right)^{mN} - \log \varrho_2 \right\}, \quad \lambda_1^{22} = \frac{N}{2\pi} \left\{ \sum_{m=1}^{\infty} \frac{1}{mN} \left(\frac{\varrho_2}{R_2} \right)^{mN} - \log R_2 \right\}$$

and

$$\begin{aligned} \langle \overline{\boldsymbol{l_1}, \boldsymbol{\xi}_1} \rangle &= \frac{\sqrt{N}}{2\pi} \left\{ \sum_{m=1}^{\infty} \frac{1}{mN} \left(\frac{R_1}{\varrho_2} \right)^{mN} \cos(mN\vartheta) - \log \varrho_2 \right\}, \\ \langle \overline{\boldsymbol{l_2}, \boldsymbol{\xi}_1} \rangle &= \frac{\sqrt{N}}{2\pi} \left\{ \sum_{m=1}^{\infty} \frac{1}{mN} \left(\frac{\varrho_2}{R_2} \right)^{mN} \cos(mN\vartheta) - \log R_2 \right\} \end{aligned}$$

Therefore

$$||u_N(\cdot\,; 1) - u(\cdot\,; 1)||_\infty = \max_{\vartheta \in [0,2\pi]} |u_N(\cos\vartheta, \sin\vartheta\,; 1) - 1| = \max_{\vartheta \in [0,2\pi]} \frac{|A - B|}{|B|},$$

where

$$A = \frac{N}{2\pi}\left\{(\lambda_1^{11}-\lambda_1^{21})\left\{\sum_{m=1}^{\infty}\frac{1}{mN}\left(\frac{\varrho_2}{R_2}\right)^{mN}\cos(mN\vartheta)-\log R_2\right\}\right.$$

$$\left.+(\lambda_1^{22}-\lambda_1^{12})\left\{\sum_{m=1}^{\infty}\frac{1}{mN}\left(\frac{R_1}{\varrho_2}\right)^{mN}\cos(mN\vartheta)-\log\varrho_2\right\}\right\}$$

and $B = \lambda_1^{11}\lambda_1^{22}-\lambda_1^{12}\lambda_1^{21}$. We thus have

$$|B| = \frac{1}{4\pi^2}\sum_{m=1}^{\infty}\frac{1}{m}R_1^{mN}\left\{N\log R_2-\sum_{m=1}^{\infty}\frac{1}{m}\left(\frac{\varrho_2}{R_2}\right)^{mN}\right\}$$

$$+\left\{N\log R_2-\sum_{m=1}^{\infty}\frac{1}{m}\left(\frac{1}{R_2}\right)^{mN}\right\}\left\{N\log\varrho_2-\sum_{m=1}^{\infty}\frac{1}{m}\left(\frac{R_1}{\varrho_2}\right)^{mN}\right\}\geqslant N^2\log R_2\log\varrho_2$$

and

$$\begin{aligned}
|A-B| =& \Bigg|\frac{N}{2\pi}\left\{(\lambda_1^{11}-\lambda_1^{21})\left\{\sum_{m=1}^{\infty}\frac{1}{mN}\left(\frac{\varrho_2}{R_2}\right)^{mN}\cos(mN\vartheta)-\log R_2\right\}\right.\\
&\left.+(\lambda_1^{22}-\lambda_1^{12})\left\{\sum_{m=1}^{\infty}\frac{1}{mN}\left(\frac{R_1}{\varrho_2}\right)^{mN}\cos(mN\vartheta)-\log\varrho_2\right\}\right\}-(\lambda_1^{11}\lambda_1^{22}-\lambda_1^{12}\lambda_1^{21})\Bigg|\\
=& \Bigg|\frac{N}{2\pi}\left\{\left(\frac{1}{2\pi}\sum_{m=1}^{\infty}\frac{1}{m}R_1^{mN}+\frac{1}{2\pi}\left[N\log\varrho_2-\sum_{m=1}^{\infty}\frac{1}{m}\left(\frac{R_1}{\varrho_2}\right)^{mN}\right]\right)\right.\\
&\left(\sum_{m=1}^{\infty}\frac{1}{mN}\left(\frac{\varrho_2}{R_2}\right)^{mN}cos(mN\vartheta)-\log R_2\right)\\
&+\left(\frac{1}{2\pi}\left[\sum_{m=1}^{\infty}\frac{1}{m}\left(\frac{\varrho_2}{R_2}\right)^{mN}-N\log R_2\right]-\frac{1}{2\pi}\left[\sum_{m=1}^{\infty}\frac{1}{m}\left(\frac{1}{R_2}\right)^{mN}-N\log R_2\right]\right)\\
&\left.\left(\sum_{m=1}^{\infty}\frac{1}{mN}\left(\frac{R_1}{\varrho_2}\right)^{mN}\cos(mN\vartheta)-\log\varrho_2\right)\right\}\\
&+\frac{1}{4\pi^2}\left\{\sum_{m=1}^{\infty}\frac{1}{m}R_1^{mN}\left[N\log R_2-\sum_{m=1}^{\infty}\frac{1}{m}\left(\frac{\varrho_2}{R_2}\right)^{mN}\right]\right.\\
&\left.+\left[N\log R_2-\sum_{m=1}^{\infty}\frac{1}{m}\left(\frac{1}{R_2}\right)^{mN}\right]\left[N\log\varrho_2-\sum_{m=1}^{\infty}\frac{1}{m}\left(\frac{R_1}{\varrho_2}\right)^{mN}\right]\right\}\Bigg|\\
=& \frac{N}{4\pi^2}\Bigg|\left\{\left(\sum_{m=1}^{\infty}\frac{1}{m}R_1^{mN}+N\log\varrho_2-\sum_{m=1}^{\infty}\frac{1}{m}\left(\frac{R_1}{\varrho_2}\right)^{mN}\right)\left(\sum_{m=1}^{\infty}\frac{1}{mN}\left(\frac{\varrho_2}{R_2}\right)^{mN}\cos(mN\vartheta)-\log R_2\right)\right.\\
&+\left(\sum_{m=1}^{\infty}\frac{1}{m}\left(\frac{\varrho_2}{R_2}\right)^{mN}-\sum_{m=1}^{\infty}\frac{1}{m}\frac{1}{R_2^{mN}}\right)\\
&\left.\left(\sum_{m=1}^{\infty}\frac{1}{mN}\left(\frac{R_1}{\varrho_2}\right)^{mN}\cos(mN\vartheta)-\log\varrho_2\right)\right\}
\end{aligned}$$

$$
\begin{aligned}
&+\frac{1}{4\pi^2}\Bigg\{\sum_{m=1}^{\infty}\frac{1}{m}R_1^{mN}\left[N\log R_2-\sum_{m=1}^{\infty}\frac{1}{m}\left(\frac{\varrho_2}{R_2}\right)^{mN}\right]\\
&+\left[N\log R_2-\sum_{m=1}^{\infty}\frac{1}{m}\left(\frac{1}{R_2}\right)^{mN}\right]\left[N\log\varrho_2-\sum_{m=1}^{\infty}\frac{1}{m}\left(\frac{R_1}{\varrho_2}\right)^{mN}\right]\Bigg\}\Bigg|\\
=&\frac{1}{4\pi^2}\Bigg|\Bigg\{N\sum_{m=1}^{\infty}\frac{1}{m}R_1^{mN}\sum_{m=1}^{\infty}\frac{1}{mN}\left(\frac{\varrho_2}{R_2}\right)^{mN}\cos(mN\vartheta)-N\log R_2\sum_{m=1}^{\infty}\frac{1}{m}R_1^{mN}\\
&+N^2\log\varrho_2\sum_{m=1}^{\infty}\frac{1}{mN}\left(\frac{\varrho_2}{R_2}\right)^{mN}\cos(mN\vartheta)-N^2\log\varrho_2\log R_2\\
&-\sum_{m=1}^{\infty}\frac{1}{m}\left(\frac{R_1}{\varrho_2}\right)^{mN}\sum_{m=1}^{\infty}\frac{1}{m}\left(\frac{\varrho_2}{R_2}\right)^{mN}\cos(mN\vartheta)\\
&+N\sum_{m=1}^{\infty}\frac{1}{m}\left(\frac{R_1}{\varrho_2}\right)^{mN}\log R_2\\
&+N\sum_{m=1}^{\infty}\frac{1}{m}\left(\frac{\varrho_2}{R_2}\right)^{mN}\sum_{m=1}^{\infty}\frac{1}{mN}\left(\frac{R_1}{\varrho_2}\right)^{mN}\cos(mN\vartheta)\\
&-N\sum_{m=1}^{\infty}\frac{1}{m}\left(\frac{\varrho_2}{R_2}\right)^{mN}\log\varrho_2\\
&-N\sum_{m=1}^{\infty}\frac{1}{m}\left(\frac{1}{R_2}\right)^{mN}\sum_{m=1}^{\infty}\frac{1}{mN}R_1^{mN}\cos(mN\vartheta)-N\sum_{m=1}^{\infty}\frac{1}{m}\left(\frac{1}{R_2}\right)^{mN}\log\varrho_2\\
&+N\log R_2\sum_{m=1}^{\infty}\frac{1}{m}R_1^{mN}-\sum_{m=1}^{\infty}\frac{1}{m}R_1^{mN}\sum_{m=1}^{\infty}\frac{1}{m}\left(\frac{\varrho_2}{R_2}\right)^{mN}\\
&+N^2\log\varrho_2\log R_2-N\log R_2\sum_{m=1}^{\infty}\frac{1}{m}\left(\frac{R_1}{\varrho_2}\right)^{mN}-N\log\varrho_2\sum_{m=1}^{\infty}\frac{1}{m}\frac{1}{R_2^{mN}}\\
&+\sum_{m=1}^{\infty}\frac{1}{m}\frac{1}{R_2^{mN}}\sum_{m=1}^{\infty}\frac{1}{m}\left(\frac{R_1}{\varrho_2}\right)^{mN}\Bigg\}\Bigg|\\
\le&\sum_{m=1}^{\infty}R_1^{mN}\sum_{m=1}^{\infty}\left(\frac{\varrho_2}{R_2}\right)^{mN}+N\log R_2\sum_{m=1}^{\infty}R_1^{mN}+N^2\log\varrho_2\sum_{m=1}^{\infty}\left(\frac{\varrho_2}{R_2}\right)^{mN}\\
&+\sum_{m=1}^{\infty}\left(\frac{R_1}{\varrho_2}\right)^{mN}\sum_{m=1}^{\infty}\left(\frac{\varrho_2}{R_2}\right)^{mN}+N\log R_2\sum_{m=1}^{\infty}\left(\frac{R_1}{\varrho_2}\right)^{mN}\\
&+\sum_{m=1}^{\infty}\left(\frac{\varrho_2}{R_2}\right)^{mN}\sum_{m=1}^{\infty}\left(\frac{R_1}{\varrho_2}\right)^{mN}+N\log\varrho_2\sum_{m=1}^{\infty}\left(\frac{\varrho_2}{R_2}\right)^{mN}\\
&+\sum_{m=1}^{\infty}\frac{1}{R_2^{mN}}\sum_{m=1}^{\infty}R_1^{mN}+N\log\varrho_2\sum_{m=1}^{\infty}\frac{1}{R_2^{mN}}\\
&+N\log R_2\sum_{m=1}^{\infty}R_1^{mN}+\sum_{m=1}^{\infty}R_1^{mN}\sum_{m=1}^{\infty}\left(\frac{\varrho_2}{R_2}\right)^{mN}+N\log R_2\sum_{m=1}^{\infty}\left(\frac{R_1}{\varrho_2}\right)^{mN}\\
&+N\log\varrho_2\sum_{m=1}^{\infty}\frac{1}{R_2^{mN}}+\sum_{m=1}^{\infty}\frac{1}{R_2^{mN}}\sum_{m=1}^{\infty}\left(\frac{R_1}{\varrho_2}\right)^{mN}
\end{aligned}
$$

$$
\begin{aligned}
&\leq 2R_1^N 2\left(\frac{\varrho_2}{R_2}\right)^N + N\log R_2 2R_1^N + N^2\log\varrho_2 2\left(\frac{\varrho_2}{R_2}\right)^N + \\
&2\left(\frac{R_1}{\varrho_2}\right)^N \frac{2}{R_2^N}2\left(\frac{\varrho_2}{R_2}\right)^N \\
&+ N\log R_2 2\left(\frac{R_1}{\varrho_2}\right)^N + 4\left(\frac{\varrho_2}{R_2}\right)^N R_1^N + 2N\log\varrho_2\left(\frac{\varrho_2}{R_2}\right)^N + \frac{2}{R_2^N}2R_1^N + N\log\varrho_2\frac{2}{R_2^N} \\
&+ 2N\log R_2 R_1^N + 4R_1^N\left(\frac{\varrho_2}{R_2}\right)^N + 2N\log R_2\left(\frac{R_1}{\varrho_2}\right)^N + 2N\log R_2\frac{1}{R_2^N} + 4\frac{1}{R_2^N}\left(\frac{R_1}{\varrho_2}\right)^N.
\end{aligned}
$$

Therefore:

$$
\begin{aligned}
|A-B| \;&\leq 4\sigma^{2N} + 2N\log R_2\sigma^N + 2N^2\log R_2\sigma^N + 4\sigma^{2N} + 2N\log R_2\sigma^N + 4\sigma^{2N} + 2N\log\varrho_2\sigma^N \\
&\quad + 4\sigma^{2N} + 2N\log\varrho_2\sigma^N + 2N\log R_2\sigma^N + 4\sigma^{2N} + 2N\log R_2\sigma^N + 4N\log R_2\sigma^N + 4\sigma^{2N} \\
&\leq 4\sigma^N + 2N\log R_2\sigma^N + 2N^2\log R_2\sigma^N + 4\sigma^N + 2N\log R_2\sigma^N + 4\sigma^N + 2N\log R_2\sigma^N + 4\sigma^N \\
&\quad + 2N\log R_2\sigma^N + 4\sigma^N + 2N\log R_2\sigma^N + 4\sigma^N + 4N\log\varrho_2\sigma^N \\
&\leq 24\sigma^N + 18N^2\log R_2\sigma^N.
\end{aligned}
$$

Thus if $\log R_2 > 1$ we have,

$$
\begin{aligned}
\frac{|A-B|}{|B|} &\leq \frac{24\sigma^N + 18N^2\log R_2\sigma^N}{N^2\log R_2\log\varrho_2} \leq \frac{24N\log R_2\sigma^N + 18N^2\log R_2\sigma^N}{N^2\log R_2\log\varrho_2} \leq \frac{42N^2\log R_2\sigma^N}{N^2\log R_2\log\varrho_2} \\
&= \frac{42\sigma^N}{\log\varrho_2}.
\end{aligned}
$$

If $\log R_2 < 1$ we have:

$$
\begin{aligned}
\frac{|A-B|}{|B|} &\leq \frac{24\sigma^N + 18N^2\log R_2\sigma^N}{N^2\log R_2\log\varrho_2} \leq \frac{24N\sigma^N + 18N^2\sigma^N}{N^2\log R_2\log\varrho_2} = \frac{42\sigma^N}{\log R_2\log\varrho_2} \\
&= \frac{42\sigma^N}{\log\varrho_2\log R_2}.
\end{aligned}
$$

Case II, $0 < k \leq N/2$: From (2.29) we have:

$$
\begin{aligned}
u_N =& \sum_{j=1}^{N} \frac{\lambda_j^{11}}{\lambda_j^{11}\lambda_j^{22} - \lambda_j^{12}\lambda_j^{21}} \langle \boldsymbol{f_2}, \boldsymbol{\xi}_j\rangle \overline{\langle \boldsymbol{l_2}, \boldsymbol{\xi}_j\rangle} - \sum_{j=1}^{N} \frac{\lambda_j^{21}}{\lambda_j^{11}\lambda_j^{22} - \lambda_j^{12}\lambda_j^{21}} \langle \boldsymbol{f_1}, \boldsymbol{\xi}_j\rangle \overline{\langle \boldsymbol{l_2}, \boldsymbol{\xi}_j\rangle} \\
&- \sum_{j=1}^{N} \frac{\lambda_j^{12}}{\lambda_j^{11}\lambda_j^{22} - \lambda_j^{12}\lambda_j^{21}} \langle \boldsymbol{f_2}, \boldsymbol{\xi}_j\rangle \overline{\langle \boldsymbol{l_1}, \boldsymbol{\xi}_j\rangle} + \sum_{j=1}^{N} \frac{\lambda_j^{22}}{\lambda_j^{11}\lambda_j^{22} - \lambda_j^{12}\lambda_j^{21}} \langle \boldsymbol{f_1}, \boldsymbol{\xi}_j\rangle \overline{\langle \boldsymbol{l_1}, \boldsymbol{\xi}_j\rangle}
\end{aligned}
$$

where

$$
\langle \boldsymbol{f_1}, \boldsymbol{\xi}_j\rangle = \begin{cases} \sqrt{N} & \text{if } j = k+1 \\ 0 & \text{otherwise}. \end{cases} \quad \text{and} \quad \langle \boldsymbol{f_2}, \boldsymbol{\xi}_j\rangle = \begin{cases} \sqrt{N}\varrho_2^k & \text{if } j = k+1 \\ 0 & \text{otherwise}. \end{cases}
$$

Thus

$$u_N = \frac{\sqrt{N}}{\lambda_{k+1}^{11}\lambda_{k+1}^{22} - \lambda_{k+1}^{12}\lambda_{k+1}^{21}}\{(\varrho_2^k\lambda_{k+1}^{11} - \lambda_{k+1}^{21})\langle\overline{\boldsymbol{l_2}, \boldsymbol{\xi}_{k+1}}\rangle + (\lambda_{k+1}^{22} - \varrho_2^k\lambda_{k+1}^{12})\langle\overline{\boldsymbol{l_1}, \boldsymbol{\xi}_{k+1}}\rangle\}.$$

We can therefore write

$$|u_N - \varrho_2^k e^{ik\theta}| = |\frac{A}{B} - \varrho_2^k e^{ik\theta}| = \frac{|A - \varrho_2^k e^{ik\theta}B|}{|B|} \tag{2.52}$$

where

$$A = \sqrt{N}\{(\varrho_2^k\lambda_{k+1}^{11} - \lambda_{k+1}^{21})\langle\overline{\boldsymbol{l_2}, \boldsymbol{\xi}_{k+1}}\rangle + (\lambda_{k+1}^{22} - \varrho_2^k\lambda_{k+1}^{12})\langle\overline{\boldsymbol{l_1}, \boldsymbol{\xi}_{k+1}}\rangle\}$$

and

$$B = \lambda_{k+1}^{11}\lambda_{k+1}^{22} - \lambda_{k+1}^{12}\lambda_{k+1}^{21}.$$

Since $\varrho_1 = 1$, we have

$$\begin{aligned}
\lambda_{k+1}^{11} =& \frac{N}{4\pi}\sum_{m=0}^{\infty}\left\{R_1^{k+mN}\frac{1}{k+mN} + R_1^{N-k+mN}\frac{1}{N-k+mN}\right\}\\
\lambda_{k+1}^{12} =& \frac{N}{4\pi}\sum_{m=0}^{\infty}\left\{\left(\frac{1}{R_2}\right)^{k+mN}\frac{1}{k+mN} + \left(\frac{1}{R_2}\right)^{N-k+mN}\frac{1}{N-k+mN}\right\}\\
\lambda_{k+1}^{21} =& \frac{N}{4\pi}\sum_{m=0}^{\infty}\left\{\left(\frac{R_1}{\varrho_2}\right)^{k+mN}\frac{1}{k+mN} + \left(\frac{R_1}{\varrho_2}\right)^{N-k+mN}\frac{1}{N-k+mN}\right\}\\
\lambda_{k+1}^{22} =& \frac{N}{4\pi}\sum_{m=0}^{\infty}\left\{\left(\frac{\varrho_2}{R_2}\right)^{k+mN}\frac{1}{k+mN} + \left(\frac{\varrho_2}{R_2}\right)^{N-k+mN}\frac{1}{N-k+mN}\right\}.
\end{aligned}$$

From equation (2.49) we have that

$$B > \frac{1}{k^2}\frac{R_1^k}{R_2^k}\left(\varrho_2^k - \frac{1}{\varrho_2^k}\right).$$

On the other hand we have

$$\begin{aligned}
&|A - \varrho_2^k e^{ik\theta}B|\\
=&\left|\sqrt{N}\{(\varrho_2^k\lambda_{k+1}^{11} - \lambda_{k+1}^{21})\langle\overline{\boldsymbol{l_2}, \boldsymbol{\xi}_{k+1}}\rangle + (\lambda_{k+1}^{22} - \varrho_2^k\lambda_{k+1}^{12})\langle\overline{\boldsymbol{l_1}, \boldsymbol{\xi}_{k+1}}\rangle\} - \varrho_2^k e^{ik\vartheta}(\lambda_{k+1}^{11}\lambda_{k+1}^{22} - \lambda_{k+1}^{12}\lambda_{k+1}^{21})\right|
\end{aligned}$$

$$
\begin{aligned}
&= \frac{N^2}{16\pi^2}\Bigg| \varrho_2^k \sum_{m=0}^{\infty} \left\{ \frac{R_1^{k+mN}}{k+mN} + \frac{R_1^{N-k+mN}}{N-k+mN} \right\} \\
&\quad \times \sum_{m=0}^{\infty} \left\{ \left(\frac{\varrho_2}{R_2}\right)^{k+mN} \frac{e^{i(k+mN)\vartheta}}{k+mN} + \left(\frac{\varrho_2}{R_2}\right)^{N-k+mN} \frac{e^{-i(N-k+mN)\vartheta}}{N-k+mN} \right\} \\
&\quad - \sum_{m=0}^{\infty} \left\{ \left(\frac{R_1}{\varrho_2}\right)^{k+mN} \frac{1}{k+mN} + \left(\frac{R_1}{\varrho_2}\right)^{N-k+mN} \frac{1}{N-k+mN} \right\} \\
&\quad \times \sum_{m=0}^{\infty} \left\{ \left(\frac{\varrho_2}{R_2}\right)^{k+mN} \frac{e^{i(k+mN)\vartheta}}{k+mN} + \left(\frac{\varrho_2}{R_2}\right)^{N-k+mN} \frac{e^{-i(N-k+mN)\vartheta}}{N-k+mN} \right\} \\
&\quad + \sum_{m=0}^{\infty} \left\{ \left(\frac{\varrho_2}{R_2}\right)^{k+mN} \frac{1}{k+mN} + \left(\frac{\varrho_2}{R_2}\right)^{N-k+mN} \frac{1}{N-k+mN} \right\} \\
&\quad \times \sum_{m=0}^{\infty} \left\{ \left(\frac{R_1}{\varrho_2}\right)^{k+mN} \frac{e^{i(k+mN)\vartheta}}{k+mN} + \left(\frac{R_1}{\varrho_2}\right)^{N-k+mN} \frac{e^{-i(N-k+mN)\vartheta}}{N-k+mN} \right\} \\
&\quad - \varrho_2^k \sum_{m=0}^{\infty} \left\{ \left(\frac{1}{R_2}\right)^{k+mN} \frac{1}{k+mN} + \left(\frac{1}{R_2}\right)^{N-k+mN} \frac{1}{N-k+mN} \right\} \\
&\quad \times \sum_{m=0}^{\infty} \left\{ \left(\frac{R_1}{\varrho_2}\right)^{k+mN} \frac{e^{i(k+mN)\vartheta}}{k+mN} + \left(\frac{R_1}{\varrho_2}\right)^{N-k+mN} \frac{e^{-i(N-k+mN)\vartheta}}{N-k+mN} \right\} \\
&\quad - \varrho_2^k e^{ik\vartheta} \sum_{m=0}^{\infty} \left\{ \frac{R_1^{k+mN}}{k+mN} + \frac{R_1^{N-k+mN}}{N-k+mN} \right\} \\
&\quad \times \sum_{m=0}^{\infty} \left\{ \left(\frac{\varrho_2}{R_2}\right)^{k+mN} \frac{1}{k+mN} + \left(\frac{\varrho_2}{R_2}\right)^{N-k+mN} \frac{1}{N-k+mN} \right\} \\
&\quad + \varrho_2^k e^{ik\vartheta} \sum_{m=0}^{\infty} \left\{ \left(\frac{1}{R_2}\right)^{k+mN} \frac{1}{k+mN} + \left(\frac{1}{R_2}\right)^{N-k+mN} \frac{1}{N-k+mN} \right\} \\
&\quad \times \sum_{m=0}^{\infty} \left\{ \left(\frac{R_1}{\varrho_2}\right)^{k+mN} \frac{1}{k+mN} + \left(\frac{R_1}{\varrho_2}\right)^{N-k+mN} \frac{1}{N-k+mN} \right\} \Bigg| \\
&= \frac{N^2}{16\pi^2}\Bigg| \varrho_2^k \left\{ \frac{R_1^k}{k} + \frac{R_1^{N-k}}{N-k} + \sum_{m=1}^{\infty} \frac{R_1^{k+mN}}{k+mN} + \sum_{m=1}^{\infty} \frac{R_1^{N-k+mN}}{N-k+mN} \right\} \\
&\quad \times \Bigg\{ \left(\frac{\varrho_2}{R_2}\right)^{k} \frac{e^{ik\vartheta}}{k} + \left(\frac{\varrho_2}{R_2}\right)^{N-k} \frac{e^{-i(N-k)\vartheta}}{N-k} \\
&\quad + \sum_{m=1}^{\infty} \left(\frac{\varrho_2}{R_2}\right)^{k+mN} \frac{e^{i(k+mN)\vartheta}}{k+mN} + \sum_{m=1}^{\infty} \left(\frac{\varrho_2}{R_2}\right)^{N-k+mN} \frac{e^{-i(N-k+mN)\vartheta}}{N-k+mN} \Bigg\} \\
&\quad - \varrho_2^k \left\{ \frac{R_1^k}{k} + \frac{R_1^{N-k}}{N-k} + \sum_{m=1}^{\infty} \frac{R_1^{k+mN}}{k+mN} + \sum_{m=1}^{\infty} \frac{R_1^{N-k+mN}}{N-k+mN} \right\} \\
&\quad \times \Bigg\{ \left(\frac{\varrho_2}{R_2}\right)^{k} \frac{e^{ik\vartheta}}{k} + \left(\frac{\varrho_2}{R_2}\right)^{N-k} \frac{e^{ik\vartheta}}{N-k} \\
&\quad + \sum_{m=1}^{\infty} \left(\frac{\varrho_2}{R_2}\right)^{k+mN} \frac{e^{ik\vartheta}}{k+mN} + \sum_{m=1}^{\infty} \left(\frac{\varrho_2}{R_2}\right)^{N-k+mN} \frac{e^{ik\vartheta}}{N-k+mN} \Bigg\}
\end{aligned}
$$

$$+\Bigg\{\left(\frac{\varrho_2}{R_2}\right)^{k}\frac{1}{k}+\left(\frac{\varrho_2}{R_2}\right)^{N-k}\frac{1}{N-k}+\sum_{m=1}^{\infty}\left(\frac{\varrho_2}{R_2}\right)^{k+mN}\frac{1}{k+mN}+\sum_{m=1}^{\infty}\left(\frac{\varrho_2}{R_2}\right)^{N-k+mN}\frac{1}{N-k+mN}\Bigg\}$$

$$\times\Bigg\{\left(\frac{R_1}{\varrho_2}\right)^{k}\frac{e^{ik\vartheta}}{k}+\left(\frac{R_1}{\varrho_2}\right)^{N-k}\frac{e^{-i(N-k)\vartheta}}{N-k}+\sum_{m=1}^{\infty}\left(\frac{R_1}{\varrho_2}\right)^{k+mN}\frac{e^{i(k+mN)\vartheta}}{k+mN}+\sum_{m=1}^{\infty}\left(\frac{R_1}{\varrho_2}\right)^{N-k+mN}\frac{e^{-i(N-k+mN)\vartheta}}{N-k+mN}\Bigg\}$$

$$-\Bigg\{\left(\frac{\varrho_2}{R_2}\right)^{k}\frac{e^{ik\vartheta}}{k}+\left(\frac{\varrho_2}{R_2}\right)^{N-k}\frac{e^{-i(N-k)\vartheta}}{N-k}+\sum_{m=1}^{\infty}\left(\frac{\varrho_2}{R_2}\right)^{k+mN}\frac{e^{i(k+mN)\vartheta}}{k+mN}$$

$$+\sum_{m=1}^{\infty}\left(\frac{\varrho_2}{R_2}\right)^{N-k+mN}\frac{e^{-i(N-k+mN)\vartheta}}{N-k+mN}\Bigg\}$$

$$\times\Bigg\{\left(\frac{R_1}{\varrho_2}\right)^{k}\frac{1}{k}+\left(\frac{R_1}{\varrho_2}\right)^{N-k}\frac{1}{N-k}+\sum_{m=1}^{\infty}\left(\frac{R_1}{\varrho_2}\right)^{k+mN}\frac{1}{k+mN}+\sum_{m=1}^{\infty}\left(\frac{R_1}{\varrho_2}\right)^{N-k+mN}\frac{1}{N-k+mN}\Bigg\}$$

$$+\varrho_2^k e^{ik\vartheta}\Bigg\{\frac{1}{kR_2^k}+\frac{1}{(N-k)R_2^{N-k}}+\sum_{m=1}^{\infty}\left(\frac{1}{R_2}\right)^{k+mN}\frac{1}{k+mN}+\sum_{m=1}^{\infty}\left(\frac{1}{R_2}\right)^{N-k+mN}\frac{1}{N-k+mN}\Bigg\}$$

$$\times\Bigg\{\left(\frac{R_1}{\varrho_2}\right)^{k}\frac{1}{k}+\left(\frac{R_1}{\varrho_2}\right)^{N-k}\frac{1}{N-k}+\sum_{m=1}^{\infty}\left(\frac{R_1}{\varrho_2}\right)^{k+mN}\frac{1}{k+mN}+\sum_{m=1}^{\infty}\left(\frac{R_1}{\varrho_2}\right)^{N-k+mN}\frac{1}{N-k+mN}\Bigg\}$$

$$-\varrho_2^k\Bigg\{\frac{1}{kR_2^k}+\frac{1}{(N-k)R_2^{N-k}}+\sum_{m=1}^{\infty}\left(\frac{1}{R_2}\right)^{k+mN}\frac{1}{k+mN}+\sum_{m=1}^{\infty}\left(\frac{1}{R_2}\right)^{N-k+mN}\frac{1}{N-k+mN}\Bigg\}$$

$$\times\Bigg\{\left(\frac{R_1}{\varrho_2}\right)^{k}\frac{e^{ik\vartheta}}{k}+\left(\frac{R_1}{\varrho_2}\right)^{N-k}\frac{e^{-i(N-k)\vartheta}}{N-k}+\sum_{m=1}^{\infty}\left(\frac{R_1}{\varrho_2}\right)^{k+mN}\frac{e^{i(k+mN)\vartheta}}{k+mN}$$

$$+\sum_{m=1}^{\infty}\left(\frac{R_1}{\varrho_2}\right)^{N-k+mN}\frac{e^{i(N-k+mN)\vartheta}}{N-k+mN}\Bigg\}\Bigg|$$

$$=\frac{N^2}{16\pi^2}\Bigg|\varrho_2^k\Bigg\{\frac{R_1^k\varrho_2^{N-k}}{R_2^{N-k}}\frac{e^{-i(N-k)\vartheta}}{k(N-k)}+\frac{R_1^k}{k}\sum_{m=1}^{\infty}\left(\frac{\varrho_2}{R_2}\right)^{k+mN}\frac{e^{i(k+mN)\vartheta}}{k+mN}$$

$$+\frac{R_1^k}{k}\sum_{m=1}^{\infty}\left(\frac{\varrho_2}{R_2}\right)^{N-k+mN}\frac{e^{-i(N-k+mN)\vartheta}}{N-k+mN}\Bigg\}$$

$$+\varrho_2^k\Bigg\{\frac{R_1^{N-k}\varrho_2^{N-k}}{R_2^{N-k}}\frac{e^{-i(N-k)\vartheta}}{(N-k)^2}+\frac{R_1^{N-k}}{N-k}\sum_{m=1}^{\infty}\left(\frac{\varrho_2}{R_2}\right)^{k+mN}\frac{e^{i(k+mN)\vartheta}}{k+mN}$$

$$+\frac{R_1^{N-k}}{N-k}\sum_{m=1}^{\infty}\left(\frac{\varrho_2}{R_2}\right)^{N-k+mN}\frac{e^{-i(N-k+mN)\vartheta}}{N-k+mN}\Bigg\}$$

$$+\varrho_2^k\Bigg\{\left(\frac{\varrho_2}{R_2}\right)^{N-k}\frac{e^{-i(N-k)\vartheta}}{N-k}\sum_{m=1}^{\infty}\frac{R_1^{k+mN}}{k+mN}+\sum_{m=1}^{\infty}\frac{R_1^{k+mN}}{k+mN}\sum_{m=1}^{\infty}\left(\frac{\varrho_2}{R_2}\right)^{k+mN}\frac{e^{i(k+mN)\vartheta}}{k+mN}$$

$$+\sum_{m=1}^{\infty}\frac{R_1^{k+mN}}{k+mN}\sum_{m=1}^{\infty}\left(\frac{\varrho_2}{R_2}\right)^{N-k+mN}\frac{e^{-i(N-k+mN)\vartheta}}{N-k+mN}\Bigg\}$$

$$+\varrho_2^k\Bigg\{\left(\frac{\varrho_2}{R_2}\right)^{N-k}\frac{e^{-i(N-k)\vartheta}}{N-k}\sum_{m=1}^{\infty}\frac{R_1^{N-k+mN}}{N-k+mN}+\sum_{m=1}^{\infty}\frac{R_1^{N-k+mN}}{N-k+mN}\sum_{m=1}^{\infty}\left(\frac{\varrho_2}{R_2}\right)^{k+mN}\frac{e^{i(k+mN)\vartheta}}{k+mN}$$

$$+\sum_{m=1}^{\infty}\frac{R_1^{N-k+mN}}{N-k+mN}\sum_{m=1}^{\infty}\left(\frac{\varrho_2}{R_2}\right)^{N-k+mN}\frac{e^{-i(N-k+mN)\vartheta}}{N-k+mN}\Bigg\}$$

$$
\begin{aligned}
&- \varrho_2^k \left\{ \frac{R_1^k \varrho_2^{N-k}}{R_2^{N-k}} \frac{e^{ik\vartheta}}{k(N-k)} + \frac{R_1^k}{k} \sum_{m=1}^{\infty} \left(\frac{\varrho_2}{R_2}\right)^{k+mN} \frac{e^{ik\vartheta}}{k+mN} \right. \\
&\left. + \frac{R_1^k}{k} \sum_{m=1}^{\infty} \left(\frac{\varrho_2}{R_2}\right)^{N-k+mN} \frac{e^{ik\vartheta}}{N-k+mN} \right\} \\
&- \varrho_2^k \left\{ \frac{R_1^{N-k} \varrho_2^{N-k}}{R_2^{N-k}} \frac{e^{ik\vartheta}}{(N-k)^2} + \frac{R_1^{N-k}}{N-k} \sum_{m=1}^{\infty} \left(\frac{\varrho_2}{R_2}\right)^{k+mN} \frac{e^{ik\vartheta}}{k+mN} \right. \\
&\left. + \frac{R_1^{N-k}}{N-k} \sum_{m=1}^{\infty} \left(\frac{\varrho_2}{R_2}\right)^{N-k+mN} \frac{e^{ik\vartheta}}{N-k+mN} \right\} \\
&- \varrho_2^k \left\{ \left(\frac{\varrho_2}{R_2}\right)^{N-k} \frac{e^{ik\vartheta}}{N-k} \sum_{m=1}^{\infty} \frac{R_1^{k+mN}}{k+mN} + \sum_{m=1}^{\infty} \frac{R_1^{k+mN}}{k+mN} \sum_{m=1}^{\infty} \left(\frac{\varrho_2}{R_2}\right)^{k+mN} \frac{e^{ik\vartheta}}{k+mN} \right. \\
&\left. + \sum_{m=1}^{\infty} \frac{R_1^{k+mN}}{k+mN} \sum_{m=1}^{\infty} \left(\frac{\varrho_2}{R_2}\right)^{N-k+mN} \frac{e^{ik\vartheta}}{N-k+mN} \right\} \\
&- \varrho_2^k \left\{ \left(\frac{\varrho_2}{R_2}\right)^{N-k} \frac{e^{ik\vartheta}}{N-k} \sum_{m=1}^{\infty} \frac{R_1^{N-k+mN}}{N-k+mN} + \sum_{m=1}^{\infty} \frac{R_1^{N-k+mN}}{N-k+mN} \sum_{m=1}^{\infty} \left(\frac{\varrho_2}{R_2}\right)^{k+mN} \frac{e^{ik\vartheta}}{k+mN} \right. \\
&\left. + \sum_{m=1}^{\infty} \frac{R_1^{N-k+mN}}{N-k+mN} \sum_{m=1}^{\infty} \left(\frac{\varrho_2}{R_2}\right)^{N-k+mN} \frac{e^{ik\vartheta}}{N-k+mN} \right\} \\
&+ \left\{ \frac{\varrho_2^k R_1^k}{R_2^k \varrho_2^k} \frac{e^{ik\vartheta}}{k^2} + \frac{\varrho_2^k R_1^{N-k}}{R_2^k \varrho_2^{N-k}} \frac{e^{-i(N-k)\vartheta}}{k(N-k)} + \left(\frac{\varrho_2}{R_2}\right)^k \frac{1}{k} \sum_{m=1}^{\infty} \left(\frac{R_1}{\varrho_2}\right)^{k+mN} \frac{e^{i(k+mN)\vartheta}}{k+mN} \right. \\
&\left. + \left(\frac{\varrho_2}{R_2}\right)^k \frac{1}{k} \sum_{m=1}^{\infty} \left(\frac{R_1}{\varrho_2}\right)^{N-k+mN} \frac{e^{-i(N-k+mN)\vartheta}}{N-k+mN} \right\} \\
&+ \left\{ \frac{\varrho_2^{N-k} R_1^k}{R_2^{N-k} \varrho_2^k} \frac{e^{ik\vartheta}}{k(N-k)} + \frac{\varrho_2^{N-k} R_1^{N-k}}{R_2^{N-k} \varrho_2^{N-k}} \frac{e^{-i(N-k)\vartheta}}{(N-k)^2} + \left(\frac{\varrho_2}{R_2}\right)^{N-k} \frac{1}{N-k} \sum_{m=1}^{\infty} \left(\frac{R_1}{\varrho_2}\right)^{k+mN} \frac{e^{i(k+mN)\vartheta}}{k+mN} \right. \\
&\left. + \left(\frac{\varrho_2}{R_2}\right)^{N-k} \frac{1}{N-k} \sum_{m=1}^{\infty} \left(\frac{R_1}{\varrho_2}\right)^{N-k+mN} \frac{e^{-i(N-k+mN)\vartheta}}{N-k+mN} \right\} \\
&+ \left\{ \frac{R_1^k}{\varrho_2^k} \frac{e^{ik\vartheta}}{k} \sum_{m=1}^{\infty} \left(\frac{\varrho_2}{R_2}\right)^{k+mN} \frac{1}{k+mN} + \frac{R_1^{N-k}}{\varrho_2^{N-k}} \frac{e^{-i(N-k)\vartheta}}{N-k} \sum_{m=1}^{\infty} \left(\frac{\varrho_2}{R_2}\right)^{k+mN} \frac{1}{k+mN} \right. \\
&+ \sum_{m=1}^{\infty} \left(\frac{\varrho_2}{R_2}\right)^{k+mN} \frac{1}{k+mN} \sum_{m=1}^{\infty} \left(\frac{R_1}{\varrho_2}\right)^{k+mN} \frac{e^{i(k+mN)\vartheta}}{k+mN} \\
&\left. + \sum_{m=1}^{\infty} \left(\frac{\varrho_2}{R_2}\right)^{k+mN} \frac{1}{k+mN} \sum_{m=1}^{\infty} \left(\frac{R_1}{\varrho_2}\right)^{N-k+mN} \frac{e^{-i(N-k+mN)\vartheta}}{N-k+mN} \right\} \\
&+ \left\{ \frac{R_1^k}{\varrho_2^k} \frac{e^{ik\vartheta}}{k} \sum_{m=1}^{\infty} \left(\frac{\varrho_2}{R_2}\right)^{N-k+mN} \frac{1}{N-k+mN} + \frac{R_1^{N-k}}{\varrho_2^{N-k}} \frac{e^{-i(N-k)\vartheta}}{N-k} \sum_{m=1}^{\infty} \left(\frac{\varrho_2}{R_2}\right)^{N-k+mN} \frac{1}{N-k+mN} \right. \\
&+ \sum_{m=1}^{\infty} \left(\frac{\varrho_2}{R_2}\right)^{N-k+mN} \frac{1}{N-k+mN} \sum_{m=1}^{\infty} \left(\frac{R_1}{\varrho_2}\right)^{k+mN} \frac{e^{i(k+mN)\vartheta}}{k+mN} \\
&\left. + \sum_{m=1}^{\infty} \left(\frac{\varrho_2}{R_2}\right)^{N-k+mN} \frac{1}{N-k+mN} \sum_{m=1}^{\infty} \left(\frac{R_1}{\varrho_2}\right)^{N-k+mN} \frac{e^{-i(N-k+mN)\vartheta}}{N-k+mN} \right\}
\end{aligned}
$$

$$
\begin{aligned}
&-\Bigg\{\frac{\varrho_2^k R_1^k}{R_2^k \varrho_2^k}\frac{e^{ik\vartheta}}{k^2}+\frac{\varrho_2^k R_1^{N-k}}{R_2^k \varrho_2^{N-k}}\frac{e^{ik\vartheta}}{k(N-k)}+\left(\frac{\varrho_2}{R_2}\right)^k \frac{1}{k}\sum_{m=1}^{\infty}\left(\frac{R_1}{\varrho_2}\right)^{k+mN}\frac{e^{ik\vartheta}}{k+mN}\\
&+\left(\frac{\varrho_2}{R_2}\right)^k \frac{1}{k}\sum_{m=1}^{\infty}\left(\frac{R_1}{\varrho_2}\right)^{N-k+mN}\frac{e^{ik\vartheta}}{N-k+mN}\Bigg\}\\
&-\Bigg\{\frac{\varrho_2^{N-k} R_1^k}{R_2^{N-k} \varrho_2^k}\frac{e^{-i(N-k)\vartheta}}{k(N-k)}+\frac{\varrho_2^{N-k} R_1^{N-k}}{R_2^{N-k} \varrho_2^{N-k}}\frac{e^{-i(N-k)\vartheta}}{(N-k)^2}+\left(\frac{\varrho_2}{R_2}\right)^{N-k} \frac{1}{N-k}\sum_{m=1}^{\infty}\left(\frac{R_1}{\varrho_2}\right)^{k+mN}\frac{e^{-i(N-k)\vartheta}}{k+mN}\\
&+\left(\frac{\varrho_2}{R_2}\right)^{N-k} \frac{1}{N-k}\sum_{m=1}^{\infty}\left(\frac{R_1}{\varrho_2}\right)^{N-k+mN}\frac{e^{-i(N-k)\vartheta}}{N-k+mN}\Bigg\}\\
&-\Bigg\{\frac{R_1^k}{\varrho_2^k}\frac{1}{k}\sum_{m=1}^{\infty}\left(\frac{\varrho_2}{R_2}\right)^{k+mN}\frac{e^{i(k+mN)\vartheta}}{k+mN}+\frac{R_1^{N-k}}{\varrho_2^{N-k}}\frac{1}{N-k}\sum_{m=1}^{\infty}\left(\frac{\varrho_2}{R_2}\right)^{k+mN}\frac{e^{i(k+mN)\vartheta}}{k+mN}\\
&+\sum_{m=1}^{\infty}\left(\frac{\varrho_2}{R_2}\right)^{k+mN}\frac{e^{i(k+mN)\vartheta}}{k+mN}\sum_{m=1}^{\infty}\left(\frac{R_1}{\varrho_2}\right)^{k+mN}\frac{1}{k+mN}\\
&+\sum_{m=1}^{\infty}\left(\frac{\varrho_2}{R_2}\right)^{k+mN}\frac{e^{i(k+mN)\vartheta}}{k+mN}\sum_{m=1}^{\infty}\left(\frac{R_1}{\varrho_2}\right)^{N-k+mN}\frac{1}{N-k+mN}\Bigg\}\\
&-\Bigg\{\frac{R_1^k}{\varrho_2^k}\frac{1}{k}\sum_{m=1}^{\infty}\left(\frac{\varrho_2}{R_2}\right)^{N-k+mN}\frac{e^{-i(N-k+mN)\vartheta}}{N-k+mN}+\frac{R_1^{N-k}}{\varrho_2^{N-k}}\frac{1}{N-k}\sum_{m=1}^{\infty}\left(\frac{\varrho_2}{R_2}\right)^{N-k+mN}\frac{e^{-i(N-k+mN)\vartheta}}{N-k+mN}\\
&+\sum_{m=1}^{\infty}\left(\frac{\varrho_2}{R_2}\right)^{N-k+mN}\frac{e^{-i(N-k+mN)\vartheta}}{N-k+mN}\sum_{m=1}^{\infty}\left(\frac{R_1}{\varrho_2}\right)^{k+mN}\frac{1}{k+mN}\\
&+\sum_{m=1}^{\infty}\left(\frac{\varrho_2}{R_2}\right)^{N-k+mN}\frac{e^{-i(N-k+mN)\vartheta}}{N-k+mN}\sum_{m=1}^{\infty}\left(\frac{R_1}{\varrho_2}\right)^{N-k+mN}\frac{1}{N-k+mN}\Bigg\}\\
&+\varrho_2^k\Bigg\{\frac{R_1^k}{R_2^k \varrho_2^k}\frac{e^{ik\vartheta}}{k^2}+\frac{R_1^{N-k}}{R_2^k \varrho_2^{N-k}}\frac{e^{ik\vartheta}}{k(N-k)}+\frac{1}{kR_2^k}\sum_{m=1}^{\infty}\left(\frac{R_1}{\varrho_2}\right)^{k+mN}\frac{e^{ik\vartheta}}{k+mN}\\
&+\frac{1}{kR_2^k}\sum_{m=1}^{\infty}\left(\frac{R_1}{\varrho_2}\right)^{N-k+mN}\frac{e^{ik\vartheta}}{N-k+mN}\Bigg\}\\
&+\varrho_2^k\Bigg\{\frac{R_1^k}{R_2^{N-k} \varrho_2^k}\frac{e^{ik\vartheta}}{k(N-k)}+\frac{R_1^{N-k}}{R_2^{N-k} \varrho_2^{N-k}}\frac{e^{ik\vartheta}}{(N-k)^2}+\frac{1}{(N-k)R_2^{N-k}}\sum_{m=1}^{\infty}\left(\frac{R_1}{\varrho_2}\right)^{k+mN}\frac{e^{ik\vartheta}}{k+mN}\\
&+\frac{1}{(N-k)R_2^{N-k}}\sum_{m=1}^{\infty}\left(\frac{R_1}{\varrho_2}\right)^{N-k+mN}\frac{e^{ik\vartheta}}{N-k+mN}\Bigg\}\\
&+\varrho_2^k\Bigg\{\frac{R_1^k}{\varrho_2^k}\frac{1}{k}\sum_{m=1}^{\infty}\left(\frac{1}{R_2}\right)^{k+mN}\frac{e^{ik\vartheta}}{k+mN}+\frac{R_1^{N-k}}{\varrho_2^{N-k}}\frac{1}{N-k}\sum_{m=1}^{\infty}\left(\frac{1}{R_2}\right)^{k+mN}\frac{e^{ik\vartheta}}{k+mN}\\
&+\sum_{m=1}^{\infty}\left(\frac{1}{R_2}\right)^{k+mN}\frac{1}{k+mN}\sum_{m=1}^{\infty}\left(\frac{R_1}{\varrho_2}\right)^{k+mN}\frac{e^{ik\vartheta}}{k+mN}\\
&+\sum_{m=1}^{\infty}\left(\frac{1}{R_2}\right)^{k+mN}\frac{1}{k+mN}\sum_{m=1}^{\infty}\left(\frac{R_1}{\varrho_2}\right)^{N-k+mN}\frac{e^{ik\vartheta}}{N-k+mN}\Bigg\}\\
&+\varrho_2^k\Bigg\{\frac{R_1^k}{\varrho_2^k}\frac{1}{k}\sum_{m=1}^{\infty}\left(\frac{1}{R_2}\right)^{N-k+mN}\frac{e^{ik\vartheta}}{N-k+mN}+\frac{R_1^{N-k}}{\varrho_2^{N-k}}\frac{1}{N-k}\sum_{m=1}^{\infty}\left(\frac{1}{R_2}\right)^{N-k+mN}\frac{e^{ik\vartheta}}{N-k+mN}
\end{aligned}
$$

$$
\begin{aligned}
&+\sum_{m=1}^{\infty}\left(\frac{1}{R_2}\right)^{N-k+mN}\frac{1}{N-k+mN}\sum_{m=1}^{\infty}\left(\frac{R_1}{\varrho_2}\right)^{k+mN}\frac{e^{ik\vartheta}}{k+mN}\\
&+\sum_{m=1}^{\infty}\left(\frac{1}{R_2}\right)^{N-k+mN}\frac{1}{N-k+mN}\sum_{m=1}^{\infty}\left(\frac{R_1}{\varrho_2}\right)^{N-k+mN}\frac{e^{ik\vartheta}}{N-k+mN}\Bigg\}\\
&-\varrho_2^k\Bigg\{\frac{R_1^k}{R_2^k\varrho_2^k}\frac{e^{ik\vartheta}}{k^2}+\frac{R_1^{N-k}}{R_2^k\varrho_2^{N-k}}\frac{e^{-i(N-k)\vartheta}}{k(N-k)}+\frac{1}{kR_2^k}\sum_{m=1}^{\infty}\left(\frac{R_1}{\varrho_2}\right)^{k+mN}\frac{e^{i(k+mN)\vartheta}}{k+mN}\\
&+\frac{1}{kR_2^k}\sum_{m=1}^{\infty}\left(\frac{R_1}{\varrho_2}\right)^{N-k+mN}\frac{e^{-i(N-k+mN)\vartheta}}{N-k+mN}\Bigg\}\\
&-\varrho_2^k\Bigg\{\frac{R_1^k}{R_2^{N-k}\varrho_2^k}\frac{e^{ik\vartheta}}{k(N-k)}+\frac{R_1^{N-k}}{R_2^{N-k}\varrho_2^{N-k}}\frac{e^{-i(N-k)\vartheta}}{(N-k)^2}+\frac{1}{(N-k)R_2^{N-k}}\sum_{m=1}^{\infty}\left(\frac{R_1}{\varrho_2}\right)^{k+mN}\frac{e^{i(k+mN)\vartheta}}{k+mN}\\
&+\frac{1}{(N-k)R_2^{N-k}}\sum_{m=1}^{\infty}\left(\frac{R_1}{\varrho_2}\right)^{N-k+mN}\frac{e^{-i(N-k+mN)\vartheta}}{N-k+mN}\Bigg\}\\
&-\varrho_2^k\Bigg\{\frac{R_1^k}{\varrho_2^k}\frac{1}{k}\sum_{m=1}^{\infty}\left(\frac{1}{R_2}\right)^{k+mN}\frac{e^{ik\vartheta}}{k+mN}+\frac{R_1^{N-k}}{\varrho_2^{N-k}}\frac{1}{N-k}\sum_{m=1}^{\infty}\left(\frac{1}{R_2}\right)^{k+mN}\frac{e^{-i(N-k)\vartheta}}{k+mN}\\
&+\sum_{m=1}^{\infty}\left(\frac{1}{R_2}\right)^{k+mN}\frac{1}{k+mN}\sum_{m=1}^{\infty}\left(\frac{R_1}{\varrho_2}\right)^{k+mN}\frac{e^{i(k+mN)\vartheta}}{k+mN}\\
&+\sum_{m=1}^{\infty}\left(\frac{1}{R_2}\right)^{k+mN}\frac{1}{k+mN}\sum_{m=1}^{\infty}\left(\frac{R_1}{\varrho_2}\right)^{N-k+mN}\frac{e^{-i(N-k+mN)\vartheta}}{N-k+mN}\Bigg\}\\
&-\varrho_2^k\Bigg\{\frac{R_1^k}{\varrho_2^k}\frac{1}{k}\sum_{m=1}^{\infty}\left(\frac{1}{R_2}\right)^{N-k+mN}\frac{e^{ik\vartheta}}{N-k+mN}+\frac{R_1^{N-k}}{\varrho_2^{N-k}}\frac{1}{N-k}\sum_{m=1}^{\infty}\left(\frac{1}{R_2}\right)^{N-k+mN}\frac{e^{-i(N-k)\vartheta}}{N-k+mN}\\
&+\sum_{m=1}^{\infty}\left(\frac{1}{R_2}\right)^{N-k+mN}\frac{1}{N-k+mN}\sum_{m=1}^{\infty}\left(\frac{R_1}{\varrho_2}\right)^{k+mN}\frac{e^{i(k+mN)\vartheta}}{k+mN}\\
&+\sum_{m=1}^{\infty}\left(\frac{1}{R_2}\right)^{N-k+mN}\frac{1}{N-k+mN}\sum_{m=1}^{\infty}\left(\frac{R_1}{\varrho_2}\right)^{N-k+mN}\frac{e^{-i(N-k+mN)\vartheta}}{N-k+mN}\Bigg\}\Bigg|\\
\leq&\frac{2N^2}{16\pi^2}\varrho_2^k\Bigg\{\frac{R_1^k\varrho_2^{N-k}}{R_2^{N-k}}+R_1^k\sum_{m=1}^{\infty}\left(\frac{\varrho_2}{R_2}\right)^{k+mN}+R_1^k\sum_{m=1}^{\infty}\left(\frac{\varrho_2}{R_2}\right)^{N-k+mN}+\frac{R_1^{N-k}\varrho_2^{N-k}}{R_2^{N-k}}\\
&+R_1^{N-k}\sum_{m=1}^{\infty}\left(\frac{\varrho_2}{R_2}\right)^{k+mN}+R_1^{N-k}\sum_{m=1}^{\infty}\left(\frac{\varrho_2}{R_2}\right)^{N-k+mN}\\
&+\left(\frac{\varrho_2}{R_2}\right)^{N-k}\sum_{m=1}^{\infty}R_1^{k+mN}+\sum_{m=1}^{\infty}R_1^{k+mN}\sum_{m=1}^{\infty}\left(\frac{\varrho_2}{R_2}\right)^{k+mN}\\
&+\sum_{m=1}^{\infty}R_1^{k+mN}\sum_{m=1}^{\infty}\left(\frac{\varrho_2}{R_2}\right)^{N-k+mN}+\left(\frac{\varrho_2}{R_2}\right)^{N-k}\sum_{m=1}^{\infty}R_1^{N-k+mN}+\sum_{m=1}^{\infty}R_1^{N-k+mN}\sum_{m=1}^{\infty}\left(\frac{\varrho_2}{R_2}\right)^{k+mN}\\
&+\sum_{m=1}^{\infty}R_1^{N-k+mN}\sum_{m=1}^{\infty}\left(\frac{\varrho_2}{R_2}\right)^{N-k+mN}\Bigg\}\\
&+\frac{\varrho_2^kR_1^{N-k}}{R_2^k\varrho_2^{N-k}}+\left(\frac{\varrho_2}{R_2}\right)^k\sum_{m=1}^{\infty}\left(\frac{R_1}{\varrho_2}\right)^{k+mN}+\left(\frac{\varrho_2}{R_2}\right)^k\sum_{m=1}^{\infty}\left(\frac{R_1}{\varrho_2}\right)^{N-k+mN}+\frac{\varrho_2^{N-k}R_1^k}{R_2^{N-k}\varrho_2^k}
\end{aligned}
$$

$$
\begin{aligned}
&+\left(\frac{\varrho_2}{R_2}\right)^{N-k}\sum_{m=1}^{\infty}\left(\frac{R_1}{\varrho_2}\right)^{k+mN}+\left(\frac{\varrho_2}{R_2}\right)^{N-k}\sum_{m=1}^{\infty}\left(\frac{R_1}{\varrho_2}\right)^{N-k+mN}+\left(\frac{R_1}{\varrho_2}\right)^{k}\sum_{m=1}^{\infty}\left(\frac{\varrho_2}{R_2}\right)^{k+mN}\\
&+\left(\frac{R_1}{\varrho_2}\right)^{N-k}\sum_{m=1}^{\infty}\left(\frac{\varrho_2}{R_2}\right)^{k+mN}+\sum_{m=1}^{\infty}\left(\frac{\varrho_2}{R_2}\right)^{k+mN}\sum_{m=1}^{\infty}\left(\frac{R_1}{\varrho_2}\right)^{k+mN}+\sum_{m=1}^{\infty}\left(\frac{\varrho_2}{R_2}\right)^{k+mN}\sum_{m=1}^{\infty}\left(\frac{R_1}{\varrho_2}\right)^{N-k+mN}\\
&+\left(\frac{R_1}{\varrho_2}\right)^{k}\sum_{m=1}^{\infty}\left(\frac{\varrho_2}{R_2}\right)^{N-k+mN}+\left(\frac{R_1}{\varrho_2}\right)^{N-k}\sum_{m=1}^{\infty}\left(\frac{\varrho_2}{R_2}\right)^{N-k+mN}+\sum_{m=1}^{\infty}\left(\frac{\varrho_2}{R_2}\right)^{N-k+mN}\sum_{m=1}^{\infty}\left(\frac{R_1}{\varrho_2}\right)^{k+mN}\\
&+\sum_{m=1}^{\infty}\left(\frac{\varrho_2}{R_2}\right)^{N-k+mN}\sum_{m=1}^{\infty}\left(\frac{R_1}{\varrho_2}\right)^{N-k+mN}\\
&+\varrho_2^{k}\Bigg\{\left(\frac{R_1}{\varrho_2}\right)^{k}\sum_{m=1}^{\infty}\left(\frac{1}{R_2}\right)^{k+mN}+\left(\frac{R_1}{\varrho_2}\right)^{N-k}\sum_{m=1}^{\infty}\left(\frac{1}{R_2}\right)^{k+mN}+\sum_{m=1}^{\infty}\left(\frac{1}{R_2}\right)^{k+mN}\sum_{m=1}^{\infty}\left(\frac{R_1}{\varrho_2}\right)^{k+mN}\\
&+\sum_{m=1}^{\infty}\left(\frac{1}{R_2}\right)^{k+mN}\sum_{m=1}^{\infty}\left(\frac{R_1}{\varrho_2}\right)^{N-k+mN}+\left(\frac{R_1}{\varrho_2}\right)^{k}\sum_{m=1}^{\infty}\left(\frac{1}{R_2}\right)^{N-k+mN}+\left(\frac{R_1}{\varrho_2}\right)^{N-k}\sum_{m=1}^{\infty}\left(\frac{1}{R_2}\right)^{N-k+mN}\\
&+\sum_{m=1}^{\infty}\left(\frac{1}{R_2}\right)^{N-k+mN}\sum_{m=1}^{\infty}\left(\frac{R_1}{\varrho_2}\right)^{k+mN}+\sum_{m=1}^{\infty}\left(\frac{1}{R_2}\right)^{N-k+mN}\sum_{m=1}^{\infty}\left(\frac{R_1}{\varrho_2}\right)^{N-k+mN}\\
&+\frac{R_1^{N-k}}{R_2^{k}\varrho_2^{N-k}}+\left(\frac{1}{R_2}\right)^{k}\sum_{m=1}^{\infty}\left(\frac{R_1}{\varrho_2}\right)^{k+mN}+\left(\frac{1}{R_2}\right)^{k}\sum_{m=1}^{\infty}\left(\frac{R_1}{\varrho_2}\right)^{N-k+mN}\\
&+\frac{R_1^{k}}{R_2^{N-k}\varrho_2^{k}}+\frac{R_1^{N-k}}{R_2^{N-k}\varrho_2^{N-k}}+\left(\frac{1}{R_2}\right)^{N-k}\sum_{m=1}^{\infty}\left(\frac{R_1}{\varrho_2}\right)^{k+mN}+\left(\frac{1}{R_2}\right)^{N-k}\sum_{m=1}^{\infty}\left(\frac{R_1}{\varrho_2}\right)^{N-k+mN}\Bigg\}\\
\le&\,2N^2\varrho_2^{k}\Bigg\{\frac{R_1^{k}\varrho_2^{N-k}}{R_2^{N-k}}+2R_1^{k}\left(\frac{\varrho_2}{R_2}\right)^{k+N}+2R_1^{k}\left(\frac{\varrho_2}{R_2}\right)^{2N-k}+R_1^{N-k}\left(\frac{\varrho_2}{R_2}\right)^{N-k}+2R_1^{N-k}\left(\frac{\varrho_2}{R_2}\right)^{k+N}\\
&+2R_1^{N-k}\left(\frac{\varrho_2}{R_2}\right)^{2N-k}+2R_1^{k+N}\left(\frac{\varrho_2}{R_2}\right)^{N-k}+4R_1^{k+N}\left(\frac{\varrho_2}{R_2}\right)^{k+N}+4R_1^{k+N}\left(\frac{\varrho_2}{R_2}\right)^{2N-k}+2R_1^{2N-k}\left(\frac{\varrho_2}{R_2}\right)^{N-k}\\
&+4R_1^{2N-k}\left(\frac{\varrho_2}{R_2}\right)^{k+N}+4R_1^{2N-k}\left(\frac{\varrho_2}{R_2}\right)^{2N-k}\Bigg\}\\
&+\frac{\varrho_2^{k}R_1^{N-k}}{R_2^{k}\varrho_2^{N-k}}+2\left(\frac{\varrho_2}{R_2}\right)^{k}\left(\frac{R_1}{\varrho_2}\right)^{k+N}+2\left(\frac{\varrho_2}{R_2}\right)^{k}\left(\frac{R_1}{\varrho_2}\right)^{2N-k}\\
&+\frac{\varrho_2^{N-k}R_1^{k}}{R_2^{N-k}\varrho_2^{k}}+2\left(\frac{\varrho_2}{R_2}\right)^{N-k}\left(\frac{R_1}{\varrho_2}\right)^{k+N}+2\left(\frac{\varrho_2}{R_2}\right)^{N-k}\left(\frac{R_1}{\varrho_2}\right)^{2N-k}+2\left(\frac{\varrho_2}{R_2}\right)^{k+N}\left(\frac{R_1}{\varrho_2}\right)^{k}\\
&+2\left(\frac{\varrho_2}{R_2}\right)^{k+N}\left(\frac{R_1}{\varrho_2}\right)^{N-k}+4\left(\frac{\varrho_2}{R_2}\right)^{k+N}\left(\frac{R_1}{\varrho_2}\right)^{k+N}+4\left(\frac{\varrho_2}{R_2}\right)^{k+N}\left(\frac{R_1}{\varrho_2}\right)^{2N-k}+2\left(\frac{\varrho_2}{R_2}\right)^{2N-k}\left(\frac{R_1}{\varrho_2}\right)^{k}\\
&+2\left(\frac{\varrho_2}{R_2}\right)^{2N-k}\left(\frac{R_1}{\varrho_2}\right)^{N-k}+4\left(\frac{\varrho_2}{R_2}\right)^{2N-k}\left(\frac{R_1}{\varrho_2}\right)^{k+N}+4\left(\frac{\varrho_2}{R_2}\right)^{2N-k}\left(\frac{R_1}{\varrho_2}\right)^{2N-k}\\
&+\varrho_2^{k}\Bigg\{2\left(\frac{R_1}{\varrho_2}\right)^{k}\left(\frac{1}{R_2}\right)^{k+N}+2\left(\frac{R_1}{\varrho_2}\right)^{N-k}\left(\frac{1}{R_2}\right)^{k+N}+4\left(\frac{R_1}{\varrho_2}\right)^{k+N}\left(\frac{1}{R_2}\right)^{k+N}+4\left(\frac{R_1}{\varrho_2}\right)^{2N-k}\left(\frac{1}{R_2}\right)^{k+N}\\
&+2\left(\frac{R_1}{\varrho_2}\right)^{k}\left(\frac{1}{R_2}\right)^{2N-k}+2\left(\frac{R_1}{\varrho_2}\right)^{N-k}\left(\frac{1}{R_2}\right)^{2N-k}+4\left(\frac{R_1}{\varrho_2}\right)^{k+N}\left(\frac{1}{R_2}\right)^{2N-k}+4\left(\frac{R_1}{\varrho_2}\right)^{2N-k}\left(\frac{1}{R_2}\right)^{2N-k}\\
&+\left(\frac{R_1}{\varrho_2}\right)^{N-k}\left(\frac{1}{R_2}\right)^{k}+2\left(\frac{R_1}{\varrho_2}\right)^{k+N}\left(\frac{1}{R_2}\right)^{k}+2\left(\frac{R_1}{\varrho_2}\right)^{2N-k}\left(\frac{1}{R_2}\right)^{k}+\left(\frac{R_1}{\varrho_2}\right)^{k}\left(\frac{1}{R_2}\right)^{N-k}\\
&+\left(\frac{R_1}{\varrho_2}\right)^{N-k}\left(\frac{1}{R_2}\right)^{N-k}+2\left(\frac{R_1}{\varrho_2}\right)^{k+N}\left(\frac{1}{R_2}\right)^{N-k}+2\left(\frac{R_1}{\varrho_2}\right)^{2N-k}\left(\frac{1}{R_2}\right)^{N-k}\Bigg\}
\end{aligned}
$$

for sufficiently large N. Therefore

$$\begin{aligned}|A-\varrho_2^k e^{ik\vartheta}B| \leq & 2N^2\left\{\varrho_2^k 30R_1^k\left(\frac{\varrho_2}{R_2}\right)^{N-k}+29\left(\frac{\varrho_2}{R_2}\right)^{k}\left(\frac{R_1}{\varrho_2}\right)^{N-k}+5\left(\frac{\varrho_2}{R_2}\right)^{N-k}\left(\frac{R_1}{\varrho_2}\right)^{k}\right.\\ &\left.+\varrho_2^k\left\{30\left(\frac{R_1}{\varrho_2}\right)^{k}\left(\frac{1}{R_2}\right)^{N-k}+5\left(\frac{R_1}{\varrho_2}\right)^{N-k}\left(\frac{1}{R_2}\right)^{k}\right\}\right\}.\end{aligned}$$

Since

$$|B| \geq \frac{1}{k^2}\frac{R_1^k}{R_2^k}\left(\varrho_2^k-\frac{1}{\varrho_2^k}\right)=\frac{1}{k^2}\frac{R_1^k}{R_2^k}\beta\varrho_2^k,$$

where $1>\beta>1-\frac{1}{\varrho_2}$, we have

$$\begin{aligned}\frac{|A-e^{ik\vartheta}B|}{|B|} \leq & \frac{2N^2k^2}{\beta}\left\{\frac{\frac{30\varrho_2^kR_1^k\varrho_2^{N-k}}{R_2^{N-k}}}{\frac{\varrho_2^kR_1^k}{R_2^k}}+\frac{\frac{29\varrho_2^kR_1^{N-k}}{R_2^k\varrho_2^{N-k}}}{\frac{\varrho_2^kR_1^k}{R_2^k}}+\frac{\frac{5\varrho_2^{N-k}R_1^k}{\varrho_2^kR_2^{N-k}}}{\frac{\varrho_2^kR_1^k}{R_2^k}}+\frac{\frac{30\varrho_2^kR_1^k}{\varrho_2^kR_2^{N-k}}}{\frac{\varrho_2^kR_1^k}{R_2^k}}+\frac{\frac{5\varrho_2^kR_1^{N-k}}{\varrho_2^{N-k}R_2^k}}{\frac{\varrho_2^kR_1^k}{R_2^k}}\right\}\\ = & \frac{2N^2k^2}{\beta}\left\{30R_2^k\left(\frac{\varrho_2}{R_2}\right)^{N-k}+\frac{29}{R_1^k}\left(\frac{R_1}{\varrho_2}\right)^{N-k}+\frac{5}{\varrho_2^k}\left(\frac{\varrho_2}{R_2}\right)^{N-2k}+\frac{30}{\varrho_2^k}\frac{1}{R_2^{N-2k}}+\frac{5}{R_1^k}\left(\frac{R_1}{\varrho_2}\right)^{N-k}\right\}\\ \leq & \frac{2N^2k^2}{\beta}99R_2^k\left(\frac{\varrho_2}{R_2}\right)^{N-k}=\frac{198N^2k^2}{\beta}R_2^k\left(\frac{\varrho_2}{R_2}\right)^{N-k}\end{aligned}$$

where $1>\beta>1-\frac{1}{\varrho_2}$.

Case III, $-N/2 \leq k < 0$:

The proof is analogous to the proof of case II in the case when the maximum is obtained on the external circle ϱ_2. As in (2.52) we now have:

$$\begin{aligned}\left|u_N-\frac{1}{\varrho_2^{|k|}}e^{-i|k|\vartheta}\right| = & \left|u_N\left(\frac{1}{\varrho_2^{|k|}}e^{-i|k|\vartheta}\right)-\frac{1}{\varrho_2^{|k|}}e^{-i|k|\vartheta}\right|=\left|\overline{u_N}\left(\frac{1}{\varrho_2^{|k|}}e^{i|k|\vartheta}\right)-\frac{1}{\varrho_2^{|k|}}e^{-i|k|\vartheta}\right|\\ = & \left|\frac{A}{B}-\frac{1}{\varrho_2^{|k|}}e^{-i|k|\vartheta}\right|=\frac{\left|A-\frac{1}{\varrho_2^{|k|}}e^{-i|k|\vartheta}B\right|}{|B|},\end{aligned}$$

where

$$A=\sqrt{N}\left\{\left(\frac{1}{\varrho_2^{|k|}}\lambda_{k+1}^{11}-\lambda_{k+1}^{21}\right)\langle\overline{\boldsymbol{l_2},\boldsymbol{\xi}_{k+1}}\rangle+\left(\lambda_{k+1}^{22}-\frac{1}{\varrho_2^{|k|}}\lambda_{k+1}^{12}\right)\langle\overline{\boldsymbol{l_1},\boldsymbol{\xi}_{k+1}}\rangle\right\}$$

and

$$B=\lambda_{k+1}^{11}\lambda_{k+1}^{22}-\lambda_{k+1}^{12}\lambda_{k+1}^{21}.$$

Thus

$$\frac{\left|A-\frac{1}{\varrho_2^{|k|}}e^{-i|k|\vartheta}B\right|}{|B|}\leq\frac{\left|A-\frac{1}{\varrho_2^{|k|}}e^{-i|k|\vartheta}B\right|}{\frac{1}{|k|^2}\frac{R_1^{|k|}}{R_2^{|k|}}\left(\varrho_2^{|k|}-\frac{1}{\varrho_2^{k}}\right)}=\frac{\left|A-\frac{1}{\varrho_2^{|k|}}e^{-i|k|\vartheta}B\right|}{\frac{1}{|k|^2}\frac{R_1^{|k|}}{R_2^{|k|}}\beta\varrho_2^{|k|}}$$

where $1>\beta>1-\frac{1}{\varrho_2}$. Therefore

$$\frac{\left|A-\frac{1}{\varrho_2^{|k|}}e^{-i|k|\vartheta}B\right|}{|B|}$$

$$\leq\frac{2N^2|k|^2}{\beta}\left\{\frac{\frac{30R_1^{|k|}\varrho_2^{N-|k|}}{R_2^{N-|k|}\varrho_2^{k}}}{\frac{\varrho_2^{|k|}R_1^{|k|}}{R_2^{|k|}}}+\frac{\frac{29\varrho_2^{k}R_1^{N-|k|}}{R_2^{|k|}\varrho_2^{N-|k|}}}{\frac{\varrho_2^{|k|}R_1^{|k|}}{R_2^{|k|}}}+\frac{\frac{5\varrho_2^{N-|k|}R_1^{|k|}}{\varrho_2^{|k|}R_2^{N-|k|}}}{\frac{\varrho_2^{|k|}R_1^{|k|}}{R_2^{|k|}}}+\frac{\frac{30R_1^{|k|}}{\varrho_2^{|k|}\varrho_2^{|k|}R_2^{N-|k|}}}{\frac{\varrho_2^{|k|}R_1^{|k|}}{R_2^{|k|}}}+\frac{\frac{5R_1^{N-|k|}}{\varrho_2^{|k|}\varrho_2^{N-|k|}R_2^{|}k|}}{\frac{\varrho_2^{|k|}R_1^{|k|}}{R_2^{|k|}}}\right\}$$

$$=\frac{2N^2k^2}{\beta}\left\{30\frac{\varrho_2^{N-|k|}R_2^{|k|}}{\varrho_2^{2|k|}R_2^{N-|k|}}+29\frac{R_1^{N-|k|}}{R_1^{|k|}\varrho_2^{N-|k|}}+5\frac{R_2^{|k|}\varrho_2^{N-|k|}}{R_2^{N-|k|}\varrho_2^{2|k|}}+30\frac{R_2^{|k|}}{\varrho_2^{2|k|}\varrho_2^{|k|}R_2^{N-|k|}}+5\frac{R_1^{N-|k|}}{\varrho_2^{2|k|}R_1^{|k|}\varrho_2^{N-|k|}}\right\}$$

$$=\frac{2N^2k^2}{\beta}\left\{\frac{30}{\varrho_2^{|k|}}\left(\frac{\varrho_2}{R_2}\right)^{N-2|k|}+\frac{29}{\varrho_2^{|k|}}\left(\frac{R_1}{\varrho_2}\right)^{N-2|k|}+\frac{5}{\varrho_2^{|k|}}\left(\frac{\varrho_2}{R_2}\right)^{N-2|k|}+\frac{30}{\varrho_2^{3|k|}}\frac{1}{R_2^{N-2|k|}}+\frac{5}{\varrho_2^{3|k|}}\left(\frac{R_1}{R_2}\right)^{N-2|k|}\right\}$$

$$\leq\frac{2N^2k^2}{\beta}\left\{30\left(\frac{\varrho_2}{R_2}\right)^{N-2|k|}+29\left(\frac{R_1}{\varrho_2}\right)^{N-2|k|}+5\left(\frac{\varrho_2}{R_2}\right)^{N-2|k|}+30\left(\frac{1}{R_2}\right)^{N-2|k|}+5\left(\frac{R_1}{R_2}\right)^{N-2|k|}\right\}$$

$$=\frac{2N^2k^2}{\beta}\left\{35\left(\frac{\varrho_2}{R_2}\right)^{N-2|k|}+29\left(\frac{R_1}{\varrho_2}\right)^{N-2|k|}+30\left(\frac{1}{R_2}\right)^{N-2|k|}+5\left(\frac{R_1}{R_2}\right)^{N-2|k|}\right\}.$$

By taking $\sigma=\max\left\{\frac{\varrho_2}{R_2},\frac{1}{R_2},\frac{R_1}{\varrho_2},\frac{R_1}{R_2}\right\}=\max\left\{\frac{\varrho_2}{R_2},\frac{R_1}{\varrho_2}\right\}<1$, we have that

$$\frac{\left|A-\frac{1}{\varrho_2^{|k|}}e^{-i|k|\vartheta}B\right|}{\left|B\right|}\leq\frac{198N^2k^2}{\beta}\sigma^{N-2|k|}$$

where $1>\beta>1-\frac{1}{\varrho_2}$.

We now find a bound for the term $u_N(\,;\log r)-u(\,;\log r)$:

Lemma 2.4.5. *We have the following estimates:*

$$|u_N(\cdot,\log r)-u(\cdot,\log r)|_\infty\leq\frac{c}{N}\sigma^N \tag{2.53}$$

where c is a constant independent of N.

Proof. Case I: When the maximum is obtained on the inner circle $r=\varrho_1=1$, from expression (2.29) we have:

$$u_N = \sum_{j=1}^{N} \frac{\lambda_j^{11}}{\lambda_j^{11}\lambda_j^{22} - \lambda_j^{12}\lambda_j^{21}} \langle \boldsymbol{f_2}, \boldsymbol{\xi}_j \rangle \overline{\langle \boldsymbol{l_2}, \boldsymbol{\xi}_j \rangle} - \sum_{j=1}^{N} \frac{\lambda_j^{21}}{\lambda_j^{11}\lambda_j^{22} - \lambda_j^{12}\lambda_j^{21}} \langle \boldsymbol{f_1}, \boldsymbol{\xi}_j \rangle \overline{\langle \boldsymbol{l_2}, \boldsymbol{\xi}_j \rangle}$$

$$- \sum_{j=1}^{N} \frac{\lambda_j^{12}}{\lambda_j^{11}\lambda_j^{22} - \lambda_j^{12}\lambda_j^{21}} \langle \boldsymbol{f_2}, \boldsymbol{\xi}_j \rangle \overline{\langle \boldsymbol{l_1}, \boldsymbol{\xi}_j \rangle} + \sum_{j=1}^{N} \frac{\lambda_j^{22}}{\lambda_j^{11}\lambda_j^{22} - \lambda_j^{12}\lambda_j^{21}} \langle \boldsymbol{f_1}, \boldsymbol{\xi}_j \rangle \overline{\langle \boldsymbol{l_1}, \boldsymbol{\xi}_j \rangle}$$

where

$$\langle \boldsymbol{f_1}, \boldsymbol{\xi}_j \rangle = 0 \quad \text{and} \quad \langle \boldsymbol{f_2}, \boldsymbol{\xi}_j \rangle = \begin{cases} \sqrt{N} \log \varrho_2 & \text{if } j = 1 \\ 0 & \text{otherwise}. \end{cases}$$

Thus we have

$$u_N = \frac{\sqrt{N}}{\lambda_1^{11}\lambda_1^{22} - \lambda_1^{12}\lambda_1^{21}} \{\log \varrho_2 \lambda_1^{11} \overline{\langle \boldsymbol{l_2}, \boldsymbol{\xi}_1 \rangle} - \log \varrho_2 \lambda_1^{12} \overline{\langle \boldsymbol{l_1}, \boldsymbol{\xi}_1 \rangle}\},$$

and therefore

$$|u_N - \log \varrho_1| = \left| \frac{A}{B} - 0 \right| = \left| \frac{A}{B} \right|$$

where

$$\begin{aligned}
|A| =& \frac{N^2}{4\pi^2} \Bigg| \log \varrho_2 \left\{ \sum_{m=1}^{\infty} \frac{1}{mN} R_1^{mN} \left(\sum_{m=1}^{\infty} \frac{1}{mN} \left(\frac{1}{R_2} \right)^{mN} \cos(mN\vartheta) - \log R_2 \right) \right. \\
& \left. - \left(\sum_{m=1}^{\infty} \frac{1}{mN} \left(\frac{1}{R_2} \right)^{mN} - \log R_2 \right) \sum_{m=1}^{\infty} \frac{1}{mN} R_1^{mN} \cos(mN\vartheta) \right\} \Bigg| \\
=& \frac{N}{4\pi^2} \Bigg| \log \varrho_2 \left\{ \sum_{m=1}^{\infty} \frac{1}{m} R_1^{mN} \sum_{m=1}^{\infty} \frac{1}{mN} \left(\frac{1}{R_2} \right)^{mN} \cos(mN\vartheta) - \log R_2 \sum_{m=1}^{\infty} \frac{1}{m} R_1^{mN} \right. \\
& \left. - \sum_{m=1}^{\infty} \frac{1}{m} R_1^{mN} \cos(mN\vartheta) \sum_{m=1}^{\infty} \frac{1}{mN} \left(\frac{1}{R_2} \right)^{mN} + \log R_2 \sum_{m=1}^{\infty} \frac{1}{m} R_1^{mN} \cos(mN\vartheta) \right\} \Bigg| \\
\leq& \frac{N}{4\pi^2} \log \varrho_2 \left\{ \frac{1}{N} \sum_{m=1}^{\infty} R_1^{mN} \sum_{m=1}^{\infty} \left(\frac{1}{R_2} \right)^{mN} + \log R_2 \sum_{m=1}^{\infty} R_1^{mN} \right. \\
& \left. + \frac{1}{N} \sum_{m=1}^{\infty} R_1^{mN} \sum_{m=1}^{\infty} \left(\frac{1}{R_2} \right)^{mN} + \log R_2 \sum_{m=1}^{\infty} R_1^{mN} \right\} \\
& \leq \log \varrho_2 \left\{ 4R_1^N \frac{1}{R_2^N} + 2N \log R_2 R_1^N + 4R_1^N \frac{1}{R_2^N} + 2N \log R_2 R_1^N \right\} \\
& = \log \varrho_2 \left\{ 8 \left(\frac{R_1}{R_2} \right)^N + 4N \log R_2 R_1^N \right\} \\
& \leq \log \varrho_2 \left\{ 8NR_1^N + 4N \log R_2 R_1^N \right\}
\end{aligned}$$

for sufficiently large N. In the case $\log R_2 > 1$, we have

$$\frac{|A|}{|B|} \leq \frac{\log \varrho_2 \log R_2 \left(8NR_1^N + 4NR_1^N\right)}{N^2 \log \varrho_2 \log R_2} = \frac{12R_1^N}{N},$$

whereas in the case $\log R_2 < 1$, we have

$$\frac{|A|}{|B|} \leq \frac{\log \varrho_2 \left(8NR_1^N + 4NR_1^N\right)}{N^2 \log \varrho_2 \log R_2} = \frac{12R_1^N}{N \log R_2}$$

Case II: When the maximum is obtained on the external circle $r = \varrho_2$ we have

$$|u_N - \log \varrho_2| = \left| \frac{A}{B} - \log \varrho_2 \right| = \frac{|A - \log \varrho_2 B|}{|B|},$$

where

$$\begin{aligned}
|A - \log \varrho_2 B| =& \frac{N^2}{4\pi^2} \left| \log \varrho_2 \lambda_1^{11} \langle \overline{\boldsymbol{l_2}, \boldsymbol{\xi}_1} \rangle - \log \varrho_2 \lambda_1^{12} \langle \overline{\boldsymbol{l_1}, \boldsymbol{\xi}_1} \rangle - \log \varrho_2 \left(\lambda_1^{11} \lambda_1^{22} - \lambda_1^{12} \lambda_1^{21} \right) \right| \\
=& \log \varrho_2 \frac{N^2}{4\pi^2} \left| \lambda_1^{11} \langle \overline{\boldsymbol{l_2}, \boldsymbol{\xi}_1} \rangle - \lambda_1^{12} \langle \overline{\boldsymbol{l_1}, \boldsymbol{\xi}_1} \rangle - \lambda_1^{11} \lambda_1^{22} + \lambda_1^{12} \lambda_1^{21} \right| \\
=& \log \varrho_2 \frac{N^2}{4\pi^2} \left| \sum_{m=1}^{\infty} \frac{1}{mN} R_1^{mN} \left(\sum_{m=1}^{\infty} \frac{1}{mN} \left(\frac{\varrho_2}{R_2} \right)^{mN} \cos(mN\vartheta) - \log R_2 \right) \right. \\
&- \left(\sum_{m=1}^{\infty} \frac{1}{mN} \left(\frac{1}{R_2} \right)^{mN} - \log R_2 \right) \left(\sum_{m=1}^{\infty} \frac{1}{mN} \left(\frac{R_1}{\varrho_2} \right)^{mN} \cos(mN\vartheta) - \log \varrho_2 \right) \\
&- \sum_{m=1}^{\infty} \frac{1}{mN} R_1^{mN} \left(\sum_{m=1}^{\infty} \frac{1}{mN} \left(\frac{\varrho_2}{R_2} \right)^{mN} \cos(mN\vartheta) - \log R_2 \right) \\
&\left. + \left(\sum_{m=1}^{\infty} \frac{1}{mN} \left(\frac{1}{R_2} \right)^{mN} - \log R_2 \right) \left(\sum_{m=1}^{\infty} \frac{1}{mN} \left(\frac{R_1}{\varrho_2} \right)^{mN} - \log \varrho_2 \right) \right| \\
=& \log \varrho_2 \frac{N^2}{4\pi^2} \left| \sum_{m=1}^{\infty} \frac{1}{mN} R_1^{mN} \sum_{m=1}^{\infty} \frac{1}{mN} \left(\frac{\varrho_2}{R_2} \right)^{mN} \cos(mN\vartheta) - \log R_2 \sum_{m=1}^{\infty} \frac{1}{mN} R_1^{mN} \right. \\
&- \sum_{m=1}^{\infty} \frac{1}{mN} \left(\frac{1}{R_2} \right)^{mN} \sum_{m=1}^{\infty} \frac{1}{mN} \left(\frac{R_1}{\varrho_2} \right)^{mN} \cos(mN\vartheta) + \log \varrho_2 \sum_{m=1}^{\infty} \frac{1}{mN} \left(\frac{1}{R_2} \right)^{mN} \\
&+ \log R_2 \sum_{m=1}^{\infty} \frac{1}{mN} \left(\frac{R_1}{\varrho_2} \right)^{mN} \cos(mN\vartheta) - \log \varrho_2 \log R_2 - \sum_{m=1}^{\infty} \frac{1}{mN} R_1^{mN} \sum_{m=1}^{\infty} \frac{1}{mN} \left(\frac{\varrho_2}{R_2} \right)^{mN} \\
&+ \log R_2 \sum_{m=1}^{\infty} \frac{1}{mN} R_1^{mN} + \sum_{m=1}^{\infty} \frac{1}{mN} \left(\frac{1}{R_2} \right)^{mN} \sum_{m=1}^{\infty} \frac{1}{mN} \left(\frac{R_1}{\varrho_2} \right)^{mN} - \log \varrho_2 \sum_{m=1}^{\infty} \frac{1}{mN} \left(\frac{1}{R_2} \right)^{mN} \\
&\left. - \log R_2 \sum_{m=1}^{\infty} \frac{1}{mN} \left(\frac{R_1}{\varrho_2} \right)^{mN} + \log \varrho_2 \log R_2 \right|
\end{aligned}$$

$$\begin{aligned}
&\leq \log \varrho_2 \left\{ \sum_{m=1}^{\infty} R_1^{mN} \sum_{m=1}^{\infty} \left(\frac{\varrho_2}{R_2}\right)^{mN} + N \log R_2 \sum_{m=1}^{\infty} R_1^{mN} + \sum_{m=1}^{\infty} \left(\frac{1}{R_2}\right)^{mN} \sum_{m=1}^{\infty} \left(\frac{R_1}{\varrho_2}\right)^{mN} \right. \\
&\quad + N \log \varrho_2 \sum_{m=1}^{\infty} \left(\frac{1}{R_2}\right)^{mN} + N \log R_2 \sum_{m=1}^{\infty} \left(\frac{R_1}{\varrho_2}\right)^{mN} + \sum_{m=1}^{\infty} R_1^{mN} \sum_{m=1}^{\infty} \left(\frac{\varrho_2}{R_2}\right)^{mN} \\
&\quad + N \log R_2 \sum_{m=1}^{\infty} R_1^{mN} + \sum_{m=1}^{\infty} \left(\frac{1}{R_2}\right)^{mN} \sum_{m=1}^{\infty} \left(\frac{R_1}{\varrho_2}\right)^{mN} + N \log \varrho_2 \sum_{m=1}^{\infty} \left(\frac{1}{R_2}\right)^{mN} \\
&\quad \left. + N \log R_2 \sum_{m=1}^{\infty} \left(\frac{R_1}{\varrho_2}\right)^{mN} \right\} \\
&= 2 \log \varrho_2 \left\{ \sum_{m=1}^{\infty} R_1^{mN} \sum_{m=1}^{\infty} \left(\frac{\varrho_2}{R_2}\right)^{mN} + N \log R_2 \sum_{m=1}^{\infty} R_1^{mN} + \sum_{m=1}^{\infty} \left(\frac{1}{R_2}\right)^{mN} \sum_{m=1}^{\infty} \left(\frac{R_1}{\varrho_2}\right)^{mN} \right. \\
&\quad \left. + N \log \varrho_2 \sum_{m=1}^{\infty} \left(\frac{1}{R_2}\right)^{mN} + N \log R_2 \sum_{m=1}^{\infty} \left(\frac{R_1}{\varrho_2}\right)^{mN} \right. \\
&\leq 2 \log \varrho_2 \left\{ 4 R_1^N \left(\frac{\varrho_2}{R_2}\right)^N + 2N \log R_2 R_1^N + 4 \frac{1}{R_2^N} \left(\frac{R_1}{\varrho_2}\right)^N + 2N \log \varrho_2 \frac{1}{R_2^N} + 2N \log R_2 \left(\frac{R_1}{\varrho_2}\right)^N \right\} \\
&\leq 2 \log \varrho_2 \left\{ 4\sigma^{2N} + 2N \log R_2 \sigma^N + 4\sigma^{2N} + 2N \log R_2 \sigma^N + 2N \log R_2 \sigma^N \right\}
\end{aligned}$$

$$\begin{aligned}
&\leq \log \varrho_2 \left\{ 16\sigma^N + 12N \log R_2 \sigma^N \right\} \\
&\leq \log \varrho_2 \, \sigma^N N \left\{ 16 + 12 \log R_2 \right\}
\end{aligned}$$

for sufficient large N.

In the case $\log R_2 > 1$, we have

$$\frac{|A - \log \varrho_2 B|}{|B|} \leq \frac{28 \log \varrho_2 \log R_2 N \sigma^N}{N^2 \log \varrho_2 \log R_2} = \frac{28\sigma^N}{N}.$$

whereas when $\log R_2 < 1$, we have

$$\frac{|A - \log \varrho_2 B|}{|B|} \leq \frac{28 \log \varrho_2 N \sigma^N}{N^2 \log \varrho_2 \log R_2} = \frac{28\sigma^N}{N \log R_2}.$$

We are now in a position to obtain a bound for $u_N\left(., f_N\right) - u\left(., f_N\right)$ by summing the bounds we have obtained so far.

$$\begin{aligned}
\left\| u_N\left(., f_N\right) - u\left(., f_N\right) \right\|_\infty \leq & \sum_{k=-\frac{N}{2}+1}^{\frac{N}{2}} |\mu_k| \left\| u_N\left(, r^k e^{ik\vartheta}\right) - u\left(, r^k e^{ik\vartheta}\right) \right\|_\infty \\
& + \sum_{k=-\frac{N}{2}+1, k\neq 0}^{\frac{N}{2}} |\nu_k| \left\| u_N\left(, r^{-k} e^{ik\vartheta}\right) - u\left(, r^{-k} e^{ik\vartheta}\right) \right\|_\infty \\
& + |\nu_0| \left\| u_N\left(\cdot, \log r\right) - u\left(\cdot, \log r\right) \right\|_\infty .
\end{aligned}$$

Using estimates (2.40), (2.48) and (2.53) we obtain

$$
\begin{aligned}
\|u_N(., f_N) - u(., f_N)\|_\infty \leq & \sum_{k=-\frac{N}{2}+1}^{\frac{N}{2}} M\gamma_4^{|k|} c N^4 \sigma^{N-2|k|} + \sum_{k=-\frac{N}{2}+1, k\neq 0}^{\frac{N}{2}} M\gamma_4^{|k|} c N^4 \sigma^{N-2|k|} + M\frac{c}{N}\sigma^N \\
\leq & 2cMN^4\sigma^N \sum_{k=0}^{\frac{N}{2}} \left(\frac{\gamma_4}{\sigma^2}\right)^k \leq 4cMN^4\sigma^N \frac{N}{4}\left\{1 + \left(\frac{\gamma_4}{\sigma^2}\right)^{\frac{N}{2}}\right\} \\
= & cMN^5\left(\sigma^N + \gamma_4^{\frac{N}{2}}\right)
\end{aligned}
\tag{2.54}
$$

The desired bound is thus obtained as follows. We take $\gamma = \max\{\gamma_3, \gamma_4\} < 1$. From the bounds on $\|u(\cdot; \boldsymbol{f} - \boldsymbol{f}_N)\|_\infty$ and $\|u_N(\cdot; \boldsymbol{f}_N) - u(\cdot; \boldsymbol{f}_N)\|_\infty$ given by (2.47), (2.48), (2.53) and (2.54), we get the desired bound.

Theorem 2.4.6.

$$
\|u_N(\cdot\,; f) - u(\cdot\,; f)\|_\infty \leq CMN^5\left(\sigma^N + \gamma^{N/2}\right). \tag{2.55}
$$

2.5 Numerical results

We considered the following numerical examples corresponding to the Dirichlet problem (2.1) in the annulus defined by $\varrho_1 = 1, \varrho_2 = 2$.

The maximum relative error in these examples was calculated on a uniform grid of m points on the boundary (since all the functions involved are harmonic and the maximum principle applies) defined by

$$
(\varrho_1 \cos\vartheta_j, \varrho_1 \sin\vartheta_j), \quad \vartheta_j = \frac{2\pi(j-1)}{m}, \quad j = 1, ..., m
$$

$$
(\varrho_2 \cos\vartheta_j, \varrho_2 \sin\vartheta_j), \quad \vartheta_j = \frac{2\pi(j-1)}{m}, \quad j = 1, ..., m
$$

The parameter m is taken to be equal to 500.

Example 1. Problem corresponding to the exact solution $u = \mathrm{e}^x \cos y$. We varied the angle of α and examined how this affected the accuracy of the solution for various values of N for different $\varepsilon = \varrho_1 - R_1 = R_2 - \varrho_2$ (Figures 2.1, 2.2). We also varied the radii R_1 and R_2 of the inner and external circle and examined how this affected the accuracy of the solution for various values of N (Figure 2.7). In addition, we varied the radius R_2 of the external circle and examined how this affected the accuracy of the solution for various values of N (Figure 2.10).

Example 2. Problem corresponding to the exact solution $u = \dfrac{x}{x^2+y^2}$. We varied the angle α and examined how this affected the accuracy of the solution for various values of N for different $\varepsilon = \varrho_1 - R_1 = R_2 - \varrho_2$ (Figures 2.3, 2.4). We also varied the radii R_1 and R_2 of the inner and external circle and examined how this affected the accuracy of the solution for various values of N (Figure 2.8).

Example 3. Problem corresponding to the exact solution $u = x^2 - y^2$. We varied the angle of α and examined how this affected the accuracy of the solution for various values of N for different $\varepsilon = \varrho_1 - R_1 = R_2 - \varrho_2$ (Figures 2.5, 2.6). We also varied the radii R_1 and R_2 of the inner and external circle and examined how this affected the accuracy of the solution for various values of N (Figure 2.9).

The numerical results indicate that for small ε the accuracy of the solution is dependent on the angular parameter α. As ε grows this dependence disappears. Further, the accuracy for a certain range of values of ε reaches an optimal value for $\alpha = 0.25$. This phenomenon was also been observed in [67, 68] and is valid for all the examples considered in this chapter (Figures 2.1-2.6). Also, we observed that as ε increases for $\alpha = 0$, the accuracy of the method improves (Figures 2.7-2.9) according to the theoretical predictions developed in this study. However, for larger values of ε the accuracy deteriorates due to ill-conditioning. This is more evident in Figure 2.10, when we kept the inner pseudoboundary fixed and equal to 0.5 and increased only the outer pseudoboundary.

From Figures 2.7, 2.8 and 2.9 it is evident that as R_1 decreases, R_2 increases and N increases the MFS solution converges exponentially fast to the exact solution for all the test problems. The same phenomenon can be observed for Figure 2.10, where R_1 is fixed and R_2 increases. However in all cases, there is a deterioration of accuracy for large values of R_2 and N due to ill-conditioning.

Note

We have also considered the case when the two pseudoboundaries are rotated independently. In particular, we take the coordinates of the points $Q_j = (x_{Q_j}, y_{Q_j})$ on the internal pseudo–boundary to be

$$x_{Q_j} = R_1 \cos \frac{2(j-1+\alpha_1)\pi}{N}, \;\; y_{Q_j} = R_1 \sin \frac{2(j-1+\alpha_1)\pi}{N}, \;\; j = 1, \ldots, N$$

and the coordinates of the points $Q_{N+j} = (x_{Q_{N+j}}, y_{Q_{N+j}})$ on the external pseudo–boundary to be

$$x_{Q_{N+j}} = R_2 \cos \frac{2(j-1+\alpha_2)\pi}{N}, \;\; y_{Q_{N+j}} = R_2 \sin \frac{2(j-1+\alpha_2)\pi}{N}, \;\; j = 1, \ldots, N\,.$$

The independent rotation produced little difference in the numerical results.

2.6 Conclusions

In this study we examine the application of the MFS to harmonic problems in annular domains subject to Dirichlet boundary conditions. The properties of the coefficient matrix are investigated, and an efficient algorithm for the numerical solution of the problem is proposed. It is shown that, for analytic boundary data, the MFS approximation converges exponentially to the exact solution. The results of the current investigation can be also applied to other second order elliptic operators such as the Helmholtz operator for problems in annular domains. Further, the application of the algorithm proposed in this chapter to the biharmonic equation in angular domains is being examined. The extension of the ideas developed in this study to the solution of harmonic and biharmonic problems in shell type axisymmetric domains (see [70]), is currently under investigation.

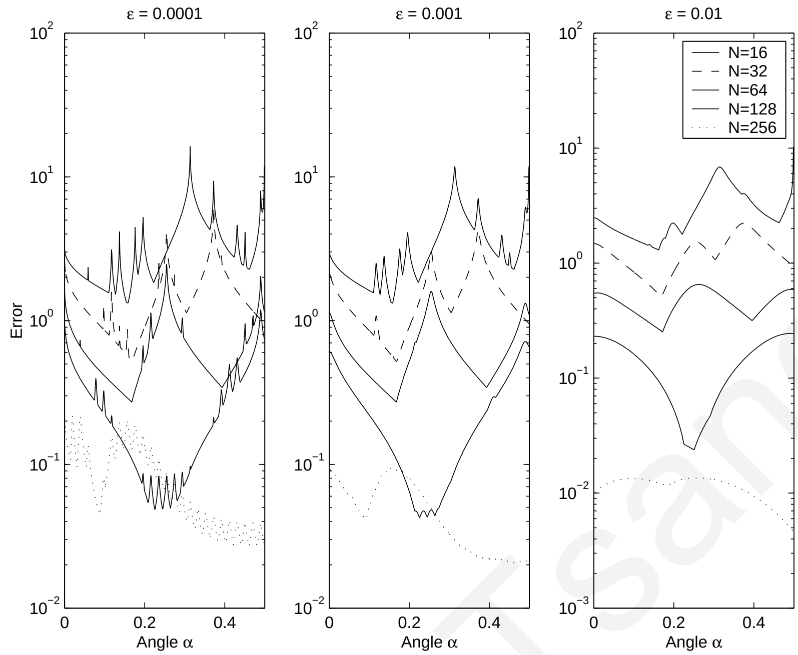

Figure 2.1: Log–plot of error versus angular parameter α for $\epsilon = 10^{-4}, 10^{-3}, 10^{-2}$ in Example 1 for different values of N

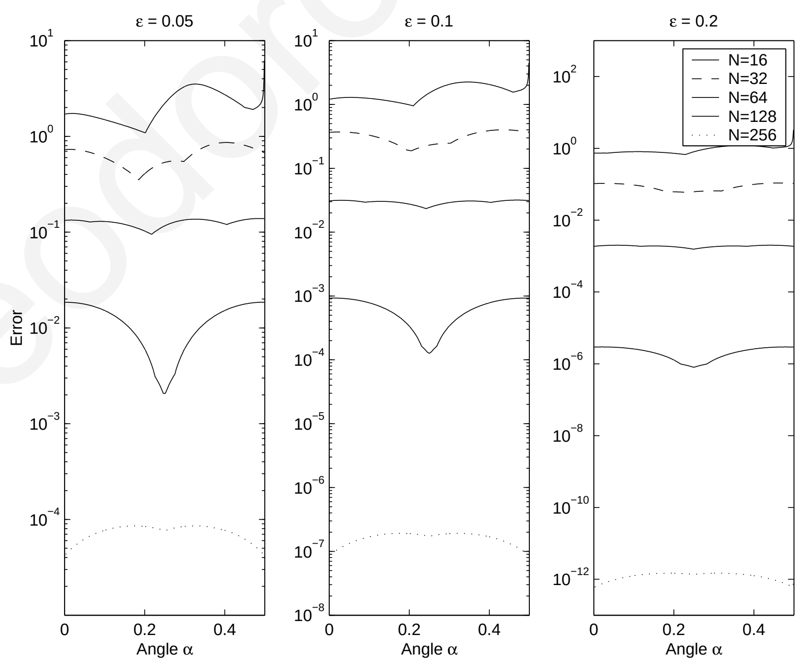

Figure 2.2: Log–plot of error versus angular parameter α for $\epsilon = 0.05, 0.1, 0.2$ in Example 1 for different values of N

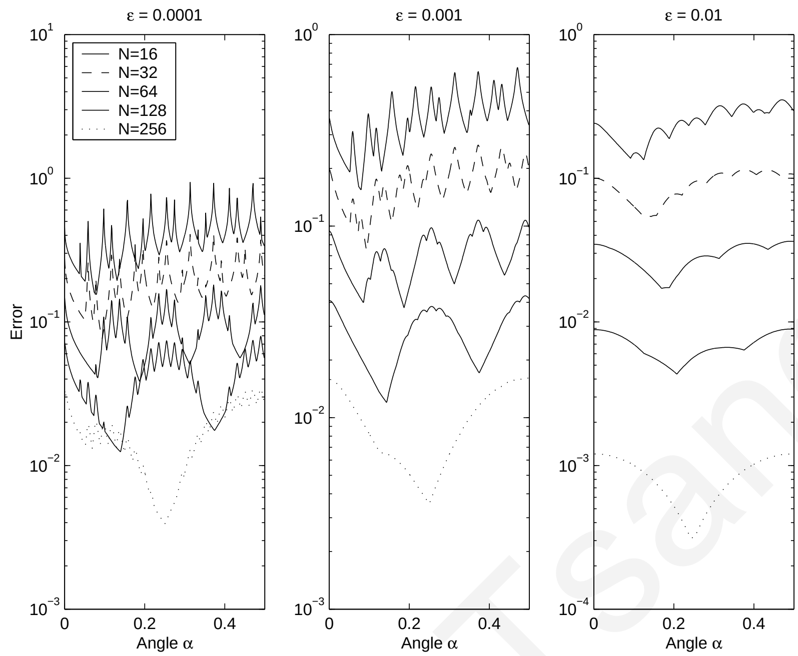

Figure 2.3: Log–plot of error versus angular parameter α for $\epsilon = 10^{-4}, 10^{-3}, 10^{-2}$ in Example 2 for different values of N

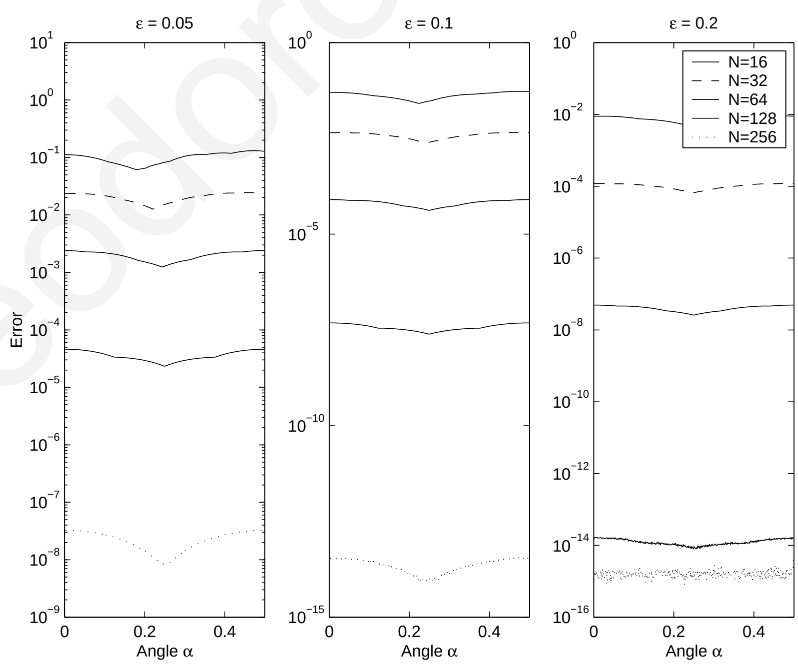

Figure 2.4: Log–plot of error versus angular parameter α for $\epsilon = 0.05, 0.1, 0.2$ in Example 2 for different values of N

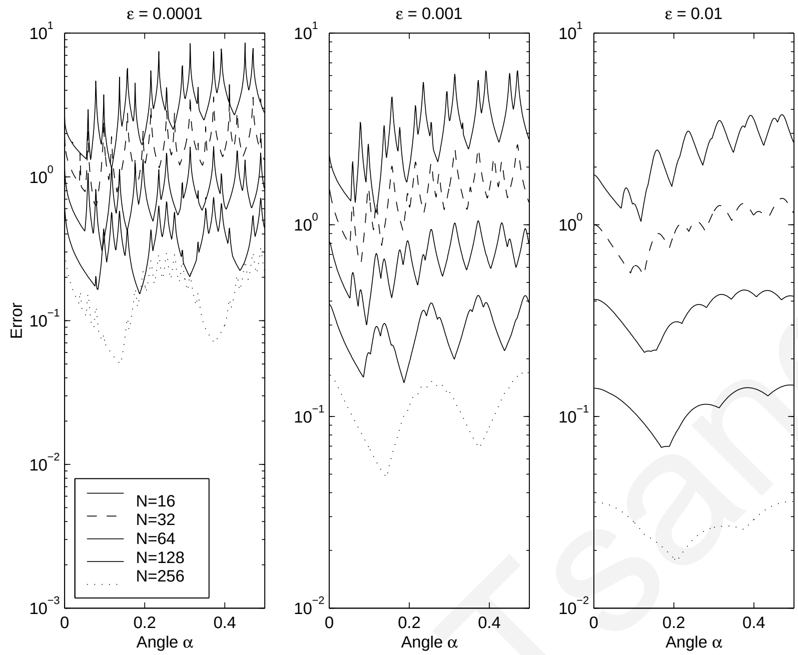

Figure 2.5: Log–plot of error versus angular parameter α for $\epsilon = 10^{-4}, 10^{-3}, 10^{-2}$ in Example 3 for different values of N

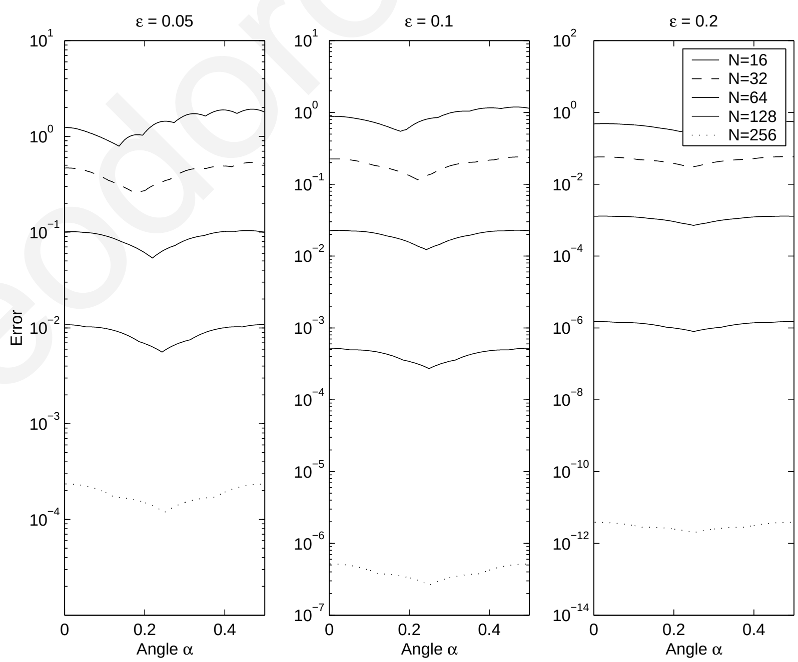

Figure 2.6: Log–plot of error versus angular parameter α for $\epsilon = 0.05, 0.1, 0.2$ in Example 3 for different values of N

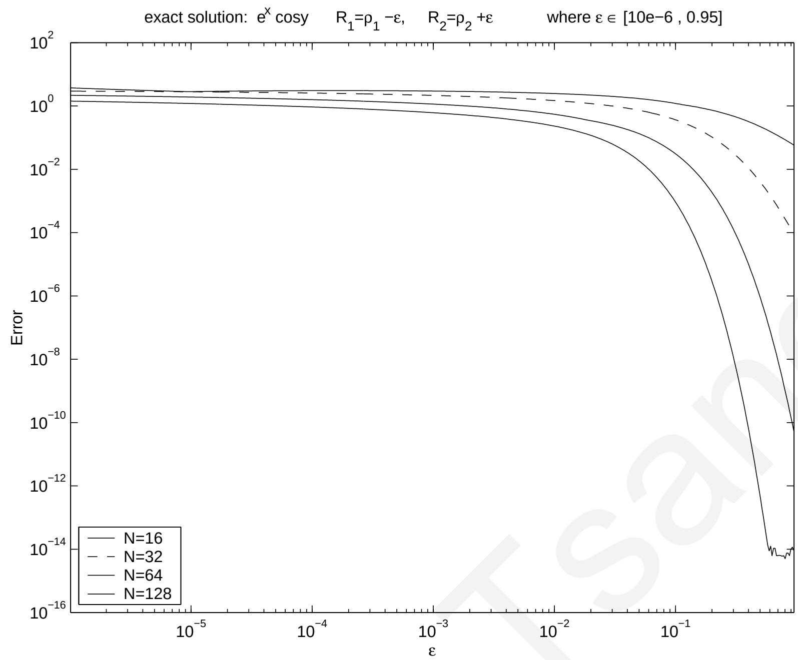

Figure 2.7: Log-log plot of maximum relative error versus ϵ in Example 1

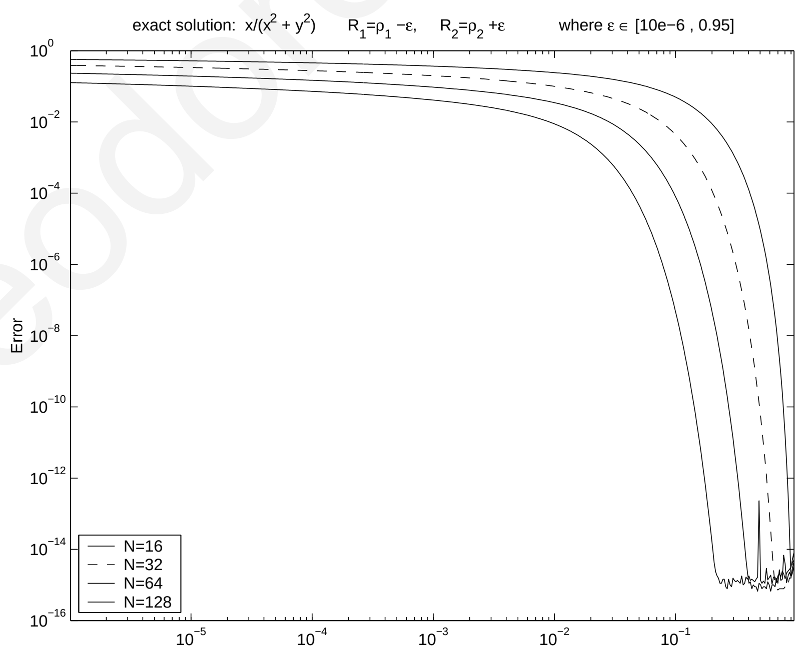

Figure 2.8: Log-log plot of maximum relative error versus ϵ in Example 2

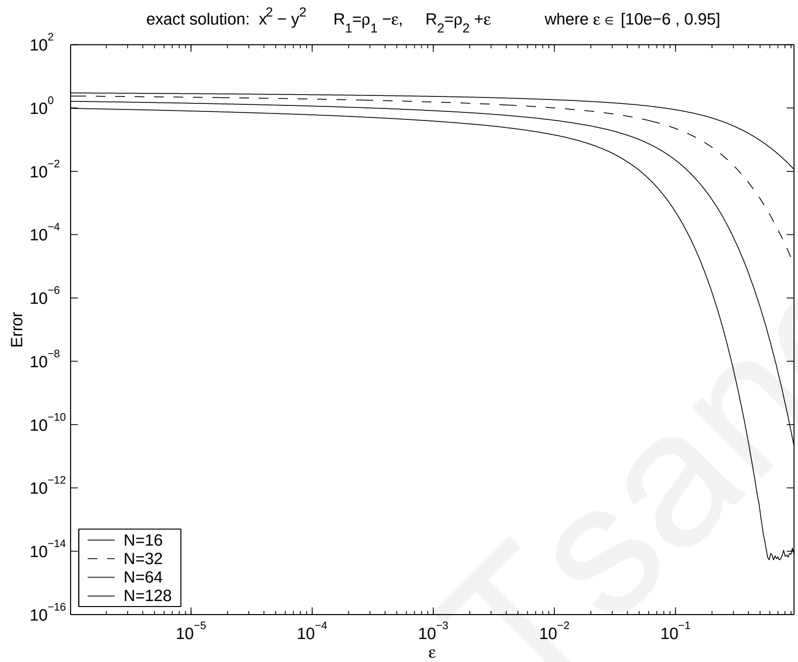

Figure 2.9: Log-log plot of maximum relative error versus ϵ in Example 3

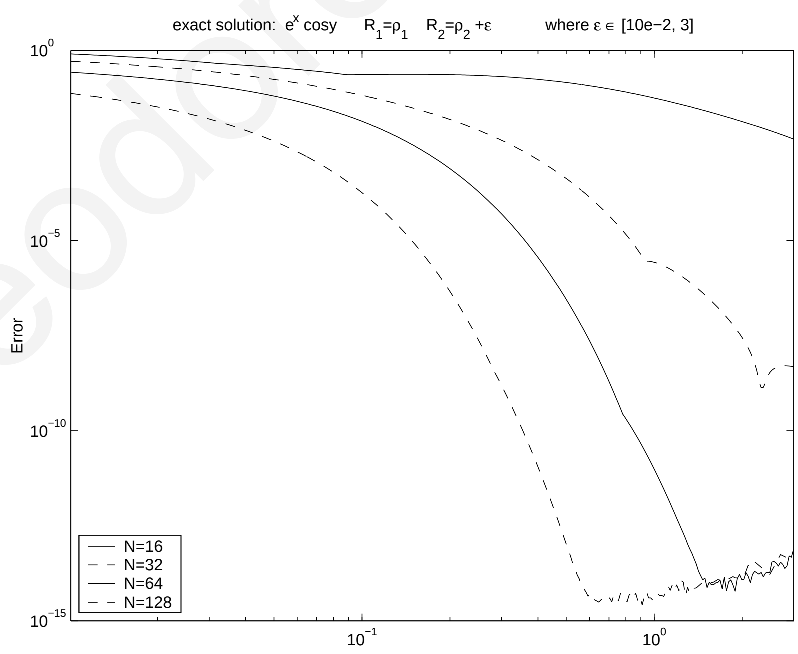

Figure 2.10: Log-log plot of maximum relative error versus ϵ in Example 1

Chapter 3

A Matrix Decomposition MFS Algorithm for Biharmonic Problems in Annular Domains

3.1 Introduction

The Method of Fundamental Solutions (MFS) is a meshless technique for the numerical solution of certain elliptic boundary value problems. It is applicable when the fundamental solution of the elliptic operator in question is known. In the MFS, singularities of the fundamental solution, are avoided by the introduction of a fictitious boundary exterior to the problem geometry (the *pseudo–boundary*). Thus the approximate solution satisfies the underlying partial differential equation. Since the method was first introduced by Kupradze and Aleksidze [49] in 1964, and was first proposed as a numerical technique by Mathon and Johnston [59] in 1977, it has been applied to a wide variety of physical problems. In recent years, this technique has become very popular because of its simplicity and ease of implementation. Details concerning the various aspects and applications of the MFS can be found in the recent survey papers [18, 19, 26].

There are two different formulations of the MFS. In one, the singularities are fixed, whereas in the other they are determined as part of the solution of the discrete problem. The latter, which results in a nonlinear least–squares problem, was used for the solution of biharmonic problems in [38, 39, 40]. The MFS with fixed singularities, which results in a linear system, was used for the solution of biharmonic problems in circular domains in [71]. This version of the MFS was also used for the solution of three–dimensional biharmonic problems in axisymmetric domains in [20]. In this study, we shall be using the MFS with fixed singularities for the solution of biharmonic problems in annular domains. We shall be extending the ideas used in [71] as well as those of chapter 2, where the MFS was used for the solution of harmonic problems in annular domains. A variant of the MFS involving Green's functions was applied to the solution of harmonic problems in annular domains in [42].

3.2 MFS formulation

We consider the boundary value problem

$$\begin{cases} \Delta^2 u = 0 & \text{in} \quad \Omega, \\ u = f_1 \quad \text{and} \quad \dfrac{\partial u}{\partial n} = g_1 & \text{on} \quad \partial\Omega_1\,, \\ u = f_2 \quad \text{and} \quad \dfrac{\partial u}{\partial n} = g_2 & \text{on} \quad \partial\Omega_2\,, \end{cases} \tag{3.1}$$

where the domain Ω is the annulus

$$\Omega = \left\{ \boldsymbol{x} \in \mathbb{R}^2 \,:\, \varrho_1 < |\boldsymbol{x}| < \varrho_2 \right\}, \tag{3.2}$$

Δ denotes the Laplace operator and f_1, f_2, g_1 and g_2 are given functions. The boundary of Ω is $\partial\Omega = \partial\Omega_1 \cup \partial\Omega_2$ where $\partial\Omega_1$ and $\partial\Omega_2$ are the circles with radii ϱ_1 and ϱ_2, respectively.

In the MFS, the solution u is approximated by (see [18, 68])

$$u_N(\boldsymbol{\mu}, \boldsymbol{\nu}, \boldsymbol{Q}\,; P) \;=\; \sum_{j=1}^{2N} \left\{ \mu_j \, k_1(P, Q_j) + \nu_j \, k_2(P, Q_j) \right\}, \quad P \in \overline{\Omega}, \tag{3.3}$$

where $\boldsymbol{\mu} = (\mu_1, \ldots, \mu_{2N})^T$, $\boldsymbol{\nu} = (\nu_1, \nu_2, \ldots, \nu_{2N})^T$ and $\boldsymbol{Q}$ is a $4N-$vector containing the coordinates of the singularities Q_j, $j = 1, \ldots, 2N$, which lie outside $\overline{\Omega}$. The function $k_1(P, Q)$ is a fundamental solution of Laplace's equation given by

$$k_1(P, Q) \;=\; -\frac{1}{2\pi} \log |P - Q|, \tag{3.4}$$

and the function $k_2(P,Q)$ is a fundamental solution of the biharmonic equation given by

$$k_2(P,Q) = -\frac{1}{8\pi}|P-Q|^2 \log|P-Q|. \tag{3.5}$$

The singularities Q_j are fixed on the pseudo–boundary $\partial\tilde{\Omega} = \partial\tilde{\Omega}_1 \cup \partial\tilde{\Omega}_2$ of an annulus $\tilde{\Omega}$ concentric to Ω and defined by

$$\tilde{\Omega} = \{\boldsymbol{x} \in \mathbb{R}^2 : R_1 < |\boldsymbol{x}| < R_2\},$$

where $R_2 > \varrho_2 > \varrho_1 > R_1$. The boundary of $\tilde{\Omega}$ comprises $\partial\tilde{\Omega}_1$ and $\partial\tilde{\Omega}_2$, the circles with radii R_1 and R_2, respectively. A set of collocation points $\{P_i\}_{i=1}^{2N}$ is placed on $\partial\Omega$. If $P_i = (x_{P_i}, y_{P_i})$, then we take

$$x_{P_i} = \varrho_1 \cos\frac{2(i-1)\pi}{N}, \quad y_{P_i} = \varrho_1 \sin\frac{2(i-1)\pi}{N}, \tag{3.6}$$

and

$$x_{P_{N+i}} = \varrho_2 \cos\frac{2(i-1)\pi}{N}, \quad y_{P_{N+i}} = \varrho_2 \sin\frac{2(i-1)\pi}{N}, \tag{3.7}$$

where $i = 1, \ldots, N$.

If $Q_j = (x_{Q_j}, y_{Q_j})$, then

$$x_{Q_j} = R_1 \cos\frac{2(j-1+\alpha)\pi}{N}, \quad y_{Q_j} = R_1 \sin\frac{2(j-1+\alpha)\pi}{N}, \quad j = 1, \ldots, N, \tag{3.8}$$

and

$$x_{Q_{N+j}} = R_2 \cos\frac{2(j-1+\alpha)\pi}{N}, \quad y_{Q_{N+j}} = R_2 \sin\frac{2(j-1+\alpha)\pi}{N}, \tag{3.9}$$

where $j = 1, \ldots, N$. The presence of the angular parameter $\alpha \in [-\frac{1}{2}, \frac{1}{2}]$ indicates that the sources are rotated by an angle $\frac{2\pi\alpha}{N}$ with respect to the boundary points. This rotation is known to improve the accuracy of the approximation significantly when the pseudo–boundary is very close to the boundary. (See [67, 69]).

The vectors of coefficients $\boldsymbol{\mu}$ and $\boldsymbol{\nu}$ are determined so that the boundary conditions are satisfied at the collocation points $\{P_i\}_{i=1}^{2N}$:

$$u_N(\boldsymbol{\mu}, \boldsymbol{\nu}, \boldsymbol{Q}; P_i) = f_1(P_i), \quad \frac{\partial u_N}{\partial n}(\boldsymbol{\mu}, \boldsymbol{\nu}, \boldsymbol{Q}; P_i) = g_1(P_i), \quad i = 1, \ldots, N, \tag{3.10}$$

and

$$u_N(\boldsymbol{\mu}, \boldsymbol{\nu}, \boldsymbol{Q}; P_{N+i}) = f_2(P_{N+i}), \quad \frac{\partial u_N}{\partial n}(\boldsymbol{\mu}, \boldsymbol{\nu}, \boldsymbol{Q}; P_{N+i}) = g_2(P_{N+i}), \quad i = 1, \ldots, N. \tag{3.11}$$

This yields a linear system of the form

$$\left(\begin{array}{c|c|c|c} A_{11} & A_{12} & A_{13} & A_{14} \\ \hline A_{21} & A_{22} & A_{23} & A_{24} \\ \hline A_{31} & A_{32} & A_{33} & A_{34} \\ \hline A_{41} & A_{42} & A_{43} & A_{44} \end{array}\right) \left(\begin{array}{c} \boldsymbol{s_1} \\ \hline \boldsymbol{s_2} \\ \hline \boldsymbol{t_1} \\ \hline \boldsymbol{t_2} \end{array}\right) = \left(\begin{array}{c} \boldsymbol{f_1} \\ \hline \boldsymbol{f_2} \\ \hline \boldsymbol{g_1} \\ \hline \boldsymbol{g_2} \end{array}\right), \tag{3.12}$$

where

$$\boldsymbol{s_1} = (\mu_1, \mu_2, \ldots, \mu_N)^T, \ \boldsymbol{s_2} = (\mu_{N+1}, \mu_{N+2}, \ldots, \mu_{2N})^T,$$
$$\boldsymbol{t_1} = (\nu_1, \nu_2, \ldots, \nu_N)^T, \ \ \boldsymbol{t_2} = (\nu_{N+1}, \nu_{N+2}, \ldots, \nu_{2N})^T.$$

The elements of the matrices $A_{mn}, \ \ m, n = 1, \cdots, 4$ are given by

$$(A_{11})_{i,j} = -\frac{1}{2\pi} \log |P_i - Q_j|,$$
$$(A_{12})_{i,j} = -\frac{1}{2\pi} \log |P_i - Q_{N+j}|,$$
$$(A_{13})_{i,j} = -\frac{1}{8\pi} |P_i - Q_j|^2 \log |P_i - Q_j|,$$
$$(A_{14})_{i,j} = -\frac{1}{8\pi} |P_i - Q_{N+j}|^2 \log |P_i - Q_{N+j}|,$$
$$(A_{21})_{i,j} = -\frac{1}{2\pi} \log |P_{N+i} - Q_j|,$$
$$(A_{22})_{i,j} = -\frac{1}{2\pi} \log |P_{N+i} - Q_{N+j}|,$$
$$(A_{23})_{i,j} = -\frac{1}{8\pi} |P_{N+i} - Q_j|^2 \log |P_{N+i} - Q_j|,$$
$$(A_{24})_{i,j} = -\frac{1}{8\pi} |P_{N+i} - Q_{N+j}|^2 \log |P_{N+i} - Q_{N+j}|,$$
$$(A_{31})_{i,j} = -\frac{1}{2\pi} \left(\frac{x_{P_i} - x_{Q_j}}{|P_i - Q_j|^2} n_x + \frac{y_{P_i} - y_{Q_j}}{|P_i - Q_j|^2} n_y \right),$$
$$(A_{32})_{i,j} = -\frac{1}{2\pi} \left(\frac{x_{P_i} - x_{Q_{N+j}}}{|P_i - Q_{N+j}|^2} n_x + \frac{y_{P_i} - y_{Q_{N+j}}}{|P_i - Q_{N+j}|^2} n_y \right),$$
$$(A_{33})_{i,j} = -\frac{1}{8\pi} \left[1 + 2\log |P_i - Q_j|\right] \left((x_{P_i} - x_{Q_j}) n_x + (y_{P_i} - y_{Q_j}) n_y \right),$$
$$(A_{34})_{i,j} = -\frac{1}{8\pi} \left[1 + 2\log |P_i - Q_{N+j}|\right] \left((x_{P_i} - x_{Q_{N+j}}) n_x + (y_{P_i} - y_{Q_{N+j}}) n_y \right),$$
$$(A_{41})_{i,j} = -\frac{1}{2\pi} \left(\frac{x_{P_{N+i}} - x_{Q_j}}{|P_{N+i} - Q_j|^2} n_x + \frac{y_{P_{N+i}} - y_{Q_j}}{|P_{N+i} - Q_j|^2} n_y \right),$$

$$(A_{42})_{i,j} = -\frac{1}{2\pi}\left(\frac{x_{P_{N+i}} - x_{Q_{N+j}}}{|P_{N+i} - Q_{N+j}|^2}n_x + \frac{y_{P_{N+i}} - y_{Q_{N+j}}}{|P_{N+i} - Q_{N+j}|^2}n_y\right),$$

$$(A_{43})_{i,j} = -\frac{1}{8\pi}\left[1 + 2\log|P_{N+i} - Q_j|\right]\left((x_{P_{N+i}} - x_{Q_j})n_x + (y_{P_{N+i}} - y_{Q_j})n_y\right),$$

$$(A_{44})_{i,j} = -\frac{1}{8\pi}\left[1 + 2\log|P_{N+i} - Q_{N+j}|\right]\left((x_{P_{N+i}} - x_{Q_{N+j}})n_x + (y_{P_{N+i}} - y_{Q_{N+j}})n_y\right),$$

for $i, j = 1, \ldots, N$, where n_x and n_y denote the components of the outward normal vector $\boldsymbol{n}$ to $\partial\Omega$ in the x and y directions, respectively.

The matrices A_{mn}, $m, n = 1, \cdots, 4$ are *circulant*[1].

3.3 Matrix decomposition algorithm

The system (3.12) can be written as

$$(I_4 \otimes U)\left(\begin{array}{c|c|c|c} A_{11} & A_{12} & A_{13} & A_{14} \\ \hline A_{21} & A_{22} & A_{23} & A_{24} \\ \hline A_{31} & A_{32} & A_{33} & A_{34} \\ \hline A_{41} & A_{42} & A_{43} & A_{44} \end{array}\right)(I_4 \otimes U^*)\,(I_4 \otimes U)\left(\begin{array}{c} \boldsymbol{s_1} \\ \hline \boldsymbol{s_2} \\ \hline \boldsymbol{t_1} \\ \hline \boldsymbol{t_2} \end{array}\right) = (I_4 \otimes U)\left(\begin{array}{c} \boldsymbol{f_1} \\ \hline \boldsymbol{f_2} \\ \hline \boldsymbol{g_1} \\ \hline \boldsymbol{g_2} \end{array}\right), \quad (3.14)$$

where

$$I_4 = \begin{pmatrix} 1 & 0 & 0 & 0 \\ 0 & 1 & 0 & 0 \\ 0 & 0 & 1 & 0 \\ 0 & 0 & 0 & 1 \end{pmatrix}$$

[1] A square matrix A is circulant (see [15]) if it has the form

$$A = \begin{pmatrix} a_1 & a_2 & \cdots & a_N \\ a_N & a_1 & \cdots & a_{N-1} \\ \vdots & \vdots & & \vdots \\ a_2 & a_3 & \cdots & a_1 \end{pmatrix}. \quad (3.13)$$

This means that the elements of each row are same as the elements of the previous row but moved one position to the right. The first element of each row is the same as the the last element of the previous row. The circulant matrix A in (3.13) is usually denoted by $A = \mathrm{circ}(a_1, a_2, \ldots, a_N)$.

and $\otimes$ denotes the matrix tensor product. The above system can be written as

$$\left(\begin{array}{c|c|c|c} UA_{11}U^* & UA_{12}U^* & UA_{13}U^* & UA_{14}U^* \\ \hline UA_{21}U^* & UA_{22}U^* & UA_{23}U^* & UA_{24}U^* \\ \hline UA_{31}U^* & UA_{32}U^* & UA_{33}U^* & UA_{34}U^* \\ \hline UA_{41}U^* & UA_{42}U^* & UA_{43}U^* & UA_{44}U^* \end{array}\right) \left(\begin{array}{c} U\boldsymbol{s_1} \\ \hline U\boldsymbol{s_2} \\ \hline U\boldsymbol{t_1} \\ \hline U\boldsymbol{t_2} \end{array}\right) = \left(\begin{array}{c} U\boldsymbol{f_1} \\ \hline U\boldsymbol{f_2} \\ \hline U\boldsymbol{g_1} \\ \hline U\boldsymbol{g_2} \end{array}\right) \tag{3.15}$$

or

$$\left(\begin{array}{c|c|c|c} D_{11} & D_{12} & D_{13} & D_{14} \\ \hline D_{21} & D_{22} & D_{23} & D_{24} \\ \hline D_{31} & D_{32} & D_{33} & D_{34} \\ \hline D_{41} & D_{42} & D_{43} & D_{44} \end{array}\right) \left(\begin{array}{c} \hat{\boldsymbol{s}}_1 \\ \hline \hat{\boldsymbol{s}}_2 \\ \hline \hat{\boldsymbol{t}}_1 \\ \hline \hat{\boldsymbol{t}}_2 \end{array}\right) = \left(\begin{array}{c} \hat{\boldsymbol{f}}_1 \\ \hline \hat{\boldsymbol{f}}_2 \\ \hline \hat{\boldsymbol{g}}_1 \\ \hline \hat{\boldsymbol{g}}_2 \end{array}\right), \tag{3.16}$$

where

$$\hat{\boldsymbol{s}}_1 = U\boldsymbol{s_1}, \quad \hat{\boldsymbol{s}}_2 = U\boldsymbol{s_2}, \quad \hat{\boldsymbol{t}}_1 = U\boldsymbol{t_1}, \quad \hat{\boldsymbol{t}}_2 = U\boldsymbol{t_2},$$

$$\hat{\boldsymbol{f}}_1 = U\boldsymbol{f_1}, \quad \hat{\boldsymbol{f}}_2 = U\boldsymbol{f_2}, \quad \hat{\boldsymbol{g}}_1 = U\boldsymbol{g_1}, \quad \hat{\boldsymbol{g}}_2 = U\boldsymbol{g_2},$$

and

$$D_{mn} = \operatorname{diag}\big(\lambda_1^{mn}, \ldots, \lambda_N^{mn}\big), \quad m, n = 1, \cdots, 4,$$

are diagonal matrices whose diagonal elements are the eigenvalues of the matrices A_{mn}, $m, n = 1, \cdots, 4$, respectively.

The solution of system (3.16) can be decomposed into the solution of the N independent 4×4 systems

$$\left(\begin{array}{c|c|c|c} \lambda_i^{11} & \lambda_i^{12} & \lambda_i^{13} & \lambda_i^{14} \\ \hline \lambda_i^{21} & \lambda_i^{22} & \lambda_i^{23} & \lambda_i^{24} \\ \hline \lambda_i^{31} & \lambda_i^{32} & \lambda_i^{33} & \lambda_i^{34} \\ \hline \lambda_i^{41} & \lambda_i^{42} & \lambda_i^{43} & \lambda_i^{44} \end{array}\right) \left(\begin{array}{c} \hat{s}_i^1 \\ \hline \hat{s}_i^2 \\ \hline \hat{t}_i^1 \\ \hline \hat{t}_i^2 \end{array}\right) = \left(\begin{array}{c} \hat{f}_i^1 \\ \hline \hat{f}_i^2 \\ \hline \hat{g}_i^1 \\ \hline \hat{g}_i^2 \end{array}\right), \quad i = 1, 2, \cdots N. \tag{3.17}$$

Having obtained $\hat{\boldsymbol{s}}_1, \hat{\boldsymbol{s}}_2$ and $\hat{\boldsymbol{t}}_1, \hat{\boldsymbol{t}}_2$, we can find $\boldsymbol{s_1}, \boldsymbol{s_2}$ and $\boldsymbol{t_1}, \boldsymbol{t_2}$, (and hence $\boldsymbol{\mu}, \boldsymbol{\nu}$) from

$$\boldsymbol{s_1} = U^*\hat{\boldsymbol{s}}_1, \quad \boldsymbol{s}_2 = U^*\hat{\boldsymbol{s}}_2, \quad \boldsymbol{t_1} = U^*\hat{\boldsymbol{t}}_1, \quad \boldsymbol{t_2} = U^*\hat{\boldsymbol{t}}_2.$$

We thus have the following matrix decomposition algorithm for solving (3.12):

Description of the algorithm

Step 1: `Compute` $\hat{\boldsymbol{f}}_1 = U\boldsymbol{f}_1,\ \hat{\boldsymbol{f}}_2 = U\boldsymbol{f}_2$ `and` $\hat{\boldsymbol{g}}_1 = U\boldsymbol{g}_1,\ \hat{\boldsymbol{g}}_2 = U\boldsymbol{g}_2$.

Step 2: `Construct the diagonal matrices` $D_{mn},\ m,n = 1,\ldots,4$.

Step 3: `Evaluate` $\hat{\boldsymbol{s}}_1, \hat{\boldsymbol{s}}_2$ `and` $\hat{\boldsymbol{t}}_1, \hat{\boldsymbol{t}}_2$ `by solving` N 4×4 `complex systems.`

Step 4: `Compute` $\boldsymbol{s}_1 = U^*\hat{\boldsymbol{s}}_1, \quad \boldsymbol{s}_2 = U^*\hat{\boldsymbol{s}}_2$ `and` $\boldsymbol{t}_1 = U^*\hat{\boldsymbol{t}}_1, \quad \boldsymbol{t}_2 = U^*\hat{\boldsymbol{t}}_2$.

Analysis of the cost

(i) In ***Step* 1** and ***Step* 4**, because of the form of the matrices U and U^*, the operations can be carried out via Fast Fourier Transforms (FFTs) at a cost of $O(N \log N)$ operations.

(ii) FFTs can also be used for the evaluation of the diagonal matrices in ***Step* 2**.

(iii) The FFT operations are performed using the NAG ([61]) routines `C06FPF, C06FQF` and `C06FRF`.

(iv) In ***Step* 3**, we need to solve N complex linear systems of order 4. This is done at a cost of $O(N)$ operations using the NAG ([61]) routine `F04ADF`.

Note. A similar algorithm can also be applied in the case of different combinations of boundary conditions associated with the biharmonic equation.

3.4 Numerical results

We considered the following numerical examples corresponding to the Dirichlet problem (3.1) in the annulus defined by $\varrho_1 = 1$ and $\varrho_2 = 2$:

Example 1. Problem corresponding to the exact solution

$$u = x^4 - y^4.$$

Example 2. In this case we consider a test example from [50], where in polar coordinates $f(\theta) = -\frac{1}{4}$ and $g(\theta) = -\frac{1}{2}(1+\cos\theta)$, which corresponds to the exact solution

$$u(r,\theta) \;=\; \frac{1}{4}(1-r^2)(1+r\cos\theta) - \frac{1}{4}.$$

Example 3. Problem corresponding to the exact solution

$$u \;=\; (x^2+y^2)\,\mathrm{e}^x\cos y + \frac{x}{x^2+y^2}.$$

Example 4. Problem corresponding to the exact solution

$$u \;=\; (x^2+y^2)\big\{(x+iy)^3+(x-iy)^3\big\} + \big\{(x+iy)^5+(x-iy)^5\big\}.$$

The maximum relative error in these examples was calculated on a grid of m^2 points on the annulus defined by

$$(r_i\cos\vartheta_j, r_i\sin\vartheta_j), \quad r_i = \varrho_1 + \frac{i-1}{m-1}(\varrho_2-\varrho_1), \quad \text{and} \quad \vartheta_j = \frac{2\pi(j-1)}{m},$$

where $i,j = 1,\ldots,m$. The parameter m was taken to be equal to 21.

In Figures 3.1–3.4, we varied the angular parameter α and examined how this affected the accuracy of the solution for various values of N for different $\varepsilon = \varrho_1 - R_1 = R_2 - \varrho_2$. The numerical results indicate that for small ε, the accuracy of the solution is dependent on the angular parameter α. As ε grows this dependence disappears. Further, for a certain range of values of ε, the approximate solution is most accurate for $\alpha \approx \frac{1}{4}$. This phenomenon was also observed in [67, 68] and is valid for all the examples considered in this chapter. (See Figures 3.1–3.4).

We also varied the radii R_1 and R_2 which define the circles of the pseudo–boundary for $\alpha = 0$ and examined how this affected the accuracy of the solution for various values of N. In this case, we observed that as ε increases, the accuracy of the method improves. See Figures 3.5-3.8. Similar results were observed for $\alpha \neq 0$.

Finally, we varied the radius R_2 of the external circle of the pseudo–boundary keeping R_1 fixed and equal to $1/2$. We examined how this affected the accuracy of the approximation of the solution for various values of N. The results of Figures 3.9–3.12 indicate that as R_2

increases the accuracy improves. However, for larger values of ε the accuracy deteriorates. This phenomenon is due to ill-conditioning and has been repeatedly reported in the literature [44, 45, 65, 67, 68]. In particular, as the radius R_2 of the external circle of the pseudo–boundary increases, the values of the eigenvalues of the submatrices A_{mn}, $m, n = 1, \dots, 4$, range from $O(1)$ to $O\big((\frac{\varrho_2}{R_2})^{N/2}\big)$. (See [69].) Such small values cannot be captured numerically and this leads to ill–conditioning of the submatrices and hence of the global matrix in the linear system (3.12). The consequences of this ill–conditioning can be observed from Figures 3.9–3.12, where the error increases for large values of R and in some cases it is even impossible to solve the linear systems.

3.5 Conclusions

In this work, we develop an efficient algorithm for the solution of biharmonic problems in annular domains. This algorithm is based on a matrix decomposition formulation and exploits the circulant nature of the matrices involved by employing FFTs. The numerical results indicate that the accuracy of the solution is affected by the angle by which the singularities are rotated with respect to the boundary points and by the distance of the pseudo–boundary from the boundary of the annulus.

The ideas developed in this study could also be applied to different elliptic equations, such as the Helmholtz equation. Also, this algorithm can be applied to three–dimensional problems. In particular, one could extend the ideas of this work to axisymmetric multiply connected shell–type biharmonic problems, in the spirit of the work of [20, 70].

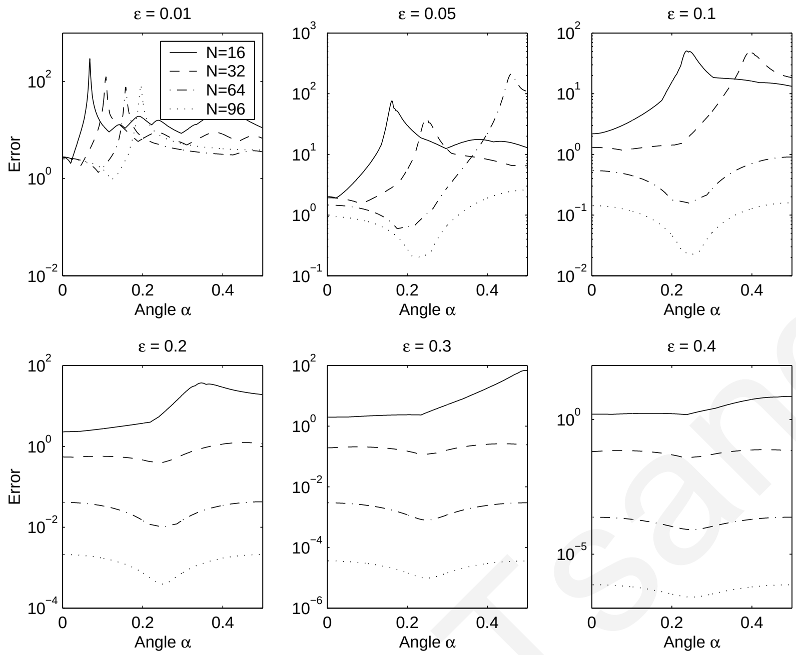

Figure 3.1: Log–plot of error versus angular parameter α for ϵ in Example 1 for different values of N.

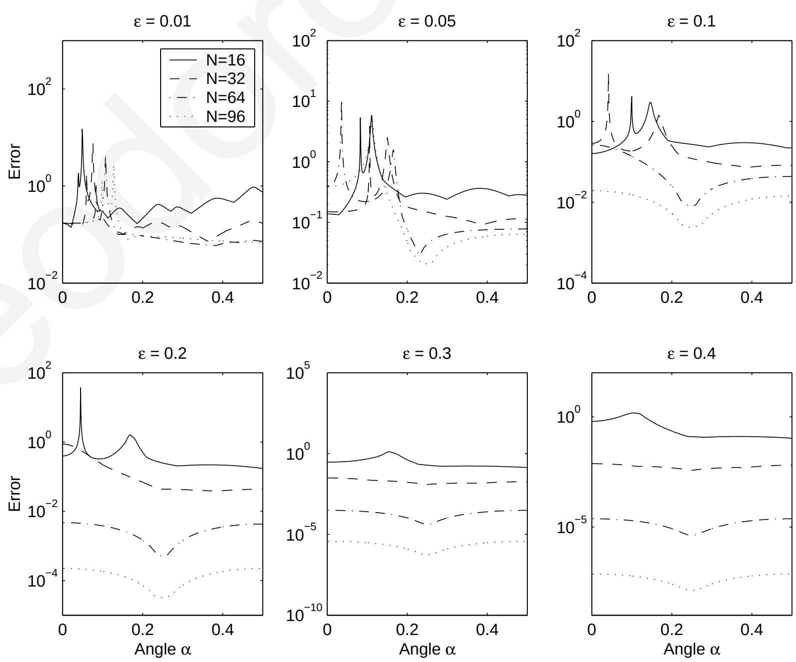

Figure 3.2: Log–plot of error versus angular parameter α for ϵ in Example 2 for different values of N.

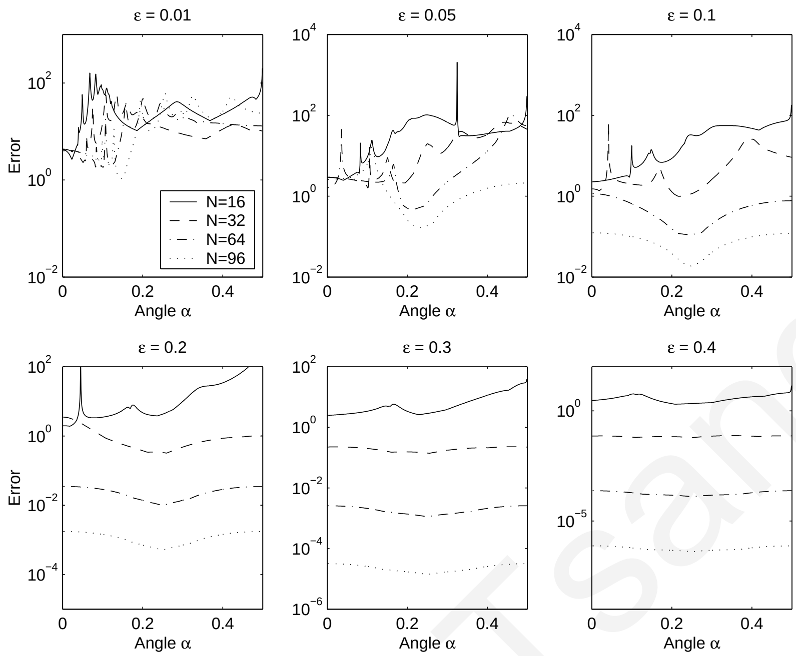

Figure 3.3: Log–plot of error versus angular parameter α for ϵ in Example 3 for different values of N.

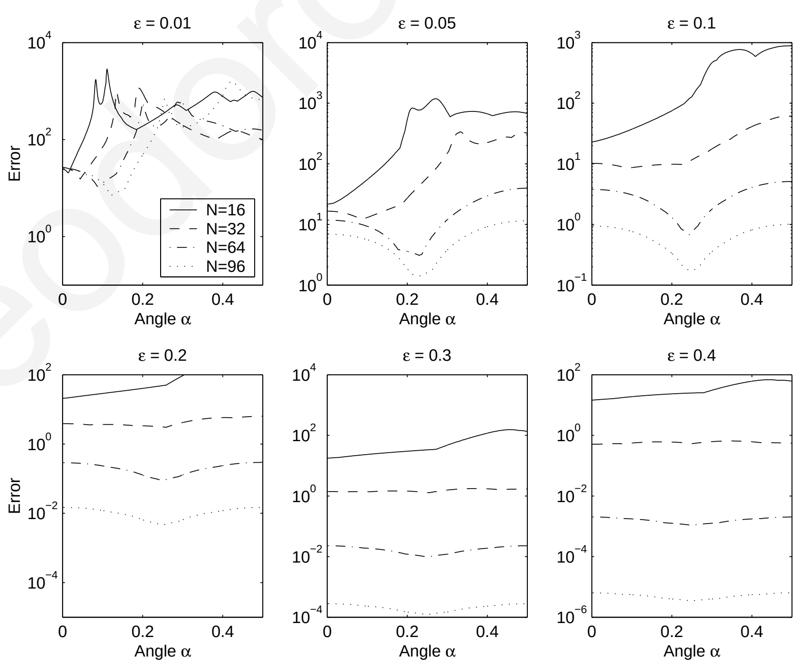

Figure 3.4: Log–plot of error versus angular parameter α for ϵ in Example 4 for different values of N.

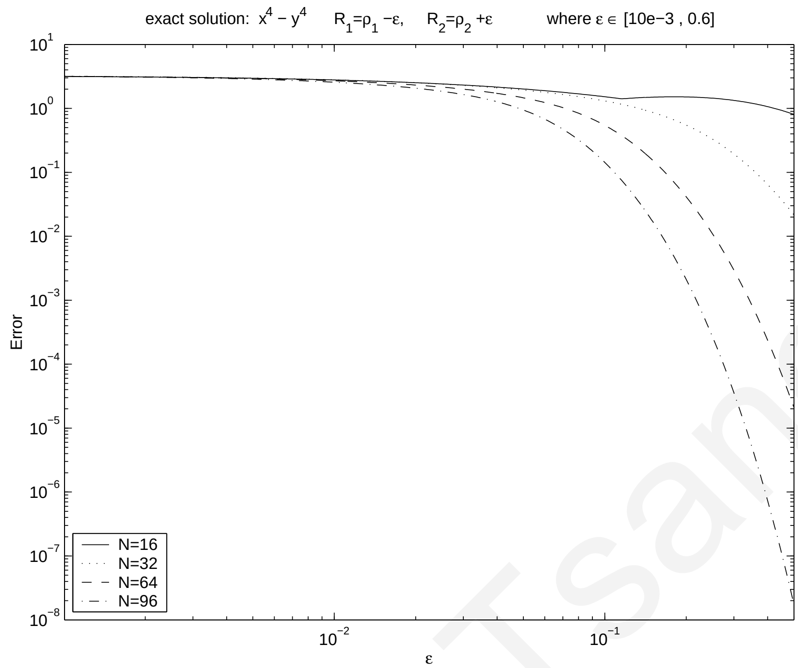

Figure 3.5: Log–plot of maximum relative error versus ϵ in Example 1 for different values of N.

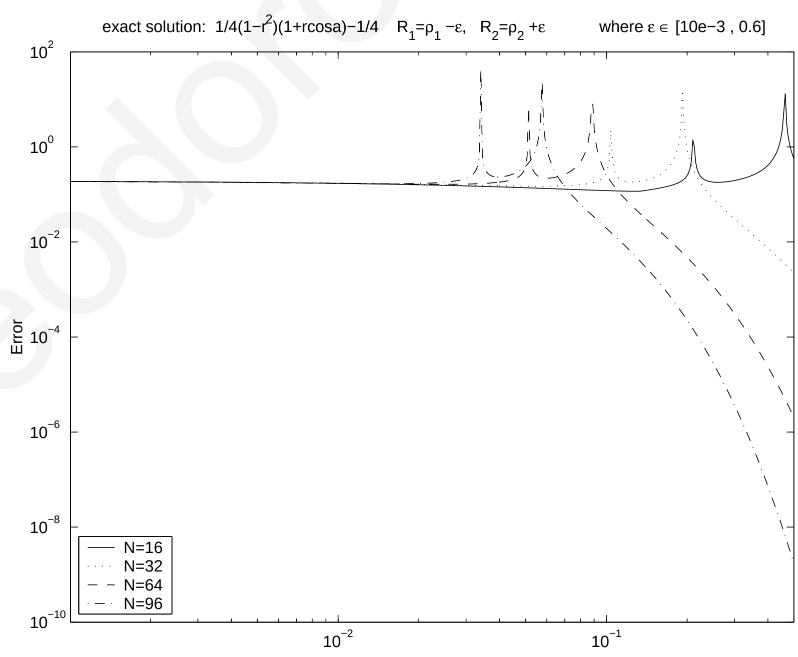

Figure 3.6: Log–plot of maximum relative error versus ϵ in Example 2 for different values of N.

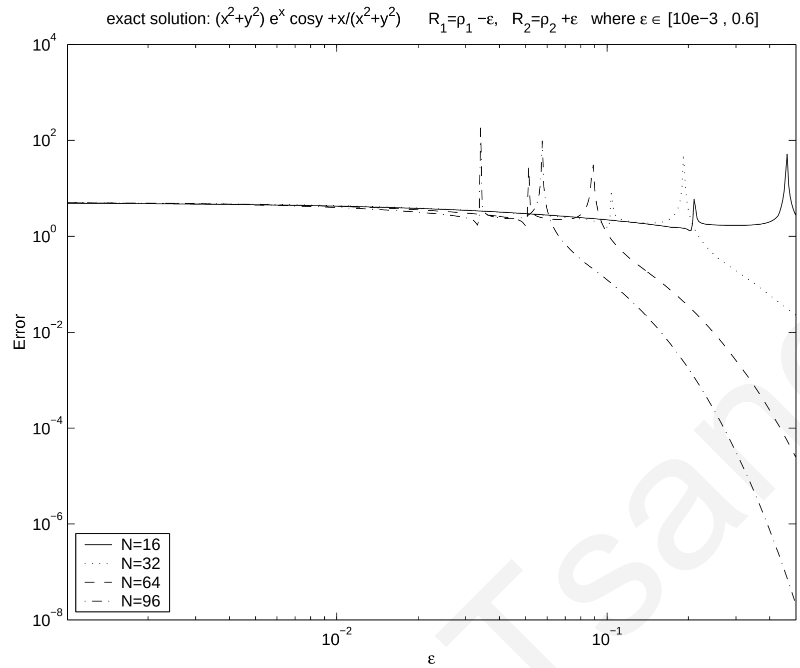

Figure 3.7: Log–plot of maximum relative error versus ϵ in Example 3 for different values of N.

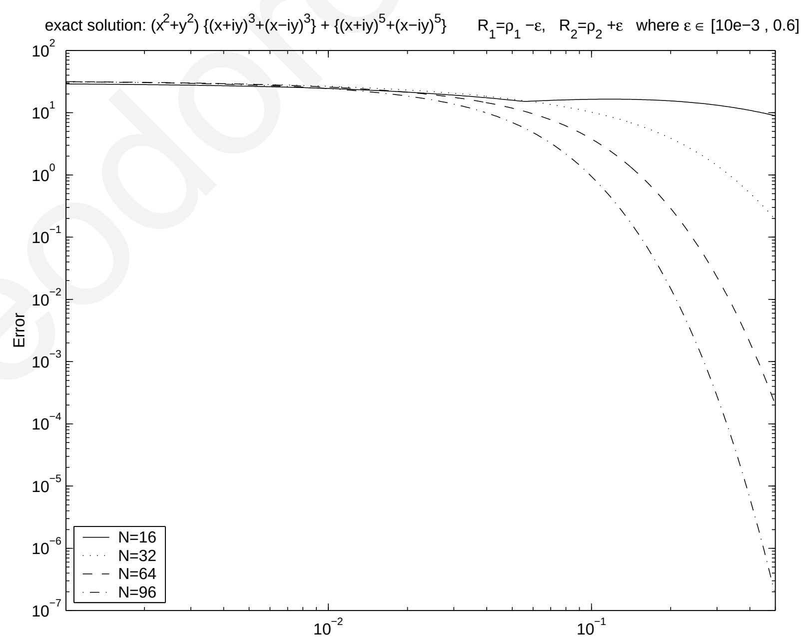

Figure 3.8: Log–plot of maximum relative error versus ϵ in Example 4 for different values of N.

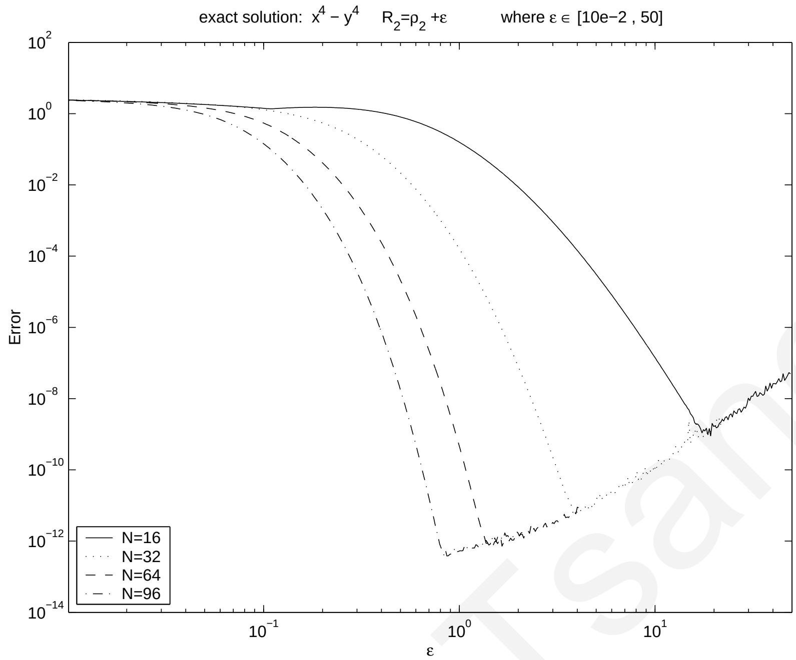

Figure 3.9: Log–plot of maximum relative error versus ϵ in Example 1 for different values of N.

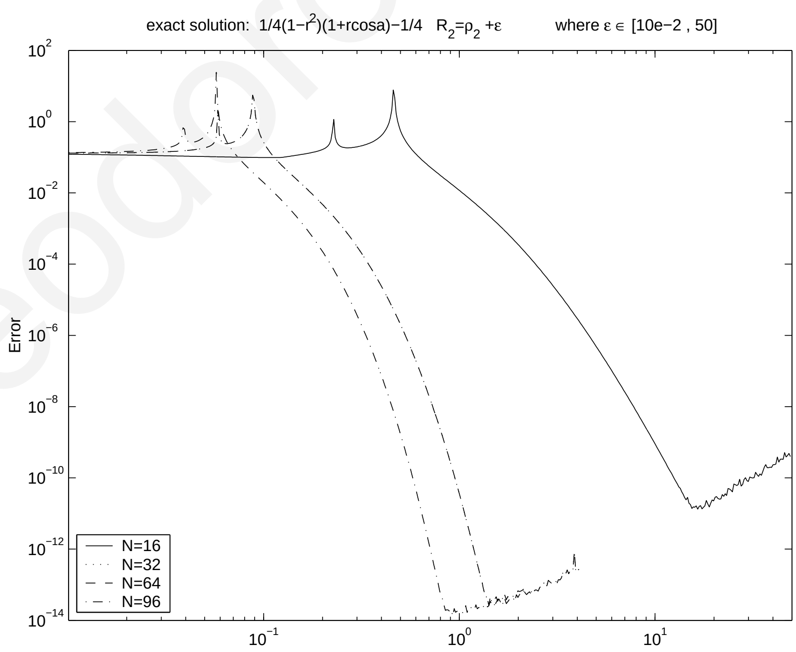

Figure 3.10: Log–plot of maximum relative error versus ϵ in Example 2 for different values of N.

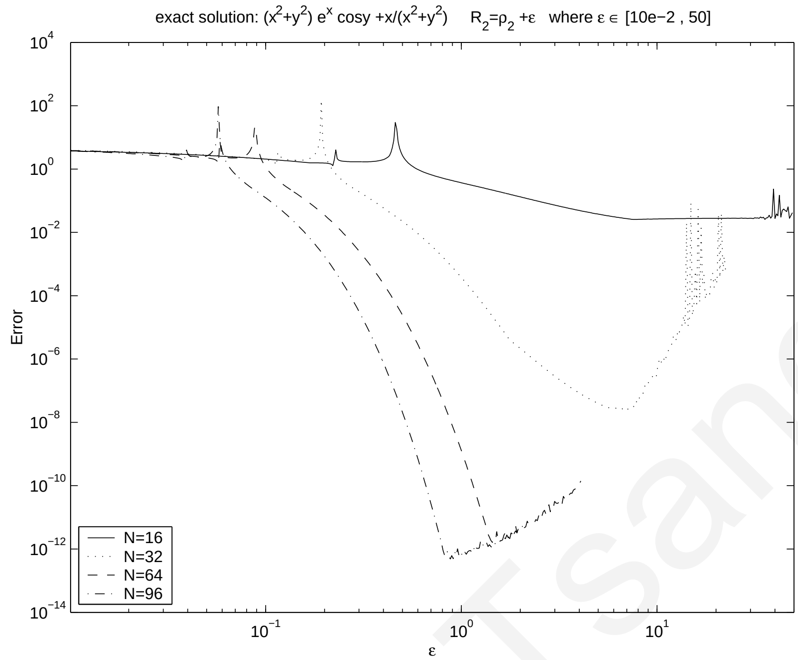

Figure 3.11: Log–plot of maximum relative error versus ϵ in Example 3 for different values of N.

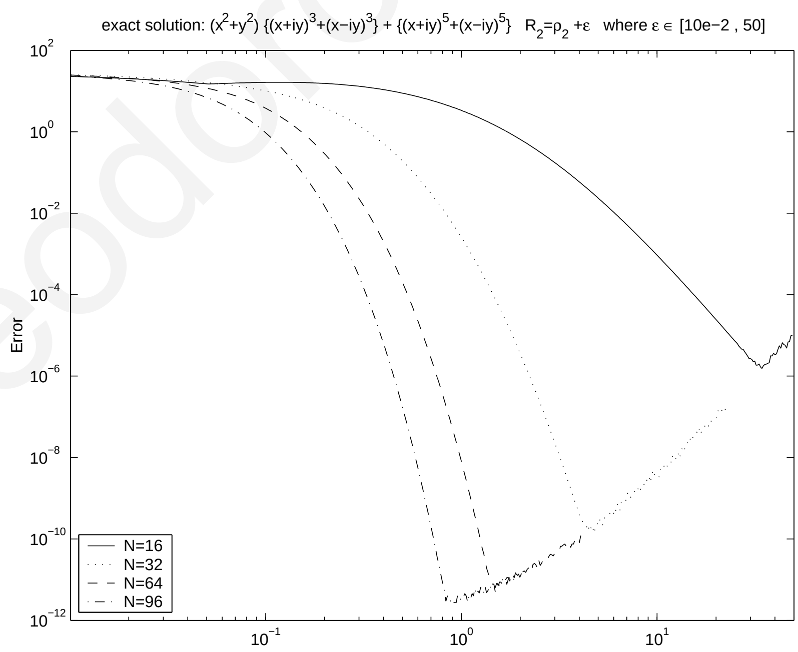

Figure 3.12: Log–plot of maximum relative error versus ϵ in Example 4 for different values of N.

Chapter 4

A matrix decomposition MFS algorithm for problems in hollow axisymmetric domains

4.1 Introduction

In this chapter, we investigate the application of the Method of Fundamental Solutions (MFS) to certain axisymmetric harmonic and biharmonic problems. In particular, we consider the MFS with fixed singularities for harmonic and biharmonic problems in axisymmetric hollow domains. In this work, we extend the ideas developed in [70], where the MFS is applied to harmonic problems in axisymmetric simply-connected domains, and [20], where the MFS is applied to the corresponding biharmonic problems. In the problems examined in this study, the MFS discretization leads to linear systems the coefficient matrices of which have block circulant structures. Matrix decomposition algorithms are developed for the efficient solution of these systems. These algorithms also make use of fast Fourier transforms (FFT).

Comprehensive reviews of the recent developments and applications of the MFS and related methods may be found in the survey papers [13, 18, 19, 26]. Also, the books [16, 25, 46] provide useful information concerning various implementational and theoretical aspects of the MFS.

The chapter is organized as follows. In Section 4.2, we present the MFS formulation and the matrix decomposition algorithm for the harmonic case. The corresponding formulation and algorithm for the biharmonic case are presented in Section 4.3. In Section 4.4 we describe various axisymmetric solids we consider. Numerical results are presented in Section 4.5. Finally, in Section 4.6, we give some concluding remarks.

4.2 The harmonic case

4.2.1 MFS formulation

We consider the three-dimensional boundary value problem

$$\begin{cases} \Delta u = 0 & \text{in} \quad \Omega, \\ u = f & \text{on} \quad \partial\Omega_1, \\ u = g & \text{on} \quad \partial\Omega_2, \end{cases}$$

where Δ denotes the Laplace operator and f is a given function. The region $\Omega \in \mathbb{R}^3$ is axisymmetric, which means that it is formed by rotating a region $\Omega' \in \mathbb{R}^2$ about the $z-$axis. The boundary of Ω is $\partial\Omega = \partial\Omega_1 \cup \partial\Omega_2$ and the boundary of Ω' is defined by the two boundary segments $\partial\Omega'_1$ and $\partial\Omega'_2$, which generate $\partial\Omega_1$ and $\partial\Omega_2$, respectively.

In the MFS [18, 71], the solution u is approximated by

$$u_{MN}(\boldsymbol{c}, \boldsymbol{d}, \boldsymbol{R}, \boldsymbol{S}; P) = \sum_{m=1}^{M}\sum_{n=1}^{N} c_{m,n}\, k_1(P, R_{m,n}) + \sum_{m=1}^{M}\sum_{n=1}^{N} d_{m,n}\, k_1(P, S_{m,n}), \qquad P \in \overline{\Omega},$$

where $\boldsymbol{c} = (c_{11}, c_{12}, \dots, c_{1N}, \dots, c_{M1}, \dots, c_{MN})^T$, $\boldsymbol{d} = (d_{11}, d_{12}, \dots, d_{1N}, \dots, d_{M1}, \dots, d_{MN})^T$ and $\boldsymbol{R}$, $\boldsymbol{S}$ are $3MN-$vectors containing the coordinates of the singularities (sources) $R_{m,n}$, $S_{m,n}$, $m = 1, \dots, M$, $n = 1, \dots, N$, which lie outside $\overline{\Omega}$. The function $k_1(P, R)$ is the fundamental solution of Laplace's equation in $\mathbb{R}^3$ given by

$$k_1(P, R) = \frac{1}{4\,\pi\,|P-R|},$$

with $|P - R|$ denoting the distance between the points P and R. The singularities $R_{m,n}$, $S_{m,n}$ are fixed on the boundary $\partial\tilde{\Omega} = \partial\tilde{\Omega}_1 \cup \partial\tilde{\Omega}_2$ of a solid $\tilde{\Omega}$ surrounding Ω. The solid $\tilde{\Omega}$ is generated by the rotation of the planar domain $\tilde{\Omega}'$ which is similar to Ω'. Clearly $\partial\tilde{\Omega}_1$ and $\partial\tilde{\Omega}_2$ are similar to $\partial\Omega_1$ and $\partial\Omega_2$, respectively. Also, the boundary of $\tilde{\Omega}'$ is defined by the segments $\partial\tilde{\Omega}'_1$ and $\partial\tilde{\Omega}'_2$, which generate $\partial\tilde{\Omega}_1$ and $\partial\tilde{\Omega}_2$, respectively. A set of MN collocation points $\{P_{i,j}\}_{i=1,j=1}^{M,N}$ is chosen on $\partial\Omega_1$ and a set of MN collocation points $\{Q_{i,j}\}_{i=1,j=1}^{M,N}$ is chosen on $\partial\Omega_2$ in the following way: We first choose N points $\{P_j\}_{j=1}^N$ on the boundary segment $\partial\Omega_1'$ and N points $\{Q_j\}_{j=1}^N$ on $\partial\Omega_2'$. These can be described by their polar coordinates (r_{P_j}, z_{P_j}), (r_{Q_j}, z_{Q_j}), $j = 1, \ldots, N$, where r_{P_j}, r_{Q_j} denotes the vertical distance of the points P_j, Q_j from the $z-$axis and z_{P_j}, z_{Q_j} denotes the $z-$coordinate of the points P_j, Q_j respectively. The points on $\partial\Omega_1$ are taken to be

$$x_{P_{i,j}} = r_{P_j}\, \cos\varphi_i, \ \ y_{P_{i,j}} = r_{P_j}\, \sin\varphi_i, \ \ z_{P_{i,j}} = z_{P_j},$$

and the points on $\partial\Omega_2$ are

$$x_{Q_{i,j}} = r_{Q_j}\, \cos\varphi_i, \ \ y_{Q_{i,j}} = r_{Q_j}\, \sin\varphi_i, \ \ z_{Q_{i,j}} = z_{Q_j},$$

where $\varphi_i = 2(i-1)\pi/M, \quad i = 1, \ldots, M$. Similarly, we choose a set of MN singularities $\{R_{m,n}\}_{m=1,n=1}^{M,N}$ on $\partial\tilde{\Omega}_1$ and a set of MN singularities $\{S_{m,n}\}_{m=1,n=1}^{M,N}$ on $\partial\tilde{\Omega}_2$ by taking $R_{m,n} = (x_{R_{m,n}}, y_{R_{m,n}}, z_{R_{m,n}})$, $S_{m,n} = (x_{S_{m,n}}, y_{S_{m,n}}, z_{S_{m,n}})$, and

$$x_{R_{m,n}} = r_{R_n}\, \cos\psi_m, \ \ y_{Q_{m,n}} = r_{R_n}\, \sin\psi_m, \ \ z_{R_{m,n}} = z_{R_n},$$
$$x_{S_{m,n}} = r_{S_n}\, \cos\psi_m, \ \ y_{S_{m,n}} = r_{S_n}\, \sin\psi_m, \ \ z_{S_{m,n}} = z_{S_n},$$

where $\psi_i = 2(\alpha + i - 1)\pi/M, \quad i = 1, \ldots, M$. The parameter $\alpha \in [-1/2, 1/2]$ describes the rotation of the singularities in the azimuthal direction. The N points R_j are chosen on $\partial\tilde{\Omega}_1'$ whereas the N points S_j are chosen on $\partial\tilde{\Omega}_2'$.

In the MFS, the coefficients $\boldsymbol{c}$ are determined so that the boundary condition is satisfied at the boundary points $\{P_{i,j}\}_{i=1,j=1}^{M,N}$, $\{Q_{i,j}\}_{i=1,j=1}^{M,N}$:

$$u_{MN}(\boldsymbol{c}, \boldsymbol{d}, \boldsymbol{R}, \boldsymbol{S}; P_{i,j}) = f_1(P_{i,j}), \quad u_{MN}(\boldsymbol{c}, \boldsymbol{d}, \boldsymbol{R}, \boldsymbol{S}; Q_{i,j}) = f_2(P_{i,j}),$$

$i = 1, \ldots, M,\ j = 1, \ldots, N$. This yields an $2MN \times 2MN$ linear system of the form

$$\left(\begin{array}{c|c} A & B \\ \hline C & D \end{array}\right) \left(\begin{array}{c} \boldsymbol{c} \\ \hline \boldsymbol{d} \end{array}\right) = \left(\begin{array}{c} \boldsymbol{f} \\ \hline \boldsymbol{g} \end{array}\right), \tag{4.1}$$

where the matrices A, B, C and D are block circulant [15] $MN \times MN$ matrices, that is

$$A = \text{circ}(A_1, A_2, \ldots, A_N), \quad B = \text{circ}(B_1, B_2, \ldots, B_N),$$
$$C = \text{circ}(C_1, C_2, \ldots, C_N), \quad D = \text{circ}(D_1, D_2, \ldots, D_N).$$

The matrices $A_\ell, B_\ell, C_\ell, D_\ell, \ell = 1, \dots, M$, are $N \times N$ matrices defined by

$$(A_\ell)_{j,n} = \frac{1}{4\,\pi\,|P_{1,j} - R_{\ell,n}|}, \quad (B_\ell)_{j,n} = \frac{1}{4\,\pi\,|P_{1,j} - S_{\ell,n}|},$$
$$(C_\ell)_{j,n} = \frac{1}{4\,\pi\,|Q_{1,j} - R_{\ell,n}|}, \quad (D_\ell)_{j,n} = \frac{1}{4\,\pi\,|Q_{1,j} - S_{\ell,n}|},$$

$\ell = 1, \dots, M$ j, $n = 1, \dots, N$. The system (4.1) can therefore be written as

$$\begin{aligned} \Big(\sum_{\ell=1}^{M} \mathcal{P}^{\ell-1} \otimes A_\ell\Big)\boldsymbol{c} + \Big(\sum_{\ell=1}^{M} \mathcal{P}^{\ell-1} \otimes B_\ell\Big)\boldsymbol{d} &= \boldsymbol{f}, \\ \Big(\sum_{\ell=1}^{M} \mathcal{P}^{\ell-1} \otimes C_\ell\Big)\boldsymbol{c} + \Big(\sum_{\ell=1}^{M} \mathcal{P}^{\ell-1} \otimes D_\ell\Big)\boldsymbol{d} &= \boldsymbol{g}, \end{aligned}$$

where the matrix $\mathcal{P}$ is the $M \times M$ permutation matrix $\mathcal{P} = \mathrm{circ}\,(0, 1, 0, \dots, 0)$ and $\otimes$ denotes the matrix tensor product[1].

4.2.2 Matrix decomposition algorithm

In the case we are examining, a Matrix Decomposition Algorithm [8] involves the reduction of the $2MN \times 2MN$ system (4.1) to M decoupled $2N \times 2N$ systems. This is achieved by exploiting the block circulant structure of the matrices A, B, C and D. Let U be the unitary

[1]The tensor (or Kronecker) product of the $m \times n$ matrix V and the $\ell \times k$ matrix W is the $m\,\ell \times n\,k$ matrix

$$V \otimes W = \begin{pmatrix} v_{11}\,W & v_{12}\,W & \cdots & v_{1n}\,W \\ v_{21}\,W & v_{22}\,W & \cdots & v_{2n}\,W \\ \cdots & \cdots & \cdots & \cdots \\ v_{m1}\,W & v_{m2}\,W & \cdots & v_{mn}\,W \end{pmatrix}.$$

Basic properties:

(i) $V \otimes (W \otimes Z) = (V \otimes W) \otimes Z$,

(ii) $(V_1 \otimes W_1)\,(V_2 \otimes W_2) = (V_1 V_2) \otimes (W_1 W_2)$,

(iii) $V \otimes (W + Z) = V \otimes W + V \otimes Z, \quad (V + W) \otimes Z = V \otimes Z + V \otimes Z.$

A comprehensive list of properties of the tensor product can be found in [15, pp. 22–23] or [58, pp. 597–598].

$M \times M$ Fourier matrix (i.e., $UU^* = \mathcal{I}_M$) which is the conjugate of the matrix (see [15, 67])

$$U^* = \frac{1}{M^{1/2}} \begin{pmatrix} 1 & 1 & 1 & \cdots & 1 \\ 1 & \omega & \omega^2 & \cdots & \omega^{M-1} \\ 1 & \omega^2 & \omega^4 & \cdots & \omega^{2(M-1)} \\ \cdots & \cdots & \cdots & \cdots & \cdots \\ 1 & \omega^{M-1} & \omega^{2(M-1)} & \cdots & \omega^{(M-1)(M-1)} \end{pmatrix}, \tag{4.2}$$

where $\omega = \mathrm{e}^{2\pi \mathrm{i}/M}$. Clearly, pre–multiplication of a vector $\boldsymbol{x}$ by U (respectively, U^*) yields the *Discrete Fourier Transform* (*DFT*) of $\boldsymbol{x}$ (respespectively, *Inverse Discrete Fourier Transform* (*IDFT*) of $\boldsymbol{x}$).

It is well–known [15] that circulant matrices are diagonalized in the following way. If

$$C = \operatorname{circ}(c_1, \ldots, c_M),$$

then $C = U^* D U$, where $D = \operatorname{diag}(\hat{c}_1, \ldots, \hat{c}_M)$, and

$$\hat{c}_j = \sum_{k=1}^{M} c_k \, \omega^{(k-1)(j-1)}.$$

In particular, the permutation matrix $\mathcal{P} = \operatorname{circ}(0, 1, 0, \ldots, 0)$ is diagonalized as $\mathcal{P} = U^* T U$, where

$$T = \operatorname{diag}(1, \omega, \omega^2, \ldots, \omega^{M-1}). \tag{4.3}$$

Next we simplify system (4.1). Let

$$\left(\begin{array}{c|c} \tilde{A} & \tilde{B} \\ \hline \tilde{C} & \tilde{D} \end{array}\right) = \left(\begin{array}{c|c} U \otimes \mathcal{I}_N & 0 \\ \hline 0 & U \otimes \mathcal{I}_N \end{array}\right) \left(\begin{array}{c|c} A & B \\ \hline C & D \end{array}\right) \left(\begin{array}{c|c} U^* \otimes \mathcal{I}_N & 0 \\ \hline 0 & U^* \otimes \mathcal{I}_N \end{array}\right),$$

and

$$\left(\begin{array}{c} \tilde{\boldsymbol{c}} \\ \hline \tilde{\boldsymbol{d}} \end{array}\right) = \left(\begin{array}{c|c} U \otimes \mathcal{I}_N & 0 \\ \hline 0 & U \otimes \mathcal{I}_N \end{array}\right) \left(\begin{array}{c} \boldsymbol{c} \\ \hline \boldsymbol{d} \end{array}\right), \qquad \left(\begin{array}{c} \tilde{\boldsymbol{f}} \\ \hline \tilde{\boldsymbol{g}} \end{array}\right) = \left(\begin{array}{c|c} U \otimes \mathcal{I}_N & 0 \\ \hline 0 & U \otimes \mathcal{I}_N \end{array}\right) \left(\begin{array}{c} \boldsymbol{f} \\ \hline \boldsymbol{g} \end{array}\right).$$

Then, after pre–multiplication by $\mathcal{I}_2 \otimes U \otimes \mathcal{I}_N$, (4.1) becomes

$$\left(\begin{array}{c|c} \tilde{A} & \tilde{B} \\ \hline \tilde{C} & \tilde{D} \end{array}\right) \left(\begin{array}{c} \tilde{\boldsymbol{c}} \\ \hline \tilde{\boldsymbol{d}} \end{array}\right) = \left(\begin{array}{c} \tilde{\boldsymbol{f}} \\ \hline \tilde{\boldsymbol{g}} \end{array}\right). \tag{4.4}$$

Since

$$A = \sum_{k=1}^{M} \mathcal{P}^{k-1} \otimes A_k,$$

then

$$\tilde{A} = (U \otimes \mathcal{I}_N)\Big(\sum_{k=1}^{M} \mathcal{P}^{k-1} \otimes A_k\Big)(U^* \otimes \mathcal{I}_N) = \sum_{k=1}^{M} \big(U\,\mathcal{P}^{k-1}\,U^*\big) \otimes A_k = \sum_{k=1}^{M} T^{k-1} \otimes A_k,$$

and similarly

$$\tilde{B} = \sum_{k=1}^{M} T^{k-1} \otimes B_k, \quad \tilde{C} = \sum_{k=1}^{M} T^{k-1} \otimes C_k \quad \text{and} \quad \tilde{D} = \sum_{k=1}^{M} T^{k-1} \otimes D_k.$$

Thus system (4.4) becomes

$$\left(\begin{array}{c|c} \sum_{k=1}^{M} T^{k-1} \otimes A_k & \sum_{k=1}^{M} T^{k-1} \otimes B_k \\ \hline \sum_{k=1}^{M} T^{k-1} \otimes C_k & \sum_{k=1}^{M} T^{k-1} \otimes D_k \end{array}\right) \left(\begin{array}{c} \tilde{\boldsymbol{c}} \\ \hline \tilde{\boldsymbol{d}} \end{array}\right) = \left(\begin{array}{c} \tilde{\boldsymbol{f}} \\ \hline \tilde{\boldsymbol{g}} \end{array}\right). \tag{4.5}$$

The solution of system (4.5) can therefore be decomposed into the solution of the M *independent* $2N \times 2N$ systems

$$G_m \left(\begin{array}{c} \tilde{\boldsymbol{c}}_m \\ \hline \tilde{\boldsymbol{d}}_m \end{array}\right) = \left(\begin{array}{c} \tilde{\boldsymbol{f}}_m \\ \hline \tilde{\boldsymbol{g}}_m \end{array}\right), \quad m = 1, \dots, M, \tag{4.6}$$

where $\tilde{\boldsymbol{f}}_m = \big(\tilde{f}_{m,1}, \dots, \tilde{f}_{m,N}\big)^T$, $\tilde{\boldsymbol{g}}_m = \big(\tilde{g}_{m,1}, \dots, \tilde{g}_{m,N}\big)^T$,

$$G_m = \left(\begin{array}{c|c} \hat{A}_m & \hat{B}_m \\ \hline \hat{C}_m & \hat{D}_m \end{array}\right), \tag{4.7}$$

and

$$\begin{aligned} \hat{A}_m &= \sum_{j=1}^{M} \omega^{(m-1)(j-1)}\, A_j, \qquad & \hat{B}_m &= \sum_{j=1}^{M} \omega^{(m-1)(j-1)}\, B_j, \\ \hat{C}_m &= \sum_{j=1}^{M} \omega^{(m-1)(j-1)}\, C_j, \qquad & \hat{D}_m &= \sum_{j=1}^{M} \omega^{(m-1)(j-1)}\, D_j, \end{aligned} \tag{4.8}$$

$m = 1, \dots, M$. We thus have the following efficient algorithm for the solution of system (4.5).

Algorithm

Step 1. `Compute` $\tilde{\boldsymbol{f}} = (U \otimes \mathcal{I}_N)\,\boldsymbol{f}$, $\quad \tilde{\boldsymbol{g}} = (U \otimes \mathcal{I}_N)\,\boldsymbol{g}$.

Step 2. `Construct the matrices` $G_m, \quad m = 1, \ldots, M$.

Step 3. `Solve the` M `systems (4.6).`

Step 4. `Compute` $\boldsymbol{c} = (U^* \otimes \mathcal{I}_N)\,\tilde{\boldsymbol{c}}$, $\boldsymbol{d} = (U^* \otimes \mathcal{I}_N)\,\tilde{\boldsymbol{d}}$.

Remarks

(i) In *Step* 1, because of the form of the matrix U, the operation is equivalent to performing N FFTs of dimension M. This can done at a cost of $\mathcal{O}(NM \log M)$ operations via an appropriate FFT algorithm. Similarly, in *Step* 4, because of the form of the matrix U^*, the operation can be carried out via inverse FFTs at a cost of order $\mathcal{O}(NM \log M)$ operations.

(ii) In *Step* 2 we need to perform an $M-$dimensional inverse FFT, in order to compute the entries of the matrices $\hat{A}_j$, $\hat{B}_j$, $\hat{C}_j$, $\hat{D}_j$, $j = 1, \ldots, M$, from (4.8). This can be done at a cost of $\mathcal{O}(N^2 M \log M)$ operations.

(iii) In *Step* 3, we need to solve M complex linear systems of order N. This is done using an $LU-$factorization with partial pivoting at a cost of $\mathcal{O}(MN^3)$ operations.

(iv) The FFT and inverse FFT operations are performed using the NAG[2] routines `C06EAF, C06FPF, C06FQF` and `C06FRF`.

[2] *Numerical Algorithms Group Library Mark 20*, NAG Ltd, Wilkinson House, Jordan Hill Road, Oxford, UK, 2001.

4.3 The biharmonic case

4.3.1 MFS formulation

We now consider the three–dimensional boundary value problem

$$\begin{cases} \Delta^2 u = 0 & \text{in} \quad \Omega, \\ u = f_1 \quad \text{and} \quad \dfrac{\partial u}{\partial n} = g_1 & \text{on} \quad \partial\Omega_1\,, \\ u = f_2 \quad \text{and} \quad \dfrac{\partial u}{\partial n} = g_2 & \text{on} \quad \partial\Omega_2. \end{cases} \tag{4.9}$$

The region $\Omega \in \mathbb{R}^3$ is axisymmetric and, as in the harmonic case, formed by rotating a region $\Omega' \in \mathbb{R}^2$ about the $z-$axis. We keep the same notation as in the harmonic case for the boundaries of Ω and Ω'.

In the MFS [18, 20], the solution u is approximated by

$$\begin{aligned} u_{MN}(\boldsymbol{c_1}, \boldsymbol{c_2}, \boldsymbol{d_1}, \boldsymbol{d_2}, \boldsymbol{R}, \boldsymbol{S}; P) = & \sum_{m=1}^{M}\sum_{n=1}^{N} c^1_{m,n}\, k_1(P, R_{m,n}) + \sum_{m=1}^{M}\sum_{n=1}^{N} c^2_{m,n}\, k_2(P, R_{m,n}) \\ & + \sum_{m=1}^{M}\sum_{n=1}^{N} d^1_{m,n}\, k_1(P, S_{m,n}) + \sum_{m=1}^{M}\sum_{n=1}^{N} d^2_{m,n}\, k_2(P, S_{m,n}), \qquad P \in \overline{\Omega}, \end{aligned} \tag{4.10}$$

where $\boldsymbol{c_1} = (c^1_{11}, c^1_{12}, \ldots, c^1_{1N}, \ldots, c^1_{M1}, \ldots, c^1_{MN})^T$, $\boldsymbol{c_2} = (c^2_{11}, c^2_{12}, \ldots, c^2_{1N}, \ldots, c^2_{M1}, \ldots, c^2_{MN})^T$, $\boldsymbol{d_1} = (d^1_{11}, d^1_{12}, \ldots, d^1_{1N}, \ldots, d^1_{M1}, \ldots, d^1_{MN})^T$, $\boldsymbol{d_2} = (d^2_{11}, d^2_{12}, \ldots, d^2_{1N}, \ldots, d^2_{M1}, \ldots, d^2_{MN})^T$, and $\boldsymbol{R}$, $\boldsymbol{S}$ are $3MN-$vectors containing the coordinates of the singularities $R_{m,n}$, $S_{m,n}$, $m = 1, \ldots, M$, $n = 1, \ldots, N$, which lie outside $\overline{\Omega}$. The function $k_2(P, S)$ is the fundamental solution of the the biharmonic equation in $\mathbb{R}^3$ given by

$$k_2(P, R) \;=\; \frac{1}{8\,\pi}\,|P - R|.$$

The $2MN$ collocation points $\{P_{i,j}\}_{i=1,j=1}^{M,N}$, $\{Q_{i,j}\}_{i=1,j=1}^{M,N}$ and the $2MN$ singularities $\{P_{m,n}\}_{m=1,n=1}^{M,N}$, $\{Q_{m,n}\}_{m=1,n=1}^{M,N}$ are chosen in exactly the same way as in the harmonic case.

The coefficients $\boldsymbol{c}_1, \boldsymbol{c}_2, \boldsymbol{d}_1$ and $\boldsymbol{d}_2$ are determined so that the boundary conditions are satisfied at the boundary points $\{P_{i,j}\}_{i=1,j=1}^{M,N}$, $\{Q_{i,j}\}_{i=1,j=1}^{M,N}$:

$$\begin{aligned} u_{MN}(\boldsymbol{c_1},\boldsymbol{c_2},\boldsymbol{d_1},\boldsymbol{d_2},\boldsymbol{R},\boldsymbol{S};P_{i,j}) \;=\; f_1(P_{i,j}),\;\; u_{MN}(\boldsymbol{c_1},\boldsymbol{c_2},\boldsymbol{d_1},\boldsymbol{d_2},\boldsymbol{R},\boldsymbol{S};Q_{i,j}) \;=\; f_2(P_{i,j}),\\ \frac{\partial}{\partial n}u_{MN}(\boldsymbol{c_1},\boldsymbol{c_2},\boldsymbol{d_1},\boldsymbol{d_2},\boldsymbol{R},\boldsymbol{S};P_{i,j}) \;=\; g_1(P_{i,j}),\;\; \frac{\partial}{\partial n}u_{MN}(\boldsymbol{c_1},\boldsymbol{c_2},\boldsymbol{d_1},\boldsymbol{d_2},\boldsymbol{R},\boldsymbol{S};Q_{i,j}) \;=\; g_2(P_{i,j}), \end{aligned} \tag{4.11}$$

$i=1,\dots,M,\; j=1,\dots,N$. This yields an $4MN\times 4MN$ linear system of the form

$$\left(\begin{array}{c|c|c|c} A^{11} & A^{12} & A^{13} & A^{14}\\ \hline A^{21} & A^{22} & A^{23} & A^{24}\\ \hline A^{31} & A^{32} & A^{33} & A^{34}\\ \hline A^{41} & A^{42} & A^{43} & A^{44} \end{array}\right)\left(\begin{array}{c} \boldsymbol{c_1}\\ \hline \boldsymbol{c_2}\\ \hline \boldsymbol{d_1}\\ \hline \boldsymbol{d_2} \end{array}\right)=\left(\begin{array}{c} \boldsymbol{f_1}\\ \hline \boldsymbol{f_2}\\ \hline \boldsymbol{g_1}\\ \hline \boldsymbol{g_2} \end{array}\right), \tag{4.12}$$

where the matrices $A^{rs},\; r,s=1,2,3,4$ are *block circulant* $MN\times MN$ matrices, that is

$$A^{rs} \;=\; \operatorname{circ}\big(A_1^{rs},A_2^{rs},\dots,A_M^{rs}\big), \quad r,s=1,2,3,4.$$

The matrices $A^{rs},\; r,s=1,2,3,4$, can be written as

$$A^{rs}=\left(\mathcal{I}_M\otimes A_1^{rs}+\mathcal{P}\otimes A_2^{rs}+\mathcal{P}^2\otimes A_3^{rs}+\cdots+\mathcal{P}^{M-1}\otimes A_M^{rs}\right).$$

For $\ell=1,\dots,M$ the $N\times N$ submatrices $A_\ell^{rs}=\big((A_\ell^{rs})_{j,n}\big)$, are defined by

$$\big(A_\ell^{11}\big)_{j,n}=\frac{1}{4\pi}\frac{1}{|P_{1,j}-R_{\ell,n}|}, \qquad \big(A_\ell^{12}\big)_{j,n}=\frac{1}{4\pi}\frac{1}{|P_{1,j}-S_{\ell,n}|},$$

$$\big(A_\ell^{13}\big)_{j,n}=\frac{1}{8\pi}|P_{1,j}-R_{\ell,n}|, \qquad \big(A_\ell^{14}\big)_{j,n}=\frac{1}{8\pi}|P_{1,j}-S_{\ell,n}|,$$

$$\big(A_\ell^{21}\big)_{j,n}=\frac{1}{4\pi}\frac{1}{|Q_{1,j}-R_{\ell,n}|}, \qquad \big(A_\ell^{22}\big)_{j,n}=\frac{1}{4\pi}\frac{1}{|Q_{1,j}-S_{\ell,n}|},$$

$$\big(A_\ell^{23}\big)_{j,n}=\frac{1}{8\pi}|Q_{1,j}-R_{\ell,n}|, \qquad \big(A_\ell^{24}\big)_{j,n}=\frac{1}{8\pi}|Q_{1,j}-S_{\ell,n}|,$$

$$\left(A_\ell^{31}\right)_{j,n} = \frac{1}{4\pi}\frac{\partial}{\partial n}\left[\frac{1}{|P_{1,j}-R_{\ell,n}|}\right]$$

$$= -\frac{1}{4\pi}\left[\frac{(x_{P_{1,j}}-x_{R_{\ell,n}})}{|P_{1,j}-R_{\ell,n}|^3}n_x + \frac{(y_{P_{1,j}}-y_{R_{\ell,n}})}{|P_{1,j}-R_{\ell,n}|^3}n_y + \frac{(z_{P_{1,j}}-z_{R_{\ell,n}})}{|P_{1,j}-R_{\ell,n}|^3}n_z\right],$$

$$\left(A_\ell^{32}\right)_{j,n} = \frac{1}{4\pi}\frac{\partial}{\partial n}\left[\frac{1}{|P_{1,j}-S_{\ell,n}|}\right]$$

$$= -\frac{1}{4\pi}\left[\frac{(x_{P_{1,j}}-x_{S_{\ell,n}})}{|P_{1,j}-S_{\ell,n}|^3}n_x + \frac{(y_{P_{1,j}}-y_{S_{\ell,n}})}{|P_{1,j}-S_{\ell,n}|^3}n_y + \frac{(z_{P_{1,j}}-z_{S_{\ell,n}})}{|P_{1,j}-S_{\ell,n}|^3}n_z\right],$$

$$\left(A_\ell^{33}\right)_{j,n} = \frac{1}{8\pi}\frac{\partial}{\partial n}|P_{1,j}-R_{\ell,n}|$$

$$= \frac{1}{8\pi}\left[\frac{(x_{P_{1,j}}-x_{R_{\ell,n}})}{|P_{1,j}-R_{\ell,n}|}n_x + \frac{(y_{P_{1,j}}-y_{R_{\ell,n}})}{|P_{1,j}-R_{\ell,n}|}n_y + \frac{(z_{P_{1,j}}-z_{R_{\ell,n}})}{|P_{1,j}-R_{\ell,n}|}n_z\right],$$

$$\left(A_\ell^{34}\right)_{j,n} = \frac{1}{8\pi}\frac{\partial}{\partial n}|P_{1,j}-S_{\ell,n}|$$

$$= \frac{1}{8\pi}\left[\frac{(x_{P_{1,j}}-x_{S_{\ell,n}})}{|P_{1,j}-S_{\ell,n}|}n_x + \frac{(y_{P_{1,j}}-y_{S_{\ell,n}})}{|P_{1,j}-S_{\ell,n}|}n_y + \frac{(z_{P_{1,j}}-z_{S_{\ell,n}})}{|P_{1,j}-S_{\ell,n}|}n_z\right],$$

$$\left(A_\ell^{41}\right)_{j,n} = \frac{1}{4\pi}\frac{\partial}{\partial n}\frac{1}{|Q_{1,j}-R_{\ell,n}|}$$

$$= -\frac{1}{4\pi}\left[\frac{(x_{Q_{1,j}}-x_{R_{\ell,n}})}{|Q_{1,j}-R_{\ell,n}|^3}n_x + \frac{(y_{Q_{1,j}}-y_{R_{\ell,n}})}{|Q_{1,j}-R_{\ell,n}|^3}n_y + \frac{(z_{Q_{1,j}}-z_{R_{\ell,n}})}{|Q_{1,j}-R_{\ell,n}|^3}n_z\right],$$

$$\left(A_\ell^{42}\right)_{j,n} = \frac{1}{4\pi}\frac{\partial}{\partial n}\frac{1}{|Q_{1,j}-S_{\ell,n}|}$$

$$= -\frac{1}{4\pi}\left[\frac{(x_{Q_{1,j}}-x_{S_{\ell,n}})}{|Q_{1,j}-S_{\ell,n}|^3}n_x + \frac{(y_{Q_{1,j}}-y_{S_{\ell,n}})}{|Q_{1,j}-S_{\ell,n}|^3}n_y + \frac{(z_{Q_{1,j}}-z_{S_{\ell,n}})}{|Q_{1,j}-S_{\ell,n}|^3}n_z\right],$$

$$\left(A_\ell^{43}\right)_{j,n} = \frac{1}{8\pi}\frac{\partial}{\partial n}|Q_{1,j}-R_{\ell,n}|$$

$$= \frac{1}{8\pi}\left[\frac{(x_{Q_{1,j}}-x_{R_{\ell,n}})}{|Q_{1,j}-R_{\ell,n}|}n_x + \frac{(y_{Q_{1,j}}-y_{R_{\ell,n}})}{|Q_{1,j}-R_{\ell,n}|}n_y + \frac{(z_{Q_{1,j}}-z_{R_{\ell,n}})}{|Q_{1,j}-R_{\ell,n}|}n_z\right],$$

$$\left(A_\ell^{44}\right)_{j,n} = \frac{1}{8\pi}\frac{\partial}{\partial n}|Q_{1,j}-S_{\ell,n}|$$

$$= \frac{1}{8\pi}\left[\frac{(x_{Q_{1,j}}-x_{S_{\ell,n}})}{|Q_{1,j}-S_{\ell,n}|}n_x + \frac{(y_{Q_{1,j}}-y_{S_{\ell,n}})}{|Q_{1,j}-S_{\ell,n}|}n_y + \frac{(z_{Q_{1,j}}-z_{S_{\ell,n}})}{|Q_{1,j}-S_{\ell,n}|}n_z\right],$$

where n_x, n_y and n_z denote the components of the outward normal vector to $\partial\Omega$ in the x, y and z directions, respectively, at the points $P_{1,j}$, $Q_{1,j}$.

4.3.2 Matrix decomposition algorithm

In this case, a Matrix Decomposition Algorithm involves the reduction of the $4MN \times 4MN$ system (4.12) to M decoupled $4N \times 4N$ systems.

Let us denote by H the $4MN \times 4MN$ matrix

$$\begin{aligned} H &= \left(\begin{array}{c|c|c|c} A^{11} & A^{12} & A^{13} & A^{14} \\ \hline A^{21} & A^{22} & A^{23} & A^{24} \\ \hline A^{31} & A^{32} & A^{33} & A^{34} \\ \hline A^{41} & A^{42} & A^{43} & A^{44} \end{array}\right) \\ &= \sum_{k=1}^{M} \left(\begin{array}{c|c|c|c} \mathcal{P}^{k-1} \otimes A_k^{11} & \mathcal{P}^{k-1} \otimes A_k^{12} & \mathcal{P}^{k-1} \otimes A_k^{13} & \mathcal{P}^{k-1} \otimes A_k^{14} \\ \hline \mathcal{P}^{k-1} \otimes A_k^{21} & \mathcal{P}^{k-1} \otimes A_k^{22} & \mathcal{P}^{k-1} \otimes A_k^{23} & \mathcal{P}^{k-1} \otimes A_k^{24} \\ \hline \mathcal{P}^{k-1} \otimes A_k^{31} & \mathcal{P}^{k-1} \otimes A_k^{32} & \mathcal{P}^{k-1} \otimes A_k^{33} & \mathcal{P}^{k-1} \otimes A_k^{34} \\ \hline \mathcal{P}^{k-1} \otimes A_k^{41} & \mathcal{P}^{k-1} \otimes A_k^{42} & \mathcal{P}^{k-1} \otimes A_k^{43} & \mathcal{P}^{k-1} \otimes A_k^{44} \end{array}\right). \end{aligned}$$

Clearly,

$$(U \otimes \mathcal{I}_N)\,(\mathcal{P}^{k-1} \otimes A_k^{rs})\,(U^* \otimes \mathcal{I}_N) = (U\mathcal{P}^{k-1}U^*) \otimes A_k^{rs} = T^{k-1} \otimes A_k^{rs},$$

for $k = 1, \ldots, M$ and $r, s = 1, 2, 3, 4$. Pre–multiplication of system (4.12) by $\mathcal{I}_4 \otimes U \otimes \mathcal{I}_N$ yields

$$(\mathcal{I}_4 \otimes U \otimes \mathcal{I}_N)\,H\,(\mathcal{I}_4 \otimes U^* \otimes \mathcal{I}_N)\,(\mathcal{I}_4 \otimes U \otimes \mathcal{I}_N)\,\boldsymbol{s} \;=\; (\mathcal{I}_4 \otimes U \otimes \mathcal{I}_N)\,\boldsymbol{t}, \tag{4.13}$$

where $\boldsymbol{s} = [\boldsymbol{c_1}|\boldsymbol{c_2}|\boldsymbol{d_1}|\boldsymbol{d_2}]^T$, $\boldsymbol{t} = [\boldsymbol{f_1}|\boldsymbol{f_2}|\boldsymbol{g_1}|\boldsymbol{g_2}]^T$, since $(U^* \otimes \mathcal{I}_N)(U \otimes \mathcal{I}_N) = \mathcal{I}_{MN}$.

The system (4.13) can be written alternatively

$$\hat{H}\hat{\boldsymbol{s}} \;=\; \hat{\boldsymbol{t}}, \tag{4.14}$$

where

$$\hat{\boldsymbol{s}} = (\mathcal{I}_4 \otimes U \otimes \mathcal{I}_N)\,\boldsymbol{s} = \left(\begin{array}{c} (U \otimes \mathcal{I}_N)\,\boldsymbol{c}_1 \\ \hline (U \otimes \mathcal{I}_N)\,\boldsymbol{c}_2 \\ \hline (U \otimes \mathcal{I}_N)\,\boldsymbol{d}_1 \\ \hline (U \otimes \mathcal{I}_N)\,\boldsymbol{d}_2 \end{array}\right) = \left(\begin{array}{c} \tilde{\boldsymbol{c}}_1 \\ \hline \tilde{\boldsymbol{c}}_2 \\ \hline \tilde{\boldsymbol{d}}_1 \\ \hline \tilde{\boldsymbol{d}}_2 \end{array}\right),$$

$$\hat{\boldsymbol{t}} = (\mathcal{I}_4 \otimes U \otimes \mathcal{I}_N)\,\boldsymbol{t} = \left(\begin{array}{c} (U \otimes \mathcal{I}_N)\,\boldsymbol{f}_1 \\ \hline (U \otimes \mathcal{I}_N)\,\boldsymbol{f}_2 \\ \hline (U \otimes \mathcal{I}_N)\,\boldsymbol{g}_1 \\ \hline (U \otimes \mathcal{I}_N)\,\boldsymbol{g}_2 \end{array}\right) = \left(\begin{array}{c} \tilde{\boldsymbol{f}}_1 \\ \hline \tilde{\boldsymbol{f}}_2 \\ \hline \tilde{\boldsymbol{g}}_1 \\ \hline \tilde{\boldsymbol{g}}_2 \end{array}\right)$$

and

$$\hat{H} = (\mathcal{I}_4 \otimes U \otimes \mathcal{I}_N)\, H\, (\mathcal{I}_4 \otimes U^* \otimes \mathcal{I}_N)$$

$$= \sum_{k=1}^{M} (\mathcal{I}_4 \otimes U \otimes \mathcal{I}_N) \left(\begin{array}{c|c|c|c} \mathcal{P}^{k-1} \otimes A_k^{11} & \mathcal{P}^{k-1} \otimes A_k^{12} & \mathcal{P}^{k-1} \otimes A_k^{13} & \mathcal{P}^{k-1} \otimes A_k^{14} \\ \hline \mathcal{P}^{k-1} \otimes A_k^{21} & \mathcal{P}^{k-1} \otimes A_k^{22} & \mathcal{P}^{k-1} \otimes A_k^{23} & \mathcal{P}^{k-1} \otimes A_k^{24} \\ \hline \mathcal{P}^{k-1} \otimes A_k^{31} & \mathcal{P}^{k-1} \otimes A_k^{32} & \mathcal{P}^{k-1} \otimes A_k^{33} & \mathcal{P}^{k-1} \otimes A_k^{34} \\ \hline \mathcal{P}^{k-1} \otimes A_k^{41} & \mathcal{P}^{k-1} \otimes A_k^{42} & \mathcal{P}^{k-1} \otimes A_k^{43} & \mathcal{P}^{k-1} \otimes A_k^{44} \end{array}\right) (\mathcal{I}_4 \otimes U^* \otimes \mathcal{I}_N)$$

$$= \sum_{k=1}^{M} \left(\begin{array}{c|c|c|c} T^{k-1} \otimes A_k^{11} & T^{k-1} \otimes A_k^{12} & T^{k-1} \otimes A_k^{13} & T^{k-1} \otimes A_k^{14} \\ \hline T^{k-1} \otimes A_k^{21} & T^{k-1} \otimes A_k^{22} & T^{k-1} \otimes A_k^{23} & T^{k-1} \otimes A_k^{24} \\ \hline T^{k-1} \otimes A_k^{31} & T^{k-1} \otimes A_k^{32} & T^{k-1} \otimes A_k^{33} & T^{k-1} \otimes A_k^{34} \\ \hline T^{k-1} \otimes A_k^{41} & T^{k-1} \otimes A_k^{42} & T^{k-1} \otimes A_k^{43} & T^{k-1} \otimes A_k^{44} \end{array}\right),$$

where T is given by (4.3). Therefore, (4.14) becomes

$$\sum_{k=1}^{M} \left(\begin{array}{c|c|c|c} T^{k-1} \otimes A_k^{11} & T^{k-1} \otimes A_k^{12} & T^{k-1} \otimes A_k^{13} & T^{k-1} \otimes A_k^{14} \\ \hline T^{k-1} \otimes A_k^{21} & T^{k-1} \otimes A_k^{22} & T^{k-1} \otimes A_k^{23} & T^{k-1} \otimes A_k^{24} \\ \hline T^{k-1} \otimes A_k^{31} & T^{k-1} \otimes A_k^{32} & T^{k-1} \otimes A_k^{33} & T^{k-1} \otimes A_k^{34} \\ \hline T^{k-1} \otimes A_k^{41} & T^{k-1} \otimes A_k^{42} & T^{k-1} \otimes A_k^{43} & T^{k-1} \otimes A_k^{44} \end{array}\right) \left(\begin{array}{c} \tilde{\boldsymbol{c}}_1 \\ \hline \tilde{\boldsymbol{c}}_2 \\ \hline \tilde{\boldsymbol{d}}_1 \\ \hline \tilde{\boldsymbol{d}}_2 \end{array}\right) = \left(\begin{array}{c} \tilde{\boldsymbol{f}}_1 \\ \hline \tilde{\boldsymbol{f}}_2 \\ \hline \tilde{\boldsymbol{g}}_1 \\ \hline \tilde{\boldsymbol{g}}_2 \end{array}\right). \tag{4.15}$$

The solution of system (4.15) can therefore be decomposed into the solution of the M independent $4N \times 4N$ systems

$$H_m \left(\begin{array}{c} \tilde{\boldsymbol{c}}_1^m \\ \hline \tilde{\boldsymbol{c}}_2^m \\ \hline \tilde{\boldsymbol{d}}_1^m \\ \hline \tilde{\boldsymbol{d}}_2^m \end{array} \right) = \left(\begin{array}{c} \tilde{\boldsymbol{f}}_1^m \\ \hline \tilde{\boldsymbol{f}}_2^m \\ \hline \tilde{\boldsymbol{g}}_1^m \\ \hline \tilde{\boldsymbol{g}}_2^m \end{array} \right), \quad m = 1, \ldots, M, \tag{4.16}$$

where

$$H_m = \left(\begin{array}{c|c|c|c} \hat{A}_j^{11} & \hat{A}_m^{12} & \hat{A}_m^{13} & \hat{A}_m^{14} \\ \hline \hat{A}_m^{21} & \hat{A}_m^{22} & \hat{A}_m^{23} & \hat{A}_m^{24} \\ \hline \hat{A}_m^{31} & \hat{A}_m^{32} & \hat{A}_m^{33} & \hat{A}_m^{34} \\ \hline \hat{A}_m^{41} & \hat{A}_m^{42} & \hat{A}_m^{43} & \hat{A}_m^{44} \end{array} \right),$$

and

$$\hat{A}_m^{k\ell} = \sum_{j=1}^{M} \omega^{(m-1)(j-1)} A_j^{k\ell}, \tag{4.17}$$

$k, \ell = 1, 2, 3, 4,$ $m = 1, \ldots, M$. We thus have the following efficient algorithm

Algorithm

Step 1. `Compute` $\tilde{\boldsymbol{f}}_{\boldsymbol{1}} = (U \otimes \mathcal{I}_N)\, \boldsymbol{f}_{\boldsymbol{1}}$, $\tilde{\boldsymbol{f}}_{\boldsymbol{2}} = (U \otimes \mathcal{I}_N)\, \boldsymbol{f}_{\boldsymbol{2}}$, $\tilde{\boldsymbol{g}}_{\boldsymbol{1}} = (U \otimes \mathcal{I}_N)\, \boldsymbol{g}_{\boldsymbol{1}}$, $\tilde{\boldsymbol{g}}_{\boldsymbol{2}} = (U \otimes \mathcal{I}_N)\, \boldsymbol{g}_{\boldsymbol{2}}$.

Step 2. `Construct the matrices` $H_m \quad m = 1, \ldots, M$.

Step 3. `Solve (4.16).`

Step 4. `Compute` $\boldsymbol{c}_{\boldsymbol{1}} = (U^* \otimes \mathcal{I}_N)\, \tilde{\boldsymbol{c}}_{\boldsymbol{1}}$, $\boldsymbol{c}_{\boldsymbol{2}} = (U^* \otimes \mathcal{I}_N)\, \tilde{\boldsymbol{c}}_{\boldsymbol{2}}$, $\boldsymbol{d}_{\boldsymbol{1}} = (U^* \otimes \mathcal{I}_N)\, \tilde{\boldsymbol{d}}_{\boldsymbol{1}}$, $\boldsymbol{d}_{\boldsymbol{2}} = (U^* \otimes \mathcal{I}_N)\, \tilde{\boldsymbol{d}}_{\boldsymbol{2}}$.

Remarks

(i) In *Step* 1, because of the form of the matrix U, the operation is equivalent to performing N FFTs of dimension M. This can done at a cost of $\mathcal{O}(NM \log M)$ operations via an appropriate FFT algorithm. Similarly, in *Step* 4, because of the form of the matrix U^*, the operation can be carried out via inverse FFTs at a cost of order $\mathcal{O}(NM \log M)$ operations.

(ii) In *Step* 2, we need to perform an $M-$dimensional inverse FFT, in order to compute the entries of the matrices $\hat{A}_k^{rs}$, $r, s = 1, 2, 3, 4$, $k = 1, \dots, M$, from (4.17). This can be done at a cost of $\mathcal{O}(N^2 M \log M)$ operations.

(iii) In *Step* 3, we need to solve M complex linear systems of order N. This is done using an $LU-$factorization with partial pivoting at a cost of $\mathcal{O}(M\, N^3)$ operations.

(iv) The FFT and inverse FFT operations are performed using the NAG routines `C06EAF, C06FPF, C06FQF` and `C06FRF`.

4.4 Examples of axisymmetric solids

Case I: Thick spherical shell

We first consider the case where the domain $\Omega \subset \mathbb{R}^3$ is the 3-dimensional domain defined by

$$\Omega \,=\, \{\boldsymbol{x} \in \mathbb{R}^3 \,:\, \varrho_1 < |\boldsymbol{x}| < \varrho_2\}. \tag{4.18}$$

In this case, the $2MN$ singularities $R_{m,n}$ and $S_{m,n}$ are fixed on the boundary $\partial\tilde{\Omega} = \partial\tilde{\Omega}_1 \cup \partial\tilde{\Omega}_2$ of the $3-$dimensional domain defined by $\tilde{\Omega} = \{\boldsymbol{x} \in \mathbb{R}^3 \,:\, R_1 < |\boldsymbol{x}| < R_2\}$ where $R_1 < \varrho_1 < \varrho_2 < R_2$. A set of $M\,N$ collocation points $\{P_{i,j}\}_{i=1,j=1}^{M,N}$ is chosen on the boundary $\partial\Omega_1$ of Ω (i.e. the surface of a sphere of radius ϱ_1) and a set of $M\,N$ collocation points $\{Q_{i,j}\}_{i=1,j=1}^{M,N}$ is chosen on the boundary $\partial\Omega_2$ (i.e. the surface of a sphere of radius ϱ_2) so that if $P_{i,j} = (x_{P_{i,j}}, y_{P_{i,j}}, z_{P_{i,j}})$ and $Q_{i,j} = (x_{Q_{i,j}}, y_{Q_{i,j}}, z_{Q_{i,j}})$, then

$$x_{P_{i,j}} = \varrho_1 \sin\vartheta_j \cos\varphi_i, \;\; y_{P_{i,j}} = \varrho_1 \sin\vartheta_j \sin\varphi_i, \;\; z_{P_{i,j}} = \varrho_1 \cos\vartheta_j,$$

$$x_{Q_{i,j}} = \varrho_2 \sin\vartheta_j \cos\varphi_i, \;\; y_{Q_{i,j}} = \varrho_2 \sin\vartheta_j \sin\varphi_i, \;\; z_{Q_{i,j}} = \varrho_2 \cos\vartheta_j,$$

where $\varphi_i = 2(i-1)\pi/M, \;\; i = 1, \dots, M$ and $\vartheta_j = j\,\pi/(N+1), \;\; j = 1, \dots, N$. Note that we avoid the points corresponding to $\vartheta_j = 0$ and $\vartheta_j = \pi$ as these remain invariant under rotation in the $\varphi-$direction and hence lead to singular matrices.

Similarly, we choose a set of $M\,N$ singularities $\{R_{i,j}\}_{i=1,j=1}^{M,N}$ on $\partial\tilde{\Omega}_1$ (i.e., the surface of a sphere of radius R_1) and a set of $M\,N$ singularities $\{S_{i,j}\}_{i=1,j=1}^{M,N}$ on $\partial\tilde{\Omega}_2$ (i.e., the surface of a sphere of radius R_2), by taking $R_{i,j} = (x_{R_{i,j}}, y_{R_{i,j}}, z_{R_{i,j}})$, $S_{i,j} = (x_{S_{i,j}}, y_{S_{i,j}}, z_{S_{i,j}})$, with

$$x_{R_{i,j}} = R_1 \sin\vartheta_j \cos\psi_i, \;\; y_{R_{i,j}} = R_1 \sin\vartheta_j \sin\psi_i, z_{R_{i,j}} = R_1 \cos\vartheta_j,$$

$$x_{S_{i,j}} = R_2 \sin\vartheta_j \cos\psi_i, \;\; y_{S_{i,j}} = R_2 \sin\vartheta_j \sin\psi_i, z_{S_{i,j}} = R_2 \cos\vartheta_j,$$

where $\psi_i = \dfrac{2(\alpha+i-1)\pi}{M}, \;\; i = 1,\ldots,M \;\;, 0 \le \alpha < 1.$

Case II: Sphere with interior cylinder removed

We next consider the domain $\Omega \subset \mathbb{R}^3$ defined by

$$\Omega \;=\; \left\{\boldsymbol{x} \in \mathbb{R}^3 \,:\, |\boldsymbol{x}| < \varrho_2\right\} \smallsetminus \left\{(x,y,z) \in \mathbb{R}^3 \,:\, x^2+y^2 < \varrho_1^2, \; -h < z < h\right\}, \quad \varrho_1, h < \varrho_2.$$

In this case a set of MN collocation points $\{P_{i,j}\}_{i=1,j=1}^{M,N}$ is chosen on the boundary $\partial\Omega_1$ of Ω (i.e., the surface of a cylinder of radius ϱ_1 and height h) and a set of $M\,N$ collocation points $\{Q_{i,j}\}_{i=1,j=1}^{M,N}$ is chosen on the boundary $\partial\Omega_2$ (i.e., the surface of a sphere of radius ϱ_2) so that if $P_{i,j} = (x_{P_{i,j}}, y_{P_{i,j}}, z_{P_{i,j}})$ and $Q_{i,j} = (x_{Q_{i,j}}, y_{Q_{i,j}}, z_{Q_{i,j}})$, then

$$x_{P_{i,j}} \;=\; r_{P_j} \cos\varphi_i, \;\; y_{P_{i,j}} \;=\; r_{P_j} \sin\varphi_i, \;\; z_{P_{i,j}} \;=\; z_{P_j},$$

$$x_{Q_{i,j}} \;=\; \varrho_2 \sin\vartheta_j \cos\varphi_i, \;\; y_{Q_{i,j}} \;=\; \varrho_2 \sin\vartheta_j \sin\varphi_i, \;\; z_{Q_{i,j}} \;=\; \varrho_2 \cos\vartheta_j,$$

where $\varphi_i = 2(i-1)\pi/M, \;\; i = 1,\ldots,M$ and $\vartheta_j = j\pi/(N+1), \;\; j = 1,\ldots,N$. The polar coordinates $\left(r_{P_j}, z_{P_j}\right)$, $j = 1,\ldots,N$, represent N points on the boundary of the rectangle $(0,\varrho_1)\times(-h,h)$.

Similarly, we choose a set of $M\,N$ singularities $\{R_{i,j}\}_{i=1,j=1}^{M,N}$ on $\partial\tilde{\Omega}_1$ (i.e., the surface of a cylinder of radius R_1 and height $2H$) and a set of $M\,N$ singularities $\{S_{i,j}\}_{i=1,j=1}^{M,N}$ on $\partial\tilde{\Omega}_2$ (i.e. the surface of a sphere of radius R_2), by taking $R_{i,j} = (x_{R_{i,j}}, y_{R_{i,j}}, z_{R_{i,j}})$, $S_{i,j} = (x_{S_{i,j}}, y_{S_{i,j}}, z_{S_{i,j}})$, with

$$x_{R_{i,j}} \;=\; \tilde{r}_{R_j} \cos\psi_i, \;\; y_{R_{i,j}} = \tilde{r}_{R_j} \sin\psi_i, \;\; z_{R_{i,j}} = \tilde{z}_{R_j},$$

$$x_{S_{i,j}} \;=\; R_2 \sin\vartheta_j \cos\psi_i, \;\; y_{S_{i,j}} = R_2 \sin\vartheta_j \sin\psi_i, z_{S_{i,j}} = R_2 \cos\vartheta_j,$$

where $\psi_i = 2(\alpha+i-1)\pi/M, \;\; i = 1,\ldots,M$. The polar coordinates $(\tilde{r}_{Q_j}, \tilde{z}_{Q_j})$, $j = 1,\ldots,N$ describe N points on the boundary of the rectangle $(0,R_1)\times(-H,H)$ with $R_1 < \varrho_1 < \varrho_2 < R_2$ and $H < h$.

Case III: Cylinder with interior sphere removed

We next consider the following domain

$$\Omega = \{(x,y,z) \in \mathbb{R}^3 \,:\, x^2+y^2 < \varrho_2^2,\ -h < z < h\} \setminus \{\boldsymbol{x} \in \mathbb{R}^3 \,:\, |\boldsymbol{x}| < \varrho_1\}, \quad \varrho_1 < h, \varrho_2. \quad (4.19)$$

In this case a set of $M\,N$ collocation points $\{P_{i,j}\}_{i=1,j=1}^{M,N}$ is chosen on the boundary $\partial\Omega_1$ of Ω (i.e. the surface of a sphere of radius ϱ_1) and a set of $M\,N$ collocation points $\{Q_{i,j}\}_{i=1,j=1}^{M,N}$ is chosen on the boundary $\partial\Omega_2$ (i.e. the surface of a cylinder of radius ϱ_2 and height h) so that if $P_{i,j} = (x_{P_{i,j}}, y_{P_{i,j}}, z_{P_{i,j}})$ and $Q_{i,j} = (x_{Q_{i,j}}, y_{Q_{i,j}}, z_{Q_{i,j}})$, then

$$x_{P_{i,j}} = \varrho_1 \sin\vartheta_j \cos\varphi_i, \quad y_{P_{i,j}} = \varrho_1 \sin\vartheta_j \sin\varphi_i, \quad z_{P_{i,j}} = \varrho_1 \cos\vartheta_j,$$

$$x_{Q_{i,j}} = r_{Q_j} \cos\varphi_i, \quad y_{P_{i,j}} = r_{Q_j} \sin\varphi_i, \quad z_{Q_{i,j}} = z_{Q_j},$$

where $\varphi_i = 2(i-1)\pi/M, \quad i = 1,\ldots,M$ and $\vartheta_j = j\,\pi/(N+1), \quad j = 1,\ldots,N$. The polar coordinates $(r_{Q_j}, z_{Q_j}), \ j = 1,\ldots,N$, represent N points on the boundary of the rectangle $(0,\varrho_2)\times(-h,h)$.

Similarly, we choose a set of $M\,N$ singularities $\{R_{i,j}\}_{i=1,j=1}^{M,N}$ on $\partial\tilde{\Omega}_1$ (i.e. the surface of a sphere of radius R_1) and a set of $M\,N$ singularities $\{S_{i,j}\}_{i=1,j=1}^{M,N}$ on $\partial\tilde{\Omega}_2$ (i.e. the surface of a cylinder of radius R_2 and height $2H$), by taking $R_{i,j} = (x_{R_{i,j}}, y_{R_{i,j}}, z_{R_{i,j}})$, $S_{i,j} = (x_{S_{i,j}}, y_{S_{i,j}}, z_{S_{i,j}})$, with

$$x_{R_{i,j}} = R_1 \sin\vartheta_j \cos\psi_i, \quad y_{R_{i,j}} = R_1 \sin\vartheta_j \sin\psi_i, z_{R_{i,j}} = R_1 \cos\vartheta_j,$$

$$x_{S_{i,j}} = \tilde{r}_{S_j} \cos\psi_i, \quad y_{S_{i,j}} = \tilde{r}_{S_j} \sin\psi_i, \quad z_{S_{i,j}} = \tilde{z}_{S_j},$$

where $\psi_i = 2(\alpha+i-1)\pi/M, \quad i = 1,\ldots,M$. The polar coordinates $(\tilde{r}_{S_j}, \tilde{z}_{S_j}), \ j = 1,\ldots,N$, describe N points on the boundary of the rectangle $(0,R_2)\times(-H,H)$ with $R_1 < \varrho_1 < \varrho_2 < R_2$ and $H > h$.

Case IV: Torus with interior torus removed

We finally consider the case where the domain $\Omega \subset \mathbb{R}^3$ is defined by

$$\Omega = \Big\{(x_1,x_2,x_3) \in \mathbb{R}^3 \,:\, \varrho_1^2 < \big(\sqrt{x^2+y^2} - \varrho_3\big)^2 + z^2 < \varrho_2^2\Big\}, \quad (4.20)$$

$\varrho_1 < \varrho_2 < \varrho_3$, where its boundary $\partial\Omega = \partial\Omega_1 \bigcup \partial\Omega_2$ can be described by the parametric equations

$$x_1 = \varrho_3 \cos\varphi + \varrho_1 \cos\varphi \cos\vartheta, \quad y_1 = \varrho_3 \sin\varphi + \varrho_1 \sin\varphi \cos\vartheta, \quad z_1 = \varrho_1 \sin\vartheta,$$

$$x_2 = \varrho_3 \cos\varphi + \varrho_2 \cos\varphi \cos\vartheta, \quad y_2 = \varrho_3 \sin\varphi + \varrho_2 \sin\varphi \cos\vartheta, \quad z_2 = \varrho_2 \sin\vartheta,$$

where $0 \le \varphi \le 2\,\pi,\;\; 0 \le \vartheta \le 2\,\pi$ with $(x_1, y_1, z_1) \in \partial\Omega_1$ and $(x_2, y_2, z_2) \in \partial\Omega_2$.

We choose a set of $M\,N$ collocation points $\{P_{i,j}\}_{i=1,j=1}^{M,N}$ on the boundary $\partial\Omega_1$ of Ω (i.e. the surface of a torus with radii ϱ_1, ϱ_3) and a set of $M\,N$ collocation points $\{Q_{i,j}\}_{i=1,j=1}^{M,N}$ on the boundary $\partial\Omega_2$ (i.e. the surface of a torus with radii ϱ_2, ϱ_3) so that if $P_{i,j} = (x_{P_{i,j}}, y_{P_{i,j}}, z_{P_{i,j}})$ and $Q_{i,j} = (x_{Q_{i,j}}, y_{Q_{i,j}}, z_{Q_{i,j}})$, then

$$x_{P_{m,n}} = \varrho_3 \cos\varphi_n + \varrho_1 \cos\varphi_n \cos\vartheta_m,\;\; y_{P_{m,n}} = \varrho_3 \sin\varphi_n + \varrho_1 \sin\varphi_n \cos\vartheta_m,\;\; z_{P_{m,n}} = \varrho_1 \sin\vartheta_m,$$

$$x_{Q_{m,n}} = \varrho_3 \cos\varphi_n + \varrho_2 \cos\varphi_n \cos\vartheta_m,\;\; y_{Q_{m,n}} = \varrho_3 \sin\varphi_n + \varrho_2 \sin\varphi_n \cos\vartheta_m,\;\; z_{Q_{m,n}} = \varrho_2 \sin\vartheta_m,$$

where $\vartheta_m = 2(m-1)\pi/N,\;\; m = 1, \ldots, M$ and $\varphi_n = 2(n-1)\pi/N,\;\; n = 1, \ldots, N$. Similarly, we choose a set of $M\,N$ singularities $\{R_{i,j}\}_{i=1,j=1}^{M,N}$ on $\partial\tilde{\Omega}_1$ (i.e. the surface of a torus with radii R_1, ϱ_3) and a set of $M\,N$ singularities $\{S_{i,j}\}_{i=1,j=1}^{M,N}$ on $\partial\tilde{\Omega}_2$ (i.e. the surface of a torus with radii R_2, ϱ_3), by taking $R_{i,j} = (x_{R_{i,j}}, y_{R_{i,j}}, z_{R_{i,j}})$, $S_{i,j} = (x_{S_{i,j}}, y_{S_{i,j}}, z_{S_{i,j}})$, where

$$x_{R_{m,n}} = R_3 \cos\psi_n + R_1 \cos\psi_n \cos\vartheta_m,\;\; y_{R_{m,n}} = R_3 \sin\psi_n + R_1 \sin\psi_n \cos\vartheta_m,\;\; z_{R_{m,n}} = R_1 \sin\vartheta_m,$$

$$x_{S_{m,n}} = R_3 \cos\psi_n + R_2 \cos\psi_n \cos\vartheta_m,\;\; y_{S_{m,n}} = R_3 \sin\psi_n + R_2 \sin\psi_n \cos\vartheta_m,\;\; z_{S_{m,n}} = R_2 \sin\vartheta_m,$$

where $\psi_n = 2(\alpha + n - 1)\pi/N,\;\; n = 1, \ldots, N$ with $0 \le \alpha < 1$.

4.5 Numerical results

The algorithms described in Sections 4.2.2 and 4.3.2 were tested in regions defined by the solids described in Section 4.4, for harmonic and biharmonic problems, respectively.

4.5.1 Harmonic case

In particular, for harmonic problems we considered two examples with boundary conditions corresponding to the exact solutions:

Example (a) $u = \cosh(0.3x)\cosh(0.4y)\cos(0.5z)$

Example (b) $u = x^2 - 2y^2 + z^2$

In the description of the numerical results we shall be referring to, say, Example (b) in the solid described in Case III, as Example 3b.

In these examples, the maximum relative error was calculated on a uniform grid on the boundary (since all the functions involved are harmonic and the maximum principle applies). In the cases of the spherical shell (Case I) and the toroidal domain (Case IV) the maximum relative error was calculated at $2 \times 23 \times 23$ points on the boundary, whereas in the Cases II and III the maximum relative error was calculated at $2 \times 20 \times 20$ points on the corresponding boundaries.

Case I

We considered Examples (a) and (b) in a thick spherical shell with $\varrho_1 = 1$, $\varrho_2 = 2$. We varied the angular parameter α and examined how this affected the accuracy of the MFS approximation for various values of N and for different $\varepsilon = \varrho_1 - R_1 = R_2 - \varrho_2$ (Figures 4.1, 4.2 for Examples (a) and (b), respectively). Because of the symmetry of the problem about $\alpha = 1/2$, we only considered $0 \leq \alpha \leq 1/2$. We present six cases for $\varepsilon = 0.05, 0.1, 0.2, 0.5, 0.8, 0.95$ for $N(= M) = 8, 12, 16, 24, 32, 48$ and 64. From these results we see that for the smaller values of ε the error appears to have a minimum value for $\alpha \approx 1/4$. This is consistent with the observations reported in [20, 71]. We also varied the radius R_2 of the external sphere when $\alpha = 0$, while keeping R_1 fixed and equal to 0.5, and examined how this affected the accuracy of the approximation for different values of N (Figures 4.9, 4.10, for Examples (a) and (b), respectively). As can be seen from the figures, the error decreases exponentially as we increase R_2 up to a certain point, beyond which it starts increasing again. This is due to the ill-conditioning of the corresponding matrices for large R_2 (and large N) and was also reported in [20, 71]. In addition, we varied both radii R_1 and R_2 (of the inner and external spheres, respectively) simultaneously and examined how this affected the accuracy of the approximation for various N (Figures 4.17, 4.18, for Examples (a) and (b), respectively). The conclusions we draw from these figures are very similar to the ones drawn from Figures 4.9, 4.10, namely that the error decreases up to a certain value of ε, beyond which it starts increasing.

Case II

We considered Examples (a) and (b) in a sphere with an interior cylinder removed with $h = 2$, $\varrho_1 = 1$ and $\varrho_2 = 2$. We varied α and examined how this affected the accuracy of the MFS approximation for different N and for different $\varepsilon = h - H = \varrho_1 - R_1 = R_2 - \varrho_2$ (Figures 4.3, 4.4 for Examples (a) and (b), respectively). We present the cases $\varepsilon = 0.05, 0.1, 0.2, 0.5, 0.8, 0.95$ for

$N(=M) = 8, 12, 16, 24, 32, 48$ and 64. In this geometry no minima appear, even for small values of ε. In Figures 4.11 and 4.12, we varied the radius R_2 of the external sphere, while keeping both H and R_1 fixed and equal to 0.5, for various values of N. The results are consistent with the results observed in Case I. The same conclusions can be drawn from Figures 4.19, 4.20 where we varied both R_2 and $H(R_1)$.

Case III

We considered Examples (a) and (b) in a cylinder with an interior sphere removed with $\varrho_1 = 1$ and $h = 4$, $\varrho_2 = 2$. When we varied α for $\varepsilon = H - h = R_2 - \varrho_2 = \varrho_1 - R_1 =$ 0.05, 0.1, 0.2, 0.5, 0.8, 0.95, in Figures 4.5 and 4.6, as in Case I, we observed that, for the smaller values of ε, the error has a minimum for $\alpha \approx 1/4$. In Figures 4.13, 4.14 we varied R_2 while while keeping both H and R_1 fixed and equal to 0.5, and in Figures 4.21, 4.22 we varied both H and R_2. The results are consistent with the previous cases, namely that the error decreases exponentially up to a certain point after which starts increasing.

Case IV

We considered Examples (a) and (b) in a torus with an interior torus removed with $\varrho_1 = 1$, $\varrho_2 = 2$ and $\varrho_3 = 5$. In Figures 4.7 and 4.8, we varied α and examined how this affected the accuracy of the approximation for various values of N and for different $\varepsilon = \varrho_1 - R_1 = R_2 - \varrho_2$. We present the cases $\varepsilon = 0.05, 0.1, 0.2, 0.5, 0.8, 0.95$ for $N(= M) = 8, 12, 16, 24, 32, 48$ and 64. As in previous cases, we see that for the smaller values of ε the error appears to have a minimum value for $\alpha \approx 1/4$. In Figures 4.15 and 4.16 we varied R_2, while keeping R_1 fixed and equal to 0.5 and in Figures 4.23 and 4.24 we varied both R_1 and R_2. In all these cases we observed that as ε increased the accuracy improved until a certain point beyond which it deteriorated.

4.5.2 Biharmonic case

For biharmonic problems we considered two examples with boundary conditions corresponding to the exact solutions:

Example (c) $u = (x^2 + y^2 + z^2)\cosh(0.3x)\cosh(0.4y)\cos(0.5z)$

Example (d) $u = x^4 - 2y^4 + z^4$

In the description of the numerical results we shall be referring to, say, Example (c) in the solid described in Case III, as Example 3c.

In these examples, the maximum relative error was calculated on a uniform grid in the interior of the domain. In the cases of the spherical shell (Case I) and the toroidal domain (Case IV) the maximum relative error was calculated at $20 \times 23 \times 23$ interior points, whereas in the Cases II and III the maximum relative error was calculated at $20 \times 20 \times 20$ interior points.

Case I

We considered Examples (c) and (d) in a thick spherical shell with $\varrho_1 = 1$, $\varrho_2 = 2$. We varied α and examined how this affected the accuracy of the MFS approximation for various values of N and for different $\varepsilon = \varrho_1 - R_1 = R_2 - \varrho_2$ (Figures 4.25, 4.26 for Examples (a) and (b), respectively). We present six cases $\varepsilon = 0.05, 0.1, 0.2, 0.5, 0.8, 0.95$ for $N(= M) = 8, 12, 16, 24, 32, 48$ and 64, and, as in the harmonic case, for certain values of ε there appears to be a minimum at $\alpha \approx 1/4$. We also varied the radius R_2 of the external sphere when $\alpha = 0$, while keeping R_1 fixed and equal to 0.5 (Figures 4.33, 4.34 for Examples (c) and (d), respectively). As in the harmonic case, the error decreases exponentially as we increase R_2 up to a certain point, beyond which it starts increasing again, due to the ill-conditioning of the corresponding matrices. We also varied both R_1 and R_2 simultaneously (Figures 4.41, 4.42 for Examples (c) and (d), respectively) and as observed in Figures 4.33, 4.34 the error decreases up to a certain value of ε beyond which it starts increasing.

Case II

We considered Examples (c) and (d) in a sphere with an interior cylinder removed with $h = 2$, $\varrho_1 = 1$ and $\varrho_2 = 2$. We varied α for various values of N and for different $\varepsilon = h - H = \varrho_1 - R_1 = R_2 - \varrho_2$ (Figures 4.27, 4.28 for Examples (c) and (d), respectively). We present the cases $\varepsilon = 0.05, 0.1, 0.2, 0.5, 0.8, 0.95$ for $N(= M) = 8, 12, 16, 24, 32, 48$ and 64. As was observed in the harmonic case, there is no indication of a minimum for this geometry, even for small values of ε. In Figures 4.35 and 4.36, we varied the radius R_2 of the external sphere, while keeping both H and R_1 fixed and equal to 0.5, for various values of N. The results were consistent with the results observed in Case I. The same conclusions can be drawn from Figures 4.43, 4.44 where we varied both R_2 and $H(R_1)$.

Case III

We considered Examples (c) and (d) in a cylinder with an interior sphere removed with $\varrho_1 = 1$ and $h = 4,\ \ \varrho_2 = 2$. In Figures 4.29 and 4.30 we present the variation of α for $\varepsilon = H - h = R_2 - \varrho_2 = \varrho_1 - R_1 = 0.05, 0.1, 0.2, 0.5, 0.8, 0.95$. Unlike the corresponding geometry in the harmonic case, no minima were observed for the values of ε we considered. In Figures 4.37, 4.38 we varied R_2 while while keeping both H and R_1 fixed and equal to 0.5, and in Figures 4.45, 4.46 we varied both H and R_2. The results are consistent with the previous cases, namely that the error decreases exponentially up to a certain point after which starts increasing.

Case IV

We considered Examples (c) and (d) in a torus with an interior torus removed with $\varrho_1 = 1$, $\varrho_2 = 2$ and $\varrho_3 = 5$. In Figures 4.31 and 4.32, we varied α and examined how this affected the accuracy of the MFS approximation for $N(= M) = 8, 12, 16, 24, 32, 48, 64$ and for different $\varepsilon = \varrho_1 - R_1 = R_2 - \varrho_2 = 0.05, 0.1, 0.2, 0.5, 0.8, 0.95$. For certain values of ε and N there is a minimum at $\alpha \approx 1/4$. In Figures 4.39 and 4.40 we varied R_2, while keeping R_1 fixed and equal to 0.5 and in Figures 4.47 and 4.48 we varied both R_1 and R_2. In all these cases we observed that as ε increased the accuracy improved until a certain point beyond which it deteriorated.

4.6 Conclusions

In this chapter we propose efficient MFS algorithms for the solution of harmonic and biharmonic problems in hollow axisymmetric domains. These algorithms, which rely on matrix decomposition techniques with the use of FFTs, can also be applied to hollow axisymmetric problems governed by other differential equations such as the Helmholtz equation and the Cauchy–Navier equations of elasticity. Further, other boundary method discretizations also lead to the block circulant structures of the matrices arising in the problems examined in this study. The algorithms proposed in this work could thus be employed in conjunction with other boundary methods, such as the Boundary Element Method.

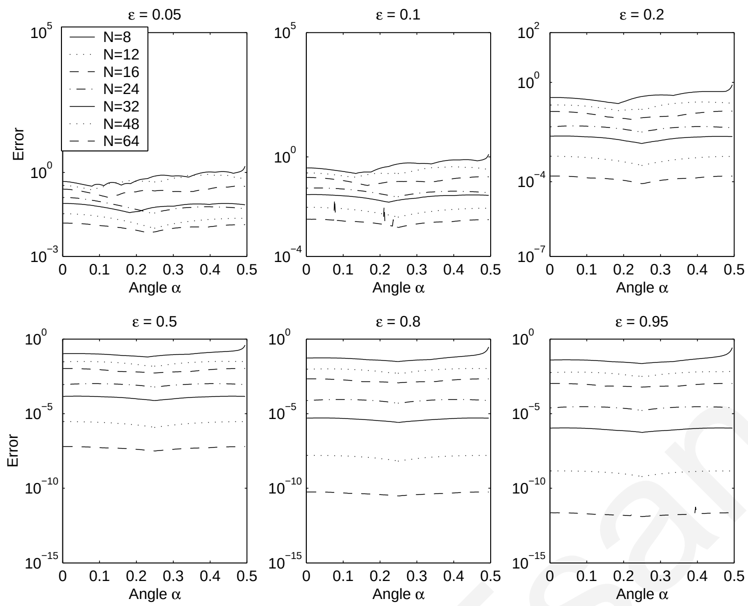

Figure 4.1: Log–plot of error versus angular parameter α for $\varepsilon = 0.05,\ 0.1,\ 0.2,\ 0.5,\ 0.8,\ 0.95$ in Example 1a for different values of N.

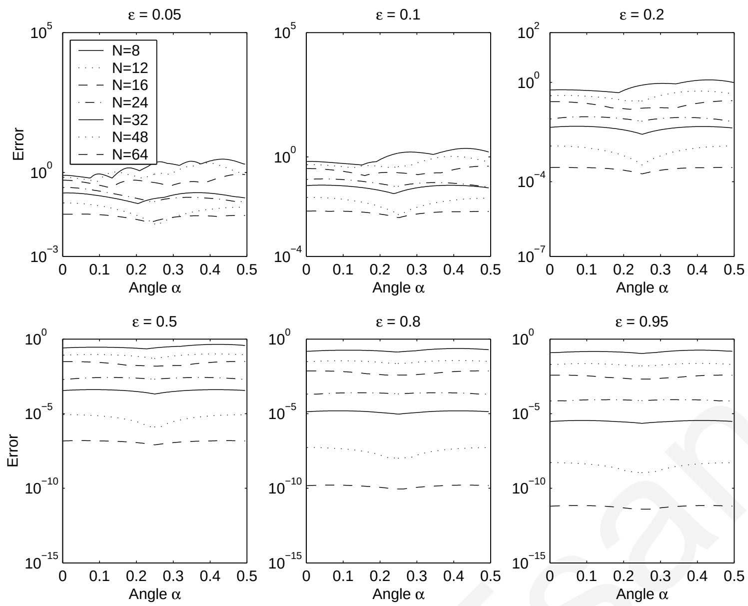

Figure 4.2: Log–plot of error versus angular parameter α for $\varepsilon = 0.05,\ 0.1,\ 0.2,\ 0.5,\ 0.8,\ 0.95$ in Example 1b for different values of N.

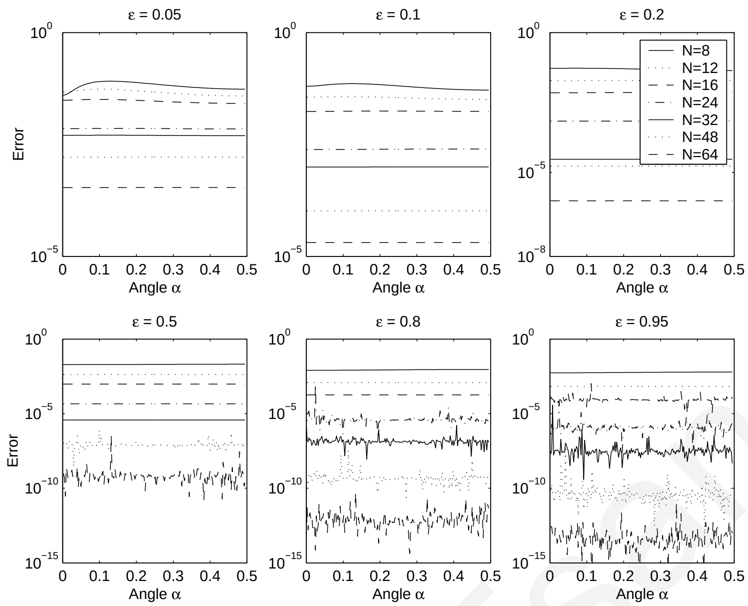

Figure 4.3: Log–plot of error versus angular parameter α for $\varepsilon = 0.05,\ 0.1,\ 0.2,\ 0.5,\ 0.8,\ 0.95$ in Example $2a$ for different values of N.

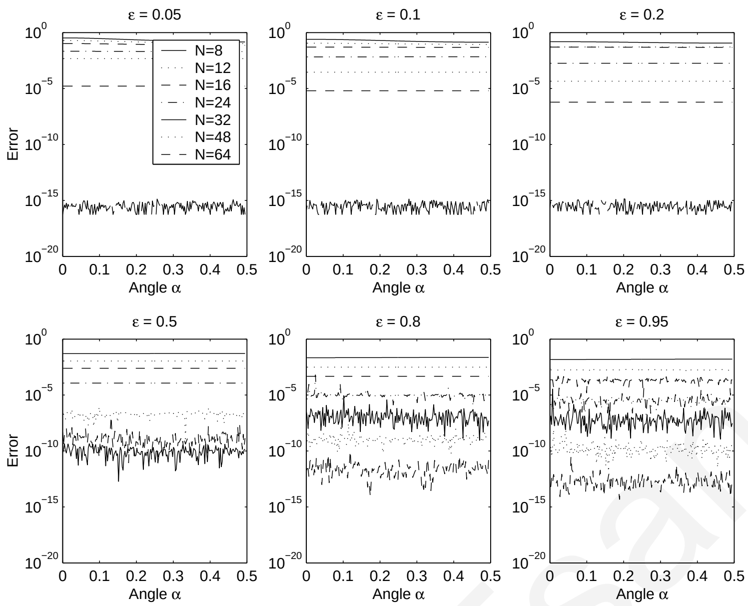

Figure 4.4: Log–plot of error versus angular parameter α for $\varepsilon = 0.05,\ 0.1,\ 0.2,\ 0.5,\ 0.8,\ 0.95$ in Example $2b$ for different values of N.

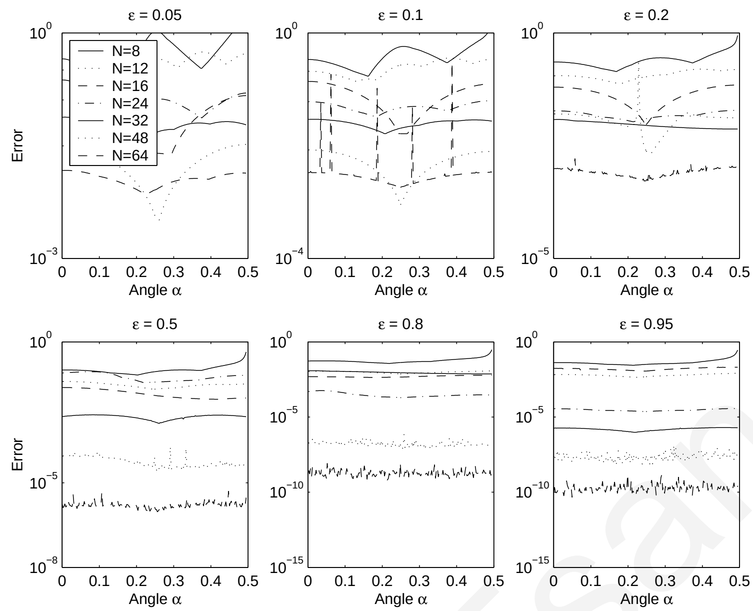

Figure 4.5: Log–plot of error versus angular parameter α for $\varepsilon = 0.05,\ 0.1,\ 0.2,\ 0.5,\ 0.8,\ 0.95$ in Example $3a$ for different values of N.

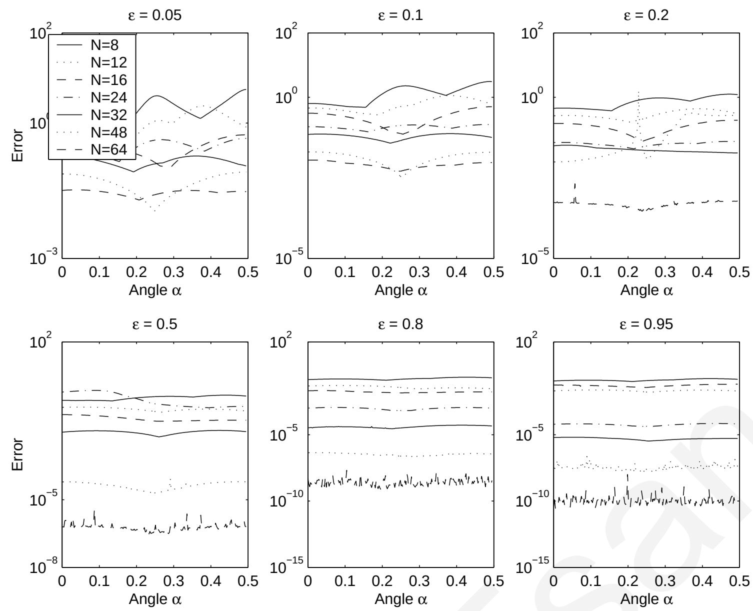

Figure 4.6: Log–plot of error versus angular parameter α for $\varepsilon = 0.05,\ 0.1,\ 0.2,\ 0.5,\ 0.8,\ 0.95$ in Example $3b$ for different values of N.

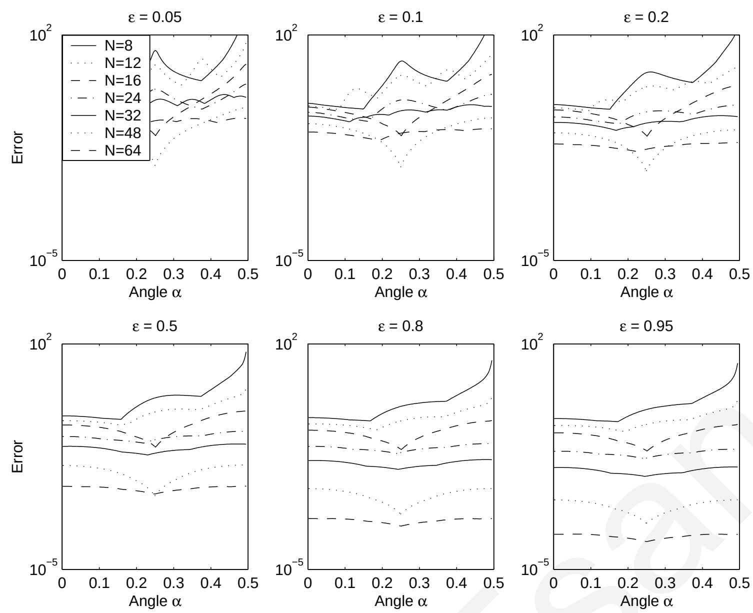

Figure 4.7: Log–plot of error versus angular parameter α for $\varepsilon = 0.05,\ 0.1,\ 0.2,\ 0.5,\ 0.8,\ 0.95$ in Example $4a$ for different values of N.

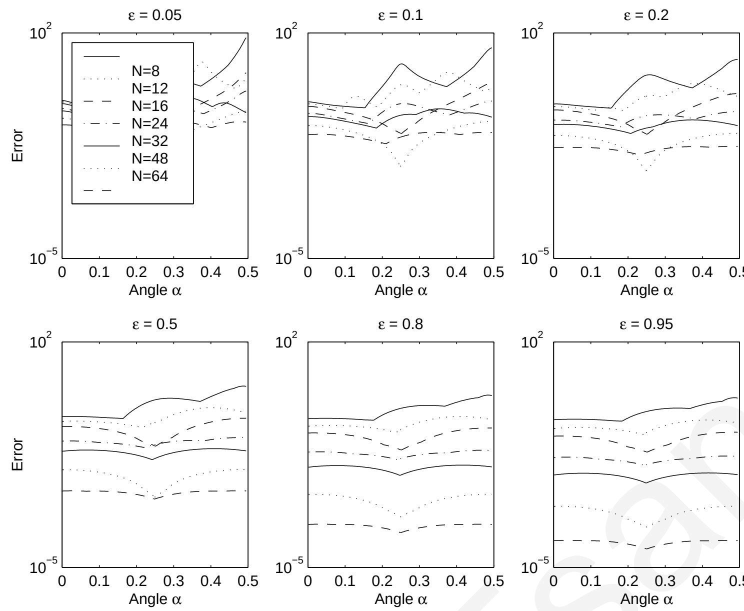

Figure 4.8: Log–plot of error versus angular parameter α for $\varepsilon = 0.05,\ 0.1,\ 0.2,\ 0.5,\ 0.8,\ 0.95$ in Example 4b for different values of N.

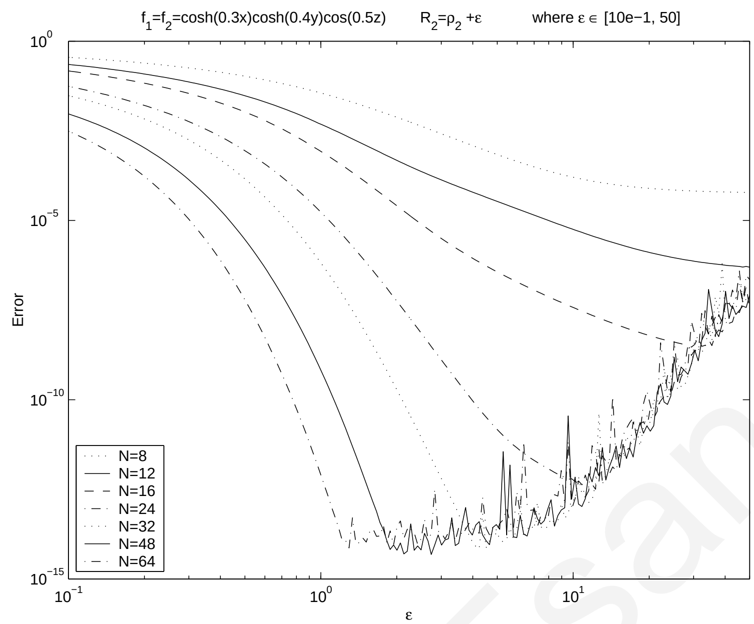

Figure 4.9: Log–log plot of maximum relative error versus ε in Example 1a.

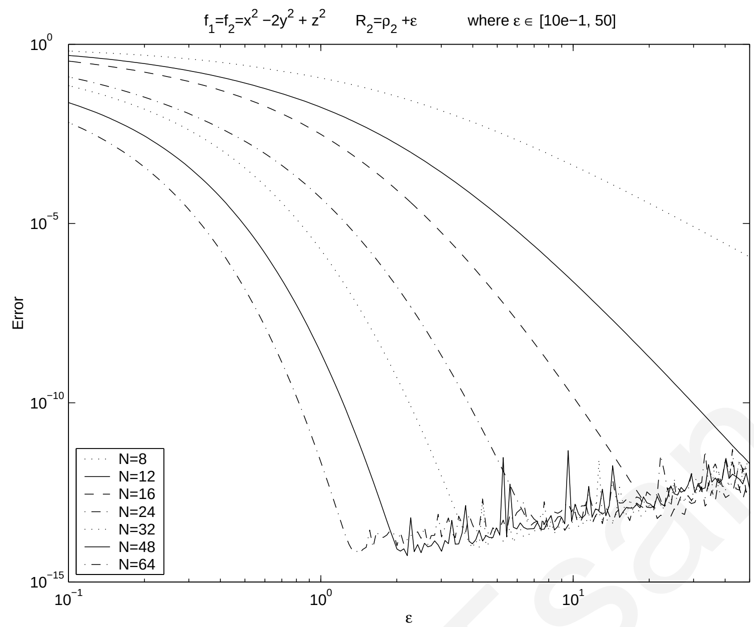

Figure 4.10: Log–log plot of maximum relative error versus ε in Example 1b.

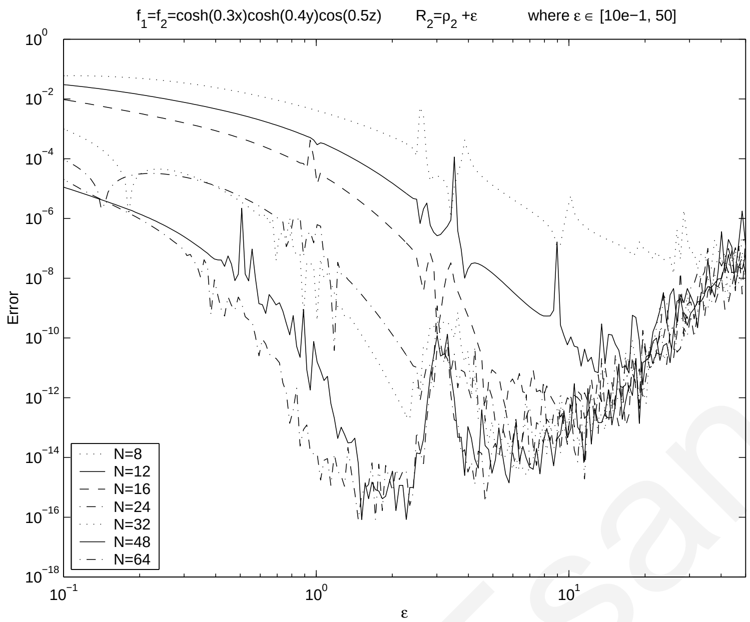

Figure 4.11: Log–log plot of maximum relative error versus ε in Example 2a.

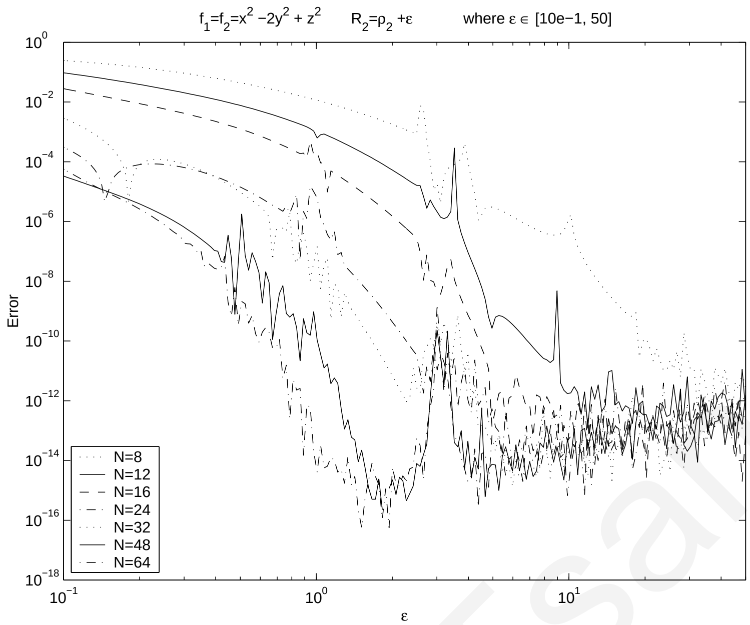

Figure 4.12: Log–log plot of maximum relative error versus ε in Example 2b.

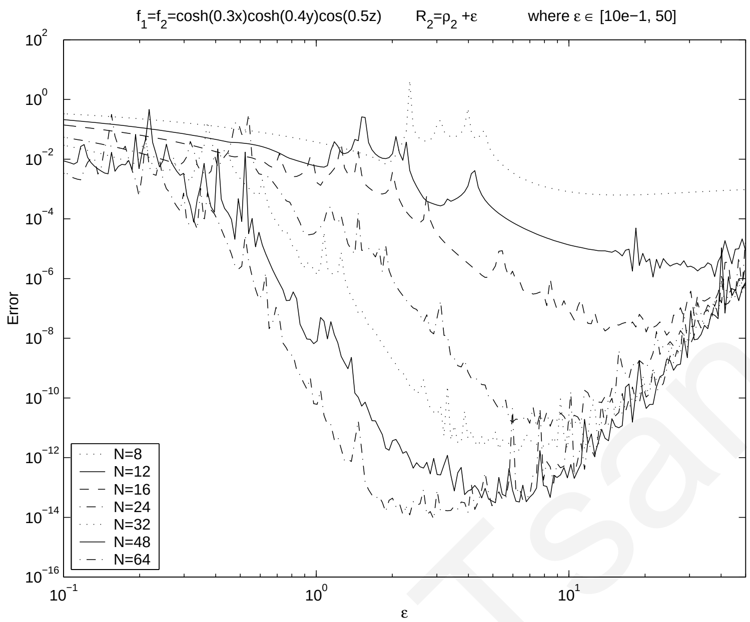

Figure 4.13: Log–log plot of maximum relative error versus ε in Example 3a.

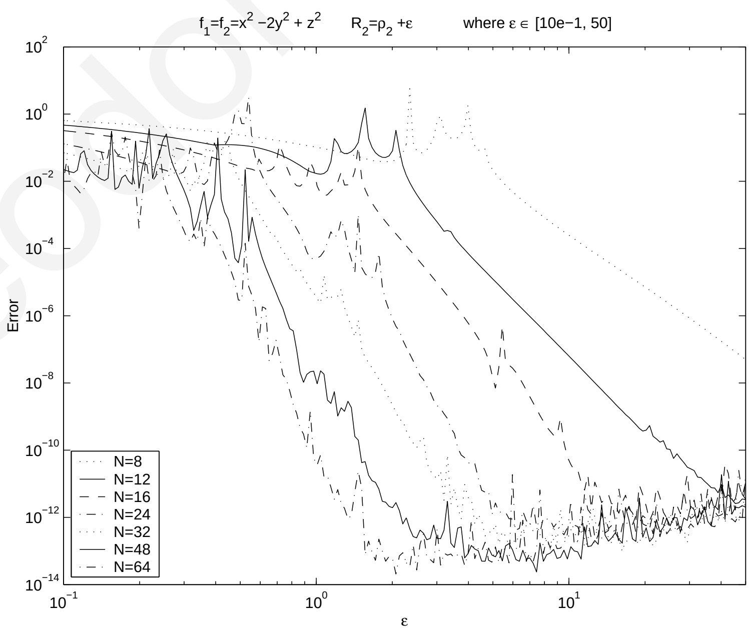

Figure 4.14: Log–log plot of maximum relative error versus ε in Example 3b.

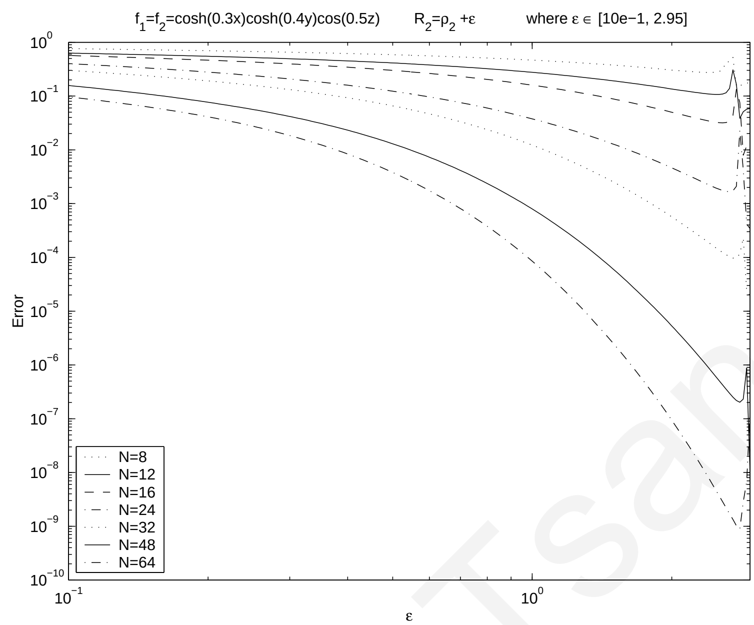

Figure 4.15: Log–log plot of maximum relative error versus ε in Example 4a.

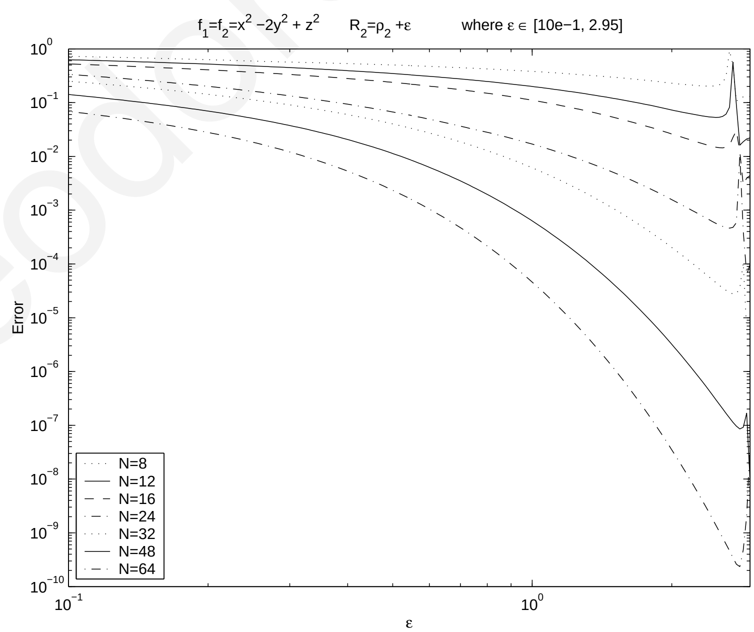

Figure 4.16: Log–log plot of maximum relative error versus ε in Example 4b.

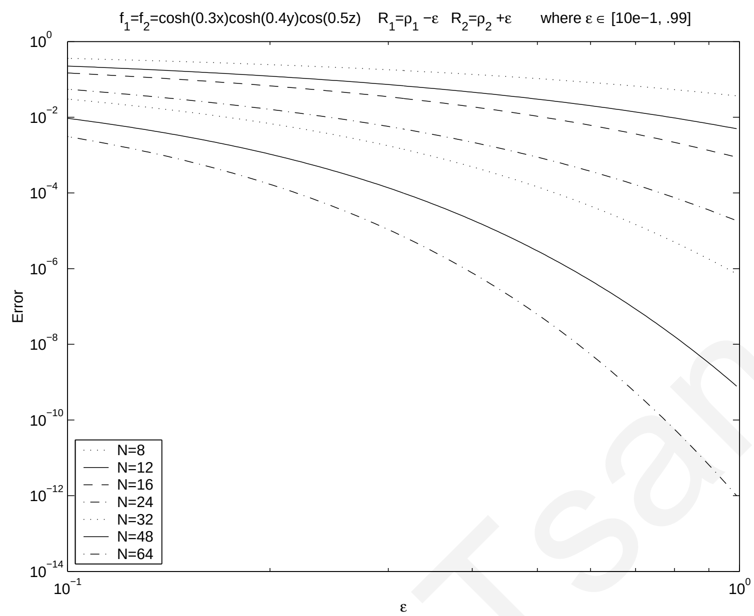

Figure 4.17: Log–log plot of maximum relative error versus ε in Example 1a.

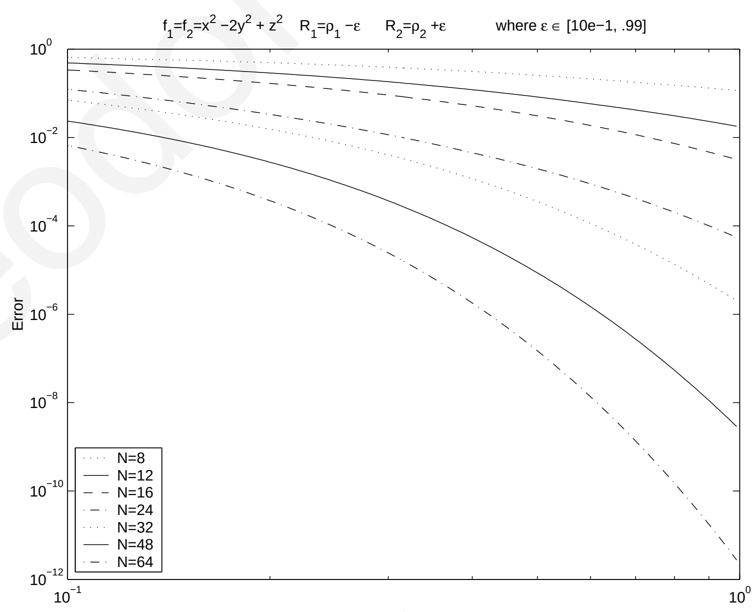

Figure 4.18: Log–log plot of maximum relative error versus ε in Example 1b.

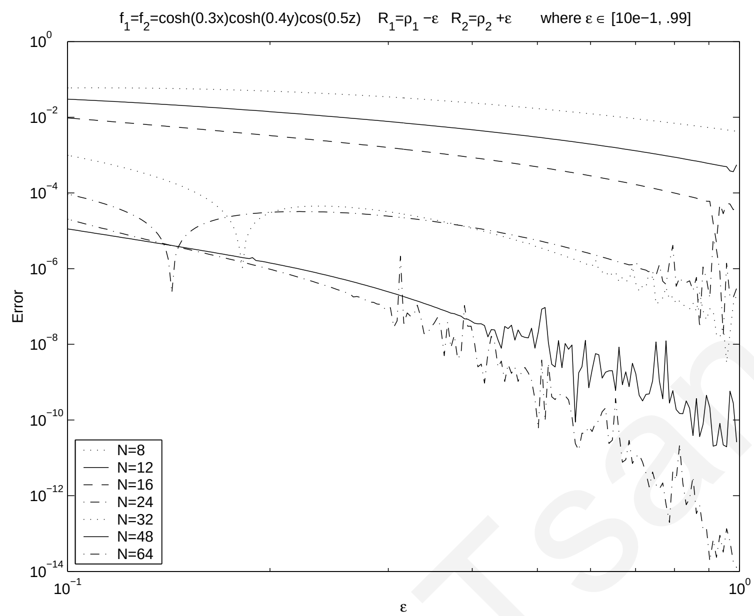

Figure 4.19: Log–log plot of maximum relative error versus ε in Example 2a.

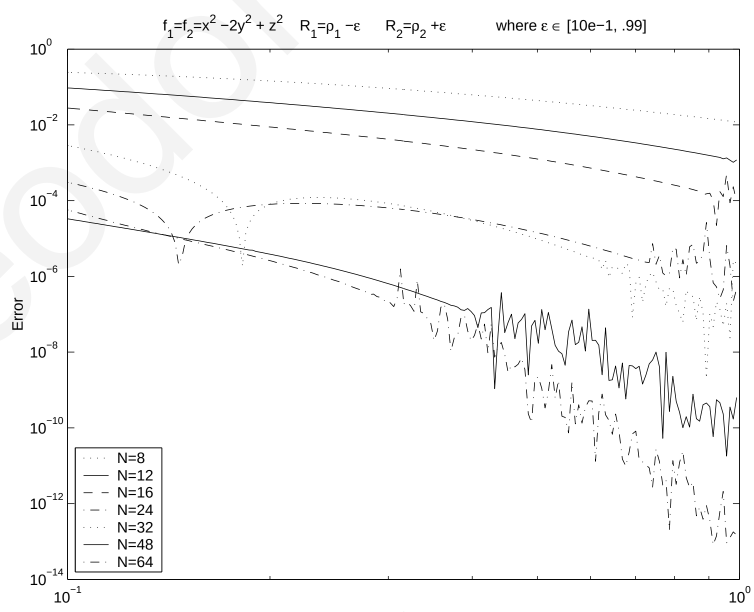

Figure 4.20: Log–log plot of maximum relative error versus ε in Example 2b.

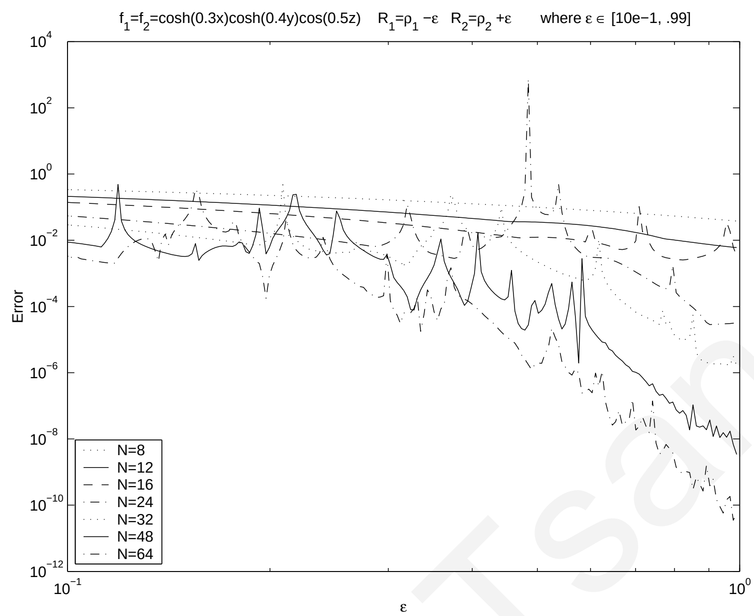

Figure 4.21: Log–log plot of maximum relative error versus ε in Example 3a.

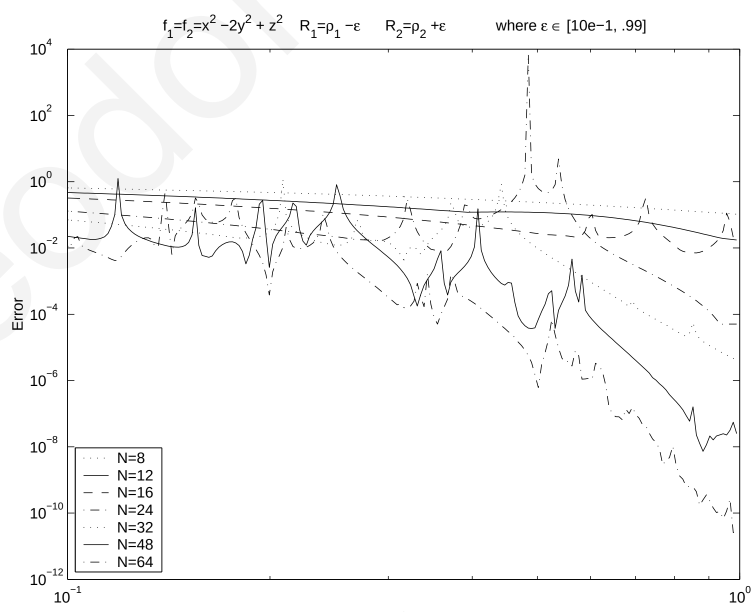

Figure 4.22: Log–log plot of maximum relative error versus ε in Example 3b.

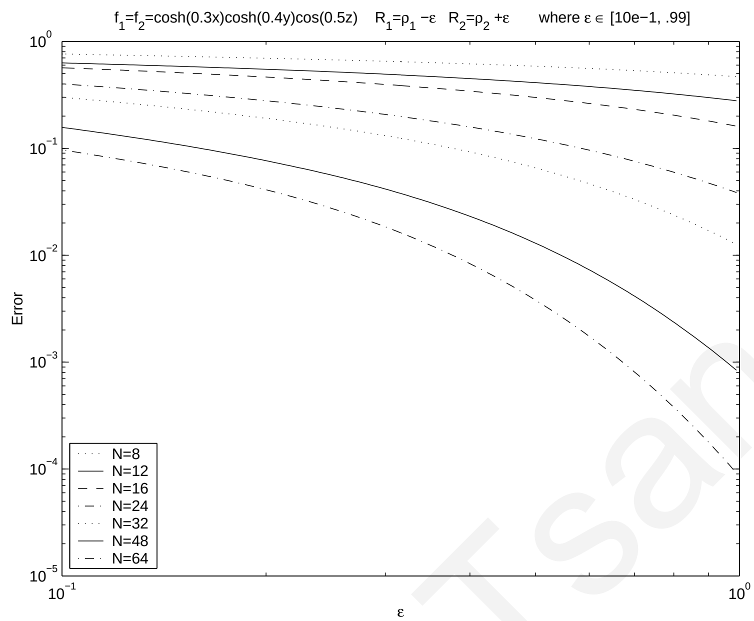

Figure 4.23: Log–log plot of maximum relative error versus ε in Example 4a.

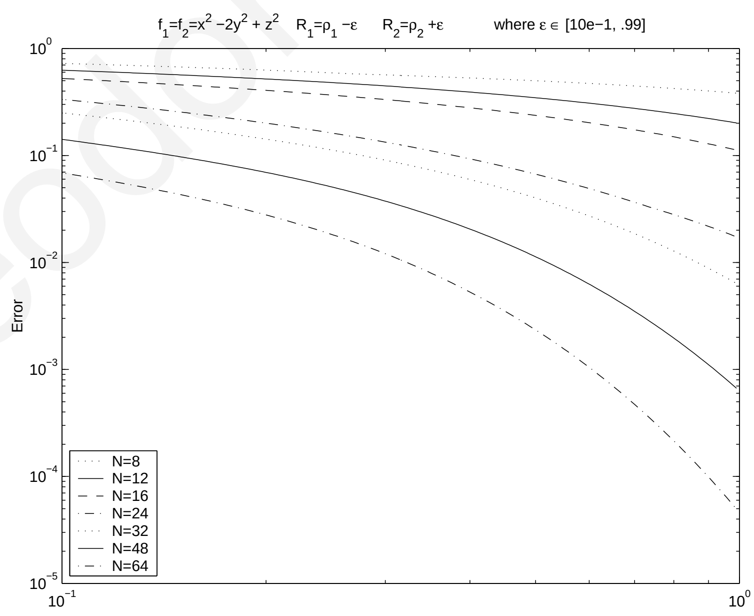

Figure 4.24: Log–log plot of maximum relative error versus ε in Example 4b.

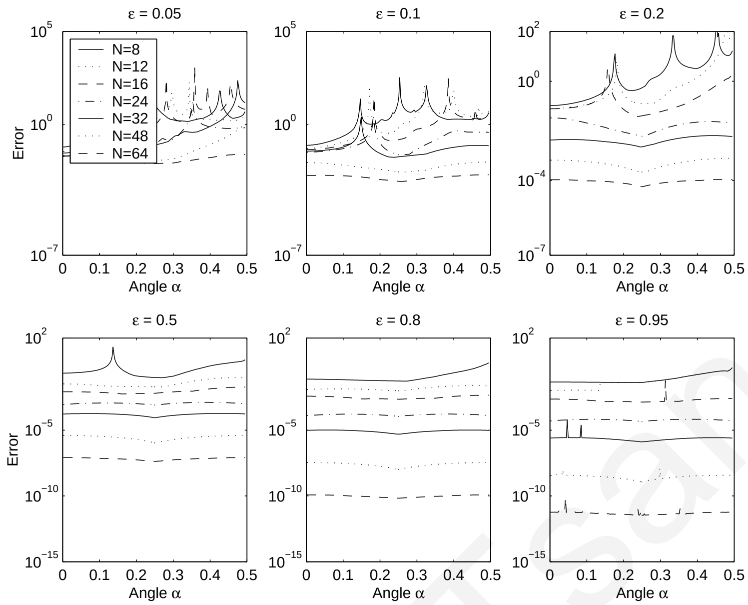

Figure 4.25: Log–plot of error versus angular parameter α for $\varepsilon = 0.05,\ 0.1,\ 0.2,\ 0.5,\ 0.8,\ 0.95$ in Example 1c for different values of N.

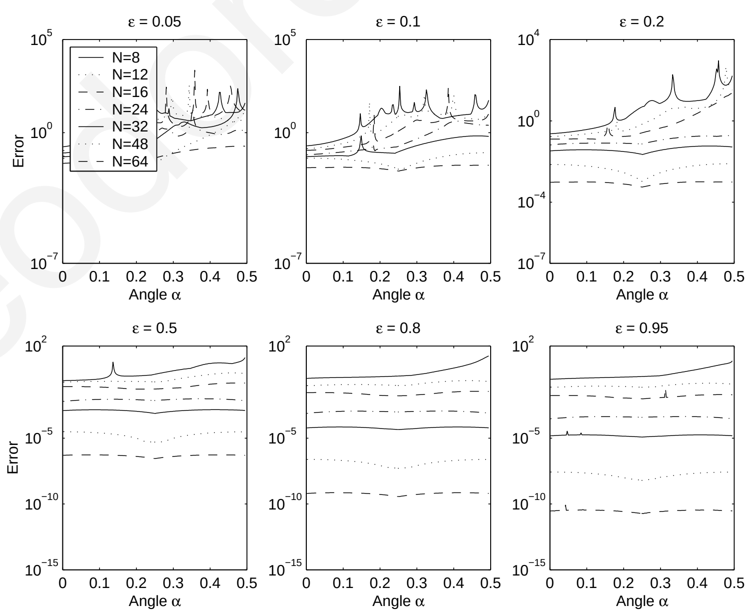

Figure 4.26: Log–plot of error versus angular parameter α for $\varepsilon = 0.05,\ 0.1,\ 0.2,\ 0.5,\ 0.8,\ 0.95$ in Example 1d for different values of N.

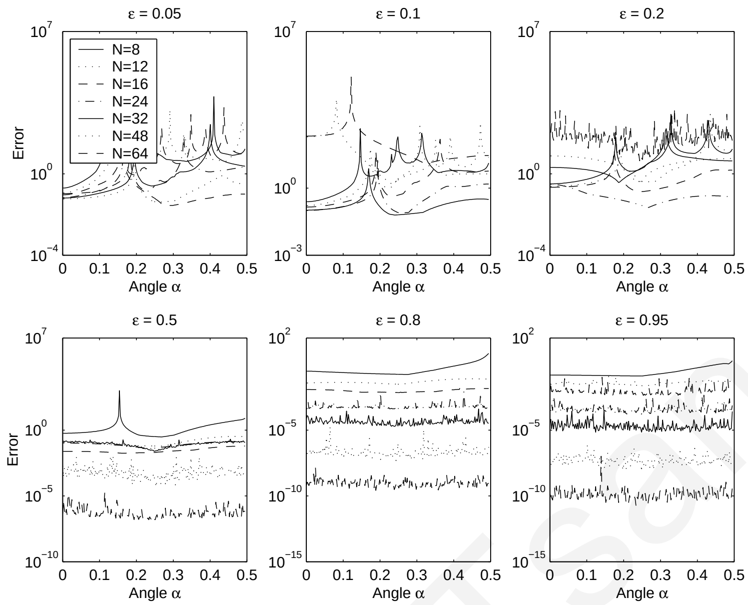

Figure 4.27: Log–plot of error versus angular parameter α for $\varepsilon = 0.05,\ 0.1,\ 0.2,\ 0.5,\ 0.8,\ 0.95$ in Example $2c$ for different values of N.

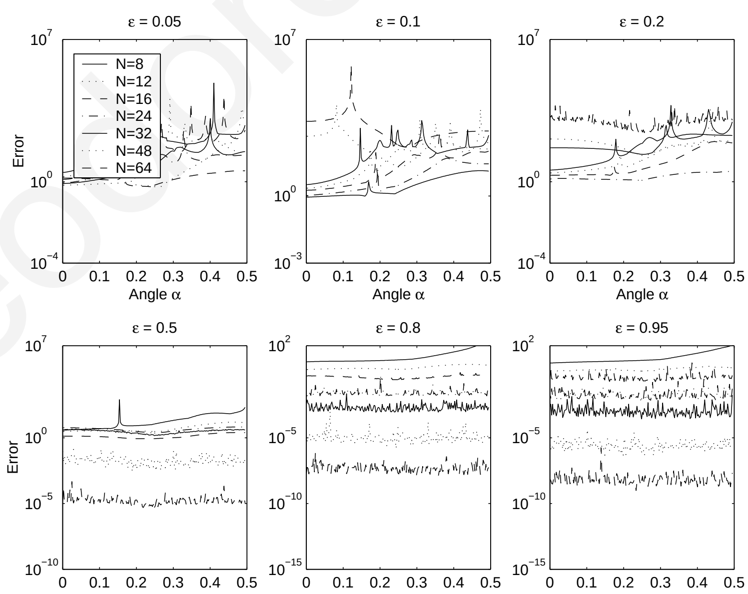

Figure 4.28: Log–plot of error versus angular parameter α for $\varepsilon = 0.05,\ 0.1,\ 0.2,\ 0.5,\ 0.8,\ 0.95$ in Example $2d$ for different values of N.

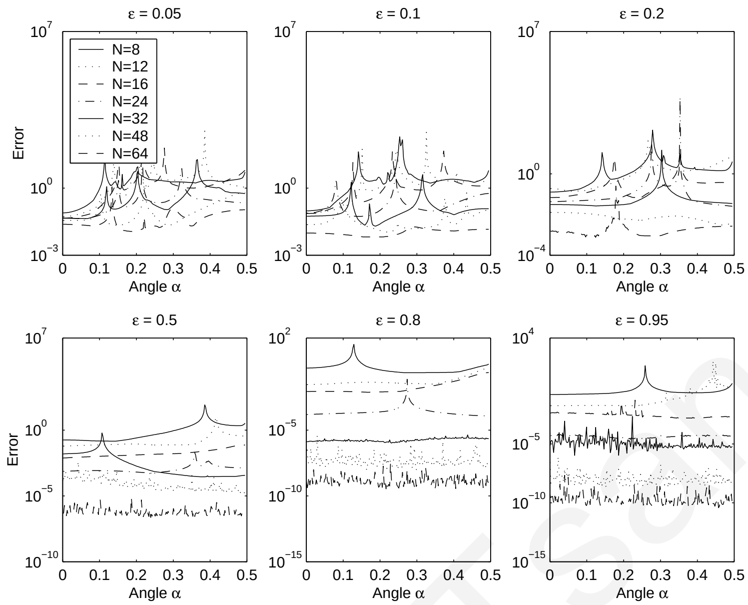

Figure 4.29: Log–plot of error versus angular parameter α for $\varepsilon = 0.05,\ 0.1,\ 0.2,\ 0.5,\ 0.8,\ 0.95$ in Example $3c$ for different values of N.

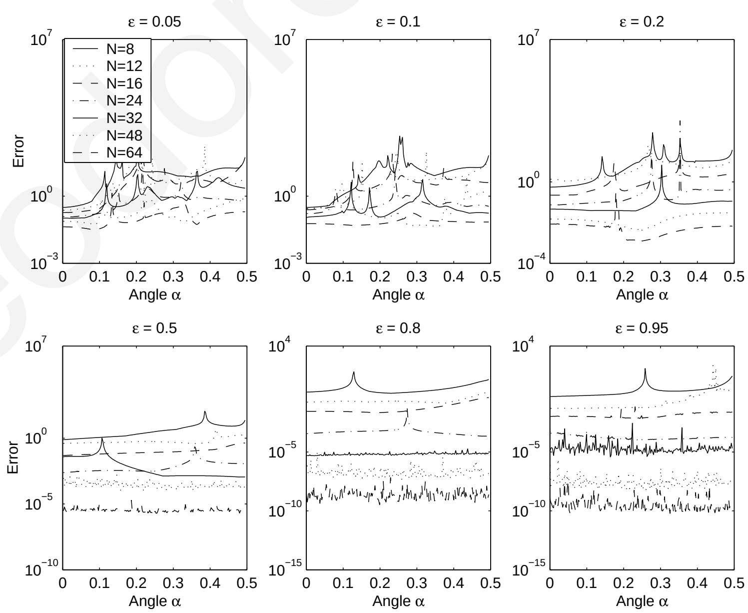

Figure 4.30: Log–plot of error versus angular parameter α for $\varepsilon = 0.05,\ 0.1,\ 0.2,\ 0.5,\ 0.8,\ 0.95$ in Example $3d$ for different values of N.

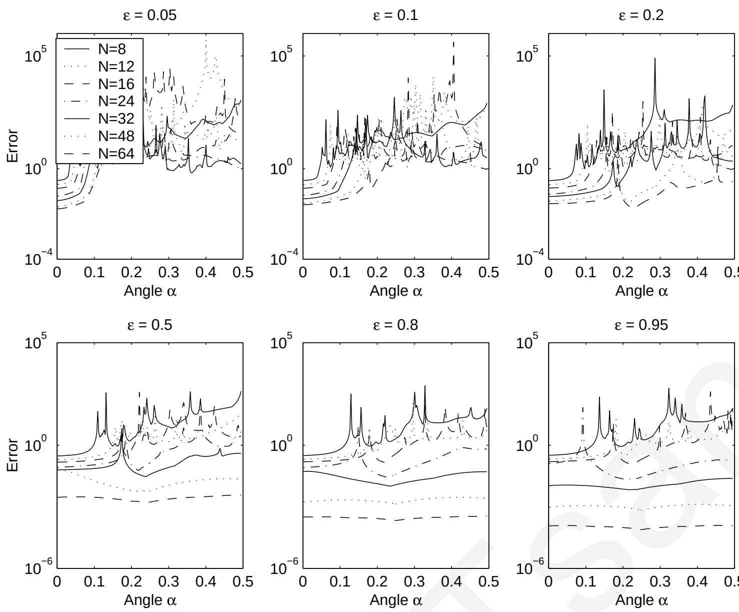

Figure 4.31: Log–plot of error versus angular parameter α for $\varepsilon = 0.05,\ 0.1,\ 0.2,\ 0.5,\ 0.8,\ 0.95$ in Example 4c for different values of N.

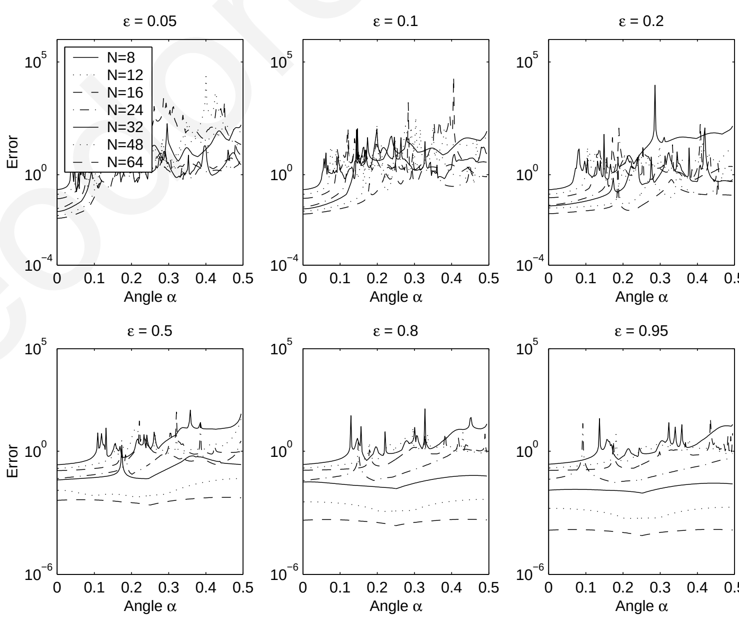

Figure 4.32: Log–plot of error versus angular parameter α for $\varepsilon = 0.05,\ 0.1,\ 0.2,\ 0.5,\ 0.8,\ 0.95$ in Example 4d for different values of N.

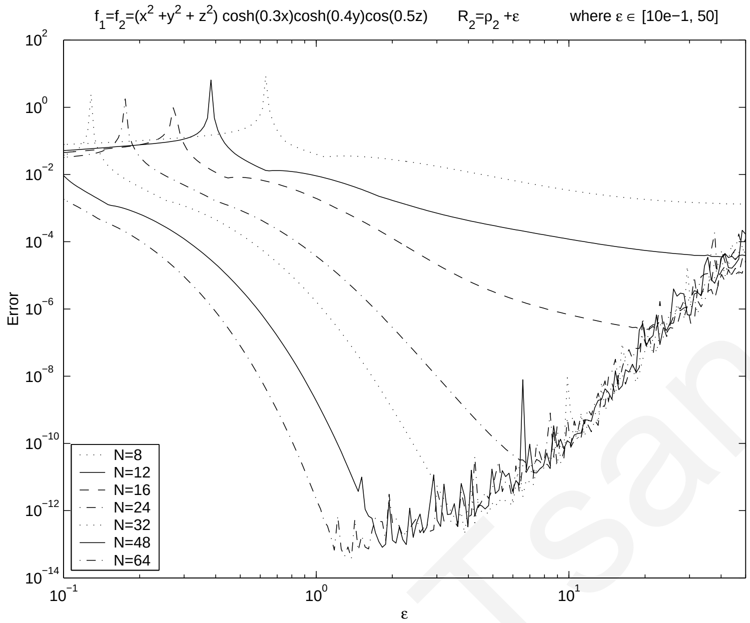

Figure 4.33: Log–log plot of maximum relative error versus ε in Example 1c.

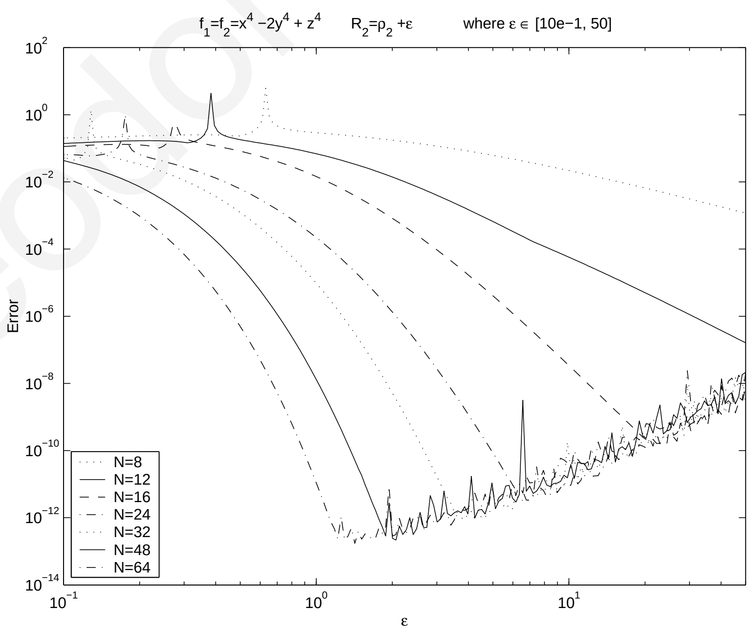

Figure 4.34: Log–log plot of maximum relative error versus ε in Example 1d.

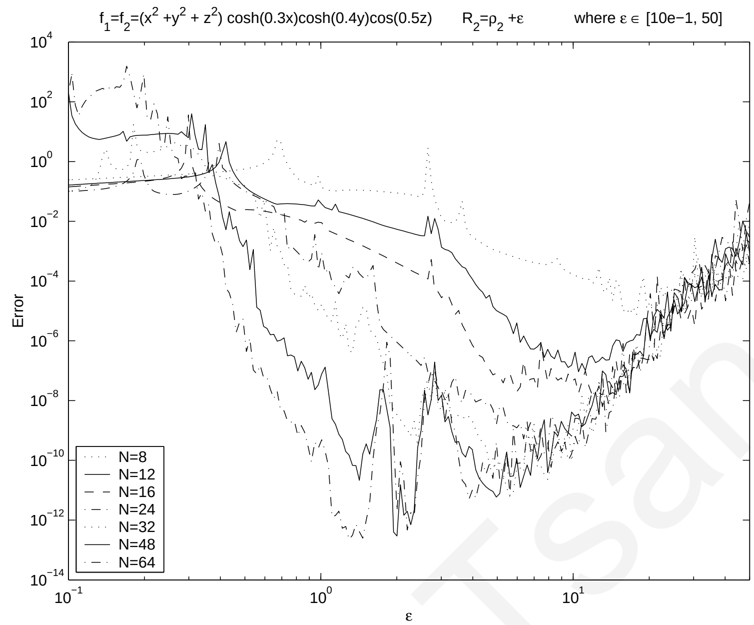

Figure 4.35: Log–log plot of maximum relative error versus ε in Example 2c.

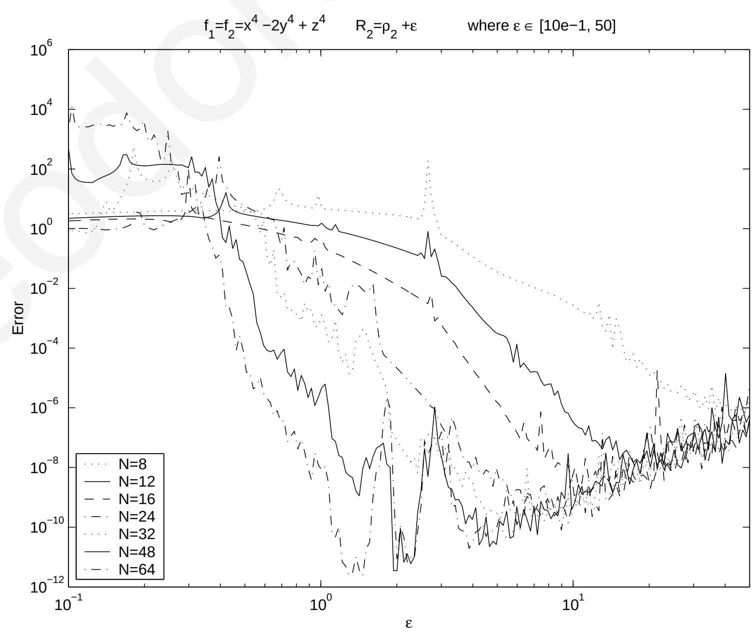

Figure 4.36: Log–log plot of maximum relative error versus ε in Example 2d.

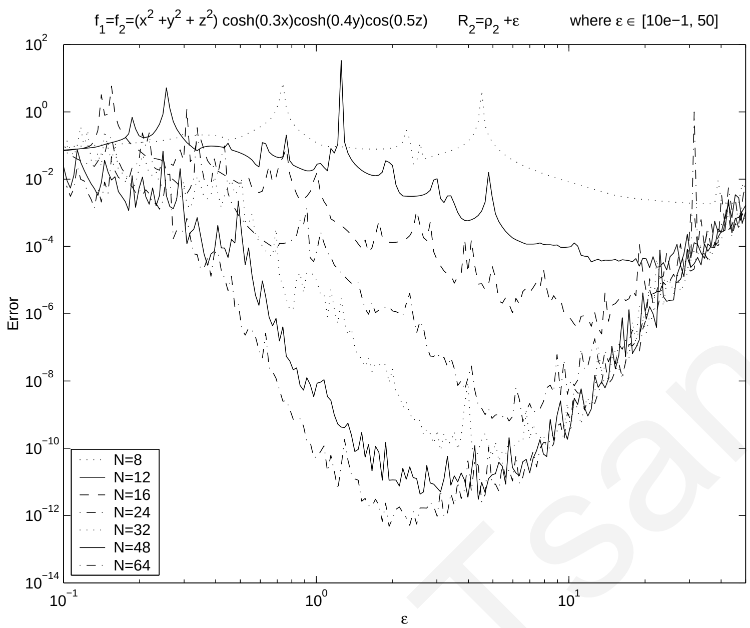

Figure 4.37: Log–log plot of maximum relative error versus ε in Example 3c.

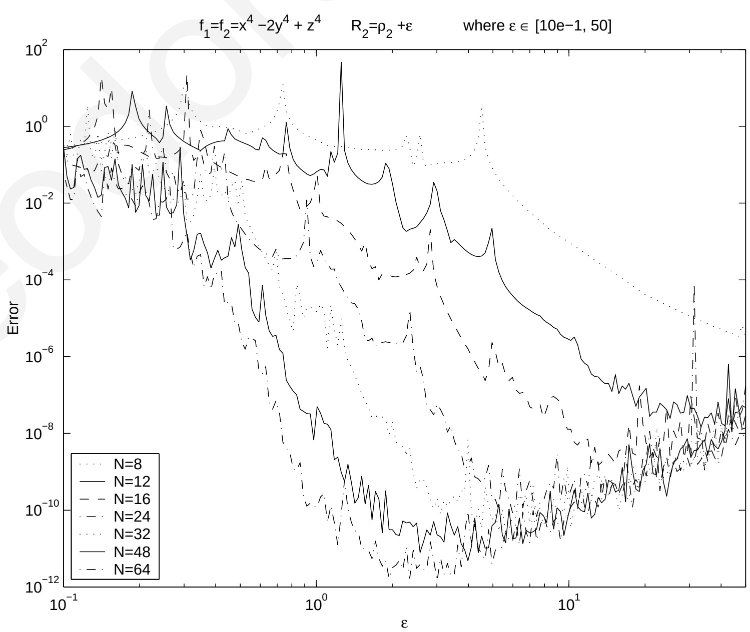

Figure 4.38: Log–log plot of maximum relative error versus ε in Example 3d.

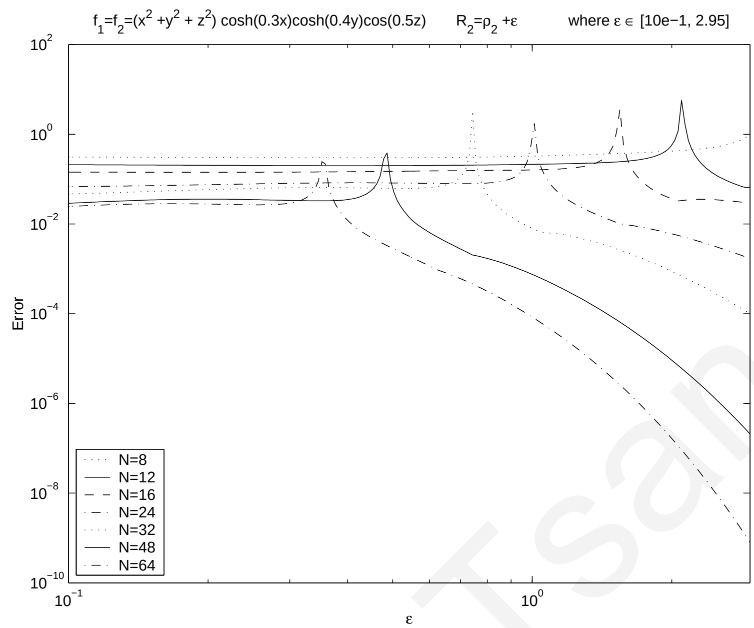

Figure 4.39: Log–log plot of maximum relative error versus ε in Example 4c.

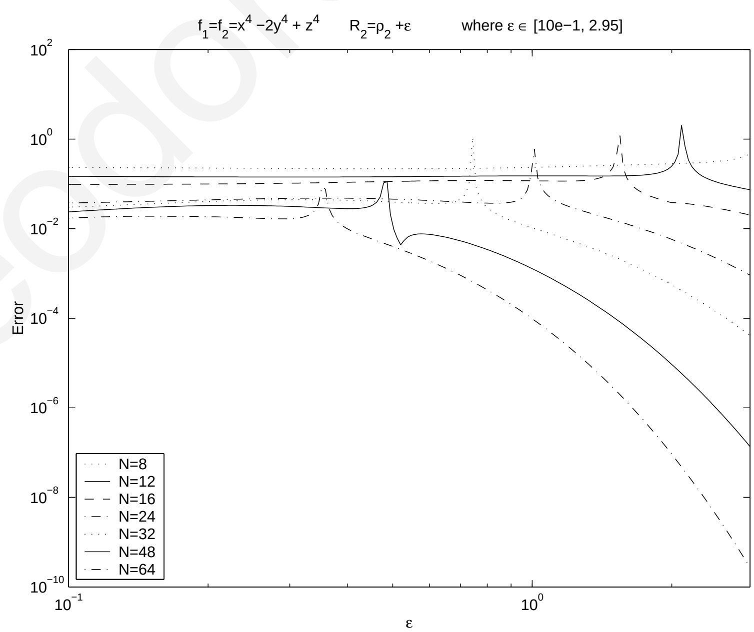

Figure 4.40: Log–log plot of maximum relative error versus ε in Example 4d.

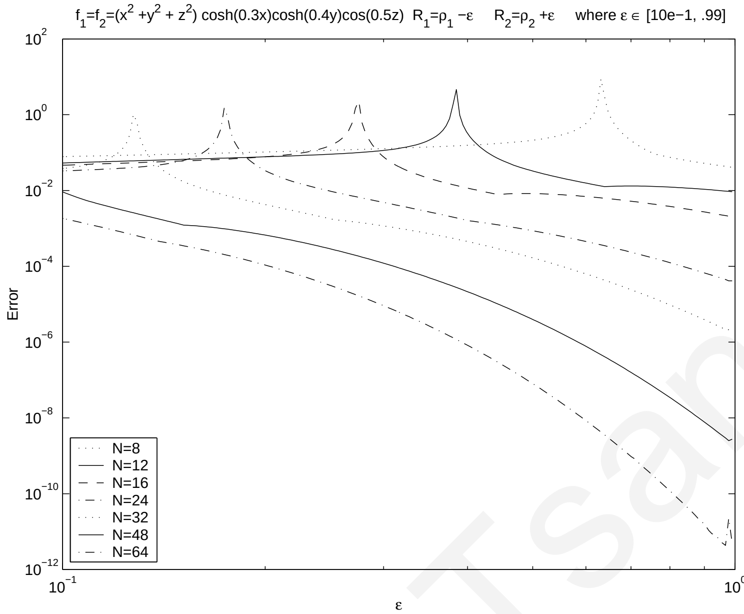

Figure 4.41: Log–log plot of maximum relative error versus ε in Example 1c.

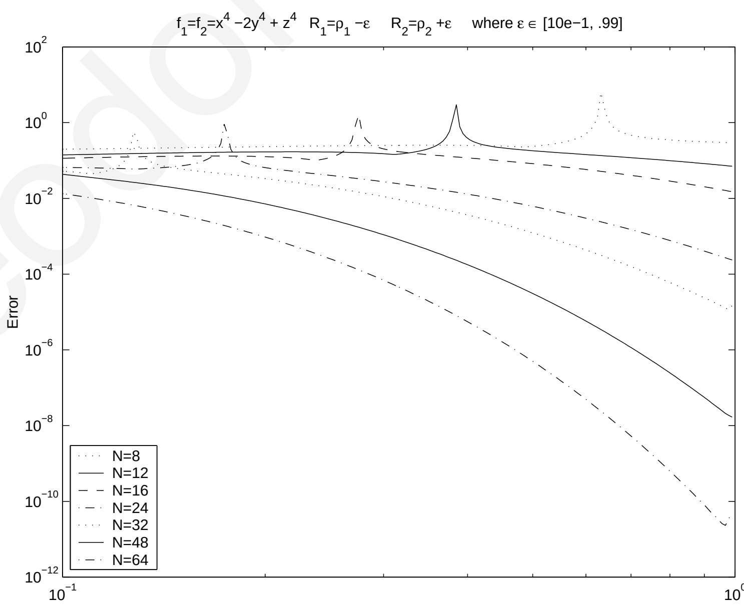

Figure 4.42: Log–log plot of maximum relative error versus ε in Example 1d.

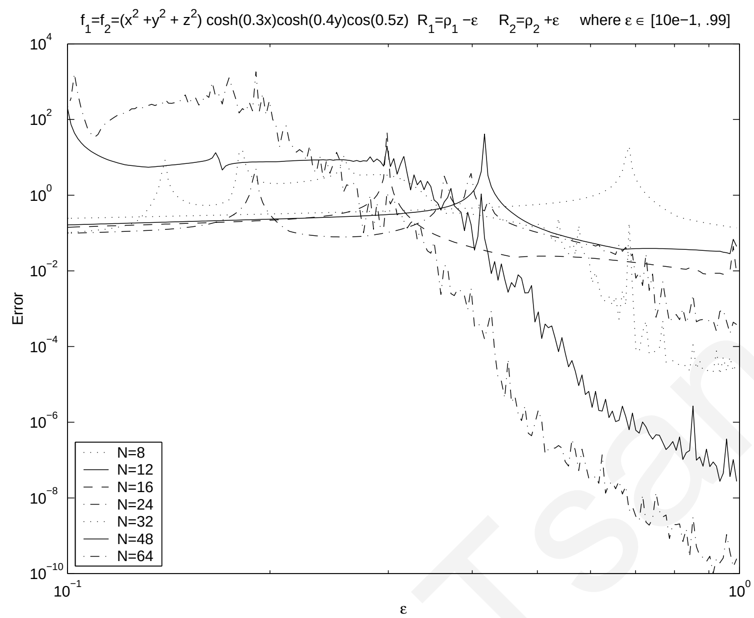

Figure 4.43: Log–log plot of maximum relative error versus ε in Example 2c.

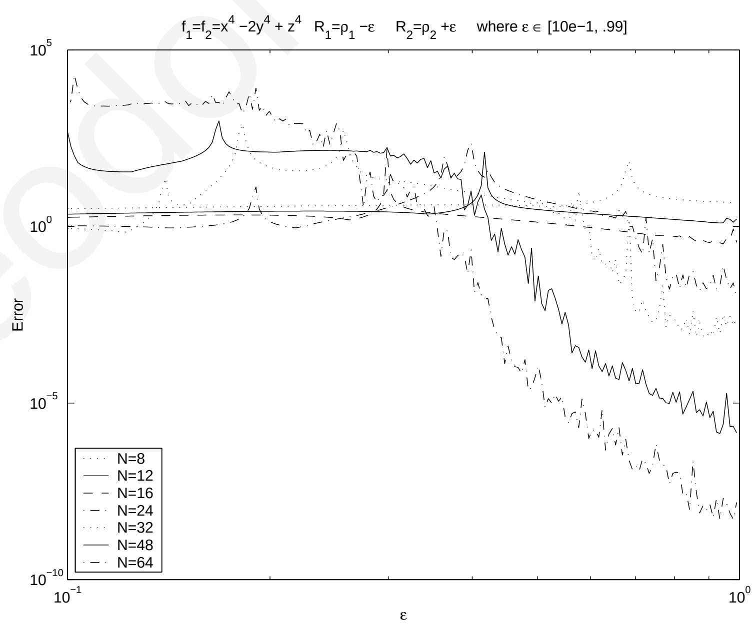

Figure 4.44: Log–log plot of maximum relative error versus ε in Example 2d.

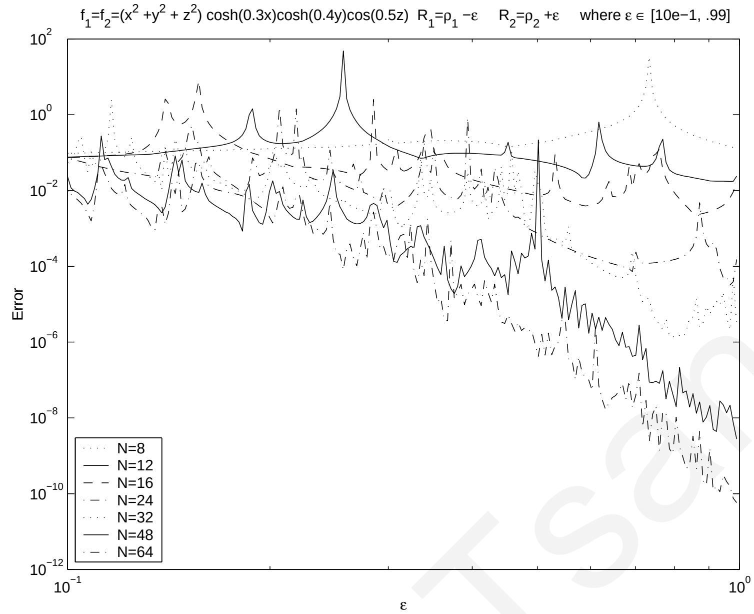

Figure 4.45: Log–log plot of maximum relative error versus ε in Example 3c.

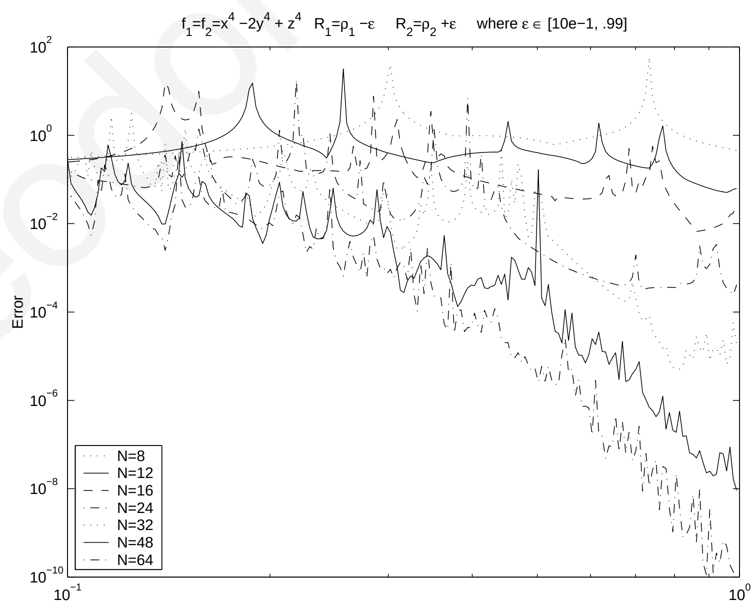

Figure 4.46: Log–log plot of maximum relative error versus ε in Example 3d.

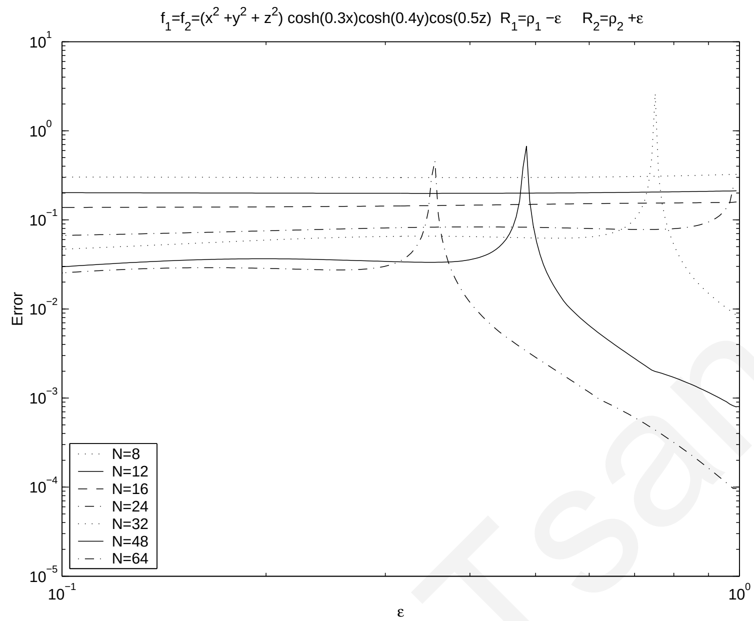

Figure 4.47: Log–log plot of maximum relative error versus ε in Example 4c.

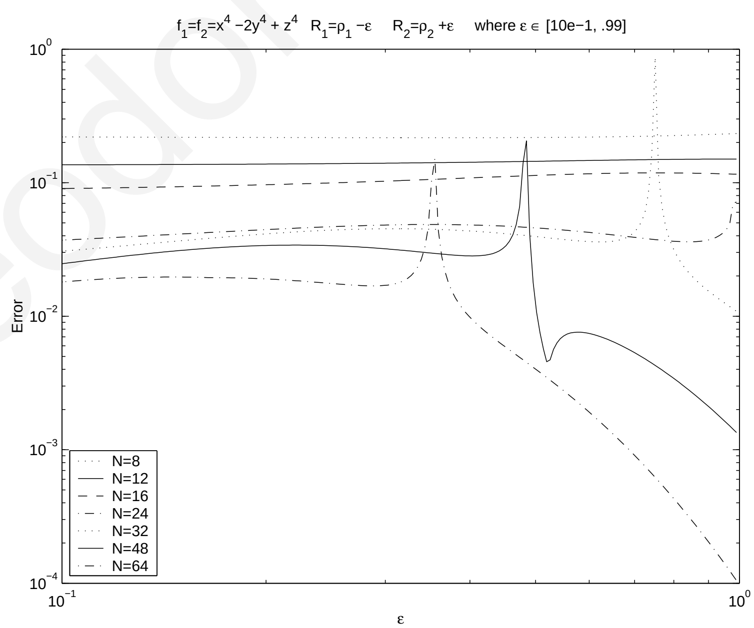

Figure 4.48: Log–log plot of maximum relative error versus ε in Example 4d.

Chapter 5

Conclusions

Our main goal in this thesis is to investigate the application of the MFS to certain problems in rotationally symmetric domains. In particular, we study the application of the MFS to certain harmonic and biharmonic problems in annular domains (Chapters 2 and 3) and to hollow axisymmetric domains (Chapter 4).

In the first chapter we apply the MFS to harmonic problems in annular domains subject to Dirichlet boundary conditions. This application is studied from both a theoretical and an implementational standpoint. The properties of the coefficient matrix are investigated in detail, and an efficient algorithm for the numerical solution of the problem is proposed. Subsequently, it is shown that, for analytic boundary data, the MFS approximation converges exponentially to the exact solution.

The second chapter is devoted to the development of an efficient algorithm for the solution of biharmonic problems in annular domains. This algorithm is an extension of the algorithm developed in the first chapter for harmonic problems and is based on a matrix decomposition formulation which exploits the circulant nature of the matrices involved by employing FFTs. The numerical results indicate that, as was the case with harmonic problems, the accuracy of the solution is affected by (i) the angle by which the singularities are rotated with respect to the boundary points and (ii) the distance of the pseudo–boundary from the boundary of the annulus.

In the third chapter we propose efficient MFS algorithms for the solution of harmonic and biharmonic problems in hollow axisymmetric domains. In particular, we consider the MFS for the solution of harmonic and biharmonic problems in axisymmetric hollow domains. We extend the ideas developed in [70], where the MFS is applied to harmonic problems in axisymmetric simply-connected domains, and [20], where the MFS is applied to the corresponding biharmonic problems. The MFS discretization leads to linear systems the coefficient matrices of which have block circulant structures. Matrix decomposition algorithms are developed for the efficient solution of these systems. These algorithms also make use of FFTs.

In all the examples we considered in this thesis, in both two and three dimansions, we observed the following phenomenon: When the distance of the pseudo–boundary from the boundary of the domain under consideration is small, the accuracy of the solution is affected by the angle by which the singularities are rotated with respect to the boundary points. Further, there appears to be optimal value for this angle. This has not been explained theoretically yet and could be an interesting question to investigate.

In the axisymmetric problems we considered, the way in which we distributed the boundary points and the singularities may not be optimal from a conditioning standpoint. For instance, in the case of the sphere we have a condensation of points in the north and south poles, while the distribution is much sparser elsewhere. A systematic way of developing a more uniform distribution of boundary points and the effect of this on the conditioning of the MFS matrices could be studied further.

The algorithms developed in this thesis could be extended to the solution of two and three-dimensional axisymmetric problems governed by the Helmholtz equation and the Cauchy-Navier equations of elasticity.

The block circulant structure of the coefficient matrices arising in the approximation of functions in two–dimensions using radial basis functions can be exploited in a way analogous to the methods described in this thesis. This has been the subject of [37] where similar matrix decomposition algorithms were developed. The (non-trivial) extension of such algorithms to the approximation of functions in three–dimensions using Radial Basis Functions is yet to be investigated.

Recently, there has been activity in the application of the MFS to problems in the area of geometric modelling [74]. This could prove to be an exciting new area of research with many applications in computer-aided design and computer-aided manufacturing applications.

In the past, the MFS has been successfully applied to two-dimensional steady-state free surface problems. The application of the MFS to three-dimensional steady-state free surface problems, as well as to two- and three-dimensional time-dependent free surface problems, could be the subject of future research.

One of the most important open questions regarding the application of the MFS is the optimal placement of the singularities. This question is to a great extent addressed by the use of the version of the MFS which uses moving singularities. This approach, however, is often prohibitively computationally costly. The improvement of the efficiency of the MFS with moving singularities could be an area of future research. One idea would be to exploit the fact that the coefficients in the MFS expansions appear linearly. This, to the best of our knowledge has not yet been exploited. We also need to investigate whether more efficient non-linear least squares solvers are available. Another open question is to what extent the use of parallelization would improve the efficiency of the method.

Finally, the ill–conditioning of the MFS matrices should be studied further. This occurs the pseudoboundary is placed far from the boundary of the domain under consideration. An interesting approach for overcoming this problem could be the use of appropriate pre–conditioning techniques.

Bibliography

[1] E. Almansi, *Sull' integrazione dell' equazione differentiale* Δ^{2n}, Annali di Mathematica Pura et Applicata, Series III, **2**, 1-51, 1897.

[2] M. Abramowitz and I. A. Stegun, *Handbook of Mathematical Functions*, Verlag Harri Deutsch, Thun, 1984.

[3] K. E. Atkinson, *The numerical evaluation of particular solutions for Poisson's equation*, IMA J. Numer. Anal. **5**, 319–338, 1985.

[4] C.J.S. Alves and C.S. Chen, *A new method of fundamental solutions applied to non-homogeneous elliptic problems*, Adv. Comput. Math., **23**, 125-142, 2005.

[5] P. K. Banerjee and R. Butterfield, *Boundary Element Methods in Engineering Science*, McGraw-Hill, Maidenhead, 1981.

[6] J. R. Berger and A. Karageorghis, The method of fundamental solutions for layered elastic materials, *Engng. Analysis with Boundary Elements*, **25**, 877-886, 2001.

[7] J. R. Berger, A. Karageorghis and P. A. Martin, *Stress intensity factor computation using the method of fundamental solutions: mixed - mode problems*, Technical Report TR–09–2005, Department of Mathematics and Statistics, University of Cyprus.

[8] B. Bialecki and G. Fairweather, *Matrix decomposition algorithms for separable elliptic boundary value problems in two space dimensions*, J. Comp. Appl. Math., **4**6, 369–386, 1993.

[9] A. Bogomolny, *Fundamental solutions method for elliptic boundary value problems*, SIAM J. Numer. Anal. **2**2, 644–669, 1985.

[10] M. D. Buhmann, *Radial Basis Functions*, Campridge University Press, Cambridge, 2003.

[11] C.S. Chen, M.A. Golberg and Y.F. Rashed, *A mesh free method for linear diffusion equations*, Numerical Heat Transfer, Part B, **3**3, 469-486, 1998.

[12] C. S. Chen, *The method of fundamental solutions for nonlinear thermal explosion*, Commun. Numer. Methods Eng. **11**, 675–681, 1995.

[13] H. A. Cho, M. A. Golberg, A. S. Muleshkov and X. Li, *Trefftz methods for time dependent partial differential equations*, Comput. Mat. Cont., **1**, 1–37, 2004.

[14] C. S. Chen, M. Ganesh, M. A. Golberg and A. H. -D. Cheng, *Multilevel compact radial functions based computational schemes for some elliptic problems*, Comput. Math. Appl., **43**, 359–378, 2002.

[15] P. J. Davis, *Circulant Matrices*, John Wiley and Sons, New York, 1979.

[16] A. Doicu, Yu. Eremin and T. Wriedt, *Acoustic and Electromagnetic Scattering Analysis Using Discrete Sources*, Academic Press, New York, 2000.

[17] G. Fairweather and R. L. Johnston, *The method of fundamental solutions for problems in potential theory,in: Treatment of Integral Equations by Numerical Methods*, eds. C. T. H. Baker and G. F. Miller (Academic Press, London, 1982) pp. 349–359.

[18] G. Fairweather and A. Karageorghis, *The method of fundamental solutions for elliptic boundary value problems*, Adv. Comput. Math., **9**, 69-95, 1998.

[19] G. Fairweather, A. Karageorghis and P. A. Martin, *The method of fundamental solutions for scattering and radiation problems*, Engng. Analysis with Boundary Elements, **27**, 759-769, 2003.

[20] G. Fairweather, A. Karageorghis, and Y.–S. Smyrlis, *A matrix decomposition MFS algorithm for axisymmetric biharmonic problems*, Adv. Comput. Math., **2**3, 55–71, 2005.

[21] R. T. Fenner, *Source field superposition analysis of two-dimensional potential problems*, Internat. J. Numer. Methods Engrg. **32**, 1079–1091, 1991.

[22] G. Fichera, *Linear elliptic equations of higher order in two independent variables and singular integral equations with applications to anisotropic inhomogeneous elasticity*, Par-

tial Differential Equations and Continuum Mechanics, ed. R. E. Langer (University of Wisconsin Press, Madison), 55–80, 1961.

[23] Garbow BS, Hillstrom KE, More JJ. *MINPACK project*, Argone National Laboratory, 1980.

[24] M. A. Golberg, *The method of fundamental solutions for Poisson's equation*, Engng. Anal. Boundary Elem. **16**, 205–213, 1995.

[25] M. A. Golberg and C. S. Chen, *Discrete Projection Methods for Integral Equations*, Computational Mechanics Publications, Southampton, 1996.

[26] M. A. Golberg and C. S. Chen, *The method of fundamental solutions for potential, Helmholtz and diffusion problems*, in: *Boundary Integral Methods and Mathematical Aspects*, ed. M. A. Golberg, WIT Press/Computational Mechanics Publications, Boston, pp. 103–176, 1999.

[27] M. A. Golberg, C. S. Chen and M. Ganesh, *Particular solution of the 3D modified Helmholtz-type equation using compactly supported radial basis functions* , Engng. Anal. Boundary Elem. **24**, 539–547, 2000.

[28] M. A. Golberg, A. S. Muleshkov, C. S. Chen and A. H. -D. Cheng, *Polynomial particular solutions for certain partial differential operators*, Numer. Methods of Partial Differential Equations, **19**, 112–133, 2003.

[29] I. S. Gradshteyn and I. M. Ryzhik, *Table of Integrals, Series, and Products*, 6th edition, Academic Press, London, 2000.

[30] Hopper MJ, ed., *Harwell subroutine library catalogue*, AERE, Harwell, UK: Theoretical Physics Division, 1973.

[31] S. Ho-Tai, R. L. Johnston and R. Mathon, *Software for solving boundary value problems for Laplace's equation using fundamental solutions*, Technical Report 136/79, Department of Computer Science, University of Toronto, 1979.

[32] M.A. Jaswon and G. T. Symm, *Integral equation methods in potential theory and elastostatics*, Academic Press [Harcourt Brace Jovanovich Publishers], London, 1977.

[33] J. H. KANE, *Boundary Element Analysis in Engineering Continuum Mechanics*, Prentice Hall, Engelwood Cliffs, NJ, 1994.

[34] E. J. KANSA, *Multiquatrics-a scattered data approximation scheme with applications to computational fluid dynamics-I-surface approximation and partial derivative estimates*, Comput. Math. Appl., **19**, 127–145, 1990.

[35] E. J. KANSA, *Multiquatrics-a scattered data approximation scheme with applications to computational fluid dynamics-II-surface approximation and partial derivative estimates*, Comput. Math. Appl., **19**, 146–161, 1990.

[36] E. J. KANSA AND Y. C. HON, *Circumventing the ill-conditioning problem with multiquadric radial basis functions: applications to elliptic differential equations*, Comput. Math, Appl. **39**, 123–137, 2000.

[37] A. KARAGEORGHIS, C. S. CHEN AND Y-S. SMYRLIS, *A matrix decomposition RBF algorithm. Part I: Approximation of functions and their derivatives*, Technical Report TR/01/2004, Dept of Maths and Stats, University of Cyprus, 2004.

[38] A. KARAGEORGHIS AND G. FAIRWEATHER, *The method of fundamental solutions for the solution of the biharmonic equation*, J. Comput. Phys., **69**, 434–459, 1987.

[39] A. KARAGEORGHIS AND G. FAIRWEATHER, *The simple layer potential method of fundamental solutions for certain biharmonic problems*, Internat. J. Numer. Methods Fluids, **9**, 1221–1234, 1989.

[40] A. KARAGEORGHIS AND G. FAIRWEATHER, *The Almansi of fundamental solutions for solving biharmonic problems*, Internat. J. Numer. Methods Engrg., **26**, 1668–1682, 1988.

[41] A. KARAGEORGHIS AND Y.S. SMYRLIS, *A matrix decomposition MFS algorithm for Helmholtz problems*, Vibrations in Physical Systems, 47–54, XXI Symposium, May 26–29, Kiekrz, Poland, 2004.

[42] M. KATSURADA, *A mathematical study of the charge simulation method II*, J. Fac. Sci., Univ. of Tokyo, Sect. 1A, Math. 36, 135-162, 1989.

[43] M. KATSURADA AND H.OKAMOTO, *A mathematical study of the charge simulation method I*, J. Fac. Sci., Univ. of Tokyo, Sect. 1A, Math. 35, 507-518, 1988.

[44] T. Kitagawa, *On the numerical stability of the method of fundamental solution applied to the Dirichlet problem*, Japan J. Appl. Math. **5**, 123–133, 1988.

[45] T. Kitagawa, *Asymptotic stability of the fundamental solution method*, Proceedings of the International Symposium on Computational Mathematics (Matsuyama, 1990). J. Comput. Appl. Math. **38**, 263–269, 1991.

[46] J. A. Kołodziej, *Applications of the Boundary Collocation Method in Applied Mechanics*, Wydawnictwo Politechniki Poznańskiej, Poznań, 2001. In Polish.

[47] V. D. Kupradze, *Potential Methods in the Theory of Elasticity*, Israel Program for Scientific Translations, Jerusalem, 1965.

[48] V. D. Kupradze, *A method for the approximate solution of limiting problems in mathematical physics*, U.S.S.R. Comp. Math. and Math. Phys. **4**, 199–205, 1964.

[49] V.D. Kupradze and M.A. Aleksidze, *The method of functional equations for the approximate solution of certain boundary value problems*, Comput. Methods Math. Phys. **4**, 82126, 1964.

[50] K. Kuwahara and I. Imai, *Steady, viscous flow with circular boundary*, Phys. Fluids Supple., **12**, II-94–II-101, 1969.

[51] Xin Li and C. S. Chen, *A mesh-free method using hyperinterpolation and fast Fourier transform for solving differential equations*, Engineering Analysis with Boundary Elements, **28**, 1253–1260, 2004.

[52] Liviu Marin , *A meshless method for the numerical solution of the Cauchy problem associated with three-dimensional Helmholtz-type equations*, Applied Mathematics and Computations, to appear.

[53] Liviu Marin , *Numerical solution of the Cauchy proplem for steady-state heat transfer in two-dimensional functionally graded materials*, International Journal of Solids and Structures, to appear.

[54] Liviu Marin and Daniel Lesnic, *The method of fundamental solutions for the Cauchy problem associated with two-dimensional Helmholtz-type equations*, Computers and Structures **83**, 267-278, 2005

[55] LIVIU MARIN AND DANIEL LESNIC, *The method of fundamental solutions for the Cauchy problem in two-dimensional linear elasticity*, International Journal of Solids and Structures **41**, 3425-3438, 2004

[56] M. MAITI AND S. K. CHAKRABARTY, *Integral equations solutions for simply supported polygonal plates*, Internat. J. Engrg. Sci. **12**, 793806, 1974.

[57] G. C. DE MEDEIROS, P. W. PARTRIGE AND J. O. BRANDAO, *The method of fundamental solutions with dual reciprocity for some problems in elasticity*, Engng. Analysis with Boundary Elements, **28**, 453–461, 2004.

[58] C. D. MEYER, *Matrix Analysis and Applied Linear Algebra*, SIAM, Philadelphia, 2000.

[59] R. MATHON AND R. L. JOHNSTON, *The approximate solution of elliptic boundary–value problems by fundamental solutions*, SIAM J. Numer. Anal., **14**, 638–650, 1977.

[60] D. NARDINI AND C. A. BREBBIA, *A new approach for free vibration analysis using boundary elements*, Boundary Element Methods in Engineering, 312–326, 1982.

[61] *Numerical Algorithms Group Library Mark 20*, NAG Ltd, Wilkinson House, Jordan Hill Road, Oxford, UK, 2001.

[62] E. R. OLIVEIRA,*Plane stress analysis by a general integral method*, J. Engrg. Mech. Div. ASCE **94**, 79-101, 1968.

[63] A. POULLIKKAS, A. KARAGEORGHIS AND G. GEORGIOU, *The method of fundamental solutions for inhomogeneous elliptic problems*, Computational Mechanics, **22**, 100-107, 1998.

[64] A. POULLIKKAS, A. KARAGEORGHIS AND G. GEORGIOU, *The method of fundamental solutions for three dimensional elastostatics problems*, Computers & Structures, **80**, 365-370, 2000.

[65] P.A. RAMACHANDRAN, *Method of fundamental solutions: singular value decomposition analysis*, Commun. Numer. Meth. Engng., **18**, 789–801, 2002.

[66] M. SHARAN AND E. J. KANSA, *Application of the multiquadic method for numerical solution of elliptic partial differential equations*, Appl. Math. Comp., **84**, 275–302, 1997.

[67] Y.S. Smyrlis and A. Karageorghis, *Some aspects of the method of fundamental solutions for certain harmonic problems*, J. Sci. Comput., **16**, 341–371, 2001.

[68] Y.S. Smyrlis and A. Karageorghis, *Some aspects of the method of fundamental solutions for certain biharmonic problems*, Computer Modeling in Engineering & Sciences, **4**, 535-550, 2003.

[69] Y.S. Smyrlis and A. Karageorghis, *Numerical analysis of the MFS for certain harmonic problems*, RAIRO Modél. Math. Anal. Numér., to appear.

[70] Y.S. Smyrlis and A. Karageorghis, *A matrix decomposition MFS algorithm for axisymmetric potential problems*, Engineering Analysis with Boundary Elements, **28**, 463–474, 2004.

[71] Y.S. Smyrlis and A. Karageorghis, *Numerical analysis of the MFS for certain harmonic problems* , Technical Report TR-04-2003, Department of Mathematics and Statistics, University of Cyprus.

[72] W. A. Strauss, *Partial Differential Equations. An Introduction*, John Wiley & Sons, Inc., New York, 1992.

[73] A. Poullikas, J. R. Berger and A. Karageorghis, *Stress intensity factor computation using the method of fundamental solutions*, Technical Report TR–16–2004, Department of Mathematics and Statistics, University of Cyprus.

[74] R. Tankelevich, G. Fairweather, A. Karageorghis and Y-S. Smyrlis, *Potential field based geometric modelling using the MFS*, preprint.

[75] G. N. Watson, *A Treatise on the Theory of Bessel Functions,* 2nd Edition, Cambridge University Press, Cambridge, 1966.

[76] S. P. Walker, *Diffusion problems using transient discrete source superposition*, Internat. J. Numer. Methods Engrg. **35**, 165–178, 1992.